NETHERLANDS GEODETIC COMMISSION

PUBLICATIONS ON GEODESY NEW SERIES

VOLUME 7 NUMBER 4

ON THE PRINCIPLES, ASSUMPTIONS AND METHODS OF GEODETIC VERY LONG BASELINE INTERFEROMETRY

by

FRITS J. J. BROUWER

1985

RIJKSCOMMISSIE VOOR GEODESIE, THIJSSEWEG 11, DELFT, THE NETHERLANDS

PRINTED BY W. D. MEINEMA B.V., DELFT, THE NETHERLANDS

ISBN 90 6132 232 4

SUMMARY

The accurary of geodetic VLBI point positioning measurements is assessed. The assessment is based on a software package developed for the purpose which incorporates all possible computing models for geodetic VLBI data analysis. Analysis of real and simulated data with this package shows that an accuracy of 10 cm in point positioning has been achieved with the ERIDOC and MERIT Short Campaign observing campaigns. This analysis has also led to the formulation of criteria for optimum design of a geodetic VLBI observing campaign, and to a general approach for evaluating experiments designed to compare VLBI with other geodetic techniques, because the ultimate accuracy of world-wide geodetic measurements for geodynamics and positioning can only be achieved by a combination of several techniques.

The DEGRIAS (DElft Geodetic Radio Interferometry Adjustment System) software package and the background of its development are described in the first three chapters of this publication. The package is the outcome of a desire to incorporate geodetic VLBI into the system for the design and computation of geodetic networks developed at the Delft Department of Geodesy, commonly known as the Delft Approach. Chapters 2 and 3 provide descriptions of the general and specific features of DEGRIAS respectively. Under general features is included a sketch of all physical phenomena relevant to VLBI observations, and the basic equations for the delay and delay rate observables in the commonly used computing model, the kinematic model. An analysis is given of the achieved level of precision of DEGRIAS in modelling the phenomena that constitute the "real world" of geodetic VLBI. The more detailed description in chapter 3 includes discussion of linearisation of the equations for delay and delay rate and a discussion on the rank deficiences of the system of normal equations in the Least Squares adjustment. Chapter 3 also presents the results of applying DEGRIAS to the VLBI data of ERIDOC (European Radio Interferometry and DOppler Campaign) and part of the MERIT (to Monitor Earth Rotation and Intercompare the Techniques of observation and analysis) Short Campaign.

The experience gained with this data analysis led to the consideration in chapter 4 of an optimized design for geodetic VLBI experiments. The SCHED-module of DEGRIAS generates a schedule of observations starting from visibility considerations for the sources and optimizing for slewing time. The design of an observing session also has to be optimized with respect to precision and reliability. The literature is mainly concerned with the precision of geodetic VLBI, hence in this study, much attention has been paid to its reliability. Simulation studies and analysis of real data has uncovered estimates of magnitudes of errors that may be present in individual observations, or in groups of observations, and which cannot be detected by statistical testing. Based on studies performed on the network designs for global networks from [Dermanis,1977], for the MERIT Short Campaign and for a possible European Geodynamics Network, the following conclusions have been reached concerning the design of an experiment:

1. The reliability is generally poor due to the large difference between the number of scheduled observations and the number of weighted observations in the final Least Squares fit; small errors may therefore have a relatively large impact on the final results for, for instance, station coordinates.
2. Low elevation observations (below about 10 degrees) should be excluded from the VLBI schedule since the magnitude of the correction for tropospheric refraction becomes less certain and since these observations are of poor reliability.
3. For accurate measurements, the operation of a network with more than two baselines (so that closed triangles can be formed) has the advantage of improved likelihood of error detection and is therefore to be recommended.
4. Furthermore, it is concluded that much can be gained from a careful design of the experiment with respect to precision and reliability, in particular when the recommendation is followed to observe for 48 hours instead of 24.

In chapter 5, the main computing models for geodetic VLBI are investigated. As discussed in chapter 2, modelling of nutation in the kinematic model is a troublesome aspect, together with refraction due to the wet component of the troposphere and to the dry component at low elevations, and instrumental effects. Ways of minimizing the risks of these errors have been sought by considering alternative computing models. The model with the least number of possible hypotheses for the description of the physical phenomena is the geometric model. This model makes use only of the simultaneity of measurements of several co-observing baselines. The ideosyncrasies of this model regarding precision and reliability are discussed. On practical grounds, an intermediate model, called short-arc computing model, is also presented, which models precession etc. only during short intervals of time. Computing results with the three types of models (geometric, short-arc, kinematic) are presented both for the European Geodynamics Network and for the MERIT Short Campaign.
It is concluded that the geometric model - although very attractive from a theoretical point of view - is hardly applicable in practice. The short-arc model, however, can be considered as a promising alternative to the common kinematic one.

In Part II, a general approach is studied to combine and compare two sets of 3-dimensional Euclidean coordinates for a number of stations. The differences in coordinates can, apart from their random character, be the result of either a systematic bias between two applied measurement techniques (intercomparison of techniques) or of a shift in position of one or more of the stations (deformation analysis). It is concluded that any comparison method should rest on a sound statistical basis. In chapter 6 an approach to intercomparison, based on the similarity transformation, is discussed which combines all the required qualities. The software developed for this approach (called FUSION) is also described in this chapter. It has been applied to analyse the differences between the Doppler and VLBI coordinates determined in the ERIDOC campaign, which were comparable at the 0.5 metre level. FUSION has also been applied to the European Geodynamics Network to establish what precision of measurement is required to detect possible (tectonic) motions of stations in the Mediterranean area reliably.

ACKNOWLEDGEMENTS

The research reported in this publication has been performed at the Delft University of Technology, Department of Geodesy, Geodetic Computing Centre (Laboratorium voor Geodetische Rekentechniek - LGR), Delft, and at the Netherlands Foundation for Radio Astronomy (Stichting Radiostraling van Zon en Melkweg - SRZM), Dwingeloo, under the financial support via grant 76-59 of the Netherlands Organization for the Advancement of Pure Research (Nederlandse Organisatie voor Zuiver Wetenschappelijk Onderzoek - ZWO), The Hague.

Further support is acknowledged from the Netherlands Geodetic Commission (Rijkscommissie voor Geodesie - RC), Delft, for travel and publishing funds and from the Royal Netherlands Institute of Engineers (Koninklijk Instituut Van Ingenieurs - KIVI), The Hague, also for granting travel funds.

To these organizations, but even more to all those individuals, too numerous to list them all here but not forgotten, who assisted me in some way during the research project, I am profoundly grateful.
I especially thank my supervisors Prof.Dr.Ir. W. Baarda and Prof.Dr. W.N. Brouw for the stimulating discussions, Prof.Dr.-Ing. J. Campbell and his VLBI group of Bonn University for their guidance and support, Prof.Dr.Ir. L. Aardoom, Dr. E. Raimond, Dr. A.R. Ritsema, Prof.Dr.-Ing. R. Rummel and Dr. R.T. Schilizzi for their comments on the manuscript and Graham Gee, Martin Jutte, Fred Pluijms and - last but not least - Tinie Visser for their help in preparing the final version of this publication.

TABLE OF CONTENTS

PART II. COMPARISON OF TECHNIQUES

PART III. CONCLUDING REMARKS

LIST OF TABLES

LIST OF FIGURES

PART I

GEODETIC VLBI

...Long baseline radio interferometry...
The field is also particularly attractive for graduate students who would not have to join the Navy to see the World !!

[Shapiro & Knight, 1969]

The solution of this complex of "shadow and substance" could only be found by a better operational definition of quantities, and consequently in a more precise analysis of the observational process. The latter becomes thus one of the basic thoughts of the new theory.

[Baarda, 1966]

Chapter 1

I N T R O D U C T I O N A N D S C O P E

Summary: This introductory chapter starts with a historical account of VLBI since its introduction in 1967. It then continues with a brief description of the VLBI concept and instrumentation. In section 1.4 the origin, aims and major constituents of the present publication are reviewed against, on the one hand, the background of the scientific objectives of geodetic VLBI (§1.2) and, on the other hand, the special "Delft" approach for point positioning which is a line-of-thought including some specific ideas and algorithms for the design and computation of geodetic networks. A guide for the reader is presented in §1.5.

1.1 VLBI, A BRIEF HISTORICAL ACCOUNT

Geodetic Very Long Baseline Interferometry (VLBI) is one of the few major world-wide positioning techniques with a non-military origin, and probably the most accurate one over large distances.

The technique originates from the field of radio astronomy. This is a relatively new science, especially in comparison to the traditional optical astronomy which is as old as the human race itself. The history of radio astronomy started accidentally in the early 1930's with the discovery by Karl Jansky of extra-terrestrial radio signals. After World War II a rapid development followed, aimed at the improvement of the quality of the observations, both in sensitivity and in angular resolution (the power to resolve neighbouring objects). The angular resolution of a receiver system is proportional to the ratio of the wavelength of the observed signal to the diameter of the receiving antenna. The study of an object at a (radio-) wavelength of 3 cm would therefore require a radio antenna of 10 km in diameter for the same resolving power as that of a 15 cm optical telescope. Such a construction is inconceivable.

As it was tried in the past for optical astronomy [Michelson,1890], the radio astronomers turned, to overcome this problem, to interferometry. With this concept two separate antennas with some kind of link between them are used to combine the signals received at two sites. In this case, the angular resolution is determined by the distance between the two antennas rather than by the size of any single antenna. The transmission of the signal from the one telescope to the other was first done by cable or radio link, a concept that was awarded the Nobel Prize for Physics in 1975 (Ryle and Hewish of Cambridge University). The separation, however, was limited to 50 km at most. This technique is called: CERI, which is an acronym for: Connected Element Radio Interferometry (Figure 1). The Westerbork Synthesis Radio Telescope (WSRT) is also based on this concept [Baars et al.,1973], [Bos et al.,1981].

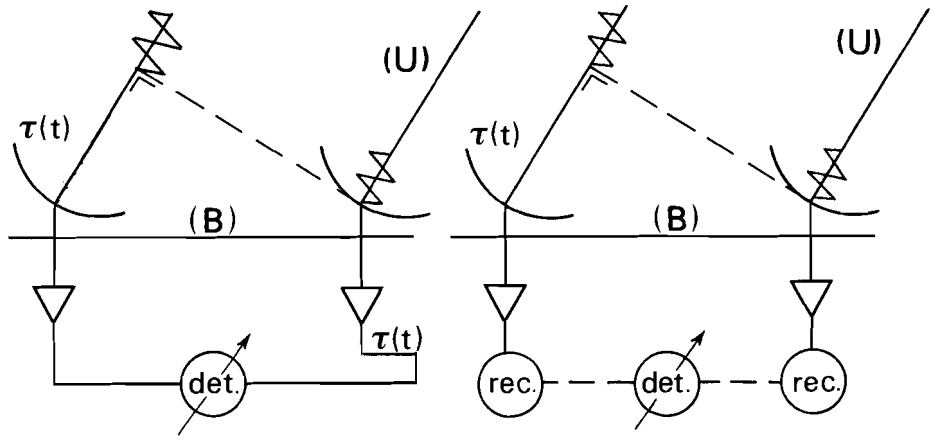

Figure 1: CERI and VLBI Concept

The need for a real-time link between the two telescopes of the interferometer was overcome by the introduction of very stable atomic clocks: VLBI was born. It is obvious that a better name for VLBI would have been: RIC, Radio-interferometry with Independent Clocks, because baseline length is not the essential feature, but independent registration of signals under the control of atomic clocks. They govern the recording of the radio signals on tape at the observatories, so that afterwards the observed data can be sent to a computing centre for further analysis by means of a correlation process. In this way the angular resolution of the astronomical observations was increased by a factor 100: from 0.1 arcsec (50 km baseline; wavelength 2.8 cm) to 0.001 arcsec (5000 km baseline), with the same point source sensitivity.

The first successful VLBI measurements at microwave frequencies were demonstrated in 1967 by two different groups: a Canadian team using an analog recording and processing technique [Broten et al.,1967] and researchers in the USA using a digital recording scheme [Bare et al.,1967], [Moran et al.,1967]. These measurements were primarily aimed at high-resolution mapping of sources.
At that time, the narrow recording bandwidth and the relatively small sizes of the available antennas limited the quality of the results. Later on, determination of accurate source positions (astrometry) and baseline components (geodesy) became possible when broader recorded bandwidths were feasible [Rogers,1970]. The precision of the measurements increased further as better atomic clocks became available and the integration time could be lengthened.

In view of the attainable high resolution, at present the most important astrophysical research by means of VLBI is concerned with:

a) the detailed mapping of compact radio sources in the nuclei of active galaxies and quasars, especially for the study of the physics of "jets". These are apparently directed streams of matter and energy from the centres of the objects. Their huge energy flux is probably connected with synchrotron radiation of relativistic electrons, trap-

ped in magnetic fields. In addition, separation velocities of radio features in these objects have been found which (seemingly) exceed the velocity of light;

b) the study of the strong compact OH and H_2O masers in our own galaxy. A maser source consists in general of 10 to 100 point sources in a relatively dense hydrogen area near a star. By repeated mapping of the relative positions of these components, the kinematics and characteristics of the maser can be determined.

For geodesy, aiming for one of its main tasks, i.e. the determination of the size and shape of the Earth ("geodetic mapping"), baseline length is bounded by the dimensions of the Earth by definition; see section 1.2. But even this baseline length is not enough for "radio astronomical mapping" of objects and proposals exist to build a telescope (QUASAT) orbiting the Earth [Schilizzi,1984], on the Moon or even at the opposite side of the Ecliptic [Schilizzi,1982] to increase the resolving power even further than the milliarcsecond level already obtained.

1.2 SCIENTIFIC OBJECTIVES OF GEODETIC VLBI

Geodetic VLBI is a pure geometric technique, i.e. it is not sensitive to the gravity field of the Earth (except for, often negligibly small relativistic effects), and yields therefore - by definition - no geocentric coordinates. On the other hand, however, the measurement concept is tied to a quasi-inertial frame of very distant and compact extra-galactic radio sources. In this coordinate system VLBI is able to measure baseline vectors (and their changes in time) between distant stations on Earth.

With this in mind, the primary scientific objectives of VLBI measurements for geodesy, geophysics and astrometry are the following; see also [Campbell,1982]:

a) defining a unified global reference frame, including the tie to a quasi-inertial coordinate system of distant radio sources in space-time of relativity, to satisfy the needs for geodetic, astrometric and navigational problems,

b) monitoring Earth tides, precession, nutation, polar motion and Earth rotation to enable a better understanding of the kinematics and dynamics of the Earth - Sun - Moon system and the structure of the Earth's interior,

c) determining plate motion and plate stability to improve the understanding of global plate tectonics,

d) investigating regional movements in order to provide input to an earthquake prediction programme,

e) enabling time transfer between remote atomic clocks, to ensure a high precision time definition on Earth and to study the effects of relativity.

The accuracy (both precision and reliability) required for these objectives are on the centimetre level over distances of up to 10,000 km. To reach this 10^{-9} relative accuracy goal is the unanimous aim of the world's geodetic VLBI-community for the 1990's.

1.3 CONCEPT OF THE VLBI TECHNIQUE

1.3.1 Introduction

Simply put, the application of VLBI for geodetic purposes consists of the following five phases, of which the first four are equivalent, though somewhat different in detail, for astrophysical VLBI:

1) experiment scheduling
2) observing session
3) correlation
4) fringe analysis
5) geodetic analysis.

The remainder of this study is completely devoted to phases 1) and 5). The geodetic analysis is concerned with the estimation and interpretation of station and source positions, polar motion and UT1 parameters, etc. from the observed data, in accordance with the objectives of geodetic VLBI mentioned in section 1.2; see chapters 2, 3 and 5. To perform this estimation in an optimal way, good scheduling of the VLBI experiment (phase 1) is required to arrive at an acceptable network design; see chapter 4.
As an introduction, therefore first the theoretical and instrumental concepts of the VLBI technique are reviewed. Most of the information presented here is taken from the following publications: [Thomas,1972], [Thomas,1981], [Campbell,1979b] and [Preuss,1984].

1.3.2 Equipment

The basic observational part of a VLBI configuration consists of two radio telescopes, two atomic clocks and two recording units (Figure 2).
This equipment is used to measure the primary geodetic observable: the time delay τ, which contains all the information for the geodetic analysis as it is dependent on the position of the telescopes, the position of the source, etc.. The time derivative of τ, called delay rate $\dot{\tau}$ is an independent second observable. Their value for each observation is derived via a correlation process. The correlator is located at a central institute, to which all recorded data are sent on magnetic tape.

Generally, the telescopes are steerable paraboloids with a diameter of more than 15m. In addition, NASA/JPL (Jet Propulsion Laboratory, California Institute of Technology) owns a few transportable antennas, especially designed for deployment in tectonically active regions, to be independent of the fixed locations of the large antennas.
The system temperature of the receiver system should preferably be below 150 K, to ensure a good signal-to-noise ratio (SNR).

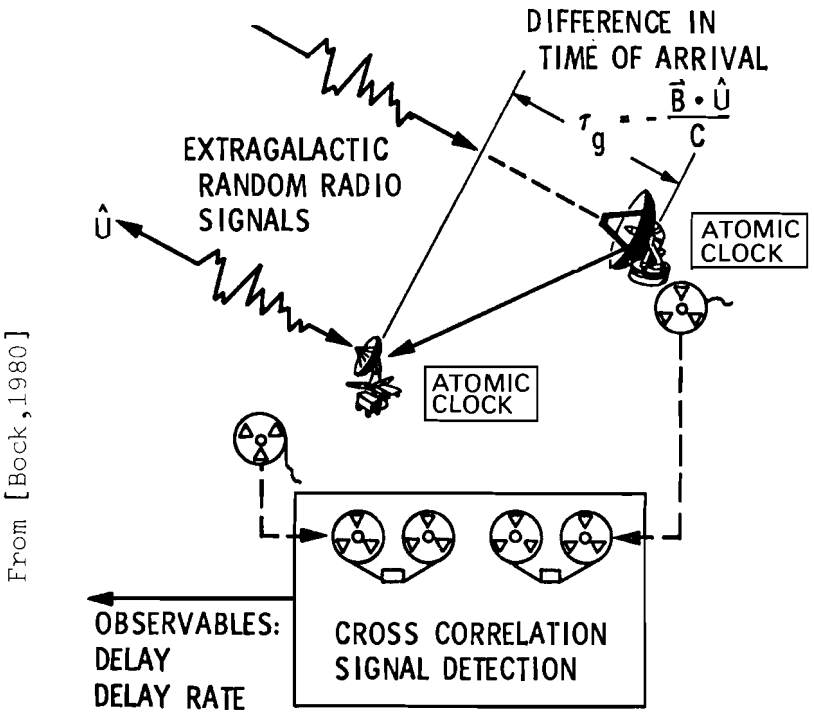

Figure 2: Basic VLBI Configuration

For geodesy, at present two observing wavelengths are in use. In the first place 6 cm observations are applied, mainly determined by the availability of many receivers for this wavelength at already existing radio astronomy observatories. In addition, a compromise is reached at this frequency between an increasing ionospheric refraction effect (on longer wavelengths) and an increasingly opaque troposphere (especially due to water vapour) on shorter wavelenghts. Second, for intercontinental experiments almost exclusively the combination of 3.8 cm (X-band) and 13 cm (S-band) is used. This dual frequency scheme offers the possibility of eliminating the influence of ionospheric refraction (§2.6.3).

It has been stated in §1.1 that the very stable atomic clocks make VLBI feasible. A rubidium standard can be applied, but most observatories possess the far more stable hydrogen maser; its relative frequency stability is around 10^{-14}.
This stability is in the first place required to achieve a sufficiently long coherent integration time for the received signals, including the time registration for the measured data. In fact, correlation of the two data streams is only possible during the interval that the two clocks of the interferometer have a relative phase variation with a standard deviation of less than 1 radian. A period (depending on source strength and system sensitivity) of about 5 minutes of observations yields one delay observable τ. This period is called a scan.

On the other hand, the clocks have to be stable with respect to one another for the duration of the entire VLBI campaign, as τ contains all relative variations of the clocks. Any variation must be modelled in the geodetic analysis phase and should therefore be rather smooth.

The recording units (terminals) for the data registration are based on broad bandwidth magnetic tape recorders. For the digital recording scheme (§1.1), the data consist of only the sign (one bit) of the voltage signal induced by the radiation field in the receiver. The process of determining this sign is indicated by (infinitely) clipping. Before clipping, the signal (in the GHz region) is heterodyned down by a series of mixers and filters to the region 0-B MHz (video band), where B is the system bandwidth. It follows from theory that for a digital recording scheme the signal must be sampled with (at least) the so-called Nyquist rate of 2*B [Van Vleck&Middleton,1966].
At present, two main types of recording systems are in use: the Mark-II system developed at the National Radio Astronomy Observatory (NRAO), USA, with a bandwidth of 2 MHz and the more advanced Mark-III system with a maximum bandwidth of 56 MHz, built by Haystack Observatory, USA. In view of its bandwidth, this system has a registration rate - with high demands for the quality - of 112,000,000 bits per second!

1.3.3 Basic Assumptions

To be able to extract a precise estimate for the delay τ from the signals recorded in the above way, the following conditions should be met:

a) The (stochastic) process of the radio waves is stationary and ergodic, which means that the statistical properties of the signal are not affected by a time shift and that an individual portion of the signal must take on all possible values of the signal with the same probabilities as those of the ensemble, which is a collection of portions of the signal, so that time averaging can be applied [Lynn,1973].

b) The system bandwidth is much smaller ($< 1/10$) than the observing frequency (to allow correlation for an "almost monochromatic" signal).

c) The source should be very distant from the interferometer to be able to receive plane wavefronts; in addition, the source should be small in diameter, i.e. smaller than the resolution of the interferometer, to define a "point-source", which is important for geodetic applications; see §2.4.1.

1.3.4 Correlation and Fringe Analysis

Under the suppositions of §1.3.3, the group delay observable τ and its time derivative $\dot{\tau}$ are estimated in two steps: (a) correlation and (b) fringe analysis.

The first step is done via a special purpose computer which performs the actual correlation in combination with a microcomputer for some additional computations. Their main tasks are the following:

First of all, a model delay τ_m is computed on the basis of a coarse model for the geometry of the interferometer. Using this model delay the bit streams of the two tapes are approximately aligned via the time-tags on the tape and a buffer. As time is measured in bits, τ_m can at best be rounded off to the nearest bit: τ_{mr}. Because the latter is constant over some time, many bits (some millions) can be shifted at once.
In addition, it should be noted that the rotation of the Earth yields a differential Doppler effect in the correlated signal due to the different velocities of the stations. On practical grounds, i.e. for a better data compression, a model value for this so-called fringe frequency is computed on the basis of a priori data such as station coordinates. By multiplying one of the bitstreams with the model fringe frequency wave, the Doppler effect is compensated for and after multiplication of the two bitstreams in an EXCLUSIVE OR operation (1*1=1, 0*0=1, 1*0=0, 0*1=0) the so-called "stopped fringes" are found which have a frequency in the 10 mHz region (Figure 3).

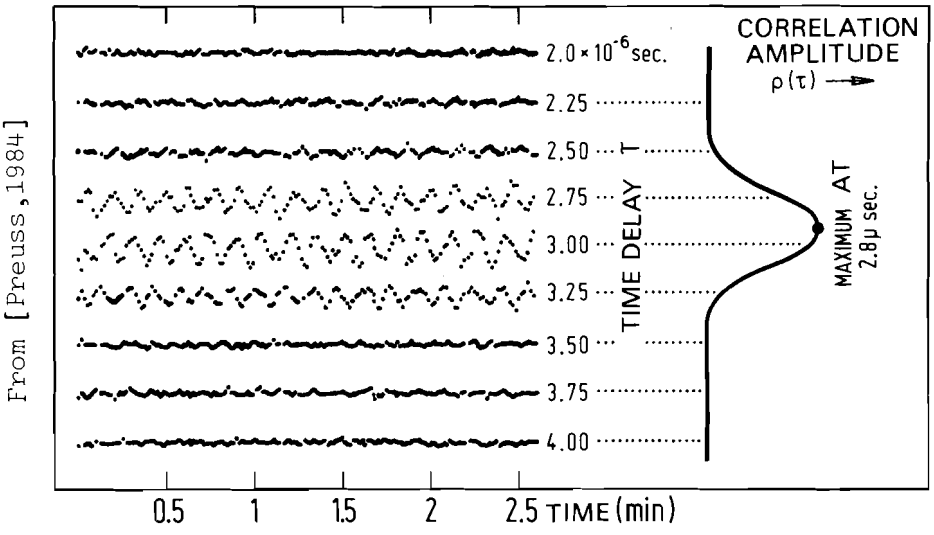

Figure 3: Stopped Fringes and Correlation Amplitude

Actually, the correlator computes the real and imaginary parts of the complex correlation function, by multiplying the second bitstream twice: once with the first bitstream multiplied by the sine wave component of the model fringe frequency, and once with the first bitstream times the cosine component. Afterwards, fringe amplitude and fringe phase can be computed from these two components. This is done simultaneously for a number of delay channels centered around the expected value of τ_m.
For the Mk-II system 32 delay-channels are used at intervals of 250 ns (Figure 3).
In this way, the cross-correlation function of the two recorded signal voltages V_i and V_j is determined as an average over a typical integration time of 2 seconds, being a function of time (a scan lasts about 5 minutes) and delay channel, according to:

$$\rho_{ij} = \langle V_i' . V_j' \rangle \; / \; \mathrm{sqrt}(\langle V_i . V_i' \rangle * \langle V_j . V_j' \rangle) \qquad (12.1)$$

The analysis is then continued on a general purpose computer with the fringe analysis phase in which the following basic observables are determined: fringe amplitude, fringe phase and BSA-delay (bit shift alignment). If the coarse delay model were perfect, the correlation maximum would be exactly in the central delay channel and the observed resulting fringe frequency would be zero. Hence a Fast Fourier Transform (FFT) is used to analyse the fringes via some trial values and to find estimates for amplitude and frequency of the stopped fringes. This FFT is at the same time used for signal detection ("search for fringes") if e.g. the source is very weak and it is not certain that the amplitude will be above the SNR thres-hold. For "monochromatic" fringes with constant amplitude, the location of the peak of the FFT (a sin(X)/X function) yields a direct estimate for the BSA-delay (Figure 3).

The correlation and fringe analysis procedure is now only possible at a few institutes; for Mk-III these are: CalTech, Haystack and Bonn. At present, a maximum of four stations can be correlated simultaneously.

1.3.5 Ancillary Techniques

The previous section presents a rather simplified version of reality. Here the complications in the entire process will be briefly summarized. To start with, most sources are extended on intercontinental baselines. Astronomers use an FFT of the sampled fringe amplitude to derive a source map. This process is called aperture synthesis. To account for extended sources, inversely, in geodetic experiments an FFT is needed in the fringe analysis phase to refer the measurements to one common point (§2.4.1).

Secondly, the fringes mentioned in §1.3.4 are not at all monochromatic with a constant amplitude; all sorts of phase excursions are present due to changing atmospheric conditions and other imperfections of the coarse model. The phase is then derived for several sub-intervals and combined afterwards. This process is called phase tracking. Combination of this phase tracking process for two separate bands which are observed simultaneously some tens of MHz apart, yields an estimate for the more accurate BWS (Bandwidth Synthesis) delay, which, however, is contaminated by 2π ambiguities (§2.3.3).

In addition, some corrections to the signal must be made. The phase calibration corrects the signal (for each BWS channel) with a phase value derived from a calibration signal of a tone generator. This calibration tone is injected in the natural source signal near the front of the instrumentation. Measured changes in the tone at the end of the instrumentation indicate phase fluctuations e.g. due to cable wrap.
Furthermore, dual frequency observations may be applied to account for refraction effects by charged particles.

From this (incomplete) list it is clear that correlation and fringe analysis is not a simple task. It may take five times longer than the

observing session itself. The bottleneck in the application of VLBI is therefore at present this correlation/fringe analysis phase.

1.4 BACKGROUND AND PHILOSOPHY OF THIS STUDY

In spite of - or perhaps even because of - the vast experience that the Delft Department of Geodesy had gained in the field of satellite geodesy (stellar triangulation and satellite laser ranging), before 1977 there was no active participation in geodetic VLBI, although some theoretical studies had been performed; e.g. [Aardoom,1972]. In that year a project was started supported by the Netherlands Foundation for Radio Astronomy (SRZM) to inventory all relevant aspects of VLBI for geodetic applications by a literature search; furthermore, the formulation of the computing model for geodetic VLBI observations was investigated, including an analysis of the accuracy. The results of this study were published as a graduate thesis [Brouwer&Visser,1978].

In this thesis much attention was given to the application of the "Delft" approach for point positioning to the VLBI case. This approach is a line-of-thought, mainly developed by Baarda at the Geodetic Computing Centre (LGR) of the Delft Department of Geodesy and consists of a number of ideas and algorithms formulated for a coherent and complete description of the tools for the design and computation of geodetic networks [Brouwer et al., 1982].
Four main items can be discerned in this approach (for a more detailed description one is referred to chapter 4):

a) the use of quantities derived from the observations which are invariant under a similarity transformation to build a computing model that describes only the shape of a geodetic network as defined by these observations. In this way one can define an adjustment problem with condition equations for an observed network using dimensionless quantities (e.g. distance ratios) [Baarda,1966].

b) the proper introduction of a coordinate system for the description of the relative positions of geodetic stations by means of a so-called S-basis. The latter consists of a selected number of non-stochastic quantities equal to the number of parameters in the similarity transformation for the dimension of the problem (1-D: 2, 2-D: 4 and 3-D: 7). The relation between different S-bases is defined by an S-transformation [Baarda,1973].

c) the analysis of the precision of a network design (even before the network is actually measured!) by the comparison of the a posteriori variance/covariance matrix (naturally, excluding the a posteriori variance factor) with an artificial criterion matrix by means of the generalized eigenvalue problem [Baarda,1973], [Alberda,1974].

d) the application of advanced statistical testing procedures for the detection of possible erroneous observations or deficiencies in the formulation of the computing model for the Least Squares adjustment problem. Use is made here of the w-test (one-dimensional) and the F-test (multi-dimensional) on the basis of the B-method of testing.

This method makes errors equally detectable by both types of tests. An analysis of the reliability of a network design can be made by computing the sizes of the by the above tests "marginally detectable errors" in the observations and by computing the impact of "marginally undetected errors" on the final results such as station coordinates [Baarda,1968], [Baarda,1972]. This reliability analysis can again be performed before the measurements are actually taken.

Because the above mentioned thesis could not cover all aspects, the study needed a follow-up. This follow-up started in 1979 as a joint research project of LGR and SRZM and was sponsored by the Netherlands Organization for the Advancement of Pure Research (ZWO). The fields of attention and the main objectives of the present research were originally formulated as:

1) First of all, an internal analysis was required of VLBI as a geodetic measuring technique, including all physical phenomena which may influence VLBI observations, such as precession, Earth tides and refraction effects. By this analysis, a consistent description should be found for possible computing models.

2) Then a software package should be built, capable of performing simulation computations for an investigation of the precision and reliability of the final results and consequently of an optimal design of a VLBI campaign. The software, however, should also be capable of analysing and adjusting observed VLBI data, albeit not necessarily to the ultimate accuracy level (1 cm).
This task is in complete agreement with the "Delft approach".

3) The theory and software developed according to the above reasoning should furthermore enable combination and comparison of geodetic VLBI measurements with observations using networks of different types (e.g. satellite laser ranging) or times (previous campaigns). This was required as it was felt that the ultimate accuracy for world-wide geodetic positioning could only be reached by a combination of several techniques. Intercomparison experiments based on a sound statistical basis are therefore of paramount importance.

4) As the proof of the pudding is in the eating, also a cooperation was foreseen in the organization and measurement (with the Dwingeloo/Westerbork telescopes, operated by SRZM) of one or more geodetic VLBI campaigns to verify the results of the above developments not only with simulations but also with "real" observations.

1.5 GUIDE FOR THE READER

From the previous section the following keynotes for the present study can be discerned:

- description of physical phenomena influencing VLBI
- study of computing models for VLBI data reduction
- development of software for geodetic VLBI analysis
- precision/reliability analysis for VLBI network design
- comparison of VLBI with other measurement techniques

- cooperation in a VLBI experiment

This publication clearly contains these items and is divided into three parts.

After the introductory chapter, Part I, devoted to geodetic VLBI in general, continues in chapter 2 with the description of all physical phenomena relevant to geodetic VLBI and their implementation in the DEGRIAS software package (an acronym for: DElft Geodetic Radio Interferometry Adjustment System). In chapter 3 this is followed by an overview of its idiosyncrasies and by some analysis results of two multi-station geodetic VLBI campaigns with the help of DEGRIAS. These campaigns are: ERIDOC (European Radio Interferometry and DOppler Campaign) and the Short Campaign of MERIT (to Monitor Earth Rotation and to Intercompare the Techniques of observation and analysis). Comparable studies about these subjects can be found in the literature so that no originality is claimed for this work. The discussions on the accuracy and validity of the models for the physical phenomena in the sections 2.3 to 2.7 may be felt to be of some use, however.
New results are presented in chapters 3 and 4, where the "typically Delft" criteria for the precision and reliability of geodetic networks are used for the optimisation of a VLBI experiment design. For these computations a module of DEGRIAS is applied to the compilation of an observing schedule for a VLBI experiment.
In chapter 5, the last chapter of Part I, the "standard" computing model for the adjustment of VLBI data as described in §2.2 (called the "kinematic" model, because it makes use of the rotational motions of the Earth) is compared with two alternatives. The first alternative model applies only the simultaneity of the observations of several baselines and is therefore called the "geometric" model. This model formulation is a typical example of a description according to the main items a) and b) of the "Delft approach" (§1.4).
In the second alternative model only knowledge about the rotation vector of the Earth during a short time interval is used. It is therefore denoted as the "short-arc" computing model. The advantages and disadvantages of the three types of models are discussed and compared, using both simulation computations and actually observed VLBI data.

Part II comprises the comparison of 3-D Euclidean coordinates of a network resulting from different measurement campaigns. A general approach for this problem is derived using invariant quantities and especially tailored testing procedures (§1.4) to search for possible errors in the two sets of coordinates. The resulting software package is applied to the data of ERIDOC. In this campaign simultaneous measurements of VLBI and satellite Doppler took place, so that the last objective of the research project, an active participation in actual measurements, was met as well.

Part III concludes this study with a summary of the results and some recommendations for future research and activities.

Chapter 2

S T A N D A R D C O M P U T I N G M O D E L

Summary: In this chapter an outline is presented of all physical phenomena relevant to VLBI observations. As an introduction, this review starts with the basic observation equations for delay and delay rate observables in the commonly used computing model: the kinematic model. It is called "kinematic" because use is made of algorithms which parameterize the rotational motions of the Earth. Next, a discussion about reference frames is presented. The physical phenomena themselves are discussed in sections 2.3 to 2.7, grouped under the following headings: instrumentation, astronomy, physics, propagation and geophysics. The discussion includes a brief general description of the phenomenon with its magnitude in relation to VLBI observations and presents also the formulae used in the implementation of the software package developed for the geodetic analysis of VLBI observations, called: DEGRIAS, DElft Geodetic Radio Interferometry Adjustment System. To conclude, an assessment is given in §2.8 of the model accuracy of DEGRIAS, also in relation to bottom-line results which are ultimately achievable by geodetic VLBI.

2.1 INTRODUCTION

In chapter 1 it is sketched out how VLBI-observations are made and how one arrives at the two basic geodetic observables: delay and delay-rate. The observed value for any of the measured delays or rates depends on a long list of physical phenomena, even ignoring noise introduced by the correlation and fringe analysis itself.
The following, non-exhaustive list presents a general idea of the types of phenomena, here arranged into five possible categories. The indication S(=signal) or N(=noise) shows whether, in the general case, the phenomenon should be regarded as an interesting subject of study for geodetic VLBI according to the objectives of §1.2, or just as "noise" present in the measurement process:

1. Instrumentation	
- clock behaviour	S
- antenna structure	N
2. Astronomy	
- source positions	N
- precession/nutation/aberration	S
3. Physics	
- gravitational deflection	N
4. Propagation effects	
- tropospheric refraction	N
- ionospheric refraction	N

5. Geophysics
   - antenna positions S
   - Earth rotation/polar motion S
   - Earth tides S

It is the task of the geodetic analysis phase (§1.3.1) to extract information about the desired aspects of these phenomena. The observed value for delay and delay rate is a function of the "physical reality", here called the "real world". As this real world is too complex to be described for computations, it is approximated by a parameterized "computing model world". Next, a choice should be made of which model-parameters will be determined from the observations (such as station coordinates) and which parameters can be regarded as known a priori (e.g. gravitational deflection).
From analyses one has an idea how well the "real world" and "model world" match; this can be expressed by a standard deviation, e.g. 1 cm. By taking more observations than required, one arrives, via linearisation and application of the algorithm of Least Squares adjustment (LSQ) [Baarda,1967] to the model formulae, on the one hand at estimated values for the model parameters and on the other hand at contradictions between "real world" observations and "model world" formula system. Application of statistics will then tell whether the discrepancy is at the assumed level of the above standard deviation, taking into account also the precision of the observations.

The "model world" used in this study is described in sections 2.3 to 2.7 and introduced in §2.2. Together with the LSQ algorithm, these models are implemented in the DEGRIAS software package, short for "DElft Geodetic Radio Interferometry Adjustment System" (§3.2), which forms the basic instrument with which all computations and analyses in the remainder of this publication were done.

2.2 BASIC OBSERVATION EQUATIONS AND FRAMES

From chapter 1 it follows that the observed delay is defined as:

$$\tau = t_b - t_a \qquad (22.1)$$

where t_a = the time of arrival of the wave at antenna "a" as measured by the clock at that site and t_b = the time of arrival of the wave at antenna "b" as measured by the clock at site "b".
On the other hand, in the most simplified form, the model delay τ' is described by the inner product of the baseline vector (B) and the unit vector in the direction of the source (U), divided by the velocity of light c (Figure 4):

$$\tau' = -((B) \cdot (U)) / c \qquad (22.2)$$

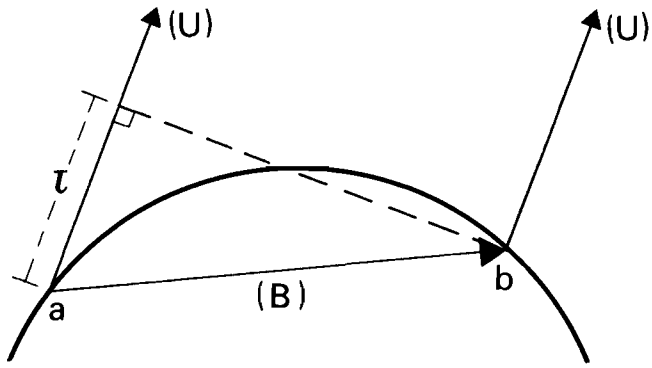

Figure 4: Basic VLBI Triangle

The negative sign follows from the fact that τ is defined as positive if the wave arrives later at station b than at station a. Note here that the distance to the (extra-galactic) objects is some Gigalight-years. The difference of direction to the source at the stations over a 10,000 km baseline is therefore about 10^{-19} radians, so that condition c) of §1.3.3 (plane wavefronts) is always met.
Combining (22.1) and (22.2) one finds the following relation between the "real world" observation and the "model world" formula system as the observation equation of the LSQ adjustment:

$$\tau = -((B) \cdot (U)) / c \qquad (22.3)$$

Differentiation with respect to time (assuming constant c) yields the observation equation for delay rate:

$$\dot{\tau} = -((\dot{B}) \cdot (U) + (B) \cdot (\dot{U})) / c \qquad (22.4)$$

Vectors are described with respect to a frame of reference. For simplicity, now some approximations are introduced and it is stated that in very general terms, the coordinate frame used in DEGRIAS is a geocentric, left-handed and Earth-fixed system, with its Z-axis through the pole and Greenwich as zero-meridian. The frame has been chosen left-handed in accordance with the BIH (Bureau International de l'Heure) definition, which counts longitude positive towards West [BIH,1978]. If the positions of the stations a and b are then represented by (Xa,Ya,Za) and (Xb,Yb,Zb) and the position of the source by its Greenwich Hour Angle GHA and its declination δ, the observation equation (22.3) becomes:

$$\begin{aligned} \tau = -(& (Xb-Xa) * \cos(GHA) * \cos\delta \\ & +(Yb-Ya) * \sin(GHA) * \cos\delta \\ & +(Zb-Za) * \sin\delta) / c \end{aligned} \qquad (22.5)$$

and similarly for (22.4), where ($\dot{U}$), which includes e.g. the effect of the motions of precession and nutation, is assumed equal to zero and the change in station coordinates only the result of Earth rotation:

$$\dot{\tau} = ((Xb-Xa) * \sin(GHA) * \cos\delta - (Yb-Ya) * \cos(GHA) * \cos\delta) * \Omega / c \qquad (22.6)$$

Ω denotes here d(GHA)/dt, which is the angular velocity of the Earth. The equations (22.5) and (22.6) are very simplified versions of the real situation. As an introduction to the detailed description, a general preview of the "real world" is presented first, starting with frames.

The most preferable coordinate system for VLBI is an inertial one. This is a frame that is not subject to any acceleration, e.g. by rotations. The frame with its origin in the solar system barycentre and its axes tied to a number of sufficiently distant radio sources can be regarded as quasi-inertial, because there will not be any noticeable change in the position of these sources at some Gigalightyears away, as seen from the solar system barycentre. Apparent changes will therefore be completely due to motions of the telescopes with respect to the frame, i.e. motions of the Earth as a whole, or deformations of the Earth.

The actual computing reference frame used in DEGRIAS, is a quasi-geocentric one. Its scale is determined by adopting a numerical value for the speed of light; its origin is defined by choosing such X,Y and Z-coordinate values for one VLBI station that the origin lies close to the geocentre; the Z-axis is parallel to the instantaneous (slowly moving) spin axis of the Earth and the X-axis points at the Greenwich meridian; the Y-axis completes a left-handed Euclidean triad.
Figure 5 shows how this computing frame is an intermediate between the quasi-inertial system and the Conventional Terrestrial System (CTS). The latter is Earth-fixed and barycentric, so that the coordinates of stations are not affected by motions of the Earth as a whole, and has CIO (Conventional International Origin) as Z-axis and Greenwich as conventional meridian. The Greenwich meridian is defined as its average over the period 1900-1905, by the assigned astronomical longitudes of the time observatories (around 50) participating in the work of the BIH (Bureau International de l'Heure). CIO is fixed, by definition, via the five observatories of the IPMS (International Polar Motion Service) located at the 39.8 degrees parallel, as the mean pole position over the period 1900-1905. The relation between instantaneous (slowly moving) spin axis and CIO is described by polar motion.

The Z-axis of the quasi-inertial system used for the source positions is defined as perpendicular to the mean equator of the reference epoch 1950.0. The X-axis points at the intersection of this mean equator with the mean ecliptic of 1950.0, the first point of Aries, or equinox. The Y-axis completes a right-handed frame. This system is "operationally defined" by the FK4 catalogue.
The reduction of the inertial position of a source in the 1950.0 system to a position in the computing frame is performed via precession, nutation, Earth rotation, etc. (see Figure 5).

In addition to these rotations of the station configuration as a whole, the observations are also affected by changes in the geometry of the station configuration. The motions of the telescopes (pointing) make their phase centres - to which the observations are referred - move, while the effect of e.g. Earth tides also modifies the geometry.

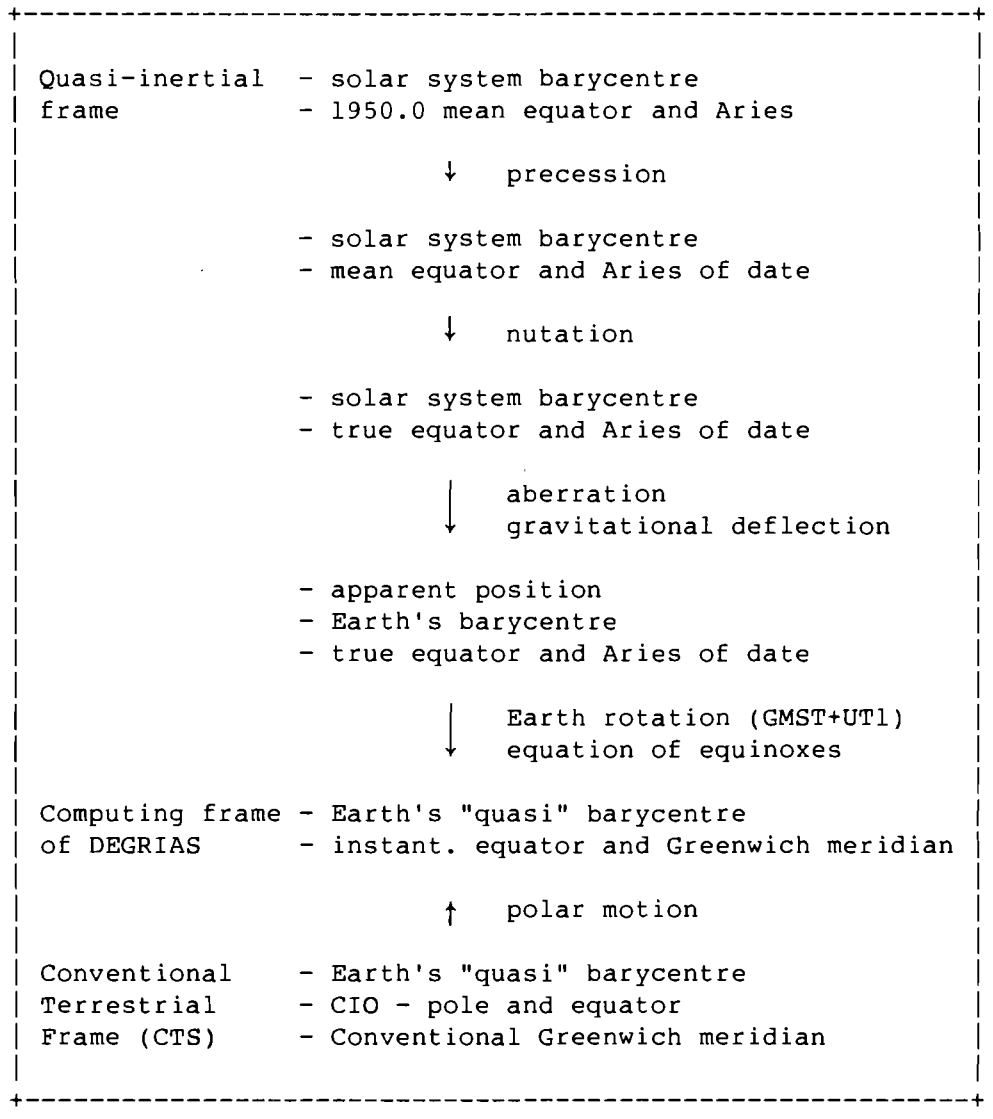

Figure 5: VLBI Reference Frames

In addition, diurnal aberration (also called retarded baseline effect), annual aberration, as well as gravitational deflection by the Sun and planets change the apparent positions of the sources. Furthermore, the effect of atmospheric refraction is a considerable source of error and finally, the equipment, e.g. the clock, is not perfect either.
In this way (22.3) is extended to the complete formulation of the kinematic computing model of (22.7). It is denoted by kinematic, because use is made of algorithms describing the rotational motions of the Earth.

$$
\begin{aligned}
\tau = & - ((W)*(B) \cdot (S)*((N)*(P)*(U) + (A) + (G))) / c \\
& + \tau_{RTB} \\
& + \tau_{TRO} \\
& + \tau_{CLO} \\
& + \tau_{ANT} \\
& + \tau_{TID} \\
& + \tau_{ION} \\
& + \tau_{AMB}
\end{aligned}
\qquad (22.7)
$$

(B) and (U) are now the station and source position vectors respectively at the reference epoch. (W) is the polar motion matrix from the CIO pole to the instantaneous spinning pole and (S) is the diurnal rotation matrix around this spin axis. (P) and (N) are the precession and nutation matrices. (A) is the annual aberration vector and (G) includes the effect of gravitational deflection. The seven correction factors are for: retarded baseline, tropospheric refraction, clock and other instrumental effects, antenna motion, Earth tides, ionospheric refraction and 2π ambiguities in the delay observations due to BWS (§1.3.5). These are the items that are taken into account in DEGRIAS. The question of what effects/parameters are estimable by an LSQ fit is left open at this stage.

Similarly, the observation equation for the delay rate observable is found from (22.4), assuming that all changes of (U) and (B) are the result of the afore mentioned effects:

$$
\begin{aligned}
\dot{\tau} = & -((\dot{W})*(B) \cdot (S)*((N)*(P)*(U) + (A) + (G))) / c \\
& -((W)*(B) \cdot (\dot{S})*((N)*(P)*(U) + (A) + (G))) / c \\
& -((W)*(B) \cdot (S)*((\dot{N})*(P)*(U) + (\dot{A}) + (\dot{G}))) / c \\
& -((W)*(B) \cdot (S)*((N)*(\dot{P})*(U) + (\dot{A}) + (\dot{G}))) / c \\
& + \dot{\tau}_{RTB} \\
& + \dot{\tau}_{TRO} \\
& + \dot{\tau}_{CLO} \\
& + \dot{\tau}_{ANT} \\
& + \dot{\tau}_{TID} \\
& + \dot{\tau}_{ION} \\
& + \dot{\tau}_{AMB}
\end{aligned}
\qquad (22.8)
$$

An extensive discussion of these phenomena will be presented in the following sections.

2.3 THE "REAL WORLD" FOR VLBI - INSTRUMENTATION

2.3.1 Clock Behaviour

From the definition of the observed delay (22.1), it is immediately obvious that time is the most important factor in the VLBI process and

that the only physically realized time (apart from the Earth's rotation itself) is the one kept by the atomic clocks at both ends of the interferometer. It is through the stability of these clocks that the user can correlate the recorded data and can relate all observations to one common reference: the length scale.
In the simple computing model of §2.2 it is assumed that the two clocks of the interferometer are running at exactly the same rate and that their "zero point of time" is also the same; see formula (22.1). In reality, this is evidently not the case for the long term (= the duration of a VLBI campaign) clock behaviour. It is in fact the major deviation (up to milliseconds!) from the simple model.
It appears however, that relative rate-changes of two clocks are very smooth and that they can easily be modelled by a polynomial or a sine wave. Therefore, in DEGRIAS the following clock model is assumed:

$$\tau_{CLO} = T0 + T1*t + T2*t^2 + T3*\sin(T4*t+T5) \qquad (23.1)$$

where t is the time measured in days from an arbitrary starting point, such as the epoch of the first observation, or, as in DEGRIAS, 0h UTC of a specific day. The coefficients Ti (i=0,...,5) denote: clock offset, clock drift, curvature and amplitude, frequency and phase of the sine wave, respectively.
For many VLBI campaigns, only a second order, or even a first order polynomial will suffice. To decide what parameters to include, judicious inspection of the observations is of paramount importance. The same holds for the possibility of accounting for clock breaks or jumps. In DEGRIAS, more than one clock function can be introduced: one valid before the event of the break and one after that.
For the delay rate observable the time derivative of (23.1) is required:

$$\dot{\tau}_{CLO} = T1 + 2*T2*t + T3*T4*\cos(T4*t+T5) \qquad (23.2)$$

It is obvious that the clock drift T1 yields an offset in the delay rate observations. Due to the set-up of the correlator [Thomas,1972] it is possible that during the correlation process an additional, artificial rate offset will be introduced. With this in view, DEGRIAS allows one to estimate a delay-rate offset independent of the clock drift in the delay observations.

Discussion

So far, no statement has been made about the origin of the deviations. It is clear that in the first place the mere stability of the instrumental design of the clock and the diurnal variations (likely to be sinusoidal!) in temperature and other environmental factors give rise to these effects. It should be added, however, that generally not only the behaviour of the atomic clock itself will have to be modelled but also the changes in electric path length in cables, mixers, antenna offset (§2.3.2), etc.; see §2.3.4 for further reference.

Hydrogen masers are claimed to be stable to a factor of at least 10^{-13} over the required time span. Therefore, the use of such a device, combined with a judicious choice for the clock parameters in the DEGRIAS LSQ adjustment, will yield a remaining uncertainty in the clock behaviour (including all instrumental clock-like errors) of less than one or two centimetres in the measured delay.

In the above, only the long term stability of the clock is discussed. For the other time frame of interest, the short term stability that enables coherent correlation over periods of several minutes, one is referred to §1.3.2.

2.3.2 Antenna Motion Correction

The receiving antennas for VLBI are steerable radiotelescopes of 10 to 100 metres in diameter, continuously following a radio source in its track through the sky. This so-called pointing can be done by rotating the telescope about two axes. One of these axes is motionless with respect to the ground (the fixed axis); the other rotates about the first. At first sight it is inconceivable that it is possible to do cm-geodesy (or, as in the case of the WSRT, even sub-mm "geodesy" [Schut,1983]) with these structures. In particular, the position of the electrical phase centre of the receiver can hardly be determined at this level.

The problem is solved, however, by the fact that the telescope is always pointed at the source and some components of the correction are thus constant. In the case of two intersecting axes, this is obvious: the appropriate choice for the baseline reference point is their point of intersection. For every observation the path length between the phase centre and the point of intersection should be subtracted from the measured delay. This path length, however, is (nearly) constant. For the construction of the Wettzell telescope, for instance, it was demanded that the point of intersection of azimuth, elevation and bore sight axis stayed within a sphere of radius 0.3 mm during the measurements and that the maximum change in the flight time of the signal via main reflector, subreflector, cassegrain focus to point of intersection was 4 mm [Nottarp&Kilger,1982]. As one knows that the extra path length is constant, the true value is not of any concern to the geodesist. It will simply be absorbed in the clock offset (§2.3.1).
Only in cases where VLBI is used to synchronize clocks, as for the Deep Space Network (DSN) with spacecraft missions, these constants (including cable delays etc.) must be measured and removed from the observations.

If the two axes do not intersect but have an offset for constructional reasons, the correction is somewhat more complicated. Being orthogonal, the second axis moves in a plane perpendicular to the fixed axis. In this case, the point of intersection of this plane and the fixed axis is the baseline reference point.
From Figure 6 it is clear (again because the telescope is always pointed at the source) that the so-called "antenna motion correction" τ_{ANT} for the delay observable is simply the component of the axis offset D in the direction of the source. If ψ is the angle between the direction of the source and the direction of the fixed axis, one finds:

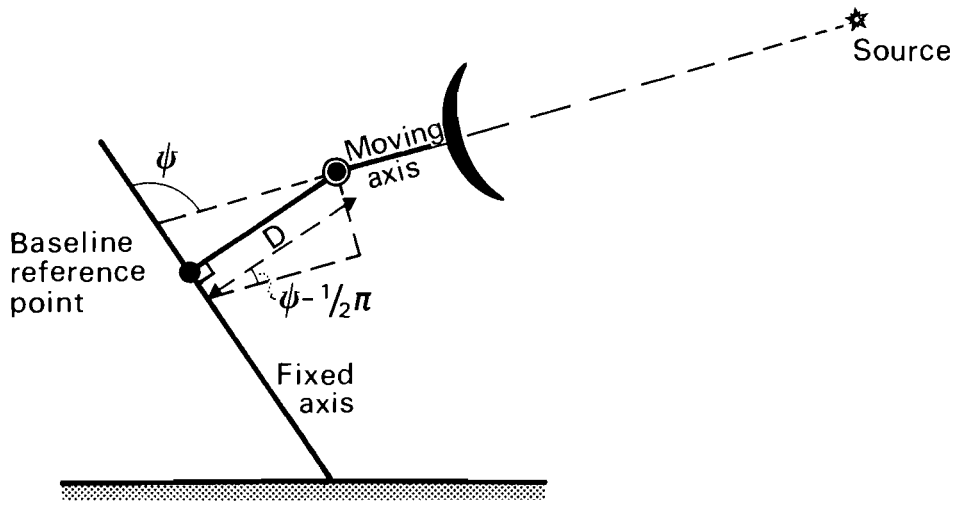

Figure 6: Telescope Axis Offset

$$\tau_{ANT} = D * \cos(\psi - \tfrac{1}{2}\pi) \qquad (23.3)$$

For an equatorially mounted telescope, $\frac{1}{2}\pi - \psi$ equals the declination δ of the source. For an Altazimuth mount, ψ is the zenith angle μ at which the source is observed, so that the following antenna motion corrections are derived:

$$\begin{array}{lll} \text{Equatorial mount} & : & \tau_{ANT} = D * \cos \delta \\ \text{Altaz mount} & : & \tau_{ANT} = D * \sin \mu \end{array} \qquad (23.4)$$

The above formulae are implemented in DEGRIAS. In the direct(ly differentiated) formula for delay rate (§3.1), however, no antenna motion correction is included.

Discussion

The axis offset D is known to a high degree of accuracy. Its magnitude is generally not very large. One of the largest is at the WSRT, where D=4.95 metres. Therefore, these formulae are correct to the millimetre level, even noting that ψ is not corrected for refraction, although the true pointing is required [Ma,1978].
A more complicated matter concerns the change of the telescope geometry due to wind loading, etc.; for this, one is referred to §2.3.4.

2.3.3 BWS - Ambiguities

When the Bandwidth Synthesis technique (BWS) is used to improve the precision of the delay observations (§1.3.5), [Rogers,1970], [Thomas,1981], an ambiguity in the delay observable may occur, which is inversely proportional to the spanned bandwidth. This is because the correlation function peaks at every integer number of (heterodyned) wavelengths.

For the ERIDOC campaign for instance (§3.6), two bands of 2 MHz each were recorded, 40 MHz apart. The ambiguity spacing is then 1/(40 MHz) = 25 ns. Consequently, the observation can be wrong by M*25 ns, with M a positive or negative integer.
In DEGRIAS this is corrected by an automatic inspection of the computed minus observed (C-O) values of the observations before the LSQ adjustment, which reduces the C-O values to the range of $+\frac{1}{2}$*25 ns to $-\frac{1}{2}$*25 ns.

Discussion

These ambiguities in no way reduce the final accuracy. It is only a tedious task to remove them from the observations in cases where no good a priori data (e.g. for station coordinates) are available. Especially in the case of an active ionosphere or in the case of a significant clock drift, some iterations will be needed to eliminate all ambiguities. Evidently, delay rate observations are not influenced by this phenomenon.

2.3.4 Miscellaneous

In addition, four instrumental effects are mentioned here that are not taken into account in DEGRIAS, viz.: phase shifts, antenna geometry, telescope pointing and system noise.

Discussion

It has been stated in §2.3.1, that the observed delay is corrupted by unknown and unstable phase shifts due to instrumentation. Such phase shifts degrade the accuracy of the measurements and are caused by e.g.: temperature variations in cables, twisting of cables, short period variations in amplifiers and filters, the influence of magnetism on the hydrogen maser, etc..
Most of these instrumental effects can be removed by using phase-calibration (§1.3.5). This also allows an absolute calibration of the interferometer phase, i.e. separation of "real" clock offset and cable delay so that clock synchronization is possible [Clark et al., 1979]. The magnitude of these phase effects may correspond to several centimetres in measured delay, but in general [Schuh,1984] their rate of change over a day is smooth. With this in view, as yet no provisions are made in DEGRIAS to include phase-calibration data; phase shifts are therefore absorbed in the estimated clock function. This will leave a residual error at the cm level (cf. §2.3.1).

The entire geometry of the antenna [Greve,1981] is of course not so rigid as presumed for the simple correction for antenna motion (23.4). Especially for older telescopes, the point of intersection of the axes is not very stable and may vary by up to 5 cm. This is due to thermal expansion, wind loading and antenna flexure, poorly adjusted bearings, focal changes, etc.. The only real remedy is to perform a special calibration of the dish using collimation procedures. The effect can then be reduced to 0.5 cm [Trask et al.,1982].

The telescope's pointing always deviates slightly from the direction to the source. If in addition the effect of multiple reflections on the

antenna [Trask et al.,1982] is included, phase errors may arise. Since this is only a second order effect, the errors are likely to be only several picoseconds.

And last but, in the VLBI case, also least, there exists the contribution of system noise. This includes the stochastic spread of the observations as computed from the stability of the clock, the local oscillator, the gain of the receiver, the size of the dish, the integration time, the bandwidth in use, the strength of the source, etc. in the ideal case. Formal reasoning [Brouwer&Visser,1978] for a standard configuration would lead to a negligible contribution to the total error budget of Mk-III equipment of a few picoseconds. This number is the bottom-line value for the error budget of geodetic VLBI that could be reached if one could govern all other factors. This, however, will hardly be the case; see sections 2.8 and 3.2.

2.4 THE "REAL WORLD" FOR VLBI - ASTRONOMY

2.4.1 Source Structure

For geodetic VLBI it is preferable to have point sources as emitting objects. Only then is one automatically assured of the necessary precondition (§1.3.3): equivalent phase-trains of the wave in all directions (= at all telescopes). An object is a point source if its size is significantly smaller than the resolution of the interferometer. Most of the relatively strong and usable sources, however, show structure on the milliarcsecond scale, which is the resolution of a 5000 km baseline at 2.8 cm (§1.1). If the structure is asymmetric, an apparent change of position occurs because the resolution changes due to a varying baseline component perpendicular to the source direction over the day. [Thomas,1972] shows that the cross-correlation expression for an extended source is identical to that of a point source if the Fourier transform of the brightness distribution (a source map) is taken into account. A correction for source structure is therefore possible, but, rarely applied.

Discussion

A source structure on the milliarcsecond scale means details of 30 lightyears in size for objects at distances of 2500 Megaparsec, or of almost 2 metres on the Moon. Resulting deviations in baseline length may reach a few millimetres on intercontinental baselines. Experimental results on 4C39.25 [Trask et al.,1982] seem to confirm this figure.

2.4.2 Precession

The gravitational forces of Sun, Moon and planets on the non-spherical Earth whose symmetry axis is not perpendicular to the ecliptic, yield smooth gyroscopic motions of the mean poles of equator and ecliptic, known as general precession. The period of these motions is 25100 years. They can be specified by three rotations (ζ_o, z and θ) with respect to the frame at the reference epoch (1950.0 for DEGRIAS).

The complement of ζ_o is the right ascension of the ascending node of the mean equator of date in the 1950.0 coordinate system and z+90° is the right ascension of the ascending node of the mean equator in the coordinate system defined by the mean equator and mean equinox of date. θ is defined as the inclination of the mean equator of date with respect to the 1950.0 equator, so that the precession matrix (P) is a function of three orthogonal rotation matrices with respect to the Z-, the Y- and again the Z-axis (see Figure 7):

$$(P) = R_z(\zeta_o) \cdot R_y(-\theta) \cdot R_z(z) \qquad (24.1)$$

Formulae for the computation of ζ_o, θ and z are obtained from Newcomb's tables [Newcomb,1895a,1895b,1897] and can be found in [Astron. Eph.Supp.,1974]. There, a precessional constant of 5025.64 arcseconds per century at the beginning of the tropical century 1900 is adopted. The formulae are a function of time T_t which is measured from 1950.0 (Julian date 2433282.423) and expressed in tropical centuries of 36524.21988 ephemeris days.

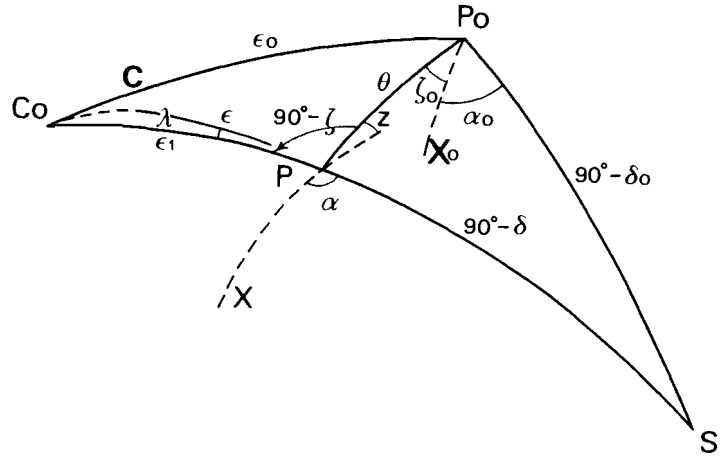

Figure 7: Polar Diagram of General Precession

The position of a source at a specific moment - denoted in rectangular coordinates (U',V',W') - referred to the mean equinox of date, can then be expressed as a function of coordinates (U0,V0,W0) at the initial epoch (1950.0-equinox) by:

$$\begin{pmatrix} U' \\ V' \\ W' \end{pmatrix} = \begin{bmatrix} Uu & Vu & Wu \\ Uv & Vv & Wv \\ Uw & Vw & Ww \end{bmatrix} \cdot \begin{pmatrix} U0 \\ V0 \\ W0 \end{pmatrix} = (P) \cdot \begin{pmatrix} U0 \\ V0 \\ W0 \end{pmatrix} \qquad (24.2)$$

where the coefficients Uu etc. can be derived by evaluating formula (24.1) [Astron.Eph.Supp.,1974].

For the delay rate observable $\dot{\tau}$ (22.8), the time derivative of (P) is required. Taking into account the small size of the angles ζ_o, θ and z, one obtains for the coefficients of ($\dot{P}$) in radians per sidereal day [Brouw,1973]:

$$\begin{aligned} \dot{U}u &= \dot{V}v = \dot{W}w = 0 \\ \dot{V}u &= -\dot{U}v = -6.102*10^{-7} \\ \dot{W}u &= -\dot{U}w = -2.654*10^{-7} \\ \dot{W}v &= \dot{V}w = 0 \end{aligned} \qquad (24.3)$$

Discussion

Small secular changes in the coefficients of the formulae for ζ_o, z and θ, amounting to about 0.001 arcsec for a century are neglected here; therefore the above quoted formulae are internally accurate to a level of below one milliarcsecond and may yield a baseline length error of less than one mm for a 5000 km baseline.

However, following a resolution of the 1976 General Assembly of the IAU (International Astronomical Union), the system of astronomical computations was changed on 1 Jan. 1984 [Kaplan,1981]. The new reference epoch is now J2000, realized by the FK5-catalogue, with a precessional constant of 5029.0966 arcsec per century at epoch time. This means a value of 5026.767 at epoch 1900, so that an increase of somewhat more than 1.1 arcsec per century is found. This number represents the "orientation error" of the old system, which is several metres on Earth scale in an absolute sense, but corresponds internally to 3 mm for a VLBI campaign duration of two days.
In view of the present aim of DEGRIAS (§1.4) the new J2000 system has not yet been implemented, but as a first step interpolated "new" values for the constants can be used in the old system; e.g. for ζ_o:

$$\begin{array}{cccc} \text{old} & + & \text{interpolation} & = \text{new} \\ 2304.948 & + & 2304.948/5025.64*1.127 & = 2305.465 \end{array} \qquad (24.4)$$

The basic angles then become:

$$\begin{aligned} \zeta_o &= 2305.465 * T_t + 0.302 * T_t^2 + 0.018 * T_t^3 \\ z &= \zeta_o + 0.791 * T_t^2 \\ \theta &= 2004.704 * T_t - 0.426 * T_t^2 - 0.042 * T_t^3 \end{aligned} \qquad (24.5)$$

This interpolation corrects most of the orientation discrepancy, but subsequent implementation of the J2000 system is of course of paramount importance for further work with DEGRIAS.

2.4.3 Nutation

Precession is defined in the preceding section as the long period motions of the mean poles of the Earth's equator and the ecliptic. In addition, nutation is the somewhat irregular motion of the true pole around the mean pole, due to the periodic motions of Sun and Moon around the Earth. The main period is about 19 years and has an amplitude of 9.210 arcseconds: the nutation constant. The shift from the mean pole to the true pole of the equatorial system can be expressed by corrections to the ecliptic longitude ($d\psi$) and to the mean obliquity ($d\varepsilon$) via three rotations; cf. Figure 7:

$$\begin{pmatrix} U'' \\ V'' \\ W'' \end{pmatrix} = (N).\begin{pmatrix} U' \\ V' \\ W' \end{pmatrix} = R_X(-\varepsilon_o).R_Z(d\psi).R_X(\varepsilon).\begin{pmatrix} U' \\ V' \\ W' \end{pmatrix} \qquad (24.6)$$

where ε is the true obliquity of the ecliptic, which equals $\varepsilon_o + d\varepsilon$ with ε_o the mean obliquity of date. The nutation matrix (N) relating the true position of date of a source in rectangular coordinates (U",V",W") to the one at the mean position (U',V',W') is then, with the usual first order approximation:

$$(N) = \begin{bmatrix} 1 & -d\psi * \cos\varepsilon & -d\psi * \sin\varepsilon \\ d\psi * \cos\varepsilon & 1 & -d\varepsilon \\ d\psi * \sin\varepsilon & d\varepsilon & 1 \end{bmatrix} \qquad (24.7)$$

The element $d\psi * \cos\varepsilon$ is called: the equation of equinoxes (EQE) and is equal to the difference between mean and true right ascension of a body on the equator; before 1960 it was therefore called: nutation in right ascension. It is used to convert mean sidereal time to apparent sidereal time (§2.7.1).

To compute $d\psi$ and $d\varepsilon$ Woolard's expansion for the rigid Earth is followed [Woolard,1953]. For $d\varepsilon$ this yields a goniometric series of 69 terms and for $d\psi$ of 40 terms, with as arguments functions of l, l', D, Ω and F, the so-called fundamental arguments. These quantities denote respectively: mean anomaly of the Moon and that of the Sun, mean elongation of the Moon from the Sun, the longitude of the ascending node of the lunar orbit on the ecliptic, and L-Ω, where L is the mean longitude of the Moon. Formulae for these quantities, including ε_o, can be found in [Astron.Eph.Supp.,1974]. In these formulae all motions with a period of more than five days are included. They are polynomials in T, where T is measured in Julian centuries of 36525 days from epoch 1900 Jan. 0.5 ET, so that T_t (§2.4.2) and T are related as:

$$T_t = 1.0000213590 * (T-0.5) - 0.000008597 \qquad (24.8)$$

These functions of fundamental arguments can be combined, so that $d\psi$ and $d\varepsilon$ are computed in DEGRIAS according to the following series' expansion (in symbolic notation), where Ai,..,Gi are constants that can be found in [Brouw,1973]:

$$\begin{aligned} d\psi &= \Sigma_i\ (Ai+Ci*T)*\sin(Ei+Fi*T+Gi*T^2+Hi*T^3) \\ d\varepsilon &= \Sigma_i\ (Ci+Di*T)*\cos(Ei+Fi*T+Gi*T^2+Hi*T^3) \end{aligned} \qquad (24.9)$$

Analogous to the precession matrix (§2.4.2), for the direct formula of the delay rate observable (§3.1) the time derivative of (N) is required. One finds with some approximation, in radians per sidereal day:

$$(\dot{N}) = \begin{bmatrix} 0 & -d\dot{\psi}*\cos\varepsilon & -d\dot{\psi}*\sin\varepsilon \\ d\dot{\psi}*\cos\varepsilon & 0 & -d\dot{\varepsilon} \\ d\dot{\psi}*\sin\varepsilon & d\dot{\varepsilon} & 0 \end{bmatrix} \qquad (24.10)$$

with

$$\begin{aligned} d\dot{\psi} &= 1.07788*10^{-3} * \Sigma_i\ Fi*(Ai+Bi*T)*\cos(Ei+Fi*T+Gi*T^2+Hi*T^3) \\ d\dot{\varepsilon} &= -1.07788*10^{-3} * \Sigma_i\ Fi*(Ci+Di*T)*\sin(Ei+Fi*T+Gi*T^2+Hi*T^3) \end{aligned} \qquad (24.11)$$

Discussion

For nutation, even more than for precession, the implementation in DEGRIAS of the J2000 system is mandatory, since the old formulation is based on an undeformable Earth. The new model (IAU 1980 resolution) is based on [Wahr,1979,1981], and includes the effect of a solid inner core and a liquid outer core and some parameters for the elasticity. The series' development includes 106 terms. But even now the end of improving the nutation theories has not been reached because all additional knowledge of the Earth's interior will improve the nutation formulae. This is important because where the new precessional constant merely changes baseline orientation, the new nutation series - due to their short period changes - lead to more complex alterations. Actually, nutation was denoted as the second major error source for geodetic VLBI at the October 1984 Crustal Dynamics Project working meeting [Aardoom,1984].

The reference axis for the Woolard model is the instantaneous rotation axis of the rigid Earth [Mueller,1980] whereas the new reference pole, denoted by Celestial Ephemeris Pole, is selected so that there are no diurnal or quasi-diurnal motions of this pole with respect to either a space-fixed or an Earth-fixed coordinate system [Kaplan,1981]; see also §2.7.4 for diurnal polar motion.
In Woolard's expansion all terms larger than 0.0002 arcseconds are included, which would mean a formal error level of below 1 cm. Considering, however, the computed deviation of instantaneous spin axis and conventional slowly-moving spin axis of more than 50 cm [Ma,1978], and in view of the difference between the rigid and the deformable model, a residual error of around 4 cm baseline length is estimated to be possible for intercontinental baseline lengths. In an absolute sense, this

means that the "orientation error" of DEGRIAS with respect to the J2000 definition, could be up to a factor of 10 higher.

2.4.4 Aberration

The apparent direction to a distant source is constantly changing due to the finite speed of light combined with the motion of the Earth-based observer. This effect is called aberration. Two types of aberration are of interest: "annual aberration" due to the rotation around the Sun and "diurnal aberration" due to the Earth's diurnal rotation. In a VLBI-context the latter is called retarded baseline correction and will be treated in a separate section (§2.7.2).

The annual aberration is caused by the actual motion of the Earth with respect to the centre of gravity of the solar system. This is a complicated motion, because of the interplay of Sun, Moon and planets according to Kepler's laws of motion. The general formula for aberration is:

$$\sin(d\theta) = \sin(\theta - d\theta) * V / c \qquad (24.12)$$

with V the scalar velocity of the centre of mass of the Earth, c the speed of light (here by IAU-definition for the 1950.0 system: 299,792.5 km/s), θ the angle between the direction of motion (apex) and the (geometric) source position (Figure 8) and $d\theta$ the apparent change in direction. Linearized, this yields [Woolard&Clemence,1966]:

$$d\theta = \sin\theta * V / c \qquad (24.13)$$

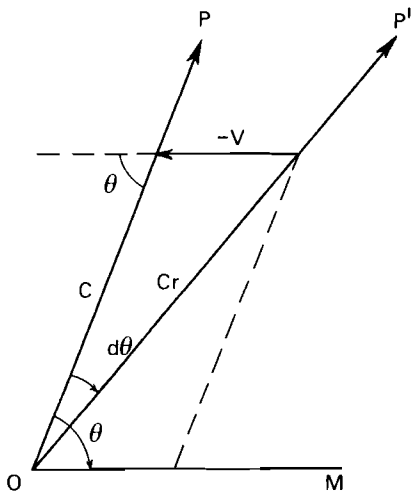

Figure 8: Aberration Diagram

The maximum $d\theta$ (θ is 90°), 20.496 arcseconds, is the aberration constant. Usually the velocity vector is computed by evaluating the ephemeris of Sun, Moon and planets from a dataset (PEP-tape = Planetary Ephemeris Program), but in DEGRIAS the closed model of [Gubanow,1973] is used which contains the most important influences, having fitted a time series of 51 terms to the PEP-data. The formulae of this model describing the velocity vector are of the form [Brouw,1973]:

$$\begin{aligned} \dot{U}_a &= \Sigma_i \, (X0i+X1i*T) * \sin(P0i+P1i*T+P2i*T^2) \\ \dot{V}_a &= \Sigma_i \, (Y0i+Y1i*T) * \cos(P0i+P1i*T+P2i*T^2) \\ \dot{W}_a &= (\dot{V}_a * \sin\varepsilon + A*\cos(B+C*T)) \,/\, \cos\varepsilon \end{aligned} \qquad (24.14)$$

The velocity vector is in metres per second with T and ε as defined in §2.4.3; X0i, X1i, Y0i, Y1i, P0i, P1i, P2i, A, B and C are constants.
From the Taylor-expansion (24.13) of the aberration formula it can be seen that the apparent position (U,V,W) can be computed from the true position (U",V",W") of the source by:

$$\begin{pmatrix} U \\ V \\ W \end{pmatrix} = \begin{pmatrix} U" \\ V" \\ W" \end{pmatrix} + \begin{pmatrix} \dot{U}_a \\ \dot{V}_a \\ \dot{W}_a \end{pmatrix} / c \qquad (24.15)$$

For the direct formula of the delay rate observable (§3.1), the time derivatives of (24.14) are needed. In the same symbolic notation as above one finds (linear approximation; in km/s/sidereal day; D and E are constants):

$$\begin{aligned} \ddot{U}_a &= D * \Sigma_i \, (P1i*(X0i+X1i*T)*\cos(P0i+P1i*T+P2i*T^2)) \\ \ddot{V}_a &= E * \Sigma_i \, (P1i*(Y0i+Y1i*T)*\sin(P0i+P1i*T+P2i*T^2)) \\ \ddot{W}_a &= \cos\varepsilon * \ddot{V}_a \end{aligned} \qquad (24.16)$$

Up to 1st Jan. 1984 the so-called E-terms - for elliptical aberration - were sometimes included in the 1950.0-positions of the sources. These E-terms describe the aberration effect due to the non-circularity of the Earth's orbit (second order effect). They vary only very slowly over the centuries for any given source and their (U,V,W)-components are a linear function of T [Brouw,1973]. If such a factor were included, the E-terms should be removed from the 1950.0-positions before applying the above calculation routine.

Discussion

The linearization via (24.13) causes second order terms of less than 0.0015 arcseconds to be neglected. This means a contribution to the er-

ror budget for baseline length of some centimetres on a 5000 km baseline.

In DEGRIAS the new J2000 data for aberration will have to be implemented, but here no such fundamental changes are required as for nutation, only an update to currently-known values. This will bring the error budget down to below 1 cm.

2.4.5 Miscellaneous

In the above, the source position was expressed in rectangular coordinates or, equivalently, in right ascension α and declination δ . Obviously, these coordinates require a frame of reference. Two aspects are of interest here: the definition of the frame and some additional time-dependences of the position: proper motion and parallax, which is the apparent change due to the Earth's rotation around the Sun.

Discussion

All commonly used VLBI point sources are extra-galactic at distances of up to 10 Gigalightyears. Even travelling at the speed of light, this would mean a proper motion of 0.02 milliarcseconds per year, which is negligible. The same holds even more strongly for parallax.

The 1950.0 system is defined as a (quasi-)inertial reference frame. Via precession, nutation and aberration, this system is made "operational" for DEGRIAS (Figure 5). This is an easy and correct way but not the best. For an alternative, a computing frame in the Space-Time sense of special relativity which includes all aberration effects, one is referred to §2.5.3.
In addition, it can be stated that in principle the coordinate values of the sources in the 1950.0 system can be defined by fixing three of them: e.g. two declinations and one right ascension. This is not how geodetic VLBI measurements are actually tied to this system. Usually only the right ascension of 3C273-B is constrained in the LSQ fit. This procedure is further pursued in §3.3.

2.5 THE "REAL WORLD" FOR VLBI - PHYSICS

2.5.1 Velocity of Light

The unit of time is defined as the time required for 9,192,631,770 cycles of the transition between the two hyperfine levels $F=4, m_F=0$ and $F=3, m_F=0$ of the fundamental state $^2S_{1/2}$ of the atom of caesium-133 in zero magnetic field as observed by a physical clock at the mean position and velocity of the Earth in a heliocentric reference frame: the SI-second. This time is maintained as International Atomic Time (TAI) by some primary caesium-standards, referred to sea level [BIH,1978]. The speed of light in vacuo is defined as: 299,792.458 km/s. From these two numbers the unit of length can be inferred.

Discussion

In a VLBI experiment, the time second is physically realized by the atomic clocks at both ends of the interferometer. The time function (23.1) models deviations of the second clock with respect to the "base"-clock. The next step is then to declare this time frame equal to the SI-second, to be able to take the adopted value for the speed of light for the conversion to metres. Consequently, the clocks have to be stable to at least a factor of $3*10^{-12}$ (which is 1 mm on Earth scale) in a kind of "absolute" sense. This causes no real difficulties, using hydrogen masers.

Since the speed of light is a fundamental constant, by definition no error can be present in its value. In this way it is a good candidate to serve as one of the seven quantities to define the reference frame: three rotations, three translations and the scale (§1.4).
One immediately sees, however, from formulae (22.3) and (22.4) that the speed of light "c" serves as a scaling factor between the measured quantities and the scale of the reference frame. It can therefore act as an unknown parameter in the LSQ adjustment, if other quantities serve as reference frame defining values; see further §3.3. Although this sounds awkward, it is not, in view of the fact that the number of 299,792.458 has once been determined with an accuracy of several metres per second and therefore leaves an uncertainty of about 5 cm in the size of the Earth due to the scale definition. Here even the question of how to go from the measured delay via the propagation effects (§2.6) to a distance in vacuo, is not considered.

2.5.2 Gravitational Deflection by the Sun

According to Einstein's theory of General Relativity, the gravitational field of the Sun deflects the radio waves, resulting in an apparent change in the position of the source. The magnitude of this change depends on the angular separation of the observed source from the centre of the Sun, as seen from the position of the observer. The magnitude of the deviation is 0.09 arcseconds for an angular distance of 5°. At the Sun's limb, this increases to 1.8 arcseconds, and even at a distance of 90° the value is still 4 milliarcsec, certainly not negligible!

In Appendix A an algorithm for computing the approximate apparent position of the Sun in the true equatorial frame of date is given. This position is denoted by the vector (Us,Vs,Ws). Now the apparent angle of deflection $\Delta\phi$, radially outward from the Sun, can be computed. In DEGRIAS the general formulae, also valid for bodies within the solar system, are implemented.

Define: β = the angular geocentric separation of the source from the Sun
Re = the distance from the Earth to the source
Rq = the distance from the Sun to the source
γ = gravitational deflection parameter
= 1 for Einstein, and 0 for Newton
GS = the heliocentric gravitational constant
and: X1 = cotan β (25.1)
X2 = (-Re + Re*cosβ) / (Re*sinβ)

Then [Misner et al.,1970]:

$$\Delta\phi = ((1+\gamma)*GS) / (Re* \sin\beta * c^2) * (X1 / \sqrt{1+X1^2} - X2 / \sqrt{1+X2^2}) / (1 + (Re/Rq)) \qquad (25.2)$$

Now the apparent position unit vector (U) of the source can be corrected for the Sun's gravitational deflection to (U)' by a rotation over angle $\Delta\phi$ in the plane defined by the position vectors of Sun and source, as:

$$\Delta\phi' = \Delta\phi / (1 + Re/Rq) \qquad (25.3)$$

$$\begin{pmatrix} U' \\ V' \\ W' \end{pmatrix} = \begin{pmatrix} U \\ V \\ W \end{pmatrix} - \Delta\phi'/\sin\beta * \begin{bmatrix} \cos\beta * \begin{pmatrix} U \\ V \\ W \end{pmatrix} + \begin{pmatrix} Us \\ Vs \\ Ws \end{pmatrix} \end{bmatrix}$$

In DEGRIAS the distances to all sources are set to 10 Megaparsec. If this and the values for γ, GS, c and Re are substituted in (25.1) and (25.2), one arrives at the more familiar formula [Kaplan,1981]:

$$\Delta\phi = 0.00407 * (1+\cos\beta) / \sin\beta \qquad \text{(arcsec)} \qquad (25.4)$$

Discussion

In the computation of the Sun's position (Appendix A), the secular terms in the orbital elements of the Sun have been neglected. The apparent latitude has been set equal to zero and also the effects of nutation and aberration have been neglected. In addition, the correction is not computed in DEGRIAS for the moment that the ray is at the point of closest approach to the Sun, which may be 8 minutes before or after the time of observation. All these effects amount to a position uncertainty of around 0.01 degrees in the Sun's position. At 1° from the Sun this uncertainty yields an error of 0.005 arcseconds in the angle $\Delta\phi$. This is generally sufficient, since a source at one degree from the Sun will rarely be observed.
In addition, it should be noted that when source coordinates are estimated in the adjustment, the major part of any error in the correction will be absorbed in the estimates for α and δ, and will thus not influence the baseline results. This is because the Sun's position changes only by 1° per day and the effect is therefore almost constant for a given source during one VLBI campaign.

No time derivatives of the Sun's gravitational deflection are computed for the delay rate observable in DEGRIAS. Only if numerical differentiation is applied (§3.1) is the effect accounted for.

2.5.3 Special Relativity

Although not applied in DEGRIAS, it should be stated that the solar system barycentric coordinate system at a certain epoch would be the most favourable computing reference frame for VLBI, since it is the nearest to the truly inertial frame (§2.2). VLBI has access to this inertial frame via the fixed directions to quasars. In this frame, VLBI data can also easily be combined with e.g. spacecraft tracking results.
The time definition belonging to this system is the coordinate second, denoted by TDB, "Barycentric Dynamical Time". Because the terrestrial clocks are not at rest with respect to this frame of reference, in the absence of a gravitational field, special relativity demands a time correction according to the Lorentz transformation [Russell,1977]:

$$t' = c / \mathrm{sqrt}(c^2-V^2) * (t - V*X/c^2) \qquad (25.5)$$

where V is the velocity of the clock with respect to the frame and X its position. Here t' is expressed in TDT, "Terrestrial Dynamical Time", which is TAI (§2.5.1) + 32.184 seconds. The latter correction is to make TDT agree with the old definition of Ephemeris Time. The transformation from TDT to TDB has annual, monthly and diurnal terms due to the three major motions of the Earth: Earth/Moon system around the Sun, Earth around the Earth/Moon barycentre and the Earth's rotation. These terms are approximately sinusoids with amplitudes [Kaplan,1981]:

annual :	1.6	milliseconds (10^{-3} / year)
monthly :	± 10	microseconds (10^{-5} / month)
diurnal :	± 1	microseconds (10^{-6} / day)

The flight time of the signal between two telescopes is 0.04s at most. Therefore, the maximum change of the annual term is $2*10^{-12}$ s over this interval, and for the monthly term: $5*10^{-14}$ s, which can be neglected. The diurnal term, however, yields changes of $5*10^{-11}$ or 0.05 ns, which is well within the scope of the VLBI-accuracy and can be approximated by (25.5) as:

$$t'-t = -((\dot{r}) \cdot (R)) / c^2 \qquad (25.6)$$

with r as the solar system barycentric position of the Earth's centre and R as the geocentric position of the clock.
If the deviations of the clock (§2.3.1) are described by a first order polynomial, the complete expression for the transformation from measured atomic time t' at telescope "a" to coordinate time t is:

$$ta = ta' + 32.184 + ((\dot{r}).(Ra)) / c^2 - T0a - T1a * (t-t0a) \qquad (25.7)$$

The observed value of the delay is:

$$\tau(t) = tb(t+ \tau_g) - ta(t) \qquad (25.8)$$

with τ_g is the geometric model delay (§2.2) and

$$(B(t)) = -[(r(t))+(Ra(t))) + ((r(t+\tau_g))+(Rb(t+\tau_g))] \qquad (25.9)$$

Now using the expansions

$$\begin{aligned}(R(t+\tau_g)) &= (R(t)) + (\dot{R}(t))*\tau_g + \tfrac{1}{2}\ldots\tau_g^2 + \ldots \\ (r(t+\tau_g)) &= (r(t)) + (\dot{r}(t))*\tau_g + \tfrac{1}{2}\ldots\tau_g^2 + \ldots\end{aligned} \qquad (25.10)$$

these formulae can be combined in a relativistic computing approach [Robertson,1975] for the delay observable:

$$\begin{aligned}\tau(t) = \tau_g &- (\dot{R}(t)) * (rb(t)-ra(t)) \\ &-((\dot{R}(t).rb(t))+((\dot{R}(t)).(\dot{r}b(t))) * \tau_g \\ &- T0a - T1a*(t-t0a) + T0b + T1b*(t-t0b+\tau_g)\end{aligned} \qquad (25.11)$$

Differentiating with respect to the time kept at station "a" yields in the same way a formula for the delay rate. It should be noted that by the inclusion of the time derivatives ($\dot{R}$) and ($\dot{r}$), the effects of annual (including elliptical) aberration and retarded baseline are implicitly included.

Discussion

In the above a tacit assumption is made. The formulae are derived via the Lorentz transformation and therefore in the absence of gravitational mass. Consequently, the changing gravitational potential of Sun and Moon and also of the Earth itself (including tides), has been neglected; in view of the distance to the Sun, however, this is justified. For further information, one is referred to [Robertson,1975] who derived the formulae starting from Einstein's weak field equations and to [Fujimoto et al.,1982] for a complete discussion.
The described approach is not followed in DEGRIAS. The effect of the above approximation, including the discrepancy between Euclidean and relativistic addition is less than 1 cm.

2.5.4 Miscellaneous

In addition to the gravitational deflection by the Sun, also the gravitational deflection by the planets and by the Earth itself is noted.

Discussion

Jupiter, the most massive planet, has a gravitational constant (or mass) that is one thousandth of that of the Sun. Due to its smaller diameter (71000 km) and its larger distance from the Earth, the angle source-Earth-Jupiter can be much smaller than for the Sun, as low as 0.0043 degrees. This results in a maximum deflection of 0.1 arcseconds! However, more than 2 degrees away from Jupiter the correction is less than 0.2 milliarcseconds. This is neglected. Also the corrections due to the other planets are neglected as these are even smaller.

On the other hand, the effect of the gravitational field of the Earth itself as regards gravitational deflection is of order 10^{-11}, which means a centimetre or so for the longest baselines. This is also neglected.

2.6 THE "REAL WORLD" FOR VLBI - PROPAGATION

2.6.1 Dry Troposphere

The displacement polarization of all air molecules in the neutral atmosphere causes a phase change in the propagation of electromagnetic waves and therefore an additional path length, known as the "dry term" of tropospheric refraction. For average tropospheric conditions at sea level, its value is 231 cm in the zenith direction.
This path excess (τ_{zd}) is scaled to other zenith angles using:

$$\tau_d = \tau_{zd} * FZ \qquad (26.1)$$

For the multiplication factor FZ, two models are implemented in DEGRIAS as a function of the zenith distance:

$$FZ1 = 1/\cos\mu \qquad (26.2)$$

$$FZ2 = 1/(\cos\mu + 0.00143/(\cot\mu + 0.0445)) \qquad (26.3)$$

with

μ = zenith angle of the observation
= $\arccos(\sin\phi * \sin\delta + \cos\phi * \cos\delta * \cos(LHA))$
ϕ = geodetic latitude of the station
LHA = local hour angle of the source (§2.7.2)

The first model is the strict cosecant law which is valid for a plane-parallel atmosphere, thus neglecting the curvature of the Earth. It will therefore only be used for simulation studies. The second formula is the so-called Chao-model [Chao,1970], which is a modified cosecant law with numerical constants derived from a best fit solution of a ray-tracing using the model through a standard troposphere. The differences between these models and several other models are reviewed in Appendix B. From data presented there, it can also be seen that a path excess of 2 metres in the zenith direction becomes approximately 20 metres at 5 degrees elevation. After the clock offset (§2.3.1), it is therefore the largest correction of the computing model (22.7).
For the delay rate observable the time derivatives of (26.1) and (26.2) are computed as (Ω is the rotation rate of the Earth):

$$\dot{FZ}1 = \Omega * \cos\phi * \cos\mu * \sin(LHA) / (\cos^2\mu) \qquad (26.4)$$

$$\dot{FZ}2 = \Omega * \cos\phi * \cos\mu * \sin(LHA)*((1-0.00143/(\cot\mu +0.0445))^2 / \sin^3\mu) /(\cos\mu + 0.0445)^2) \qquad (26.5)$$

The excess dry path is the integral of the refractive index n of dry air along the path through the troposphere. The refractivity Nd of dry air, defined as $10^6*(n-1)$, is described by the equation [Smith & Weintraub,1953]:

$$Nd = 77.6 * P / T \qquad (26.6)$$

where P is the total pressure in millibars and T the temperature in Kelvin.
By taking average values for the relevant quantities, the following excess path in the zenith direction due to dry air can be computed [Van Antwerpen et al.,1978], assuming a fourth-degree model for Nd as a function of height [Hopfield,1977]:

$$\begin{aligned} Hd &= \text{model height of the dry troposphere above sea level} \\ &= 40{,}082.0 + 148.198 * (T-273.16) \quad (m) \\ \tau_{zd} &= 0.2 * 10^{-6} * Nd * Hd \end{aligned} \qquad (26.7)$$

Ignoring the additional contribution of the wet component (§2.6.2) for the time being, the zenith path excess can be estimated from the adjustment by adding the coefficients (26.3) and (26.5) to the observation equations. The estimated value is then an average over some time, e.g. one day. As temperature and pressure are changing continuously due to weather variations and day/night cycle, this will not yield optimal results.
The estimate can be improved if weather data are available. In this case (26.7) is used to compute the zenith path delay for every observation. The maximum change of this value due to varying weather conditions over one day is about 5 cm; at day-time the excess is less than at night. Relative changes derived from the model, however, are more reliable than the absolute values for the zenith path delay. Therefore, the latter is always estimated in the LSQ adjustment. Consequently, the τ_{zd} computed from weather data is used to "scale" the coefficient FZ2 (26.3) via:

$$FZ2' = FZ2 * (\tau_{zd} / \tau_{zd}^{\circ}) \qquad (26.8)$$

where τ_{zd}° is the value of the tropospheric dry path excess according to (26.7) at the moment of the first observation at that station.
Figure 9 presents the change of the tropospheric zenith delay during the first five days of the MERIT-Short Campaign (§3.7) at the Harvard Radio Astronomical Observatory, Texas, USA.

Discussion

[Moran&Rosen,1979] state that τ_{zd} can be estimated to an accuracy of less than one cm if the pressure is measured with a few millibars standard deviation. Together with an LSQ estimate of the parameter this

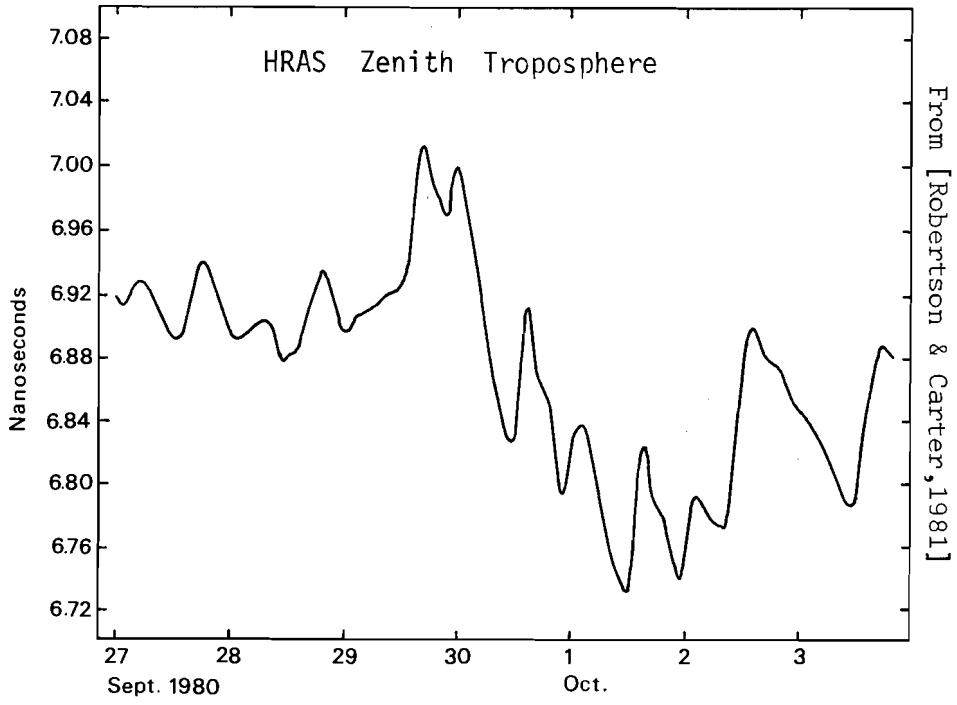

Figure 9: Changes of Tropospheric Zenith Delay

would yield a negligible contribution to the error budget. From the table in Appendix B, however, where several models to correct T_{zd} to other zenith angles are compared, it can be seen that large differences exist. Although these models all serve their own purpose, the conclusion is that:

observations taken below 10° elevation are suspect and those below 5° should not be allowed in the analysis of VLBI data.

At this point, it should also be mentioned that the integral was computed along the direction vector of the source. For a proper solution this should have been done along the actual ray-path. For 10° elevation the difference between the two is in the centimetre region; for 1° it becomes two metres. Furthermore, it should be noted that one is assuming constant weather data over an area of several hundreds of kilometres, the distance at which the ray is above the troposphere for lower elevations.

An improvement of DEGRIAS would be the use of the Marini-model which is similar to (26.3) but allowing the coefficients to depend on latitude and weather data; see [Schuh,1984] and Appendix B. It should also be

added that (26.6) is slightly dependent on frequency due to the CO_2 contents. A more optimal solution lies naturally in a ray-tracing approach; e.g. [Van Antwerpen et al.,1978].

Summarizing, it is estimated that for observations at an acceptable elevation, the contribution from dry troposphere to the error budget of DEGRIAS will be around 2 cm.

2.6.2 Wet Troposphere

The dipoles of the water molecules in the air give rise to a delay in the propagation of the electro-magnetic waves: the "wet" component of tropospheric refraction. The magnitude of the correction depends on the integrated water vapour content of the air along the line of sight. The path excess in the zenith direction is about 20 cm, but this number is highly variable depending on weather conditions.
In the same way as for the dry component, [Smith & Weintraub,1953] and [Hopfield,1977] yield the following model correction:

$$Nw = 3.73*10^5 * E / T^2 \qquad (26.9)$$

where E is the water vapour pressure in millibars and T the absolute temperature in Kelvin; furthermore:

$$Hw = \text{model height of the wet troposphere above sea level} = 13{,}268.0 - 97.96 * (T-273.16) \quad (m) \qquad (26.10)$$

$$\tau_{zw} = 0.2 * 10^{-7} * Nw * Hw \qquad (26.11)$$

In DEGRIAS, τ_{zw} is simply added to τ_{zd}, before the scaling to other elevations via the Chao-formula, or to other instants in time via (26.8) is performed.

Discussion

The scaling of τ_{zw} via the same Chao-model as for the dry path excess is theoretically incorrect (cf. [Lawlinakis,1976]) but acceptable for elevations above five degrees. Since water vapour is not well-mixed in the air, the correction may vary by as much as 50 percent of its nominal value derived from surface meteo readings. There are large differences between geographical locations, the scale height differs by 2 or 3 kilometres between Summer and Winter [Hopfield,1977], the diurnal effect is considerable and there also seems to be a relation to the Sunspot cycle. This makes it extremely difficult to extrapolate the measured E and T at the observatory to a realistic value for the wet component along the line of sight. Typically, an RMS of 5 cm between predicted and measured path is present [Moran&Rosen,1979]. A small part of this effect will be absorbed in the estimated tropospheric parameter (§2.6.1).

A real solution can therfore only be reached by an independent estimate of the total water vapour content along the ray path. This has been tried with balloons and radiosondes in satellites but microwave radiometry (WVR) seems to be the most successful method. This technique provides the required estimate by measuring the strength of the water vapour emission line at 22.2 GHz along the line of sight. In this way an accuracy of below 1 cm for the wet component should be possible. Unfortunately, the technique is not yet fully reliable due to a number of problems, both technical and conceptual (e.g. what to do with "water clouds"?)

2.6.3 Ionosphere

The charged particles in the ionosphere yield a path delay for the radio signal. Its magnitude is dependent on the total electron content (TEC) of the ionosphere along the line of sight. The electron density in the ionosphere is highly variable and decreases rather capriciously by a factor of around five from day to night due to the influence of solar radiation. Furthermore it depends on the season (Figure 10), the (geomagnetic) latitude, the sunspot cycle and many not well-known phenomena in the ionosphere, such as TID's (travelling ionospheric disturbances), probably connected to acoustic-gravity waves [Spoelstra,1983a,b].
The ionosphere consists of several layers, denoted by D, E, F1 and F2 respectively. In the lower layers the collision frequency is so high [Hagfors,1976] that few free electrons are present. Therefore the F2-layer (between about 180 and 1000 km) is the most troublesome for VLBI.
The ionosphere is dispersive. As an example, upper limits for the refraction effect as a function of frequency and zenith angle are presented in Table 1 for the VLBI-frequencies mentioned in §1.3.2, based on data presented in [De Munck,1982]. For reference, values are also shown for the two frequencies of the NNSS doppler satellite navigation system: 150 and 400 MHz (§3.6.1).
One could say that for the higher VLBI frequencies, the ionospheric effect is roughly 10-20% of the tropospheric path delay, but it is not so extreme at low elevations.

DEGRIAS has two ways of correcting the observations for ionospheric refraction, one based on observing simultaneously at two frequencies, and one based on the measurement of the peak electron density by an ionosonde.

Dual-frequency method

The dependence on the frequency offers the possibility of removing the ionospheric path excess by a dual-frequency scheme (§1.3.5).
Let the ionospheric path excess be τ_I, defined as:

$$\tau_I = ION / f^2 \qquad (m) \qquad (26.12)$$

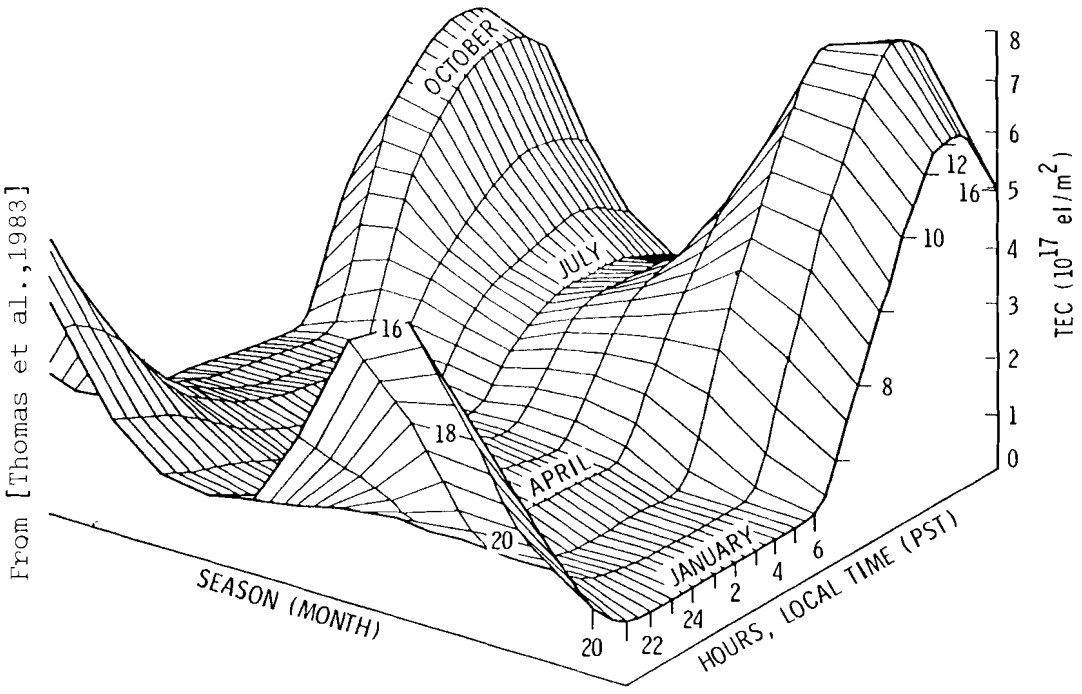

Figure 10: 1979 Monthly Average of TEC for Goldstone, Ca.

Table 1.

Maximum Ionospheric Path Delay (metres)

Elevat. / Freq.	90°	40°	10°	2°	0°
8.1 GHz	0.40	0.60	1.00	1.15	1.15
5.0 GHz	1.00	1.50	2.60	2.90	2.90
2.3 GHz	4.90	6.90	12.40	13.70	13.70
0.4 GHz	162.00	230.00	409.00	452.00	454.00
0.15GHz	1150.00	1640.00	2910.00	3210.00	3230.00

with ION ≈ 40.3*TEC [Flock et al.,1982] and f the observing frequency in Hz. Define the observed values for delay at the two frequencies as:

$$\tau_1 = \tau + \tau_{I1}$$
$$\tau_2 = \tau + \tau_{I2} \qquad (26.13)$$

Now the difference between the two frequencies can be used to correct the measured delay by:

$$\tau_1 - \tau_2 = ION/f_1^2 - ION/f_2^2$$

$$ION = (\tau_1 - \tau_2) / (1/f_1^2 - 1/f_2^2) \qquad (26.14)$$

$$\tau = \tau_1 - (\tau_1 - \tau_2) / (1-(f_1^2 / f_2^2))$$

This delay τ is now free of all charged particle effects and can be used for the LSQ adjustment. For the delay rate observable one can handle the correction in the same way. This, however, is not yet implemented in DEGRIAS.

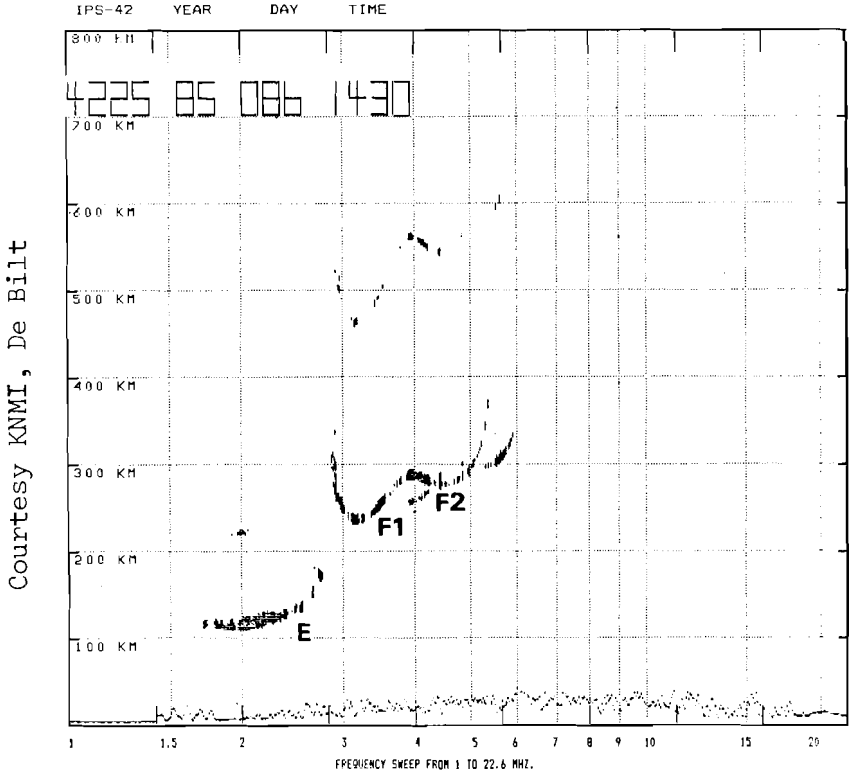

Figure 11: Typical Ionogram observed during Day-time

Ionosonde method

Ionosonde observations measure the peak electron density in the F2-layer (and other layers) by means of a vertical looking HF-radar, sweeping the frequency from 1 to 20 MHz. The highest frequency for which an echo can be received (called the plasma frequency and denoted by f_oF2), is a direct measure for the density of free electrons. This f_oF2 is measured continuously via an ionogram at many weather stations all over the world (Figure 11).

[De Munck,1982] presents a simple ionospheric model, where the plasma frequency squared is assumed to be a discontinuous linear function of R^2, with R the distance to the centre of the Earth. The model divides the F2-layer into two zones, which is a fair approximation to reality. If Rl, Rm and Ru are the distances to the lower limit, the maximum and the upper limit of the ionosphere respectively, and Ra the Earth's radius (Figure 12), the model is formulated as (in DEGRIAS these values are taken as: 6370, 6570, 6770 and 7270 km respectively):

$$
\begin{array}{lll}
R \leq Rl & f_o^2 = 0 & \\
Rl < R \leq Rm & f_o^2 = f_oF2*(R^2-Rl^2)/(Rm^2-Rl^2) & (26.15) \\
Rm < R \leq Ru & f_o^2 = f_oF2*(R^2-Ru^2)/(Rm^2-Ru^2) & \\
Ru \leq R & f_o^2 = 0 &
\end{array}
$$

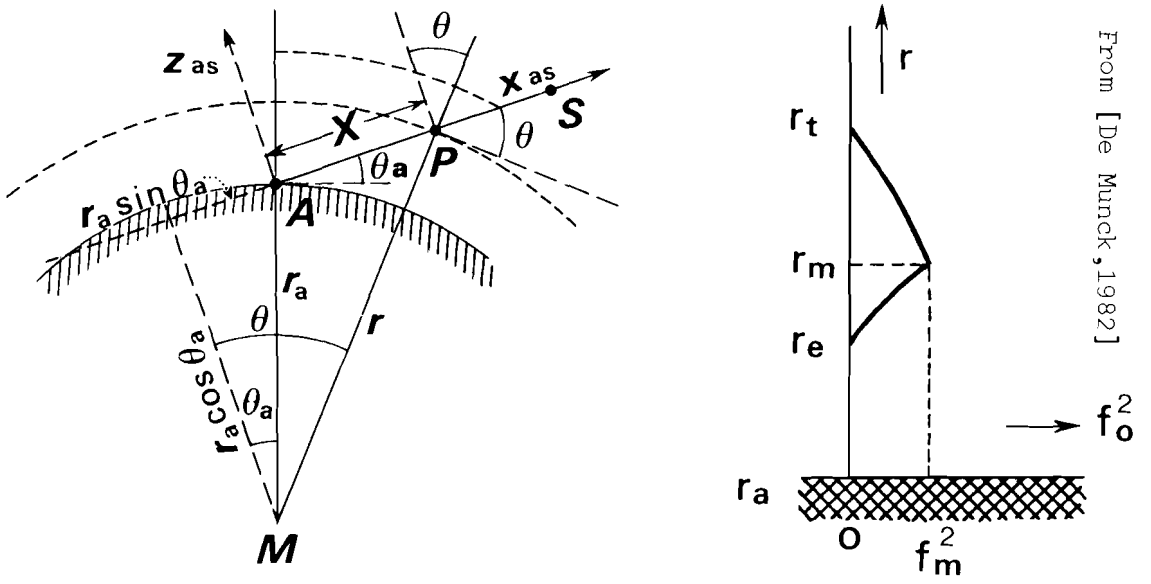

Figure 12: Model for the Ionosphere

If X is defined as a coordinate axis along the line of sight (Figure 12), the ionospheric path delay can be computed as:

$$\tau_{ion} = -(f_o^2/(2*f^2)) *$$

$$[(1/3*(Xm^3-Xe^3) + (Xm^2-Xe^2)*Ra*\sin\theta a + (Ra^2-Re^2)*(Xm-Xe))/(Rm^2-Re^2)+$$

$$+(1/3*(Xt^3-Xm^3) + (Xt^2-Xm^2)*Ra*\sin\theta a + (Ra^2-Rm^2)*(Xt-Xm))/(Rm^2-Rt^2)] \quad (26.16)$$

Since the f_oF2-values are measured at weather stations (in general hourly) and not at the observatories, DEGRIAS applies the following procedure. It is assumed that the quiet ionosphere changes at a given position over short time intervals mainly as a function of the position of the Sun and therefore of time. Consequently, a change in the time registration for the measured f_oF2 values, equivalent to the difference in geographical longitude between the VLBI station and the weather station, will result in a reasonable f_oF2 estimate. This time difference must be adjusted because the f_oF2 value is required where the ray crosses the ionosphere and not at the VLBI-observatory itself, as looking towards the East or the West at an elevation of 10 degrees makes a difference of over an hour in "ionospheric" time. With some approximation one can write this time correction (in hours) as:

$$t_i = 24*200*\sin(A) / (\cot\mu * \cos\phi *40000) \quad (26.17)$$

where A is the azimuth, counted from South towards West.
Furthermore, it is known that the number of free electrons is a function of the incoming solar radiation. The ionosphere is therefore more active at lower geographical latitudes. In DEGRIAS, the measured f_oF2 is thus increased by 7 percent for every 10 degrees that the VLBI station is located South of the weather station. This average number of 7 percent is inferred from some global f_oF2 profiles presented in [Klobuchar,1978] and [Campbell&Lohmar,1982]. Due to its special character, this ionosonde correction cannot be applied directly to delay rate data.

Discussion

The accuracy of the dual frequency correction depends on the separation of the two frequency channels. For simultaneous observations at 2.3 and 8.1 GHz, for instance, the factor $(1-(f_1^2/f_2^2))$ in (26.14) has a value of -12.3, so that a standard deviation of somewhat less than 0.05 ns in the correction for the ionospheric path delay is found.

The ionosonde method in its present form is not meant to be a real alternative to dual-frequency observations. Rather, it is useful in eliminating the ambiguities of the BWS method (§1.3.5) where they are only slightly larger than the ionospheric path delays, because one has to remove the ambiguities before the dual-frequency correction can be computed (§3.4).
Another application would be to interpolate ionospheric corrections for pieces of observations where one frequency is lacking. In this respect it has the advantage over Doppler-derived corrections [Campbell & Lohmar,1982] that the latter requires additional Doppler satellite observations (plus equipment and data processing), whereas the ionosonde approach makes use of available data measured on a routine basis.

Appendix C shows an RMS-difference between the correction from dual-frequency observations and the ionosonde model of around 0.2 ns for an example of the MERIT Short Campaign (§3.7). The overall accuracy of the ionosonde model is therefore conservatively estimated as about 10 cm.

Dual-frequency observations are expensive (receivers) and time consuming (double correlation effort). Therefore, the need for a cheap alternative is obvious. Doppler derived corrections are an alternative especially if the horizontal density gradients in the electron density are also included [Spoelstra&Kelder,1984].
The ionosonde model presented here, is currently based on observations of f_oF2 at only one station. For better results, an interpolation between f_oF2 data of more weather stations will be required, combined with the introduction of the horizontal gradients and a more sophisticated F2-layer model. Even then, the results will probably not be much better than 0.1 ns.
A combination of ionosonde plus Doppler may yield the best results as an alternative to dual frequency observations. Additional information about the behaviour of the ionosphere can then also be acquired by measuring the Faraday rotation of polarized radiation.

2.6.4 Miscellaneous

Some additional features of propagation have a small influence on VLBI observations and are therefore neglected in DEGRIAS: solar corona, solar wind and interstellar gas.

Discussion

The charged particles in the corona of the Sun and in the solar wind yield an effect similar to those in the ionosphere. The number of particles in the solar wind, however, is too small to be of interest. The brightness of the corona is only one part in 10^6 of that of the Sun itself at one solar radius away from the Sun. This gives an indication how near to the Sun one would have to observe a source to find a noticeable effect of the corona. [Ma,1978] mentions a safe distance of 10 solar radii, which corresponds to an angle of 2.5 degrees as seen from the Earth. Hence, no real problems exist, unless one wants to study gravitational deflection. Correction models do exist [Ma,1978], but when dual-frequency observations are applied the correction is automatically taken into account.

Interstellar (and also interplanetary) gas causes more attenuation effects of the signal than phase changes. Anyway, the influence is the same for both telescopes and vanishes therefore in the measured delay.

2.7 THE "REAL WORLD" FOR VLBI - GEOPHYSICS

2.7.1 Earth Rotation and Time

Since time immemorial, time as defined by the periodic motions of the celestial bodies was used by men to organize their lives. Even with

modern techniques such as VLBI, nothing has changed in this respect, as the stellar and terrestrial frames of reference should be related (§2.2) and the key to this still is: time.
The hour angle of the First Point of Aries with respect to the Greenwich conventional meridian (§2.2) is a direct measure of the diurnal rotation of the Earth, called: Greenwich Mean Sidereal Time (GMST). This measure can directly be derived from observing star transits through the local meridian. All civil time-keeping, however, is not based on the diurnal motion with respect to the stars but to the Sun. This time measure is denoted by Universal Time (UT). [Newcomb,1895b] derived a rigorous formula, based on theory but mostly on observations, relating GMST and UT for 0h UT of a specific day:

$$GMST0 = 23925.836 + 8640184.542*T + 0.0929*T^2 \qquad (s) \qquad (27.1)$$

with T the time in Julian centuries since 1900, 0.5 Jan. (§2.4.3). A linear term of exactly 8,640,000 seconds in (27.1) would imply that in addition to the diurnal rotations every year precisely one more rotation occurs due to the motion around the Sun. Most of the deviation from this figure (including the quadratic term) is due to the diurnal precession in right ascension which amounts to approx. 0.0084 seconds per day [Woolard&Clemence,1966]. From (27.1) it follows that the ratio of the mean solar day to the mean sidereal day is:

$$UTCONV = 1.002737909265 + 0.589*10^{-10} * T \qquad (27.2)$$

However, 24 hours of mean sidereal time do not yield exactly one rotation of the Earth with respect to the stars due to nutation. The variable shift of the true equinox with respect to the mean equinox is denoted by EQE (equation of equinoxes) and represents apparent minus mean sidereal time (§2.4.3).
The angular velocity of the Earth is not constant but subject to periodic and sudden changes due to e.g. Earth tides, atmospheric mass motions, changes in sea level, volcanic eruptions, earthquakes and other movements in the interior of the Earth and possibly due to solar radiation. These daily changes in the length of day (LOD) amount to about 0.4 ms/day, and the amplitude of the integrated effect (with a yearly signature) is about 40 ms (Figure 13). An additional secular retardation due to tidal friction lenghtens the day by 0.0016 s per century.

A transit instrument on Earth measures the duration of a full rotation of a star and via (27.1), (27.2) and EQE a measure for Universal Time is derived, denoted by UT0. In the BIH-1968 system the "0" is added to indicate that these are the raw observed values. UT0 corrected for the effect of polar motion is denoted by UT1. This measure represents the real angular position of the Earth and comparison of UT1 with a uniform time-scale reveals the irregularities of the Earth's rotation [Enslin,1978]. The notation UT used thus far, may therefore be identified with UT1.

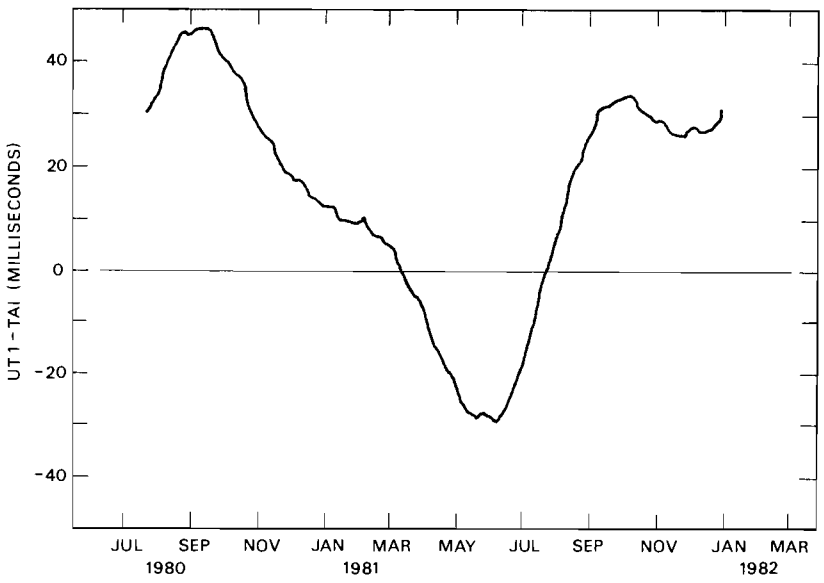

After [Preuss, 1984]

Figure 13: Changes in the Length of Day

On the other hand, the VLBI station clocks are running at UTC (=Coordinated Universal Time), which is TAI (§2.5.3) as maintained by caesium-standards minus a number of leap seconds to ensure an approximate agreement of UT1 and UTC (within limits of 0.9 seconds). From data of some 75 observatories, the BIH publishes values for UT1-UTC at 0h UTC as 5-days (weighted) averages in its Circular D. DEGRIAS uses a linearly interpolated value for UT1-UTC so that the 'apparent' Greenwich sidereal time becomes:

$$GAST = GMST0 + (UT + UT1\text{-}UTC)*UTCONV + EQE \qquad (27.3)$$

GAST is thus the rotational angle of the X-axis of the conventional terrestrial system with respect to the first axis of the true equator and equinox frame of date measured in the equator of the ephemeris pole defined by the nutation routines.
From the above data, the LOD can be derived as:

$$LOD = 86400 - (UT1\text{-}UTC - EQE) \quad (s) \qquad (27.4)$$

and consequently the instantaneous angular velocity is:

$$\Omega = 2*\pi * UTCONV/86400 * (86400/LOD) \qquad (27.5)$$
$$= 72.921151463*10^{-6} * 86400 / LOD \quad (rad/s)$$

This - linearly interpolated - instantaneous angular velocity is used in DEGRIAS for the delay rate observable (22.6). A refinement would be a quadratic interpolation of UT1-UTC. The changes due to EQE are at present only included if numerical differentiation is applied (§3.1).

Discussion

The UT1-UTC data provided by the BIH are estimated to be precise to a factor of 0.0016s [BIH,1978], which is about 70 centimetres in orientation. In the above, the BIH-1968 system has been described. Since May 1979, UT1 has been refined by including some corrections for instrumental effects and diurnal polar motion (up to 1984). Since March 1982 the effects of zonal Earth tides have also been removed. This makes a difference of maximally 1.5 ms. To find the real orientation in space, the influence of the tides must be added to the published values. For DEGRIAS, this implies a possible error of up to 1 metre in orientation, propagating to 1 cm in baseline length if the data are taken as a priori.
When UT1 is estimated from the observations, the same holds as with polar motion (§2.7.3): DEGRIAS can compute averages over a minimum of one day.

2.7.2 Retarded Baseline Correction

The maximum flight time of a signal between two Earth-based stations is 0.04s. Over this interval the baseline cannot be regarded as motionless with respect to the incoming wavefront: a station on the equator moves about 19 metres due to Earth rotation. The compensation for this effect is called "retarded baseline" correction and is in fact diurnal aberration plus a constant; see §2.4.4 and [Campbell,1979b].

Now, consider baseline AB. The plane wavefront first reaches station A with coordinates (Xa,Ya,Za) and after a time τ_g station B with coordinates (Xb,Yb,Zb). Let Ω be the rotation rate of the Earth, then station B has moved from position (Xb,Yb,Zb) to position (Xb',Yb',Zb') during this time τ_g, descibed by a (R_z)-matrix about the instantaneous rotation axis (§2.7.1). With the usual approximation one finds $Xb'=Xb-(\Omega^* \tau_g)^*Yb$ and $Yb'=Yb+(\Omega^* \tau_g)^*Xb$, so that the difference between $\tau_g(AB)$ and $\tau_g(AB')$ of formula (22.5) becomes:

$$\tau_{RTB} = -(\cos(GHA) * \cos\delta * (\Omega^* \tau_g * YB) - \sin(GHA) * \cos\delta * (\Omega^* \tau_g * XB)) / c \qquad (27.6)$$

or, more familiarly (with ReB = sqrt(Xb^2+Yb^2), the equatorial radius for station B and LHA = GAST- α - λ , the local hour angle):

$$\tau_{RTB} = -\Omega * \tau_g * \cos\delta * ReB * \sin(LHA) / c \qquad (27.7)$$

Consequently, one obtains the following retarded baseline correction for the delay rate:

$$\dot{\tau}_{RTB} = -\Omega * \cos\delta * ReB * (\dot{\tau}_g * \sin(LHA) + \tau_g * \cos(LHA)) / c \qquad (27.8)$$

It should be stressed that the same formulae hold when the wavefront first reaches station B and therefore τ_g is negative; cf. [Campbell,1979b].

Discussion

In the above, apart from the linearization of the rotation matrix, also the tacit assumption is made that the change in baseline orientation is completely due to a well-known Earth rotation. This approximation is estimated to have only a negligible contribution to the total error budget, say at most a few millimetres in DEGRIAS.

2.7.3 Polar Motion

The effect that the Earth's crust is moving with respect to its spin axis is known as polar motion. This motion consists of various components, the most prominent being the Chandler Wobble with a period of approximately 14 months and an amplitude of around 0.15 arcseconds; this means about 5 metres at the pole. The Chandler Wobble is the free Eulerian motion that the Earth undergoes due to a difference between the axis of figure (3rd moment of inertia) and the instantaneous rotation axis. Its period is defined by the moments of inertia and the amplitude is the result of the initial conditions ("when the Earth started rotating"), somewhat damped by the motion of masses in the Earth's interior. In addition, an annual and a semi-annual motion exist, with amplitudes of 0.09 and 0.01 arcseconds, which are related to the continuous redistribution of masses in the atmosphere and in the seas (e.g. ice). Furthermore, a secular movement of 0.003 arcseconds per year exists in the direction of Greenland and the Markowitz oscillation with a period of 40 years and an amplitude of 0.02 arcseconds [Aardoom,1983].

The Bureau International de l'Heure (BIH) publishes 5-days average values for the X- and Y-coordinates of the pole position in the CIO-system via its Circular D, here denoted by Xp and Yp.
In DEGRIAS the values of these two components at a specific instant in time are determined by a linear interpolation between two 5-days values.
The polar motion matrix is thus defined as: $(W) = R_X(Yp).R_Y(Xp)$.
Then, using the fact that the angles Xp and Yp are small, one finds as a first order approximation:

$$\begin{pmatrix} X' \\ Y' \\ Z' \end{pmatrix} = \begin{bmatrix} 1 & 0 & -Xp \\ 0 & 1 & -Yp \\ Xp & Yp & 1 \end{bmatrix} . \begin{pmatrix} X \\ Y \\ Z \end{pmatrix} \quad \text{or} \quad (X') = (W).(X) \qquad (27.9)$$

where (X,Y,Z) are the coordinates of a station in the CIO-system and (X',Y',Z') the coordinates in the coordinate system with the instantaneous, slowly moving rotation axis of the Earth as Z-axis.

In the direct formula for the delay rate observable (§3.1) no changes due to polar motion are included.

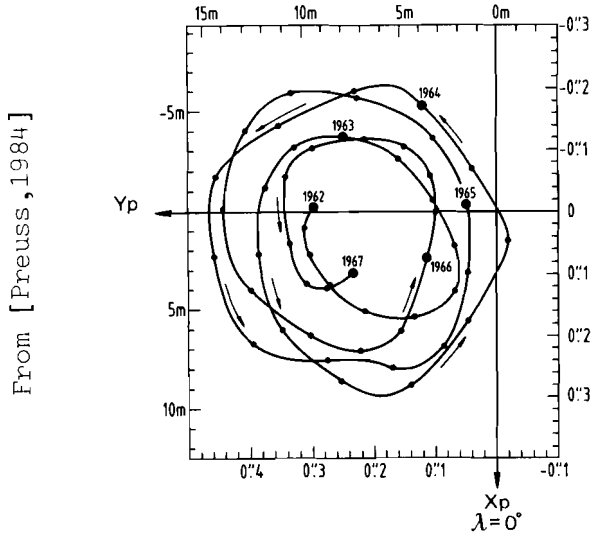

Figure 14: Path of the North Pole in 1962-67

When the polar motion components are solved for in the LSQ adjustment, as for UT1-UTC (§2.7.1), averages are estimated for sections of a minimum of one day.

Discussion

The only approximation in the above reasoning is the linearization of the rotation matrices for Xp and Yp. This, however, holds to a very high level of accuracy, even on long baselines. An improvement could be reached by a quadratic interpolation of the BIH-data instead of a linear one.

The BIH-data are claimed to be accurate to a level of 0.01 arcsec [BIH,1978], which results in a baseline orientation inaccuracy of approximately 30 cm for a 5000 km baseline. Since polar motion is a pure rotation, the influence on baseline length is negligible.
On the other hand, the real problem lies not in the value of the components, but in where they do refer to in view of the combination of precession, nutation, polar motion and diurnal polar motion. This is discussed in §2.7.4.

2.7.4 Diurnal Polar Motion

Although the effect of diurnal polar motion is not implemented in DEGRIAS and is obsolete in the J2000 reference system (§2.4.3), a short description is nevertheless given here, albeit as a historical review of how the new nutation series was arrived at.
Polar motion mainly consists of changes of the slowly moving pole (§2.7.3). In addition, the lunar and solar torques acting on the equatorial bulge of the Earth cause a change in the angular momentum axis, which is followed by a change in the spin axis. In the fixed terrestrial reference frame this is seen as diurnal polar motion [Ma,1978]; previously it was called "dynamical variation of latitude".

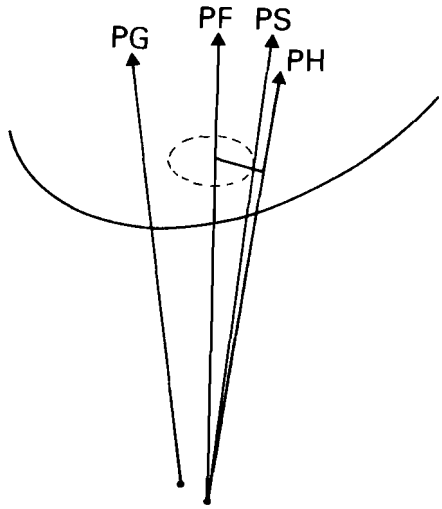

Figure 15: Definition of Polar Motion Axes

The situation is illustrated in Figure 15, where PG is the geographical Pole (CIO), PF is the pole of figure, PH is the angular momentum pole and PS the instantaneous rotation pole. From kinematic considerations (Euler's equations) PF, PH and PS lie in one plane. PS is moving on an epicycle around the Eulerian pole position. The amplitude PH-PS of the epicycle is only 2 or 3 cm and its radius about 30 cm.
The above situation is valid for a non-deformable Earth. Due to the elastic response of the Earth (e.g. the changing mass distributions due to tides) the situation becomes more complicated: the Eulerian pole path becomes the Chandler pole path, PF may move as much as 60 metres and PH-PS may be up to 21 cm and the epicycle radius up to 62 cm [Ma,1978].
The centre of the quasi-diurnal pole path is defined as the Celestial Ephemeris Pole. This point shows neither diurnal motions in the Earth-fixed nor in the space-fixed system and is accessible for IPMS (International Polar Motion Service) measurements. It is therefore the ideal reference for the new nutation series (§2.4.3), which in this way include the traditional diurnal polar motion.

Discussion

For diurnal polar motion, in general the same holds as for nutation: the influence is dependent on the relative direction of the baseline vector and the polar vector. Consequently, a sinusoidal delay change is produced with a maximum amplitude of approximately 0.5 ns for intercontinental baselines and a daily period with a fortnightly envelope [Ma,1978].
A correction for this effect has not been applied in DEGRIAS because of the envisaged introduction of the J2000 system and because of the fact that it averages out during 24 hours of observations in the final results and that it only increases the estimated RMS of the observations somewhat. Only for shorter campaigns is this not the case.

2.7.5 Solid Earth Tides

The gravitational forces of Sun and Moon yield tidal motions of the Earth's surface. To correct these motions to arrive at time-independent station coordinates, in DEGRIAS the approach is followed of the classical development of Laplace for the spherical harmonics of the disturbing potential W of a perturbing body (up to second order) [Melchior,1978]:

$$
\begin{aligned}
W \;=\; & 3/4 * G*M * R^2 / D^3 * \qquad (27.10)\\
& (+\cos^2\phi \;*\; \cos^2\delta \;*\; \cos(2*LHA) \qquad a\\
& \;+\sin(2\phi\,) * \sin(2\delta\,) * \cos(LHA) \qquad b\\
& \;+3*(\sin^2\phi - 1/3) * (\sin^2\delta - 1/3)) \qquad c
\end{aligned}
$$

with

R = distance of a station to the geocentre
D = distance to the perturbing body
G = gravitational constant
M = mass of Sun and Moon respectivily

One discerns three types of spherical harmonics: the sectorial (a), the tesseral (b) and the zonal (c).
The sectorial functions have an absolute maximum at the equator if the declination of the perturbing body is zero; the amplitude is zero at the poles. The period is semi-diurnal. Because of this symmetry the sectorial tides do not change the position of the pole nor the major moment of inertia, which determines the rate of rotation, but it is believed that these tides are responsible for the secular retardation of the Earth's rotation (§2.7.1) by energy dissipation.

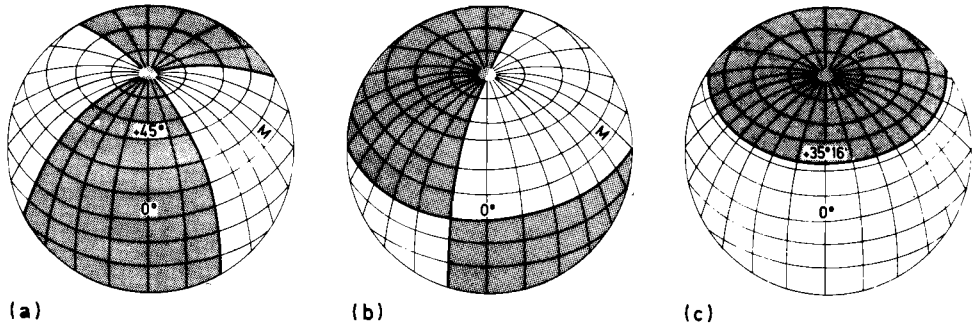

From [Melchior,1978]

Figure 16: The Three Kinds of Earth Tides

The tesseral functions have an absolute maximum at plus and minus 45° latitude if the declination of the perturbing body is also 45°. The tide is anti-symmetric with respect to the equator and has a diurnal period. These tidal variations do affect the position of the pole but not the moment of inertia. It is clear that they correspond to the precession/nutation forces which tend to rotate the equatorial bulge of the Earth to the ecliptic plane.

The zonal functions are only dependent on latitude and have a maximum at the poles, a minimum at the equator and are zero at plus and minus 35° latitude. The constant part results in the equipotential surface being lowered by 28 cm at the poles and raised by 14 cm at the equator, thus causing a slight increase of the Earth's flattening (Honkasalo term). These tides have no effect on the position of the pole but do affect the principal moment of inertia so that slight variations are caused in the rotation rate of the Earth, with a period of half a year for the Sun and fourteen days for the Moon.

The tide of the geoid, expressed by the displacement H, is defined by:

$$H = -W / g \qquad (27.11)$$

where g is the gravity of the Earth (defined positive downwards). This follows from the fact that the work accomplished in transporting a unitary mass from the initial level to the perturbed level (which is H*g) equals the potential variation W. Since only this variation is important, a mean value for W is defined in (27.10) by adopting a mean radius and gravity for the Earth and mean distances to Sun and Moon.
The constant part of (27.10) is called Doodson's Constant [Melchior,1978]. With these mean values a maximum tidal displacement of the geoid due to the Moon of 26.8 cm, called Hl in (27.12) and due to the Sun of 12.3 cm is found. The total range of the geoid tide is therefore in an exceptional case: 78.1 cm.
The trigonometric part of W in (27.10) can vary from -1 to +1. Using the basic astronomical developments for the positions of Sun and Moon, the eleven main terms of the series' expansion for the disturbing potential U are implemented in DEGRIAS after (27.12). The phase lag of the tides is chosen to be zero. The constants Ai allow for the relative weighting of Sun (S) and Moon (L) and are given in [Melchior,1966] or [Robertson,1975].

$U = Hl *$ (27.12)

	tidal symbol	origin	period
$(\cos^2\phi \quad *$			
$*(+A1*\cos(2*HA1)$	M2	L	12.42 h
$+A2*\cos(2*HA1-\mu+\Omega)$	N2	L	12.66 h
$+A3*\cos(2*HAs)$	S2	S	12.00 h
$+A4*\cos(2*(GAST-\lambda))$	K2	L+S	11.97 h
$+\sin(2*\phi) *$			
$*(+A5*\cos(GAST-\lambda-\frac{1}{2}\pi)$	K1	L+S	23.93 h
$+A6*\cos(HA1-\mu+\frac{1}{2}\pi)$	O1	L	25.82 h
$+A7*\cos(HAs-\sigma+\frac{1}{2}\pi))$	P1	S	24.07 h
$+(1\frac{1}{2}*\sin^2\phi - \frac{1}{2}) *$			
$*(+A8$	Mo+So	L+S	-
$+A9*\cos(\mu-\Omega)$	Mm	L	27.55 d
$+A10*\cos(2*\mu)$	Mf	L	13.66 d
$+A11*\cos(2*\sigma))$	Ssa	S	0.5 y

with (T is measured in Julian centuries since 1900.0):

HA1 = Lunar hour angle = GAST - μ - λ

HAs = Solar hour angle = GAST - σ - λ
μ = Mean longitude of the Moon = 4.719967 + 8399.709*T (rad)
σ = mean longitude of the Sun = 4.881628 + 628.3319*T (rad)
Ω = longitude of lunar perigee = 5.835152 + 71.01803*T (rad)

The potential changes in the vertical and the North/South and East/West horizontal directions can be derived from the above formulae by differentiating (27.12) according to:

$$\begin{aligned} &\text{height} &&: -\partial W/\partial r \\ &\text{North/South} &&: -\partial W/\partial\phi \;/\; R \\ &\text{East/West} &&: -\partial W/\partial\lambda \;/\; (R*\cos\phi) \end{aligned} \qquad (27.13)$$

so that the following displacements are found:

$$\begin{aligned} H &= h * U && \text{(cm)} \\ \Delta\phi &= l/g * \partial U/\partial\phi \;/\; R && \text{(rad)} \\ \Delta\lambda &= l/g * \partial U/\partial\lambda \;/\; (R*\cos^2\phi) && \text{(rad)} \end{aligned} \qquad (27.14)$$

where h and l are the relevant Love numbers describing the elasticity of the Earth. They have an average value in DEGRIAS of 0.608 and 0.0845 respectively. The actual difference in delay due to solid Earth tides is computed by applying (22.5) twice, once with and once without the correction (27.14). No correction is present in the direct formula for delay rate (§3.1).

Discussion

As mentioned above, the total range of tides would reach about 78 cm if the Earth were fluid and the sine waves in phase. The actual range of displacement of the equipotential level has a maximum of around 35 cm. The horizontal displacements reach only a few centimetres. Due to a not well-known phase lag in the elastic response of the Earth and due to irregularities in its interior by which the Love numbers may vary by 10 percent from site to site, a contribution to the total error budget of DEGRIAS can be expected of around 2 centimetres.

An improvement would be not to use spherical harmonics, but to compute the rigorous formula for W directly. In this case more exact positions of Sun and Moon are required, which can be taken from a PEP-tape [Ma,1978]. In addition, separate Love numbers for different positions on Earth and degrees of harmonics could then be used, since they are affected by different aspects of the Earth's structure.
A last remark concerns special relativity: if the approach of §2.5.3 is chosen, from (27.14) velocity vectors due to Earth tides can also be computed which are added to the other velocity vectors [Ma,1978].

2.7.6 Ocean Loading

The changing loads of ocean masses on the continental shelves due to tides generate a tidal motion of the continents. The relative phase lag of the ocean tide to the corresponding Earth tide and the height displacement amplitude can be computed for the main tides using e.g. the [Schwiderski,1978] model. As yet, this is not implemented in DEGRIAS.

Discussion

For MERIT, the ocean loading displacements due to the 9 main tides are computed for 25 stations all over the world [Melbourne et al.,1983]. For the majority of these stations (including Westerbork/Kootwijk) the displacement is less than 1 cm. Only for stations like Bermuda has a maximum displacement of 5 cm been computed. On the average, therefore a contribution to the total error budget of DEGRIAS of one centimetre in regions near the oceans can be expected.

2.7.7 Miscellaneous

To conclude, a number of geophysical phenomena are mentioned influencing site positions, notably: groundwater, atmospheric loading and crustal dynamics.

Discussion

Changing groundwater storage due to seasonal variations and changes in the atmospheric masses (atmospheric loading) may vary the positions of telescopes by one centimetre in height [Larden,1980]. It will, however, be hard to model this reliably.
Furthermore, there exists some speculation about a secular expansion of the Earth [Dicke,1969]. The possible rate of this expansion is estimated to be 10-100 mm/century.
Finally, the effect of crustal movements and plate tectonics is mentioned, which is well-accepted but still a hypothesis to be confirmed by direct measurements; cf. the objectives of geodetic VLBI in §1.2. The average relative motions of the major plates are shown in Figure 17. Typically the plates move at rates of a few cm per year, with a maximum of nearly 20 cm per year along the Pacific-Nazca boundary. A direct measure of these motions will shed light on the rheology of the crust and upper mantle and the responsible (convection) mechanism, ultimately enabling the prediction of earthquake activity.

2.8 ASSESSMENT OF ACCURACIES

In the preceding sections an idea is conveyed of the various phenomena composing the "real world" for geodetic VLBI. Algorithms have been discussed composing the "model world" in DEGRIAS, together with an indication of their level of accuracy. In this section an assessment will be made of these accuracies, and compared to "bottom line" results that will be possible in the near future.

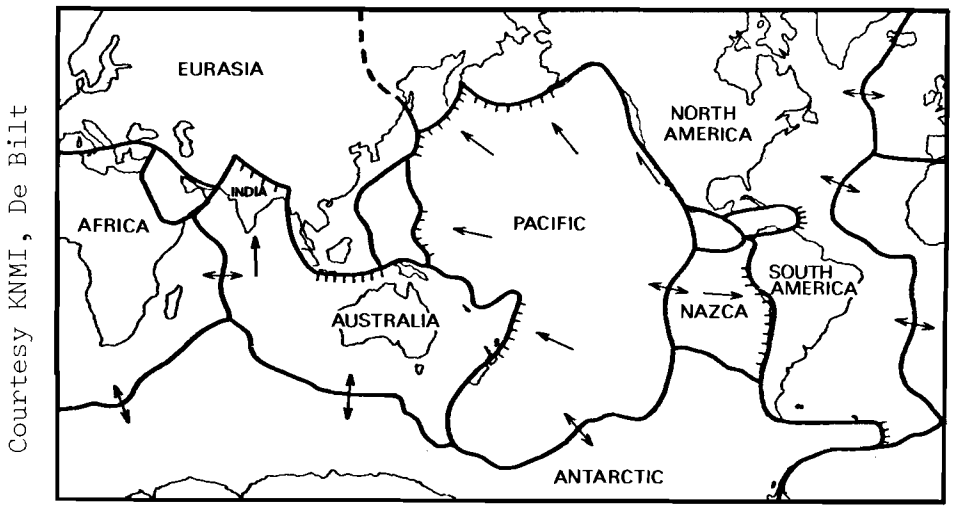

Figure 17: Motions of Tectonic Plates

In this assessment a careful distinction must be made between "relative" and "absolute" accuracy. "Relative" is defined here as: influencing the relative positions of stations, whereas "absolute" is defined as: influencing the position of the polyhedron formed by all stations with respect to the adopted frame of reference. It may be clear that these definitions are directly related to the primary goal of geodetic VLBI (§1.2): world-wide positioning of stations. It may also be clear that this refers to the definition of "form-elements" [Baarda, 1966]; see §1.4. An example may illustrate the difference.
In §2.4.2 the difference between the 1950.0 precessional constant and the J2000 one was given as about 1.1 arcsec per century. Between DEGRIAS coordinates and results of other software packages using the J2000-ephemeris, a rotation is therefore present; this can be regarded as absolute accuracy. If, however, from the coordinates (presuming that all other algorithms are the same) the baseline lengths and the angles between baselines are computed, the results will be (almost) identical: relative accuracy.

This is also shown by a computational example. With DEGRIAS simulated observations are generated for the MERIT-SC schedule (§3.7), during 48 hours on two baselines: Effelsberg (Bonn, FRG) - OVRO (Cal., USA) and Effelsberg-Haystack (Mass., USA). Next, two adjustments are made, one using the 1950.0-system precessional constant and one using the interpolated new precessional constant. From the results under item 2 in Tables 2 and 3 it is clear that an apparent rotation of the network occurs of 0.317 arcsec (which equals 7 metres) but that baseline lengths stay the same. In the same way 11 other examples have been computed pertaining e.g. to gravitational deflection and nutation, as follows:

1 = standard simulation fit, using full DEGRIAS model;
delays only; a priori standard deviation 0.2 ns
2 = using 1950.0 instead of interpolated new precessional constant
3 = no nutation included

4 = no E-terms in aberration included
5 = no gravitational deflection correction applied
6 = tropospheric refraction without weather data
7 = no ionospheric refraction correction applied
8 = changing all polar motion Xp-components by 0.01 arcsec
9 = changing Xp as in 8, but only for one day
10 = with a 10% change in Earth tide Love numbers
11 = no Earth tides included
12 = with a 5% error in retarded baseline correction
13 = 1 cm axis offset introduced in Haystack

Table 2.

Simulated Distortions of EFF-OVRO Baseline

	RMS (ns)	dX (cm)	dY (cm)	dZ (cm)	dL (cm)	dAzim. (mas)
1	0.17	-	-	-	-	-
with sigma:		11	24	9	11	7
2	0.17	-764	-991	0	0	317
3	0.98	552	733	18	8	-233
4	0.17	-64	-83	0	0	27
5	0.24	-120	-157	9	-1	50
6	0.21	-14	-21	-8	0	7
7	0.25	-55	-28	1	26	14
8	0.17	5	0	-31	0	-1
9	0.18	3	-2	-11	-2	0
10	0.17	0	2	1	1	0
11	0.22	4	-16	6	-12	3
12	0.23	12	26	15	5	-7
13	0.17	0	0	1	1	0

A few remarks about the results of these simulations can be made. Firstly, it is immediately clear that the introduction of an error in the adjustment model affects the "relative" positions of stations far less than their "absolute" ones. This means that most phenomena have about the same influence on all baselines. A good example is nutation. Adjustment 3 of the tables shows that completely neglecting nutation in the adjustment increases RMS residuals by a factor of five and changes station positions by several metres, but the rotation of both baselines around the Z-axis (azimuth) is the same and the change in length is approximately proportional to baseline length (EFF-OVRO 8200 km and EFF-HAY 5600 km). This is of course correct, as nutation is to a first order approximation a pure rotation and deviations from this are mainly seen as residuals and only partly as a change in the estimated parameters. For instance, ionospheric refraction (example 7) and Earth tides (example 11) can obviously not be described by a rotation and/or a change in scale alone.

Table 3.

Simulated Distortions of EFF-HAY Baseline

	RMS (ns)	dX (cm)	dY (cm)	dZ (cm)	dL (cm)	dAzim. (mas)
1	0.20	-	-	-	-	-
with sigma:		13	13	3	7	6
2	0.20	760	391	0	0	317
3	0.66	-554	-293	-7	6	-233
4	0.20	64	32	0	0	27
5	0.24	121	61	-9	0	50
6	0.24	14	5	4	2	6
7	0.32	42	6	0	14	15
8	0.20	-3	0	12	0	-1
9	0.21	-1	2	4	-2	0
10	0.21	-1	-1	0	0	0
11	0.27	2	9	0	-6	2
12	0.25	-15	11	-11	-18	-3
13	0.20	0	0	0	0	0

In the above examples some effects are completely neglected, but in the same way this discussion holds if an error in the model is present of e.g. 10 percent in the total magnitude of the corresponding correction. The considerable rotation over 1.5 metres due to neglect of gravitational deflection is caused by the position of the reference source 3C273-B, which was at an angular separation of only 6 degrees from the Sun at the time of the MERIT Short Campaign.
The other examples speak for themselves.

With the above in mind, Table 4 is composed as an assessment of the discussions of sections 2.3 to 2.7 for the delay observable. In the first column, the estimated "absolute" accuracy of DEGRIAS is mentioned where appropriate; in the second column the "relative" DEGRIAS accuracy is shown and in the last column the expected [Trask et al.,1982] "bottom line" results for VLBI on the basis of one-day datasets are given, all for a 5000 km baseline.
From the table it appears that the accumulated error budget of DEGRIAS modelling is 7.1 cm. To avoid optimism, it is preferable to state the conclusion that:

DEGRIAS model accuracy at its present stage is one decimetre for intercontinental baselines.

For shorter baselines, this accuracy increases to a few centimetres.

Table 4.

Assessment of DEGRIAS and VLBI Accuracy

units = cm phenomenon	DEGRIAS modelling accuracy "absolute"	DEGRIAS modelling accuracy "relative"	Bottom line results
1. clock behaviour		2.0	0.6
2. antenna structure		3.0	0.7
3. source structure		0.5	0.3
4. precession	200.0	0.2	-
5. nutation	50.0	4.0	0.9
6. aberration	20.0	3.0	-
7. grav. deflection		0.5	-
8. (special) relativity		0.7	-
9. dry troposphere		1.5	0.5
10. wet troposphere		3.0	1.5
11. ionosphere		0.2	0.2
12. Earth rotation	20.0	1.0	-
13. retarded baseline		0.2	-
14. polar motion	20.0	0.2	-
15. solid Earth tides		2.0	-
16. ocean loading		1.0	-
17. miscellaneous		1.0	-
TOTAL	210.0	7.1	1.9
ESTIMATED RESULTS			
baseline length (cm)	-	7.1	1.9
pole position (mas)	19	7.0	2.0
UT1-UTC (ms)	1.3	0.5	0.06
source positions (mas)	70	7.0	2.0

The last column of Table 4 (cf. also [Schaffer,1984]) clearly demonstrates that the "wet" tropospheric refraction component is the major VLBI error source. In addition, the "dry" component is a major error source at low elevations (0.5 cm is for elevations above 10 degrees). If a significant improvement (1.5 cm includes WVR-measurements) can be reached in their determination, the way is open to an approach using phase-delay observables [Campbell,1979a] instead of the present group-delays. This could bring VLBI accuracy to the level of Connected Element Radio Interferometry (§1.1), meaning millimetre precision.

As the computed observation of the delay rate observable is found by a numerical differentiation using computed delay observations (§3.1), the level of accuracy of this type of observation is in principle the same as for delay, noting, however, the inherent limitation of delay-rate: its insensitivity to the Z-component of the baseline.

Chapter 3

"D E G R I A S" S O F T W A R E P A C K A G E

Summary: In the preceding chapter the "real world" for geodetic VLBI has been described. In §3.1 all relevant phenomena will be combined to arrive at the standard "model world" (formula system) for the DEGRIAS software package (DElft Geodetic Radio Interferometry Adjustment System). For this so-called "kinematic" model the linearized observation equations for delay and delay rate observables are derived. This is followed by a brief description of the idiosyncrasies of DEGRIAS and a discussion about rank deficiencies of the system of normal equations of Least Squares adjustment. The description concludes with an indication of some envisaged improvements of DEGRIAS (§3.5).
As an example of the capabilities of this software package, the results of analysis of two multi-station geodetic VLBI experiments are presented in sections 3.6 and 3.7, viz.: ERIDOC (European Radio Interferometry and DOppler Campaign) and a part of the MERIT Short Campaign (to Monitor Earth Rotation and to Intercompare the Techniques of observation and analysis). For the latter, the differences in estimated results are also studied when several choices are made for the set of observations or model parameters.

3.1 FULL COMPUTING MODEL OF DEGRIAS

In §2.2 the simple computing model (22.3) and the related non-linear observation equation (22.5) have been presented. Now the full computing model (22.7) as implemented in DEGRIAS will be described. This computing model is called kinematic model, since it is based on the rotational motions of the Earth with respect to the fixed sources, or - in other words - since the positions with respect to the Earth-fixed interferometer of a given source at several instants of observation are related via the (presumably) known algorithms for precession, nutation, Earth rotation, etc..
The following models and quantities for chapter 2 are applied:

(W) = $R_X(Yp) * R_Y(Xp)$, polar motion matrix (27.9)
(S) = $R_Z(GAST)$, the Earth's spin (27.3)
(P) = precession matrix (24.2)
(N) = nutation matrix (24.7)
(A) = aberration vector (24.15)
(G) = gravitational deflection vector (25.3)
X,Y,Z = coordinates of stations a and b in the CIO-system
(B) = (Xb-Xa, Yb-Ya, Zb-Za)
= (DX,DY,DZ), the baseline vector
(U) = the source position vector in the 1950.0 system, expressed by α (right ascension) and δ (declination)

$$= \begin{bmatrix} \cos\alpha * \cos\delta \\ \sin\alpha * \cos\delta \\ \sin\delta \end{bmatrix} \qquad (31.1)$$

τ_{CLO} = the clock function for stations a,b (23.1)
τ_{ANT} = antenna motion correction (23.3) for stations a,b
τ_{RTB} = retarded baseline correction (27.6)
τ_{ION} = ionospheric refraction correction for a,b (26.13 or 26.15)
τ_{AMB} = BWS-ambiguity correction (§2.3.3)
τ_{TRO} = tropospheric refraction correction for a,b (26.2,26.7,26.11)
τ_{TID} = solid Earth tides correction for a,b (27.14)

In DEGRIAS the following parameters are estimable in the LSQ fit:

- X,Y,Z = station coordinates in the CIO-system
- α_o, δ_o = right ascension and declination of a source in the 1950.0 system
- T0,...,T5 = six coefficients of the clock function (23.1)
- Xp, Yp = X- and Y-component (as one-day's averages) of polar motion (27.9)
- UT1 = UT1-UTC value, as one-day's averages (27.3)
- τ_{tz} = tropospheric zenith delay, the sum of (26.1) and(26.11)
- c = velocity of light in vacuo.

Differentiating the full computing model (22.7) with respect to these estimable parameters (using their approximate values) yields the following linearized observation equation (being one row of the design matrix for the LSQ fit) for stations "a" and "b" and source "i" (GHAi is the actual Greenwich hour angle, δi is the apparent declination, both corrected for gravitational deflection).

$$
\begin{aligned}
d\tau = {} & + \cos(GHAi) * \cos\delta i / c && * dXa \\
& + \sin(GHAi) * \cos\delta i / c && * dYa \\
& + \sin\delta i / c && * dZa \\
& - \cos(GHAi) * \cos\delta i / c && * dXb \\
& - \sin(GHAi) * \cos\delta i / c && * dYb \\
& - \sin\delta i / c && * dZb \\
& - 1 && * dT0a \\
& - t && * dT1a \\
& - t^2 && * dT2a \\
& - \sin(T4a*t+T5a) && * dT3a \\
& - T3a * \cos(T4a*t+T5a) * t && * dT4a
\end{aligned}
$$

$$
\begin{aligned}
&- T3a * \cos(T4a*t+T5a) && * dT5a \\
&+ 1 && * dT0b \\
&+ t && * dT1b \\
&+ t^2 && * dT2b \\
&+ \sin(T4b*t+T5b) && * dT3b \\
&+ T3b * \cos(T4b*t+T5b) * t && * dT4b \\
&+ T3b * \cos(T4b*t+T5b) && * dT5b \\
&- FZ2a && * d\tau_{tz}{}^{a} \\
&+ FZ2b && * d\tau_{tz}{}^{b} \\
&+ (\cos(GHAi) * \cos\delta i * DZ \\
&\qquad -\sin\delta i * DX) / c && * dXp \\
&+ (\sin(GHAi) * \cos\delta i * DZ \\
&\qquad -\sin\delta i * DY) / c && * dYp \\
&+ \cos\delta i * (\sin(GHAi)*DX \\
&\qquad - \cos(GHAi)*DY) / c && * dUT1 \\
&- \tau / c && * dc \\
&- \cos\delta i * (\sin(GHAi)*DX \\
&\qquad - \cos(GHAi)*DY) / c && * d\alpha_o i \\
&+(\sin\delta i * (\cos(GHAi)*DX \\
&\quad +\sin(GHAi)*DY)-\cos\delta i*DZ) / c && * d\delta_o i
\end{aligned}
\qquad (31.2)
$$

For computing the model value of the delay rate observable two possible methods exist: (1) a direct formula via the differentiated formula (22.8) and (2) a numerical differentiation of (22.7) during execution time of the input module of DEGRIAS. The disadvantage of (1) is that it is a tedious task to completely implement all the chain-rule differentiations. Therefore, in DEGRIAS only an approximate direct model for (22.8) is implemented, in which only the time-derivatives of clock function (23.2), of precession (24.3), of nutation (24.10), of aberration (24.16), of tropospheric refraction (26.4) and of retarded baseline correction (27.8) are present, so that the time-dependence of the following phenomena is neglected: gravitational deflection, ionospheric refraction, solid Earth tides, antenna motion correction and equation of equinoxes in GAST.
The numerical differentiation of option (2) is computed as:

$$\dot{\tau}(t) = (\tau(t+dt) - \tau(t-dt)) / (2*dt) \qquad (31.3)$$

with "dt" having a value of 0.5 or 5 seconds, depending on the baseline length. It is clear that the latter approach requires more computer time since precession, nutation, etc. are computed for three time-points (t,t+dt and t-dt). The advantage is that all phenomena are automatically included in the computed observation for delay rate.
The coefficients of the linearized observation equation for delay rate - which need not be so accurate - can be computed by directly differentiating the delay coefficients, using the approximation that changes result only from Earth rotation. From (27.3) one finds:

$$\Omega = dGAST/dt = 2\pi \ / \ (\text{mean sidereal day} + dUT1 + dEQE) \qquad (31.4)$$

This yields:

$$
\begin{aligned}
\dot{d\tau} = \;& - \sin(GHAi) * \cos\delta i * \Omega / c && * dXa \\
& + \cos(GHAi) * \cos\delta i * \Omega / c && * dYa \\
& + \sin(GHAi) * \cos\delta i * \Omega / c && * dXb \\
& - \cos(GHAi) * \cos\delta i * \Omega / c && * dYb \\
& - 1 && * dT1a \\
& - 2 * t && * dT2a \\
& - T4a * \cos(T4a*t+T5a) && * dT3a \\
& + T3a * T4a * \sin(T4a*t+T5a) * t \\
& \quad - T3a * \cos(T4a*t+T5a) && * dT4a \\
& + T3a * T4a * \sin(T4a*t+T5a) && * dT5a \\
& + 1 && * dT1b \\
& + 2 * t && * dT2b \\
& + T4b * \cos(T4b*t+T5b) && * dT3b \\
& - T3b * T4b * \sin(T4b*t+T5b) * t \\
& \quad - T3b * \cos(T4b*t+T5b) && * dT4b \\
& - T3b * T4b * \sin(T4b*t+T5b) && * dT5b \\
& - \dot{F\tau}2a && * d\tau_{tz}a \\
& + \dot{F\tau}2b && * d\tau_{tz}b \\
& - \sin(GHAi) * \cos\delta i * \Omega * DZ / c && * dXp
\end{aligned}
\qquad (31.5)
$$

+ cos(GHAi) * cos δ i * Ω * DZ / c	* dYp
- cos δ i * (-cos(GHAi)*DX -sin(GHAi)*DY) * Ω / c	* dUT1
- $\dot{\tau}$ / c	* dc
+ cos δ i * (-cos(GHAi)*DX -sin(GHAi)*DY) * Ω / c	* $d\alpha_o i$
+ sin δ i * (-sin(GHAi)*DX +cos(GHAi)*DY) * Ω / c	* $d\delta_o i$

No effort has been made here to express all quantities in appropriate units; therefore multiplication by 2π , etc. has been omitted. The actual units used in DEGRIAS to scale the system of normal equations are (for the most important quantities): station coordinates in Mm, observed delays in ms and source coordinates in radians.

3.2 FUNCTIONAL DESCRIPTION OF DEGRIAS

The DEGRIAS package is integrated in the SCAN-II (System for Computerized Adjustment of Networks) modular software system of the Computing Centre of the Delft Department of Geodesy which is written in FORTRAN-IV and developed by J.J.Kok. It is running on the AMDAHL 470-V7-B computer of the Computing Centre of the Delft University of Technology. An outline of DEGRIAS is presented in Figure 18.

DEGRIAS starts with the input of a number of steering parameters. These include such items as: number of stations and observed sources, parameters for statistical testing and an option list indicating the choice for the computing model (included subroutines and formula system).
DEGRIAS uses a special format for the input of the observations. One observation card contains the following data: the stations of the interferometer, the observed source, the day and time of observation and the observed delay and delay rate with their respective standard deviations. These cards can be in any sequence: per time of observation or per baseline in observing sequence, or just randomly. Observations which are not to be included in the LSQ fit can be indicated by the character "X" in the first column of the card and will automatically be skipped. If dual-frequency observations are used to eliminate ionospheric refraction, two files are read simultaneously. If one of the two observations is missing, the observation is also skipped. A third input file is used when weather data are available, for a tropospheric refraction correction according to (26.7). If required, this file can be created by separate software, called METEOINT (§3.5) which interpolates observed values for temperature, pressure and relative humidity (e.g. from weather map data if no on-site values are available) for every instant of observation.

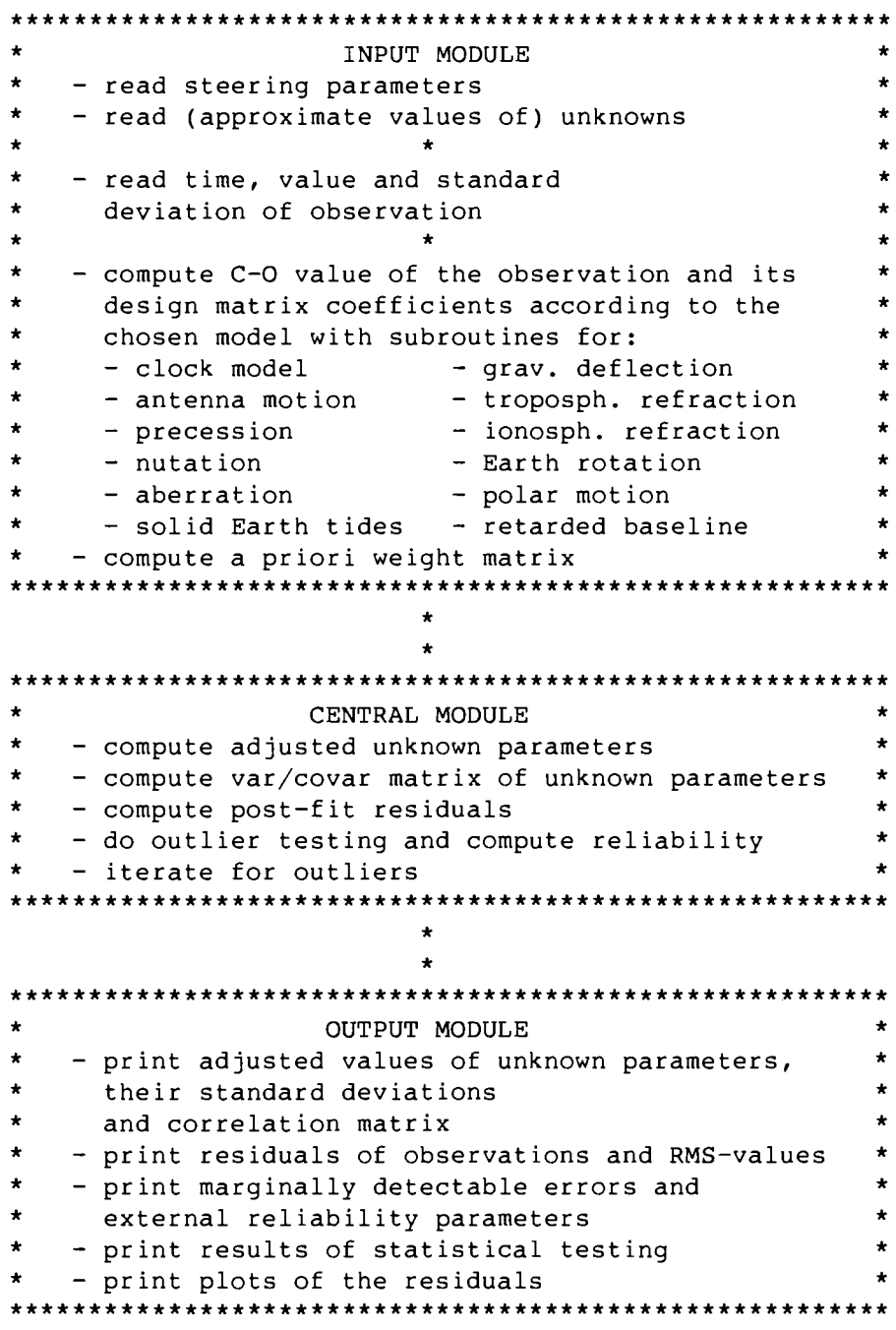

Figure 18: Outline of DEGRIAS

As a consequence of the correlation process, the a priori weight matrix of the observations is always chosen to be diagonal [Bock,1983], although DEGRIAS allows a full weight matrix. This would be especially useful for simulation studies to investigate the effect of the introduction of off-diagonal elements caused by common factors such as tropospheric refraction for baselines forming a closed triangle. The correlation process yields a standard deviation based on the signal-to-noise-ratio (SNR) of the observation which depends mainly on source strength

and length of the coherent correlation interval [Brouwer&Visser,1978]. For stronger sources, even using Mk-II BWS, the standard deviation for delay typically scatters around 0.01 ns, which equals 3 mm. This is evidently too optimistic, for the SNR is not the only item of interest, but also the behaviour of the "real world" during the entire experiment. In DEGRIAS it is therefore possible to change this SNR standard deviation by a multiplication factor or by adding an ad hoc number. In particular the latter accounts in an acceptable way for error sources that are not merely a function of signal strength (correlated flux) and provides a more equal weighting of the observations. In addition, it is possible to divide the standard deviations by the sine of the elevation, to suppress the influence of low elevation observations.

The central module applies Choleski decomposition using sparse matrix techniques [Kok,1981]. This computer storage and CPU-time saving approach allows a large number of observations and estimable parameters to be included. In the standard version of DEGRIAS therefore the following dimensions are valid for the estimable parameters:

- number of stations	20
- number of sources	40
- number of clock polynomials	50
- number of tropospheric parameters	50
- number of polar motion parameters	10
- number of UT1 parameters	10
- speed of light	1

This amounts to a total of 521 unknowns with a maximum of 2500 observations. Any of these unknowns can be constrained in the LSQ adjustment. The number of observations can easily be extended to 10000, as computer storage is no major limitation.

The statistical testing is done in two steps following the B-method of testing [Baarda,1968]. The first step makes use of the overall Fisher-test to test the zero hypothesis Ho, which consists of: (a) mathematical or computing model (design matrix and linearization), (b) probabilistic model (normal distribution and a priori variance/covariance matrix) and (c) the validity of the vector of observations with respect to these two models:

$$\sigma^2 / \sigma_o^2 \quad <? \quad F_{1-\alpha\ ;m-b,\infty} \tag{32.1}$$

with

$$\begin{aligned} \sigma^2 &= \text{a posteriori variance factor} \\ &= (\Sigma_i\ (\ v_i^2 / \sigma x_i^2)) \ /\ (m-b) \qquad (32.2) \\ \sigma_o^2 &= \text{a priori variance factor} \\ F^o &= \text{critical value of F-test} \\ \alpha &= \text{level of significance of the test (§4.3.3)} \\ m &= \text{total number of observations} \\ b &= \text{number of estimated parameters} \\ v_i &= \text{the correction (or post-fit residual) of the observation} \\ \sigma x_i &= \text{the standard deviation of the observation.} \end{aligned}$$

If the above test fails, the normalised test values "w" are computed for all observations. They are related to the alternative hypothesis that only one observation at a time is erroneous. The process of computing this series of test values is denoted by "data-snooping" [Baarda,1968]. The general formula for "w" is valid for correlated observations (43.7), but in the case of a diagonal a priori weight matrix one finds:

$$w_i = - v_i / \sigma_{v_i} \quad <? \quad \mathrm{sqrt}(F_{1-\alpha_o;1,\infty}) \qquad (32.3)$$

with σ_{v_i}= the standard deviation of the correction of the i-th observation and F the critical value and α_o the level of significance.

To enable faster operation, it is possible to iterate the LSQ solution on the basis of this w-test. It may e.g. be that a comparatively small number of observations are rejected, for instance due to a low elevation or due to an inappropriate SNR-sigma. If the option for iteration is chosen, DEGRIAS automatically downweights all rejected observations by a factor of four and computes a new LSQ solution and new test-values. This process may be repeated several times. The approach is of course only allowed if some observations are rejected more or less randomly and therefore no systematic trends are present in the residuals. Appendix D shows the validity of this process for the case of VLBI. As the LSQ solution (=the estimated parameters) hardly changes during the iterations (N.B. one should of course check this!), the main advantage of this approach is the smoother appearance of the residuals (32.5) and the test-values.

DEGRIAS enables one also to compute the marginally detectable error (m.d.e.) connected with the w-test as a measure for the so-called internal reliability. The m.d.e. is the size of error in an observation which causes the w-test to just fail. In addition, the measure $\overline{\lambda}$ is computed for the so-called external reliability [Baarda,1972]. This is the normalized length of the vector of deviations in adjusted parameters due to the above error with size m.d.e. [Brouwer,1982a]. These quantities are of special interest for design studies (chapter 4). For this purpose a random observation generator is present as well.

In addition to the data-snooping which tests for individual errors, a number of special alternative hypotheses are also formulated to test for systematic trends. The following three types are used:

- a constant bias is present in all delay observations including one specific station
- a constant bias is present in all delay observations of one specific baseline
- a constant bias is present in all delay observations made at one specific source.

For the mathematical formulation of these tests one is referred to §4.3.2 and Appendix G.

The results of the output module are clear. Due to a reordering process, the results can be printed either per baseline or in time sequence. A plot of delay and delay rate residuals is produced per baseline.
Two RMS (Root Mean Squared)-values are computed, an unweighted and a weighted one, defined as:

$$RMSu = \mathrm{sqrt}\left(\sum_{ml} (v_i^2) \;/\; (ml*(m-b)/m)\right) \qquad (32.4)$$

$$RMSw = \mathrm{sqrt}\left(\sum_{ml} (v_i^2/\sigma x_i^2) \;/\; \sum_{ml} (1/\sigma x_i^2) \;/\; (ml*(m-b)/m)\right) \qquad (32.5)$$

with ml = number of relevant observations (per baseline, delay or delay rate observables).

3.3 ESTIMABLE PARAMETERS IN DEGRIAS

In §3.1 the parameters have been mentioned that serve in DEGRIAS as unknowns in the LSQ fit. It should be recalled that every station may have several clock polynomials, depending on clock jumps or re-starts of the measurements. Furthermore, tropospheric zenith delays can be chosen for several time intervals; it may e.g. be favourable to split the measurements into night and day sections with separate tropospheric parameters. In addition, it is recalled that polar motion and UT1 parameters are computed as - at least one - day averages.
It is obvious that not all these parameters are estimable at the same time: in general the system of normal equations of the LSQ fit will be singular. This can be due to two reasons:

a) rank deficiencies due to coordinate system definition
b) rank deficiencies due to a critical configuration.

An example of the latter is the single baseline experiment with sources at only one declination. In this situation clock offset and vertical baseline component become inseparable; see e.g. [Schut,1983]. These critical configurations, however, will be dealt with in §4.4.1.

As for item a) a short discussion is necessary here:
Since Euclidean coordinates in 3-D are defined as distances with respect to certain (orthogonal) planes, they are not estimable as such [Baarda,1973]. In a Euclidean space the coordinate system definition requires 7 "conventions", because the definition is related to the number of parameters in the similarity transformation (seven for 3-D). The most common way to define the coordinate system is to constrain 7 well-chosen parameters in the LSQ adjustment. The more or less international "standard" choice for these seven parameters for VLBI is:

- the X, Y and Z coordinate of one station, to define the origin (3 translations),
- the epoch (1950.0 in DEGRIAS) ephemeris pole position to define the equatorial plane (2 rotations),

- the right ascension of one source, to define the orientation in the equatorial plane (1 rotation),
- the velocity of light in vacuo, as a scale parameter.

The Cartesian coordinate system in use in DEGRIAS is left-handed, geocentric and Earth fixed, as described in §2.2. The origin of this system is operationally defined by some arbitrary coordinates adopted for the point of intersection of the azimuth and elevation axes of one antenna, mostly Haystack, if included (e.g. MERIT Short Campaign; §3.7), as derived from, for instance, spacecraft tracking. The origin of right ascension is taken as 12h 26m 33.246s for the radio source 3C273-B at epoch 1950.0 (elliptic aberration removed) which is the quasar with the highest radio intensity and therefore practically always included in geodetic VLBI experiments. The value for the speed of light used to convert measured delays to distances is 299,792.458 km/s.
The introduction of precession and nutation in the computing model defines the ephemeris pole position at epoch time. Consequently, the definition of the Z-axis is tacitly included in the precession/nutation formulae (see (24.1): R_Z, etc.) and no unknown parameters have to be constrained explicitly.

In addition, a rank deficiency occurs as a combined effect of coordinate system definition and a critical configuration. The unknowns for polar motion and UT1 yield a singular system of normal equations if they are not held fixed to a priori values for at least one moment (=one observation; in DEGRIAS thus one day). This is due to the fact that these parameters describe a rotation of the Earth-fixed frame with respect to the stellar frame, and evidently only changes in these rotations can be monitored. It is probably more precise to state that with the kinematic model for VLBI one has to define two coordinate frames: a stellar one with only orientations (thus three directions fixed: ephemeris pole and origin of right ascension) and a terrestrial one with the standard seven parameters: three station coordinates, one scale factor and polar motion and UT1 as three orientations.
However, other conventions for the coordinate system definition may be chosen; for example:

a) Constrain seven coordinates of VLBI-stations (plus the additional three values for polar motion and UT1). As yet, this is not possible with DEGRIAS for the kinematic model since the ephemeris pole position is already implicitly fixed in the precession formulae. If one therefore fixed seven station coordinates in DEGRIAS, the LSQ fit would be overconstrained.

b) From a) it follows that a valid choice for DEGRIAS would be: to constrain five station coordinates. With the implicit assumption of pole position (and again the three Earth orientation parameters) this would define the coordinate frame completely and make e.g. the right ascension of 3C273-B estimable.

c) The use of a minimum norm solution: this yields a minimal trace for the variance/covariance matrix so that smoother looking variances appear (cf. the larger sigma ellipses in plane geodetic networks, away from the two constrained points). This solution is not directly pos-

sible in DEGRIAS because the inversion routine cannot handle a general inverse, but requires an explicit indication of the constrained unknowns.

It is stressed, however, that in principle these solutions are the same, because the "real world" does not change when describing it with the aid of a different coordinate frame. Therefore, a relation exists between these solutions. [Baarda,1973] called this relation S-transformation. For the background to this, one is referred to chapter 6 and Appendix E.

In addition it is mentioned that for the clock polynomial the same situation occurs as for the station coordinates. Time is a one dimensional phenomenon. Therefore origin ("zero point" of time) and scale (the length of the second) must be defined. For the origin this can be done by assuming the clock offset at one of the stations to be zero. By putting the clock drift of this station also equal to zero, the unit of time is defined as the length of the second of this clock at any given moment. The same holds for other terms in the clock function (23.1). This is because only time differences are measured.

An interesting interdependence, however, can be observed between clock-drift and speed of light. Consider the situation of Figure 19. The times of arrival of the signals are recorded as ta and tb. Let the rates with which the two clocks are running with respect to "real" time be: la and lb. For "real" time one can think of the time frame belonging to the adopted speed of light (coordinate time).

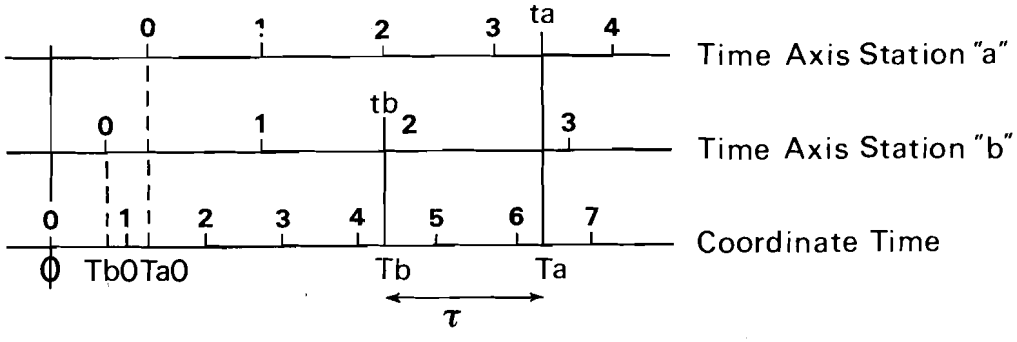

Figure 19: Clock Time-scales

Then the following relations hold:

$$ta = (Ta - Ta0) / la$$
$$tb = (Tb - Tb0) / lb \qquad (33.1)$$

The delay resulting from the correlation process is (22.1): $\tau = tb-ta$. The time difference, however, that belongs to the coordinate time frame is $\tau_g = Tb-Ta$, where τ_g is the geometric delay, or the inner product (22.2) of (B) and (U). Now the following relation exists:

$$(tb - ta) = (Tb/lb - Ta/la) - (Tb0/lb - Ta0/la) \qquad (33.2)$$

so that

$$\tau = \tau_g/lb - (Tb0-Ta0)/lb + (la-lb)/lb*ta \qquad (33.3)$$

One immediately sees the scaling effect of the clock drift at station "b". The speed of light and the clock drift have therefore the same background and consequently they have also an equal impact on the solution. Constraining the speed of light in the LSQ adjustment thus makes the clock drift at one station ("b") estimable.
Due to the term (la-lb)/lb*ta, the clock drift of station "a" is in principle also estimable. However, because of the very small coefficient - (la-lb) is of order 10^{-14} - this is not possible in practice. Hence not all clock drifts are estimable if the speed of light is constrained, or, put the other way, constraining one clock drift does not yield an estimable speed of light.

3.4 DATA ANALYSIS PROCEDURE

This section is included here to present an idea of how the data handling for ERIDOC and MERIT-SC was done and to serve as a guide to others.

The analysis starts with a tape containing approximate values for source and station coordinates plus observations with timing and corresponding formal errors. DEGRIAS input requires a special format for the observations (§3.2). Therefore, an interface exists to transform the observation file from the commonly used NGS-format [Carter,1981] to the DEGRIAS-format. This programme is called NGSFORMAT; see §3.5. Possible other formats can, via some minor actions , also be transferred to the DEGRIAS-format. Four files are needed, containing: steering parameters and station/source coordinates, observations, observations at a second frequency (for ionospheric refraction correction) and meteo data respectively, of which the last two are optional.
Then the analysis is continued with the following steps:

1. Delete observations via the character X (§3.2) with an obviously poor formal error, since a formal error considerably above the average noise level of the observations usually indicates that there is something wrong with the corresponding observation, rather than that this observation is simply of lower precision.

2. Make an LSQ fit of the first 2-3 hours of data of the experiment with clock offset and clock drift as the only unknown parameters. Apply - if required - the automatic ambiquity elimination procedure here (§2.3.3). At the same time, the C-O values can be used to eliminate large outliers. This should be done for n-1 baselines, if n is the number of stations, to establish values of clock offset and drift parameters for all stations. Note that dual-frequency observations for the determination of ionospheric refraction cannot be applied before all ambiguities are eliminated. In particular, when ionospheric

corrections have almost the same magnitude as the ambiguity spacing, the application of the ionosonde model is helpful (§2.6.3).

3. Now one has some estimates for clock offset and drift, iterate step 2 for larger portions of observations to find better estimates for the clock parameters and station coordinates and to eliminate the ambiguities on all other baselines as well. Do not hesitate to introduce clock breaks in the clock function of a station to speed up this iteration procedure by separating the observations into sections.
   It is advisable to exclude observations taken at elevations below 10 degrees in this procedure, because of the uncertainties in the tropospheric refraction correction.

   Note: It is probably advisable to eliminate observations taken at elevations below 10 degrees completely, even in the final adjustment; see §2.6.1 and Appendix B.

4. The triangle-condition, commonly known as closure phase, can be used to eliminate any remaining ambiguities in the delay observations and - as only single baselines have been considered so far - any confusion between clock offset and ambiguity spacing. Since the closure phase relation is implicitly included in the adjustment model (31.2), special software exists to compute the closures in the triangles. The input to this TRIANGLE programme is the observation file. These observations are then corrected for retarded baseline (27.6), because otherwise the triangle will not close. The output consists of a list of all closures and a list of the observations not included in any triangle condition. The latter observations are somewhat suspect since they are less well-checked in the LSQ adjustment and errors may pass undetected. Also on the basis of these closures, observations can be excluded.

5. Make an improved LSQ adjustment for all single baselines with more unknown parameters. This offers the opportunity of eliminating bad observations on the basis of the w-test (§3.2). In the present approach, only at this stage are delay rate observations included in the adjustment since the following rule, although not strictly necessary, is applied: if the delay observable is excluded in the LSQ fit, the delay rate observable is excluded as well; the opposite does not hold.

6. Compute the overall multi-station LSQ solution with all possible estimable parameters using, where required, the iteration procedure and applying the special alternative hypothesis testing (§3.2) to assess the final accuracy.

For a single baseline experiment the analogous procedure is followed with DEGRIAS, without step 4, of course.

3.5 DEGRIAS SYSTEM SUMMARY AND IMPROVEMENTS

The complete data-flow through the DEGRIAS system is shown in Figure 20. The tasks of the input, output and central module of DEGRIAS are presented in detail in Figure 18.
As yet, DEGRIAS is a prototype software package: all relevant items are present, but both the coding and the internal organization are not (yet) optimal for use in a production manner. The envisaged improvements are mentioned here:

- the change of programming language from standard FORTRAN-IV to standard FORTRAN-77,
- the introduction of the improved IAU J2000 system in the computing model, plus some other (minor) changes in this model,
- an automatic iteration with improved estimates for unknown parameters,
- further optimization of use of CPU time and computer storage in view of the large number of observations compared to the number of estimable parameters,
- the integration of NGSFORMAT, METEOINT, TRIANGLE and SORTOBS in the INPUT and OUTPUT modules of DEGRIAS,
- better plot facilities for post-fit residuals,
- additional non-conventional hypotheses, e.g. tests for errors in certain corrections, or the introduction of multi-variate linear hypothesis tests [Kok,1984],
- the introduction of more estimable parameters. Good candidates are: the precessional constant, the aberration constant, the Love numbers and phase lag of solid Earth tides and the gravitational bending parameter (25.2),
- the improvement of the numerical differentiation for delay rate. Computations are in principle only required for two time points (t+dt and t-dt) if the data for the observation equation are determined via interpolation as well.

3.6 EXAMPLE I: ERIDOC VLBI CAMPAIGN

3.6.1 General Information

The fourth objective (§1.4) of the research project which led to this publication was to cooperate in the organization of VLBI experiments and to carry out the analysis of the data obtained.
In 1980 a programme of four geodetic VLBI experiments was started within the European network of radio astronomy observatories. This programme was denoted by the acronym WEJO, for the initials of the four major participants. The joint responsibility lay with the Geodetic Institute of the University of Bonn (D) and the Department of Geodesy of the Delft University of Technology. The programme was designed to gain experience with geodetic VLBI measurements on a European scale and to finally serve the objectives of §1.2.

The first campaign took place in October 1980 but due to a number of technical failures only the measurements on the baseline Effelsberg (D) to Metsähovi (SF) could be correlated. Baseline results were presented in [Beyer et al.,1982]. WEJO-3 was a complete failure in December 1981.

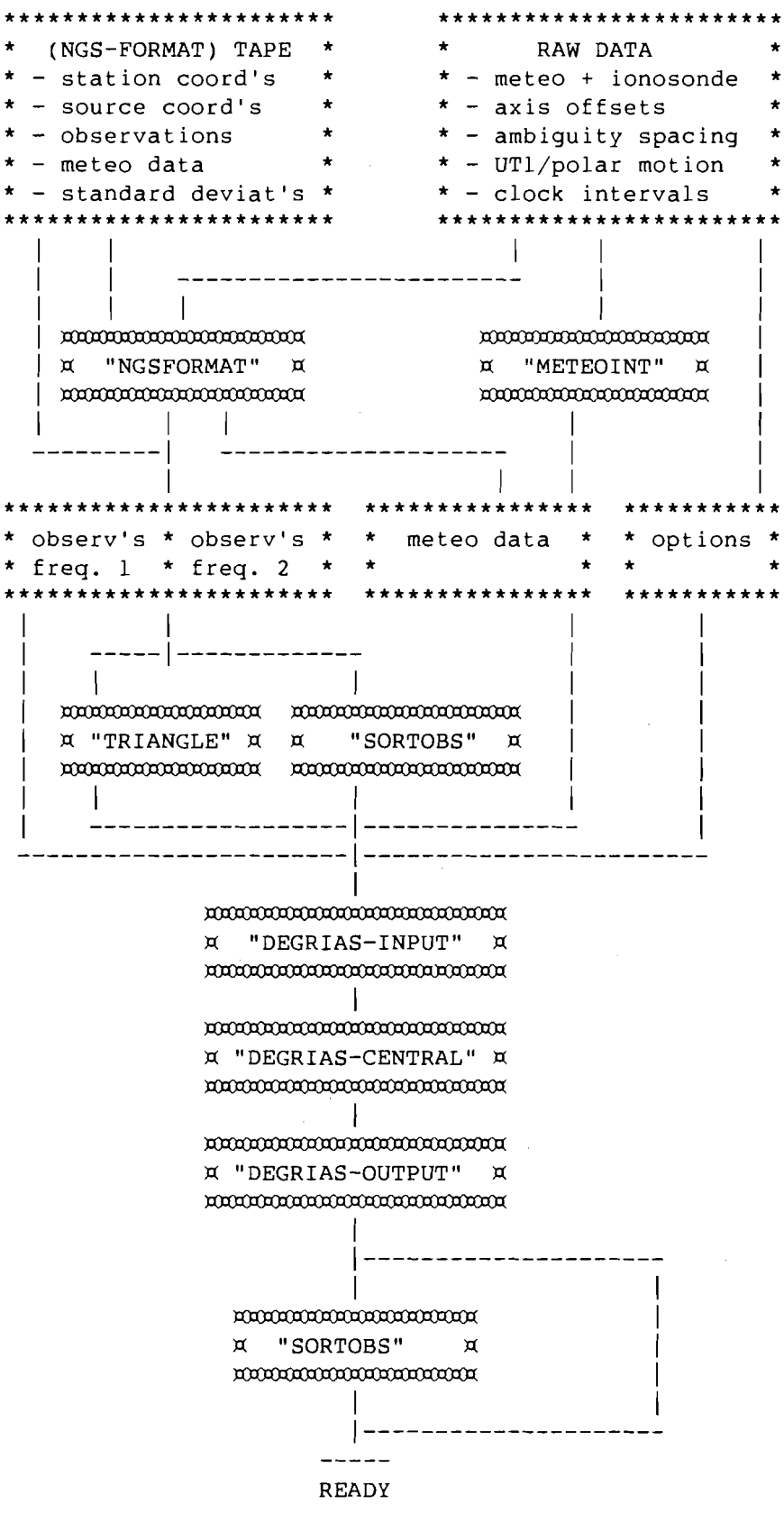

Figure 20: Data Flow in DEGRIAS Software Package

Snowfall and high winds prevented any observations at Onsala (S); the recording equipment was out of order at Jodrell Bank (GB) and a wrong frequency setting hampered observations at Westerbork (NL). As Effelsberg was the only station left, no correlation could be done. The last campaign with the same four observatories (December 1982) has been successfully correlated for the most part, but no baseline results are reported.

The second, most successful experiment took place in April 1981 and was called: Project ERIDOC (European Radio Interferometry and DOppler Campaign). In the project, simultaneous VLBI and Doppler satellite positioning campaigns were conducted between those European radio observatories that were or may in the future be equipped with VLBI recording systems. In this way, the performance of the VLBI system on a European scale could be tested and compared with the Doppler system; in addition, precise Doppler positions would be available for as yet non-operational VLBI observatories.
Co-located VLBI and Doppler satellite observations were thus made at five radio observatories: Effelsberg (D), Westerbork (NL), Chilbolton (GB), Jodrell Bank (GB) and Onsala (S); see Table 5. Thirteen other Doppler stations also took part in the campaign, five of them located at satellite laser observatories, to provide a connection to the laser network as well. Those stations were: Dwingeloo (NL), Robledo (E), Weilheim (D), Wettzell (D), Bologna (I), Graz (A), Leeuwarden (NL), Herstmonceux (GB), Kootwijk (NL), Dionysos (GR), Florence (I), Brussels (B) and Metsähovi (SF); see Figure 21.

Table 5.

ERIDOC VLBI Stations

Station	Antenna diameter (m)	Mount type	Axis offset (m)	Clock system
Westerbork (dish B)	25	EQ	4.95	Rubidium
Effelsberg	100	AltAz	0.0	H-Maser
Jodrell Bank (MkII)	26*38	AltAz	0.47	Rubidium
Onsala (OSO 25.6)	25.6	EQ	2.15	H-Maser
Chilbolton	20	AltAz	0.31	H-Maser

The VLBI session lasted from April 12, 18h UT to April 13, 18h UT and the Doppler observations from April 7, 0h UT to April 16, 24h UT. By this simultaneity of the observations uncertainties in the changes of orientation of the reference frames due to precession and nutation on the one hand and polar motion and UT1 on the other, do not enter into the comparison results.

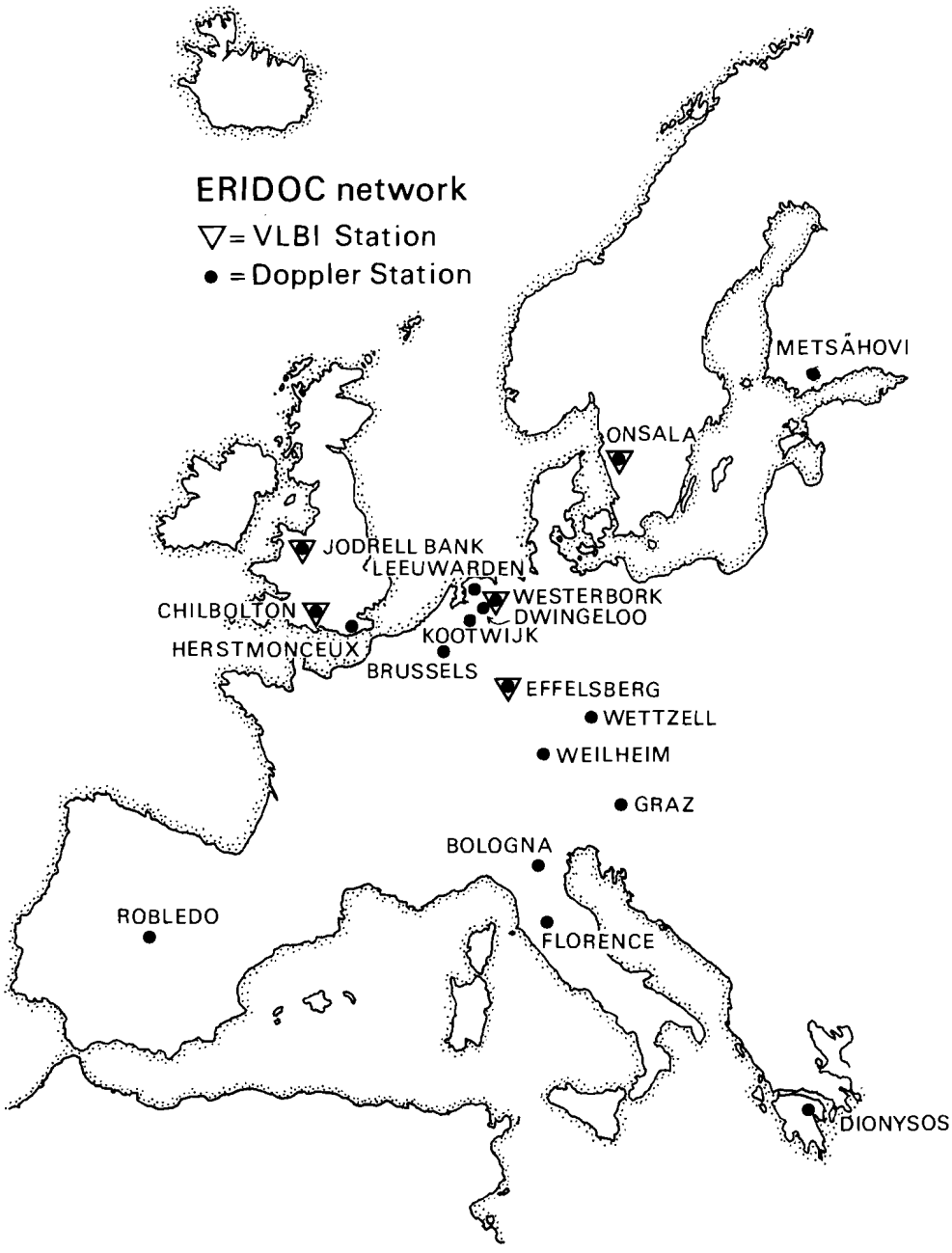

Figure 21: ERIDOC Network

The data were analysed independently at the two computing centres Bonn and Delft, and a report is presented in [Brouwer et al.,1983]. Although most of the results are already available in this paper, a short review of the achievements is given here, because the data are connected to one of the main objectives of the present research project (§1.4) and the results of the updated VLBI solution presented here with the aid of DEGRIAS are used in chapter 6 to illustrate the necessity of the use of rigorous comparison techniques.

At the time of ERIDOC, not all observatories were equipped with a Mk-III recording system. Due to the accuracy limitations of the Mk-II system, a sequential bandwidth synthesis (BWS) technique was used in order to improve the delay resolution of the 6-cm observations (§2.3.3). On the European scale a two channel approach was considered to be the best choice, because it minimizes the loss in sensitivity and was relatively easy to implement. This 40 MHz two channel approach (odd seconds on 4990 MHz; even seconds on 5030 MHz) yields a theoretical precision of about 0.25 ns in the BWS-delay, but leaves an ambiguity spacing of 25 ns. With the relatively high signal-to-noise-ratio (SNR) provided by the rather sensitive European station configurations, the non-ambiguous single channel BSA-delays (§1.3.4) tend to be fairly accurate (between 1.5 and 5 ns) and can thus be included in the LSQ solution.

A relatively simple observing schedule was used with fixed 15 minute scans, including a varying portion of time for slewing. This schedule was compiled by the SCHED module of DEGRIAS (§4.3).

3.6.2 ERIDOC multi-station solution

The ERIDOC VLBI measurements were not completely successful from a technical point of view due to a number of factors. Onsala, for instance, could only observe during the second half of the campaign due to a recorder malfunction. The BWS-delays on all baselines involving either Westerbork or Jodrell Bank were corrupted by strong sinusoidal phase variations during the integration interval. The exact cause of these variations has not been established, but is connected to insufficient stability of the rubidium standards or the two synthesizers. At Chilbolton, the H-maser was not operational during 12 hours of the session and also showed a somewhat lower stability performance than usual for the remainder of the campaign. Moreover, its 6 cm receiver had a relatively high system temperature.
In this way, the BWS-delays on the Effelsberg-Onsala baseline proved to be the only ones fully consistent with the two channel 40 MHz BWS-accuracy level expected from theory.

For the ERIDOC analysis, the "standard" coordinate system definition of §3.3 was used, with for the Effelsberg coordinates as the arbitrary values of Table 6. For the LSQ adjustment the "kinematic" model of DEGRIAS was chosen with the following features:

- fixed source positions as published in [Fanselow et al.,1981],
- precession defined by the J2000 precessional constant transformed to the 1950.0-system,
- second order polynomials as clock function where required,
- tropospheric zenith path delays computed from interpolated weather data based on readings every 3 or 6 hours,
- the ionosonde ionospheric correction model, based on data observed at the KNMI in De Bilt (The Netherlands)

The latter three items in particular, are included as improvements in the present solution as compared to that presented in [Brouwer et al.,1983].

In the ERIDOC campaign 10 baselines are present, each with two BSA channels and one BWS channel. Due to the technical problems described above, only the BWS data of the EFF-ONS baseline were fully usable so that a simultaneous LSQ fit was made to the observations of one BWS and 20 BSA baselines. After removing bad observations with the w-test (32.3), a total number of 1029 group delay observations and 877 delay-rate observations were used in the adjustment, each with a weight based on its SNR.

Table 6.

ERIDOC VLBI Coordinates

STATION	X (m)	Y (m)	Z (m)
Effelsbg	4033911.00	-487046.00	4900424.00
+/-	.0	.0	.0
Westerbk	3828565.81	-443931.86	5064915.40
+/-	0.07	0.04	0.13
Chilbltn	4008274.97	100595.26	4943788.22
+/-	0.17	0.18	0.41
Jod.Bank	3822812.23	153747.33	5086279.44
+/-	0.10	0.08	0.20
Onsala	3370929.24	-711520.42	5349657.18
+/-	0.02	0.02	0.04

In the LSQ fit 58 unknowns were estimated, comprising: coordinates of four stations and 18 clock polynomials. The latter is due to a number of clock breaks. Second-order terms were only introduced at those stations where the Googe number (§4.2.1) indicated that the parameter would be estimable. The multi-dimensional F-test (32.1) yielded a result of 0.795 with critical value 1.000 with α = 5%, indicating that the estimated formal error is a little pessimistic. The estimated coordinates and their (formal) standard deviations are presented in Table 6.
In Table 7 the computed baseline lengths are shown, together with their formal errors and the weighted RMS-values of the post-fit residuals (32.5). In general it can be stated that the overall precision of the ERIDOC Mk-II BWS VLBI results is around 20 cm.
The major conclusion of this campaign, however, was that it proved to be feasible to perform geodetic VLBI on a European scale at the cm level, even using a two channel 40 MHz Mk-II BWS-scheme if hydrogen masers were to become available at all stations.

Table 7.

ERIDOC Baseline Lengths

BASELINE	length (m)	formal error (m)	RMS (ns)
EFF-JOD	699,800.71	0.09	1.70
EFF-CHI	589,796.51	0.18	2.01
EFF-WES	266,613.77	0.09	1.56
EFF-ONS	831,711.51	0.02	0.20
JOD-ONS	1,011,065.95	0.09	3.54
CHI-ONS	1,109,266.01	0.22	13.01
WES-ONS	601,758.04	0.07	3.59
JOD-WES	598,088.57	0.09	3.86
CHI-WES	586,069.08	0.20	5.32
JOD-CHI	239,844.36	0.29	14.93

3.7 EXAMPLE II: MERIT SHORT CAMPAIGN

3.7.1 General Information

Project MERIT is the cooperative effort of IAU and IUGG, sponsored by COSPAR, "to Monitor Earth Rotation and to Intercompare the Techniques of observation and analysis". The main objective of this project is to measure polar motion and UT1-UTC as accurately and intensively as possible with all available techniques (optical astrometry, Satelite Laser Ranging (SLR), Lunar Laser Ranging (LLR), Satellite Doppler, CERI (§1.1) and, naturally, VLBI), to intercompare the results of the individual techniques and thus to have a better understanding of the phenomena that excite the regular and sudden changes in Earth rotation and polar motion [Wilkins,1980]. The main measurement campaign of MERIT was held from 1983 September 1 to 1984 October 31, thus spanning a complete period of the Chandler Wobble.
To provide realistic tests of the types of operational arrangements that were required during the main campaign and to provide high-quality observational data for scientific analysis and for use in a preliminary intercomparison of the techniques, a test was held during a three-month period (1980 August 1 to October 31), called: the MERIT Short Campaign, here denoted by: MERIT-SC. One part of this MERIT-SC consisted of a series of fourteen sessions of 24 hour VLBI observations at the following observatories (not all stations observed for the whole series); see Figure 22:

1. Haystack Radio Observatory, USA
2. Harvard Radio Astronomy Observatory, USA
3. Owens Valley Radio Observatory, USA
4. Onsala Space Observatory, Sweden
5. Chilbolton Radio Observatory, United Kingdom
6. Effelsberg Radio Observatory, Federal Republic of Germany

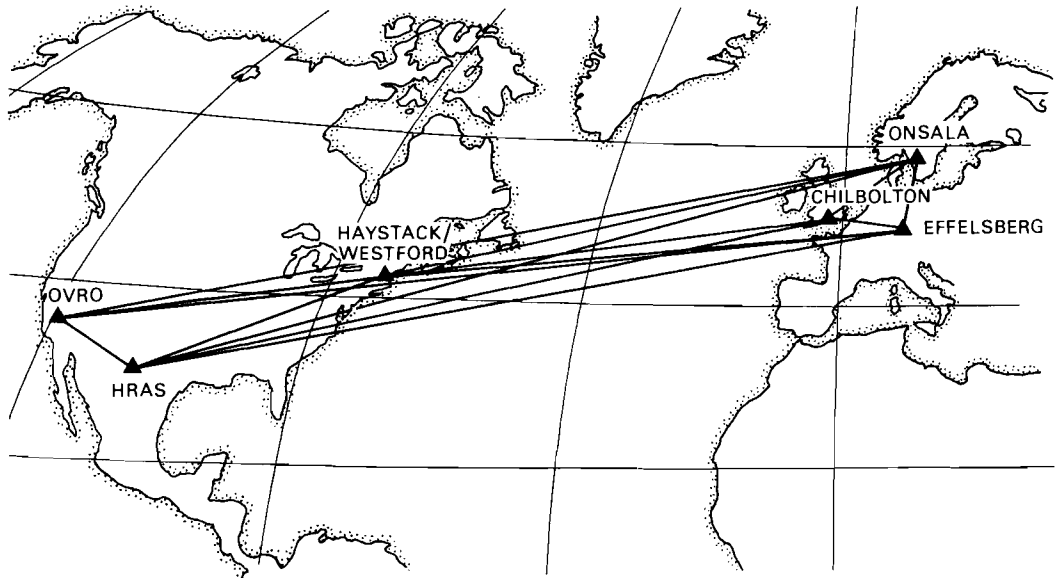

Figure 22: MERIT-SC Network

The observations were made using the Mk-III recording system with approximately 140 scheduled delay and delay rate S- and X-band values per baseline per day. Each value represents an observation (integration) of about 110 seconds. For the elimination of ionospheric refraction and for increasing the precision of the observations by means of the BWS-technique, eight X-band channels (near 8.3 GHz) and six S-band channels (near 2.2 GHz) were recorded. The ambiguity spacing was 20 ns for X-band and 40 ns for S-band, and theoretically, depending on the sensitivity of the telescopes, a delay accuracy of about 0.2 to 0.3 ns could be expected.

Here an analysis is made of the observations during the first 48 hours of this MERIT-SC (September 26, 21h UT to September 28, 20h UT). The cooperating observatories during this period were the above stations except Chilbolton. Information about the MERIT-SC for Earth rotation determination can be found in [Robertson&Carter,1981].
The objective of the present analysis is twofold. In the first place, it provides a validation of the DEGRIAS software package by comparing the results with previously reported data, especially [Carter,1983]. Secondly, some studies are done in §3.7.3 about "deformations" of the network when slight changes in the computing model or in the number of observations are made. The latter analysis is comparable to the one in §2.8, but now a network is considered with actually observed data.

Table 8.

Number of Scans per MERIT-SC Baseline

BASE-LINE	SCHEDULED SCANS	CORRELATED SCANS	ACCEPTED DELAYS	
			no.	%
HAY-ONS	240	231	89	39
HAY-OVR	240	194	57	29
HAY-HRA	240	183	56	31
HAY-EFF	240	209	90	43
EFF-ONS	240	226	179	79
EFF-OVR	240	160	95	60
EFF-HRA	240	151	108	72
ONS-OVR	240	180	88	49
ONS-HRA	240	173	85	49
OVR-HRA	240	185	136	74
%	100%	79%		41%

3.7.2 MERIT-SC: Reference Fit

The "reference fit" is a DEGRIAS LSQ fit to the data of the part of MERIT-SC described above, which includes all relevant options. The phrase "optimal solution" is deliberately not used, as this thesis is concerned with the principles, assumptions and methods of geodetic VLBI. The objective was therefore not to deliver an optimal solution for the MERIT-SC, but to assess a general validation of DEGRIAS and geodetic VLBI.

This reference fit is taken as the one with delays only. The analysis of the observed data was carried out on the basis of the procedure of §3.4. From Table 8 the large drop-out of observations on all Haystack baselines is immediately obvious. The reason for this is that due to an error in the steering computer, all pointings of the Haystack antenna towards the West were wrong and the observations therefore useless; compare the percentages: about 30% for the baselines to HRAS and OVRO (West) and about 40% to Effelsberg and Onsala (East)! Of course this has some impact on the reliability and comparability of the results presented here. For the other baselines, the figures in Table 8 are typical for a global VLBI-experiment. Reasons for the differences between the number of scheduled scans and successfully correlated scans are primarily visibility (some sources are not observable by the longest baselines and the telescopes were idle at that moment) and in addition equipment failures, bad spots on the tape, etc.. The additional decrease in the number of accepted observations is partly due to the same problems and partly to poor environmental conditions (e.g. low elevations) so that the observations do not fit the computing model. They are excluded from the LSQ fit either on the basis of the closed triangle condition (§3.4) or on the basis of the w-test (32.3).

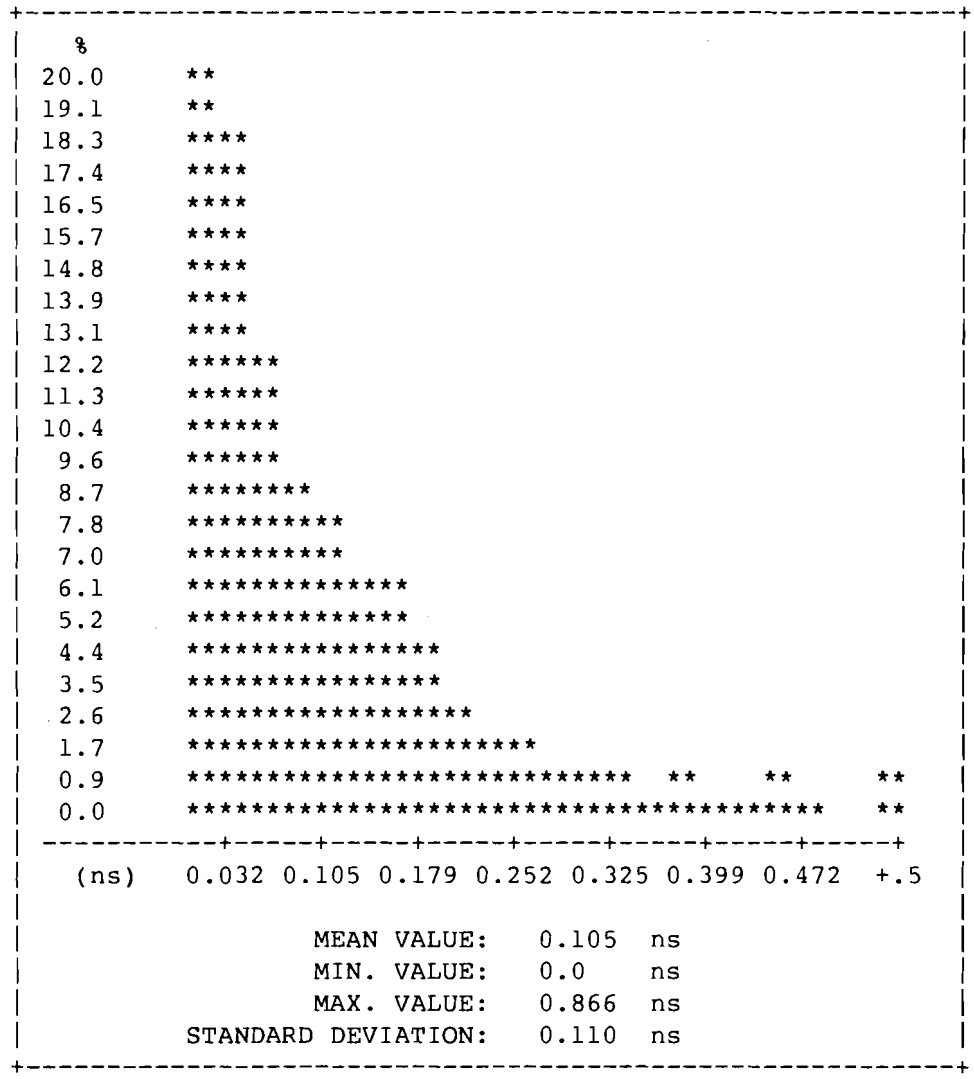

Figure 23: Closures of MERIT-SC Triangles

A histogram with the closures of 768 triangles before the final editing of the observed data was done, is shown in Figure 23. From this histogram it follows that the maximum closure is 0.866 ns. The mean value, however, is only 0.105 ns. Hence, a few observations still have to be excluded! To compute these closures, the observations are corrected for the retarded baseline effect. Without this correction, closures will be found with a mean value of 4.6 ns and a maximum value of up to 22.8 ns, which equals about 7 metres.
The distribution per source of the 983 delays which were finally accepted is given in Table 9. Note that relatively few observations are present for low declination sources.

As regards the LSQ fit, the coordinate system definition is the same as for ERIDOC, but with adopted arbitrary coordinates for Haystack (Table 10). For the computing model the kinematic model was chosen for epoch 1950.0 with the J2000 precessional constant; the corrections for tropos-

Table 9.

Sources Used in MERIT-SC

OBJECT	No. OBS	RIGHT ASCENSION h m s (1950.0)			DECLINATION o ' " (1950.0)			SPECIAL HYPOTHESIS w-TEST
0106+013	17	1	6	4.518	1	19	1.074	5.91
4C67.05	62	2	24	41.134	67	7	39.338	3.25
0235+164	55	2	35	52.619	16	24	3.880	1.08
NRAO150	75	3	55	45.228	50	49	20.068	1.42
0552+398	123	5	52	1.373	39	48	21.924	0.16
OJ287	90	8	51	57.230	20	17	58.596	0.08
4C39.25	126	9	23	55.294	39	15	23.828	0.26
3C273-B	15	12	26	33.246	2	19	43.471	5.78
OQ208	69	14	4	45.628	28	41	29.524	0.04
3C345	97	16	41	17.640	39	54	10.991	1.20
1642+690	105	16	42	18.142	69	2	13.428	2.94
2134+00	11	21	34	5.226	0	28	25.020	0.10
VRO	88	22	0	39.388	42	2	8.331	0.40
3C454.3	50	22	51	29.534	15	52	54.184	0.84

pheric zenith delay were based on surface meteo readings and a clock function was chosen which was valid for two days with five unknowns: offset, linear drift and sine wave. All source positions were estimated except those of the low declination sources 0106+013, 2134+00 and 3C273-B which were scarcely observed. The pole position and UT1-parameter were determined for the 28th September. The a priori standard deviations, based on the SNR of the correlated signals, ranged from 0.09 to 0.35 ns (depending on baseline and observed source) with an average value of 0.19 ns.

In this way, 62 unknowns were estimated in the LSQ fit. The most important results of this adjustment are shown in Table 10: the coordinates of the stations and their corresponding formal errors.
The multi-dimensional F-test (32.1) with a level of significance of 5%, yielded a value of 1.5, indicating that some improvements in the model or updating of the observed material would be possible. Only four individual observations were left rejected as they had a w-value just above the critical value. As regards the special alternative hypothesis testing (Table 9), it became clear that there are indeed some problems with the low declination sources, because both 0106+013 and 3C273-B are rejected with a w-value of about 5.8 (critical value 3.3). The marginally detectable error (§4.2.3) for these tests was about 0.18 ns, so that a constant bias of more than 0.3 ns for the corresponding observations is present. This indicates the influence of refraction, because all the observations were made at low elevations.

Table 10.

MERIT-SC Station Coordinates

STATION	X (m)	Y (m)	Z (m)
Haystack	1492406.691	4457267.330	4296882.102
+/-	.0	.0	.0
OVRO	-2409598.948	4478357.281	3838603.839
+/-	.029	.062	.060
HRAS	-1324207.728	5332028.819	3232118.815
+/-	.030	.097	.069
Onsala	3370598.846	-711919.776	5349830.519
+/-	.060	.047	.084
Effelsbg	4033940.609	-486993.888	4900430.445
+/-	.059	.048	.079

Since hardly any baseline components can be found in the literature, for reference purposes the baseline lengths as computed from these coordinates are listed in Table 11, together with the differences with respect to the results of [Carter,1983] and the corresponding formal errors and weighted RMS-values and special alternative hypothesis test values (critical value 3.3). From these tests it is clear that error sources as a function of source are more significant than biases per baseline. The error detectable by these tests was about 0.1 ns.

As was to be expected, the estimated baseline lengths are not the same as the ones of [Carter,1983]; exact similarity would even have been suspicious, e.g. because in this reference fit no delay rate observations are included and because of the problems with the Haystack pointings. It is obvious from the differences (column 3 of Table 11) that the overall scale of the network of this DEGRIAS solution is smaller: the four longest baselines are all about 20 cm shorter. In addition, it can be stated that Haystack "moves" to the East, because HAY-EFF and HAY-ONS are both 10 cm shorter and HAY-HRAS and HAY-OVRO both about 10 cm longer. This leads to the conclusion that Haystack also moves in height. The explanation is of course that the lack of observations towards the West means that the estimated tropospheric zenith delay parameter is poorly determinable. Consequently, via the correlation, the local height coordinate of the station becomes biased. With this in view, the correspondence between the DEGRIAS results and those of [Carter,1983] can be considered as within the error limits.
At any rate, for the Haystack-Onsala baseline e.g., the following results can be found as adjustment results (in metres):

5,599,714.63 [Shapiro et al.,1979]
5,599,714.69 [Herring et al.,1981]
5,599,714.54 [Robertson&Carter,1981]

Table 11.

MERIT-SC Baseline Lengths

BASELINE	DEGRIAS length (m)	DEGRIAS minus [Carter,83] (cm)	formal sigma (cm)	RMS (ns)	baseline bias hypothesis test	one observ. more (cm)
EFF-ONS	832210.535	0	1	0.12	4.52	0
EFF-OVR	8203742.438	- 20	5	0.28	4.85	+6
HRA-ONS	7940732.094	- 13	8	0.27	1.80	+19
HRA-OVR	1508195.371	0	2	0.19	0.91	+4
EFF-HRA	8084184.714	- 30	8	0.25	0.18	+19
OVR-ONS	7914130.941	- 16	5	0.22	0.78	+6
HAY-ONS	5599714.414	- 11	3	0.24	3.44	+1
HAY-HRA	3135641.130	+ 10	3	0.16	0.17	+7
HAY-OVR	3928881.745	+ 9	3	0.21	2.44	+3
HAY-EFF	5591903.458	- 16	3	0.28	1.10	+1

5,599,714.53 [Carter,1983]
5,599,714.43 [Rogers et al.,1983]
5,599,714.51 [Lundqvist,1984]
5,599,714.41 [present publication]

The most recent information about a series of intercontinental baseline determinations can be found in [Lundqvist,1984]; cf. also [Thomas et al.,1983].

3.7.3 MERIT-SC: Alternative Fits and Stability

3.7.3.1 One observation more

To demonstrate the possible influence of one single observation on the LSQ estimates, the results are reproduced here of an alternative fit for MERIT-SC. The difference is just that one additional observation of source 2134+00 by the baseline Effelsberg-HRAS is included. The observing elevations are 32.6 and 11.1 degrees respectively. At the time of the observation (day 270, 22h 58m UT) the local zenith angles of the Sun were 131 and 68 degrees.
The differences in estimated baseline lengths with the reference fit are shown in the last column of Table 11. From these numbers it follows that a difference of only one observation yields a maximum change in baseline length of 19 cm!!! Inspection of the test results reveals that the w-test for this observation has a value of 3.95 with a critical value of 3.29, so that the observation is only narrowly rejected, with a post-fit residual of 0.75 ns. The marginally detectable error (43.8) is, in addition, about twice the average value for this baseline and the

external reliability parameter (43.11) has a value 5.45, whereas the average value is one. Possible errors in this observation therefore have a large impact on the estimated parameters.
Hence, this observation has a very poor reliability, and when an error is present, the geometry of the solution is severely corrupted. The main reason for such an error in this observation is of course the low elevation. The effect is so large because the source was not observed often, twelve times in total and only once by this baseline. In addition, it should be noted that the results of the special hypothesis test remain about the same: 0.23 vs. 0.10 (Table 11) with a critical value of 3.29. It is therefore obvious that just this single observation is erroneous. Even taking into account the non-optimal DEGRIAS computing model (of which the sizes of the m.d.e. and $\bar{\lambda}$, however, are independent), it follows from this example that for many observations it is also necessary to inspect all observations individually.

3.7.3.2 Excluding subsets of observations

To analyse the stability of the multi-station fit further, in Table 12 the differences with respect to the reference fit are shown for the following cases:

1. No EFF-OVR baseline observations included
2. No HRA-ONS baseline observations included
3. No HRA-OVR baseline observations included
4. No EFF-HRA baseline observations included
5. No OVR-ONS baseline observations included
6. No HAY-ONS baseline observations included
7. No HAY-OVR baseline observations included
8. No HAY-HRA baseline observations included
9. No EFF-ONS baseline observations included
10. No HAY-EFF baseline observations included
11. All baselines with station OVRO excluded
12. All baselines with station HRAS excluded
13. All baselines with station EFF excluded
14. All baselines with station HAY excluded
15. All baselines with station ONS excluded
16. All observations of source 0106+013 excluded

Run 16 was included because of the results of the special alternative hypothesis testing of §3.7.2. The analogous elimination of observations of all sources other than 0106+013 yielded changes in baseline length below the 2 cm threshold, which are not reproduced here.
As a main impression from these results, it can be stated in the first place that the stability of the network solution is not very good. Several examples can be found where changes with a magnitude of about the standard deviation of the estimated baseline length are caused by excluding a number of observations. That this is purely a matter of poor reliability is indicated by the fact that no significant differences are found between the multi-dimensional F-test values (32.1). Since possible errors in the set of observations or in the computing model cannot therefore be detected by statistical testing of the main LSQ fit alone, it is recommended that such a comparison of a series of fits should al-

Table 12.

Comparison of MERIT-SC Results I (cm)

RUN	1	2	3	4	5	6	7	8
EF-ON	0	0	0	0	0	0	0	- 1
EF-OV	-	0	3	- 1	1	1	- 1	0
HR-ON	- 4	-	- 6	- 2	0	0	1	6
HR-OV	- 1	0	-	- 1	0	0	- 1	2
EF-HR	- 5	0	- 5	-	- 1	0	0	6
OV-ON	- 3	0	2	- 1	-	1	0	- 1
HA-ON	- 2	1	2	1	0	-	0	1
HA-HR	- 2	0	- 1	0	0	0	- 1	-
HA-OV	- 1	0	3	0	0	0	-	3
HA-EF	- 2	1	3	1	2	- 1	- 1	2

RUN	9	10	11	12	13	14	15	16
EF-ON	-	0	0	0	-	0	-	- 2
EF-OV	8	5	-	0	-	13	7	- 7
HR-ON	- 7	6	-11	-	- 1	23	-	-10
HR-OV	- 1	1	-	-	0	0	- 1	- 2
EF-HR	7	6	-13	-	-	23	5	- 9
OV-ON	- 7	5	-	- 1	- 1	14	-	- 8
HA-ON	- 5	0	-	7	- 4	-	-	- 4
HA-HR	0	0	- 6	-	- 2	-	0	- 3
HA-OV	0	0	-	6	- 2	-	0	- 2
HA-EF	4	-	- 2	7	-	-	4	- 3

ways be performed when adjusting a set of VLBI observations, as this gives a better indication of the true accuracy (precision + reliability) of the experiment than the quoted formal errors of the final LSQ fit.

In addition, attention is drawn to the fact that for run 14 (where all Haystack observations are excluded) a value of about two decimetres is found equal to the number by which the DEGRIAS baselines of the reference fit are shorter than the ones presented in [Carter,1983]. This justifies the conclusion that the DEGRIAS computing model accuracy is indeed at the 10 cm level and that the main deviations for these MERIT-SC data are caused by the Haystack pointing error bias.

3.7.3.3 Changes in the computing model

Analogous to the computations in §2.8, this section describes the influence of some changes in the computing model on the behaviour of the LSQ fit.
Column 1 of Table 13 shows the differences in baseline lengths with respect to the reference fit, due to a change in the a priori standard de-

viation: now a fixed value of 0.2 ns is chosen for all observations. By comparison with the reference fit, this means that the observations of EFF-ONS and HRA-OVR are down-weighted and those of EFF-HRA and ONS-HRA up-weighted. In view of the standard deviations of the estimated baseline lengths of Table 11, no significant changes can be found, although there exists a trend that baseline lengths increase proportional to their length. The coordinates of Onsala and of Effelsberg change somewhat more than their standard deviation: in the X- and Y-directions by -7 cm and in the Z-direction by -17 cm. The network shape, however, remains constant in view of the above.
The results of such statistical testing as data-snooping, multi-dimensional F-test, special alternative hypothesis tests and RMS-values are also in complete agreement.

Table 13.

Comparison of MERIT-SC Results II (cm)

RUN	1	2	3	4	5
EF-ON	0	+ 1	0	+ 1	- 2
EF-OV	+ 3	+ 6	- 1	+15	+ 2
HR-ON	0	+ 2	+11	+ 8	-12
HR-OV	+ 1	0	+ 2	+ 7	+ 4
EF-HR	+ 2	+ 4	+11	+13	- 6
OV-ON	0	+ 5	0	+10	- 4
HA-ON	+ 1	+ 2	+ 2	+ 9	- 9
HA-HR	+ 3	- 3	+ 5	+ 1	+ 1
HA-OV	+ 4	- 3	0	+ 4	+ 5
HA-EF	+ 3	+ 3	+ 2	+12	- 5

In the second example, all standard deviations of the observations are multiplied by $1/(2*\cos\mu)$; this is a down-weighting as a function of zenith angle. The factor of 2 is applied to arrive at about the same formal errors for the estimated unknowns. Although the changes in baseline length are somewhat larger and more random than in the previous example, no surprising effects are found. The considerable changes in estimated coordinates should be noted again, with a maximum for X,Y and Z of EFF of +18, +9 and +28 cm respectively. Here one sees again that the shape of the network is better defined than its orientation or its scale. In these fits all observations below 10 degrees elevation had already been excluded, otherwise the changes would have been considerably greater.

As regards the introduction of delay rate observations in run 3, only the changes in the length of the intercontinental baselines to HRAS are

worth noting. Further inspection of the adjustment results shows that the estimated tropospheric zenith delay of HRAS changes by about 10 cm as a result of the introduction of delay rates. Its value becomes 2.16 metres, a more realistic number in view of the height of HRAS above sea level. The conclusion is therefore that with delay observations only a correlation between zenith delay and local height-coordinate for the HRAS station exists for this experiment, which is too high (N.B. the shift in HRAS coordinates compared to the reference fit is exactly 14 cm in height direction!) and that the additional delay rate observations remedy this situation.

In the 4th example the correction for ionospheric refraction is omitted. It can be concluded from Appendix C that this includes corrections of up to 2.2 ns. It is immediately obvious from Table 13 that the changes in baseline length are more or less proportional to baseline length, which means that the scale is ill-determined. Such errors cannot therefore be detected easily. This follows also from the multi-dimensional F-test, which yields 2.1 (compared to the 1.53 for the reference fit) for a 5% level of significance. This is probably also the main reason for effects such as the large differences between published lengths for HAYONS (§3.7.2).

In the last example, in view of fit 12 of §2.8 and the results of Figure 23, a 5% error in the retarded baseline correction is introduced, which has a smaller magnitude than the error for the previous example. The differences are immediately obvious: the multi-dimensional test-variate F rises to 2.22, compared to 1.53 for the reference fit. As regards the special hypothesis, the tests for source biases remain about the same, but almost all baseline bias tests are rejected and also one station bias test. The largest test value is 11.0 (with critical value 3.3) for a baseline bias in EFF-OVR. The problem is also indicated by the increase of the RMS value of the residuals from 0.28 to 0.44 ns for the same baseline. In addition, the number of rejected observations by the data-snooping is seven times as large. All these factors indicate that the geometry of the network (especially the closed triangles!) and therefore of the LSQ fit is severely disturbed. Consequently, such an error, unlike that of the preceding example, can be easily detected.
The changes in estimated station coordinates are also considerable: about 0.5 metres. In geographical coordinates this means a rotation of about 0.015 arcsec to the East for the European stations and a change of about -65 cm in height. OVRO and HRAS change mainly in height: by +60 and +37 cm respectively.

3.7.4 Conclusions

The first conclusion of these MERIT-SC computations is that the claimed DEGRIAS computing model accuracy of §2.8 is indeed achieved and may even be somewhat better than the quoted number of 10 cm.

Furthermore, it can be stated that one should be careful in claiming a certain precision for the estimated station coordinates or baseline lengths, on the basis of formal errors and RMS-values only. It is shown that the "stability" of the estimated MERIT Short Campaign baseline

lengths is significantly poorer than indicated by the formal errors. Perhaps the MERIT-SC is a comparatively bad example due to the Haystack pointing error, but it is stated here that such factors will always hamper a completely successful observing session. Mention should be made of the following points: the ionosphere can suddenly become very active, parts of some observations will lack a second frequency or an error in the clock system lasting for several hours may occur. These factors determine for the most part the final accuracy of the experiment, as they cause situations like that of §3.7.3.1, where one observation has a tremendous influence on the LSQ estimates.

Even though the recommendation is based on the example of the MERIT-SC which has some very significant problems, and noting that DEGRIAS does not have a computing model accuracy of 1 cm, it is to be recommended that computations such as those described above (deleting all observations of one baseline, of one source, etc.) should always be carried out so that the final solution is accompanied with a better indication of its accuracy. One thus has a reliable estimate of the internal consistency or repeatability. The reproducibility (independent observations, correlation, geodetic analysis software) will then be about a factor of two worse.

Another conclusion is that a marked difference exists between error sources that corrupt the geometry of a closed triangle of VLBI baselines and those that do not, with respect to the possibility of detecting those sources of error. This is because the former type of error source tends to increase the shifting variate and therefore can be detected by statistical testing, whereas the latter kind of error source leads mainly to changes in the scale and orientation of the network.
An example of the first kind of error source is an error in the computation of the retarded baseline correction, which results in considerable closing errors for the triangles. An example of the second error source is the neglect of the ionospheric refraction correction.
This leads to the conclusion that in general the relative positions of VLBI observatories can be determined to one order of magnitude better than the position, orientation and scale of the entire network. This is due to the coordinate system definition (§3.3) and the fact that errors in certain corrections or observations yield a considerable common effect on all baselines and therefore on the position, orientation and scale of the network.

The last conclusion is that tropospheric refraction, both "dry" at low elevations and "wet", is the most prominent source of error, especially because it is of the second type mentioned above. To avoid problems, no observations below 10 degrees elevation should be included in the experiment. In addition, care should be taken with sources which have not been observed on many occasions. For the Northern hemisphere telescopes, these are mostly low declination sources, observed in a small section of the sky. The estimate of the tropospheric zenith delay parameter then becomes less well determined due to correlation, and also the situation of observations with a poor reliability may occur. The source position then becomes biased as well and affects the estimated station locations.

Chapter 4

D E S I G N O F V L B I E X P E R I M E N T

Summary: In this chapter first some general considerations relevant to the design of a geodetic VLBI experiment are discussed. Next, two items of the "quality control" of a geodetic network, i.e. precision and reliability, are discussed in §4.2 with a view on the special "Delft" approach for point positioning. The quantities of this approach for describing precision and reliability are derived and discussed. In connection with this, the characteristics of the SCHED-module of the DEGRIAS software package are briefly summarized. This module generates a schedule for a geodetic VLBI campaign starting from visibility considerations for the sources and optimizing for telescope slewing times. This is defined as "costs", the third constituent of quality control.
In §4.4 the above is applied to some simulation studies for optimizing the quality of a geodetic VLBI network. Examples are the network studies previously performed in [Dermanis,1977], the MERIT-SC configuration and a European geodynamics network.

4.1 INTRODUCTION

Generally speaking, every geodetic VLBI experiment is conducted for the determination of station coordinates and Earth orientation parameters at a specific moment. The "quality control" [Teunissen,1984a] of such a geodetic network demands a design which is precise and reliable enough at minimal costs. Precision is defined here as a measure of the characteristics of the network in propagating random errors. Reliability describes the ability of the redundant observations to check model errors. Costs of geodetic VLBI are mainly determined by the number of telescopes involved (especially via correlator time) and the duration of the campaign.

First of all, choices must be made regarding the design of a VLBI experiment. This concerns: number and location of stations, a number of candidate sources, approximate period of observation and equipment. The latter choice (i.e. Mk-II or Mk-III) is also of interest for the probabilistic model: the a priori standard deviations. According to [Bock,1983] a diagonal matrix is always sufficient; see §3.2.
Furthermore, a number of limiting conditions should be considered, such as the minimum elevation angle, which will be allowed (in connection with tropospheric refraction) and some critical configurations, by which is meant measurement designs that yield a (nearly) singular system of normal equations in the LSQ fit. A well-known example of such a singular case is the single baseline experiment with observed sources at only one declination.

In view of the fact that the radiotelescopes mostly have fixed locations on Earth and that the (relatively few) sources have fixed positions in the sky, the main way of achieving an optimal quality is to choose the sequence and timing of the observations.

4.2 INSTRUMENTATION FOR JUDGING A NETWORK DESIGN

4.2.1 Estimability of Parameters

In §3.3 some remarks were made concerning the estimability of parameters in the LSQ fit; they were mainly to do with the definition of the coordinate system.
To investigate whether it makes sense to estimate e.g. a second order term for the clock polynomial in view of the available observations (cf. ERIDOC fit, §3.6.2), so-called Googe-numbers are computed for every unknown parameter [Nibbelke,1984]. This Googe-number is computed during the Choleski decomposition of the system of normal equations as the sine squared - cf. (D.21)- of the angle between the row (vector) of a certain unknown parameter with respect to all previously handled parameters in the space described by the Choleski factor. A Googe-number of zero therefore means complete dependence on (a linear combination of) other unknown parameters. A value of 10^{-8} is regarded as the computer limit for a singular situation. Values of less than 10^{-5} indicate hardly estimable parameters. In this way it can be investigated what parameters to include in the final LSQ fit. The Googe-number is evidently closely connected with the correlation coefficients derived from the variance/covariance matrix of the estimated parameters; see below.

4.2.2 Precision of Networks

Precision is defined (§4.1) as the characteristics of a network in propagating random errors. In LSQ adjustment this is expressed by the a posteriori variance/covariance matrix of the unknown parameters. From this matrix e.g. standard deviations of the estimated station coordinates can be computed, or the length and direction (correlation!) of the three axes of the point standard ellipsoids, comparable to the standard ellipses in plane geodetic networks.
These quantities yield an indication of the precision, but two major disadvantages are encountered.
In the first place: the results are dependent on the choice of the S-basis (§3.3). If, for instance, the ERIDOC VLBI measurements of §3.6 were re-adjusted with Westerbork instead of Effelsberg as the station with arbitrarily-fixed coordinates, the quoted standard deviations would change, most drastically for Effelsberg and Westerbork themselves. It should be noted that if in the second adjustment the arbitrary Westerbork coordinates are chosen to be equal to those shown in Table 6, the coordinates of the other stations do not change either, only their precision. This, in a nutshell, is the essence of the S-transformation (Appendix E).
A second disadvantage follows in that only a restricted judgement can be made about the precision results of several network designs. An example is station coordinates for which only functions connected with the point

standard ellipsoids are considered; and also the standard deviations of the baseline lengths do not give a complete picture of the precision of the network.

To remedy this situation it is stated that all relevant unknown parameters Y play a role in the precision analysis and that one network design is better than another if the standard deviations of all the permitted functions f of Y are better for the former. Denoting the a posteriori variance/covariance matrices of the designs 1 and 2 by Q1 and Q2, this is mathematically formulated as (42.1) [Teunissen,1984a]. Note here that the a posteriori variance/covariance matrix can be computed before the network is actually measured if a level for the variance factor σ_o (32.1) is assumed:

$$f'.Q1.f \;/\; f'.Q2.f \;\leq\; 1 \qquad \text{for all permitted } f \tag{42.1}$$

The upper bound of the above ratio is represented by the maximal eigenvalue μ_{max} of the generalized eigenvalue problem:

$$|Q1 - \mu * Q2| = 0 \tag{42.2}$$

Criterion (42.1) is met if $\mu_{max} \leq 1$ [Baarda,1973]. The generalized eigenvalue problem (42.2) yields a maximal eigenvalue independent of the chosen S-basis (§3.3); the only demand is that Q1 and Q2 are defined in the same S-system. As a consequence, the first disadvantage is remedied as well.

For levelling networks and plane geodetic surveying an artificial variance/covariance matrix has been constructed for Q2 based on a covariance function, derived from results for ideal, schematic networks [Baarda,1973], [Alberda,1974] to serve as a so-called criterion matrix. The eigenvalue problem is then computed for the entire network (for which μ_{max} should not exceed the value of 1 by too much) and for a number of partial networks to locate weak parts.
Such an approach is not yet possible for geodetic VLBI. Design 1 is therefore considered to be better than design 2 for a certain VLBI experiment if the maximum eigenvalue of their mutual eigenvalue problem is smaller than one.

4.2.3 Reliability of Networks

In §4.1 reliability was defined as the ability of the redundant observations in an adjustment problem to detect model errors. These errors can be three-fold, according to the definition of the zero hypothesis Ho in §3.2: (a) an error in the formulation of the computing model (22.7), (22.8) or its linearization, (b) an error in the adopted probabilistic model (a priori standard deviations), or (c) outliers in the observations due to some (unknown) cause.

From this definition one can see that networks with no redundant observations have no reliability at all. In all other cases, the post-fit residuals of the LSQ adjustment allow one to detect errors. The magnitude of a post-fit residual is (the vector Ci^T denotes which observation is meant, A is the design matrix, P the weight matrix, x the observations):

$$vi = Ci^T.(I-A.(A^T.P.A)^{-1}.A^T.P).x \qquad (42.3)$$

Following Baarda's convention [Baarda,1968] at least all hypotheses are tested where only one observation at a time is supposed to be erroneous (data-snooping). The row vector Ci^T then has the following form:

$$Ci^T = (0,0,0,...,0,1,0,...,0) \quad i=1,...,m \qquad (42.4)$$
$$\qquad\quad 1,2,3,.....,i,.....,m$$

For the general case of correlated observations it can be proven that the vector v is not as sensitive to an error in one of the observations, as the vector P.v, so that in this case one should test (see Appendix D):

$$Pii*vi = Ci^T.P.(I-A.(A^T.P.A)^{-1}.A^T.P).x \qquad (42.5)$$

If one now wants to have a standard normally-distributed test value for (42.5) one should divide Pii*vi by its standard deviation, the square of which can be found by applying the error propagating law as:

$$Ni = Ci^T.(P-P.A.(A^T.P.A)^{-1}.A^T.P).Ci \qquad (42.6)$$

The above formulated test is known as the w-test, defined as:

$$wi = -Pii*vi \;/\; sqrt(Ni) \qquad (42.7)$$

The quantity wi can thus be seen as the normalized projection of the shifting variate onto the direction defined by Ci.
In the case of uncorrelated observations it is clear from the formulae (42.6) and (42.3), that (42.7) reduces to the simple (32.3), which defines the w-test as the post-fit residual divided by its standard deviation.

In the general case of non-conventional hypothesis testing, C can have different forms as one expects several observations to be erroneous. One could formulate a probable error on physical grounds in terms of a C-vector. For instance, $Cp^T = (1,1,1,0...0)$ means that a common bias is suspected in the first three observations. Since hypothesis testing is the same as "relaxing" the computing model, an accepted w-test for

this Cp^T means nothing more than the fact that the introduction of an additional constant as an extra unknown parameter in the observation equations of the first three observations would bring all test values below their critical level (if no other errors are present).

To be able to describe the reliability beforehand, it seems worthwhile choosing a fixed value for Pii*vi and computing the size of the corresponding error which would yield a w-test that just failed. Then the size of the marginally detectable error (m.d.e.) describing the internal reliability is defined as:

$$\nabla p = \text{sqrt}(\lambda o/Np) \qquad (42.8)$$

The quantity λo describes the distance between the centres of the Gaussian distributions of Ho and of the alternative hypothesis Ha. λo can be computed on the basis of assumed values for the level of significance α and the power β which gives the chance of detecting an outlier of size λo (Figure 24). Larger outliers are more likely to be detected, smaller ones less likely. Baarda first suggested making errors equally detectable in both the multi-dimensional F-test (32.1) and the w-test, the so-called B-method of testing, so that λo can be found via the following relation:

$$\begin{aligned} \lambda o &= \lambda(\alpha o, \beta o, 1, \infty) \\ &= \lambda(\alpha, \beta o, b, \infty) \end{aligned} \qquad (42.9)$$

The usual procedure is then: choose, for instance, $\alpha o = 0.1\%$, $\beta o = 80\%$ and compute α and λo with the use of (42.9). The problem with this approach is that α becomes very large for a considerable number of redundant observations. One should then adjust and test the data in phases. For multi-station VLBI campaigns, however, this is not done and α is held fixed at 5%.

It is clear that for an optimal network design equivalent observations (e.g. same baseline, same standard deviation) in general should have equivalent m.d.e.'s under the conventional hypothesis. For geodetic VLBI with only delays as observables, one is therefore justified in stating that all observations should have approximately the same ratio of m.d.e. to a priori standard deviation, with an average level which is as low as possible. Any delay observation with a relatively large m.d.e. is therefore suspect, because it may contain larger undetected outliers after the LSQ adjustment and can thus contaminate the solution of the parameters.
Due to the large number of observations and the fact that they have approximately the same a priori standard deviation and equal observation equations, one is justified in applying statistical means to the comparison of two different designs of a VLBI-network. With this in mind, histograms of the m.d.e.'s under the conventional hypothesis are made and a design for a network is defined as better than a second design if the computed mean and standard deviation of all its m.d.e.'s is smaller.

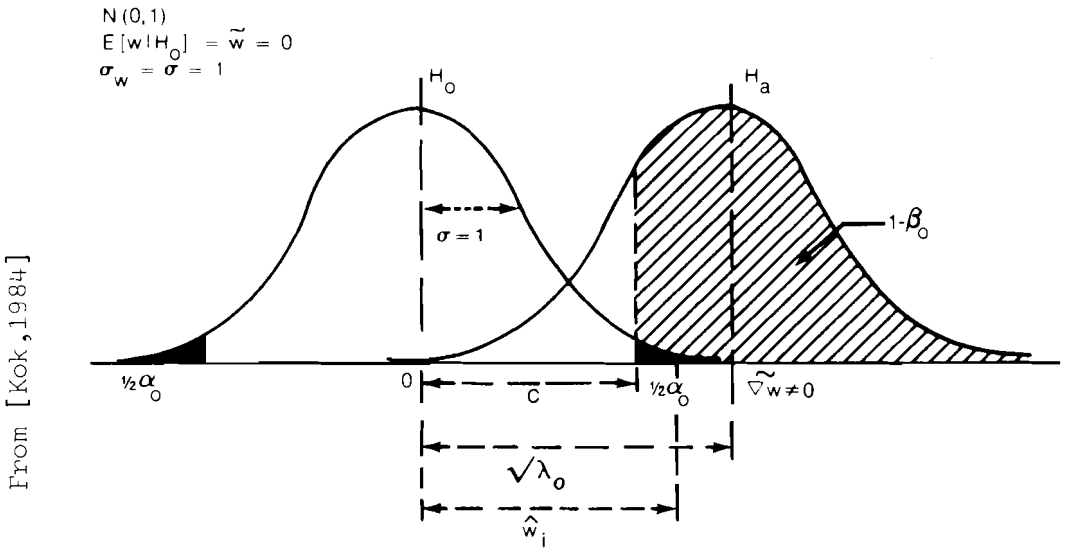

Figure 24: Gaussian Distribution and w-test

The presence of comparably large m.d.e.'s should be avoided at all times.

In addition to the internal reliability described above, there exists also external reliability. This is defined as the impact of the m.d.e.'s on the estimated parameters Y and is expressed - via the LSQ formula - as:

$$\nabla Yp = (A^T.P.A)^{-1}.A^T.P.Cp.\nabla p \qquad (42.10)$$

For every hypothesis p a vector ∇Yp can be computed. Due to the amount of data involved in a judgement on the basis of ∇Y, usually the (weighted) squared length of this vector is taken as a measure of the external reliability [Baarda,1972] according to:

$$\overline{\lambda} p = \nabla Yp^T.(A^T.P.A).\nabla Yp \qquad (42.11)$$

This quantity $\overline{\lambda}$ is therefore a measure of the upper bound of the influence of a model error with size ∇ on the estimated unknown parameters. One can compute the influence on all parameters, or only on a subset.

The same holds for the external reliability as for the internal reliability: for an optimal network design, observations should all have about equal $\overline{\lambda}$'s under the conventional hypothesis. Therefore, as for the m.d.e.'s, the mean and standard deviation are computed for sqrt($\overline{\lambda}$) and presented in a histogram, which can be compared for different network designs. In §3.7.3.1 the effect of an observation with a large $\overline{\lambda}$ was shown.

To conclude this section, a short remark is added concerning non-conventional hypothesis testing. As yet, DEGRIAS applies three types of test (§3.2): a constant bias per station, a constant bias per baseline and a constant bias per source. It follows from the above that these tests are mathematically formulated by C-vectors of the type (cf. Appendix G): Cp^T = (0,0,1...1,0...0,1...1,0...0) where the ones are at the positions of the sequence numbers of the observations of the specified station, baseline or source, respectively. Due to the limited number of these special hypotheses a comparison of the reliability of different network designs can be made directly.

4.3 THE SIMULATION SOFTWARE "SCHED"

The simulation software SCHED, which forms a module of DEGRIAS, generates an observing schedule from data such as station and source coordinates, mainly by minimizing slewing time. In this way one can analyse the precision and reliability of different network designs. The main disadvantages of SCHED are that only fixed scan lengths are allowed and that slewing time itself is not actually minimized but telescope hour angle rotations, starting from the assumption that this usually requires most time. For a more optimal schedule the incorporation of idiosyncrasies such as slew-rates and cable wrap of the individual telescopes will be required. This is a foreseen extension, but it has not been implemented yet. Then a variable scan length, depending on the correlated flux of the source, should be possible as well.
The main advantage of SCHED is that a complete schedule is presented directly and no additional work is required; cf. the SKED programme [Vandenberg et al.,1980].
In SCHED the following steps can be discerned:

1) Input of station coordinates, start and stop time of the experiment, scan-length and "candidate" sources.

2) Computation of the simultaneous visibility of the sources for all stations. This takes into account such questions as: is the source above the horizon? (or any given minimum elevation), and: can the telescope be pointed at the source? The latter is not always the case due to e.g. hour angle and declination limitations. Westerbork, for instance, can only observe in the hour angle range from -6h to +6h. The visibility is presented in a diagram so that one can easily see which sources are observable by all stations at which times; Figure 25 presents an example for the WEJO-4 experiment (§3.6.1). It is obvious that it is hardly possible to schedule a pure simultaneous experiment for very distant observatories. In this case, the skipping of a scan from time to time for the more remote (or less important) stations cannot be avoided.

3) Compilation of an optimized schedule at the time of observation of all scans. For this, a subroutine called SCORE determines a point-result for all sources by means of a system of faults and bonus-points. The items that influence this point-result are:

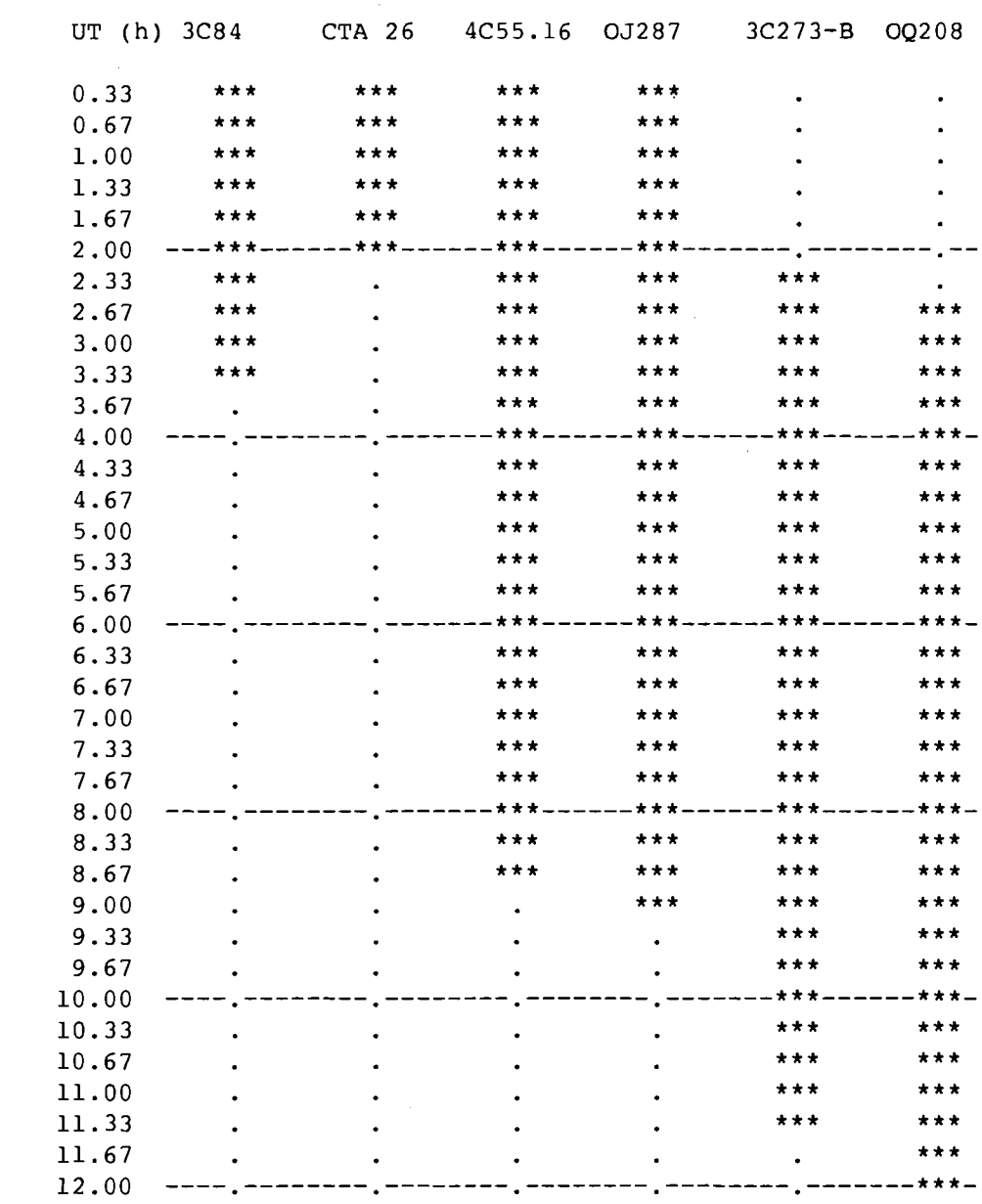

Figure 25: Simultaneous Visibility of Sources

visibility	is the source observable for all participating telescopes (elevation, hour angle limitations, etc.)?
slewing-time	the source with the smallest hour angle difference with respect to the last observed source gets the highest priority in this class.
rising/setting	if a source has just risen above the horizon or is about to set, the observation gets more priority.
observation gap	the larger the number of scans (which corresponds to time) since the last observation made of this source, the higher the priority.

The procedure now is that, starting from a chosen first source, a total point-result is computed for every "candidate" source in the second scan by a relative weighting of these items [Brouwer,1982b]. The source with the lowest result will be chosen as the source to be observed next. The process is then repeated for the third scan and so on, so that for a 24 hour campaign with a scan length of about 10 minutes some 2000 calls of SCORE are required.

4) The final result of the SCHED module is a computer output containing start and stop times of the scans in UT and GMST, source number and start and stop hour angle and elevation. In addition, some data required by the observatories will be printed, such as: observing frequencies, source coordinates, request for meteo data, etc.. In this way, a complete, user-ready log can be mailed to the participating observatories. This feature of DEGRIAS was used for the WEJO-3 and WEJO-4 campaigns (§3.6.1).
Finally, for network design studies, a file is created with observations in the format required by the input module of DEGRIAS. The a priori standard deviation of each observation is taken as a fixed value, or computed as a function of both the flux of the source and the elevation at which it is observed via a formula based partly on theory, partly on experimental data (Figure 26):

$$\sigma_i = 2/\mu + \mathrm{sqrt}(F_{max} / F) * \sigma \qquad (43.1)$$

where

μ = the elevation angle (in degrees)
F_{max} = the flux (in Jy) of the strongest observed source present
F = the flux (in Jy) of the present source
σ = bottom level for the standard deviation for the campaign (e.g. 0.1 ns)

The observation itself is computed in the input module of DEGRIAS, using a random generator with a 3-sigma cut-off for the normal distribution (§3.2).

4.4 SOME SIMULATIONS

4.4.1 Critical Configurations

To start this section, a brief review is presented of the requirements which the choice of estimable parameters should meet to avoid a singular system of normal equations. For more information one is referred to: [Schut,1983], [Dermanis,1977], [Bock,1980] and for a general approach to [Tsimis,1973]. For minimum requirements (e.g. minimal number of sources and stations) one is also referred to [Aardoom,1972] or [McLintock,1980].
For the unknown parameters the ones chosen from §3.1 are: station and source coordinates, clock parameters, length scale factor, Earth orientation parameters and tropospheric zenith delays.

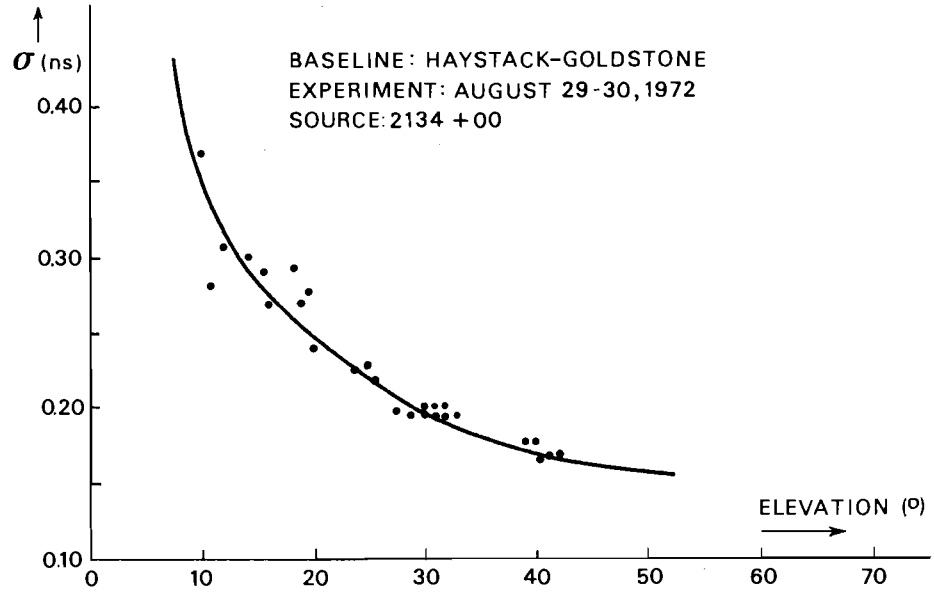

Figure 26: σ as a Function of Elevation

The requirements for the definition of a coordinate system have been discussed in §3.3; there the dependence of clock drift and scale factor was also indicated. Furthermore, it has been stated that the Earth orientation parameters should be held fixed for at least one observation. Even if these requirements are met, a singular system of normal equations may occur. For a single baseline experiment the following situations should be considered:

a) for observations of sources at only one declination, clock offset and Z-component of baseline become inseparable.

b) for shorter baselines the observing elevations at both stations are almost equal and consequently the tropospheric zenith delay parameters become inseparable; at least one of them should be constrained.

c) the fact that a direction is defined by only two rotations means that a single baseline can only determine two Earth orientation parameters at a time. The two to be chosen, depends on the direction of the baseline with respect to the Earth-fixed frame. This is shown in Table 14 [Dermanis,1977], which also includes estimability of source positions. In addition, it can be stated that a baseline parallel to the Equatorial plane should not be also parallel to X- or Y-axis as then either Xp or Yp are no longer estimable.

With the above in view, the simulations of the following sections can be studied.

Table 14.

Estimability as a function of Baseline Orientation

Parameter	Baseline parallel to Equatorial plane		Baseline parallel to rotation axis	
	Equatorial sources	Polar sources	Equatorial sources	Polar sources
Xp, Yp	NO	YES	YES	NO
UT1, α	YES	NO	NO	NO
δ	NO	YES	YES	NO

4.4.2 MERIT-SC Network

In the first place, the effect on both precision and reliability of the omission of about 50 percent of the observations for the part of MERIT-SC described in §3.7.2 is investigated. Whereas in that section the w-test was applied to eliminate errors, here the size of errors that will just be detectable (m.d.e.'s) and their influence on the estimable parameters ($\overline{\lambda}$) will be investigated (§4.2). The precision will be examined by comparing formal errors of baseline lengths only.

For this simulation, four computations are carried out on the following sets of observations:

1. all observations of the official schedule for one day
2. only the observations of the reference fit (§3.7.2) for one day
3. all observations of the official schedule over two days
4. only the observations left in the reference fit over two days

For all fits the following estimable parameters have been chosen: station coordinates, one second order clock polynomial plus one tropospheric zenith delay parameter per 24 hours of observations, all source coordinates except the right ascension of 3C273-B, and a pole position and UT1-value per day. All observations have an a priori standard deviation of 0.2 ns.

The results of these simulations are summarized in Table 15 and are illustrated by the Figures 27 to 32, in which histograms are shown of the runs 3 and 4 for the m.d.e.'s and $\overline{\lambda}$'s for the influence both on all unknown parameters and on station coordinates only. The histograms for the runs 1 and 2 look similar and are not published here.
It is obvious from the results of Table 15 that the precision of the estimated baseline lengths behaves as one might expect, or even somewhat better. Doubling the number of observations (run 1 vs. run 2 and run 3 vs. run 4) makes the formal standard deviation decrease by a factor of

Table 15.

Precision and Reliability Results of MERIT-SC Design

I T E M	RUN 1	RUN 2	RUN 3	RUN 4
number of observations	977	487	1893	983
formal sigma EF-ON baseline (cm)	1.4	2.9	1.0	2.2
formal sigma EF-OV baseline (cm)	6.4	16.1	4.3	11.6
formal sigma HR-ON baseline (cm)	6.8	19.1	5.0	13.7
formal sigma HR-OV baseline (cm)	2.0	4.5	1.4	3.3
formal sigma EF-HR baseline (cm)	6.9	18.6	4.9	13.2
formal sigma OV-ON baseline (cm)	6.0	16.3	4.2	11.8
formal sigma HA-ON baseline (cm)	3.7	11.3	2.4	8.3
formal sigma HA-HR baseline (cm)	3.1	8.7	2.2	6.7
formal sigma HA-OV baseline (cm)	2.8	8.2	2.0	6.3
formal sigma HA-EF baseline (cm)	3.5	10.7	2.3	7.9
mean m.d.e. data-snooping (ns)	0.85	0.84	0.84	0.87
maximum m.d.e. data-snooping (ns)	1.14	2.74	1.10	2.84
sigma m.d.e. data-snooping (ns)	0.02	0.12	0.02	0.06
mean $\overline{\lambda}$ (all unknowns)	1.01	1.52	0.83	1.19
max. $\overline{\lambda}$ (all unknowns)	3.91	13.06	3.61	11.68
sigma $\overline{\lambda}$ (all unknowns)	0.35	0.92	0.27	0.57
mean $\overline{\lambda}$ (only coordinates)	0.44	0.65	0.30	0.43
max. $\overline{\lambda}$ (only coordinates)	2.06	4.53	1.98	4.47
sigma $\overline{\lambda}$ (only coordinates)	0.21	0.39	0.15	0.28
mean m.d.e. spec. test stations (ns)	0.05	0.08	0.04	0.06
max. m.d.e. spec. test stations (ns)	0.06	0.09	0.04	0.06
mean m.d.e. spec. test baselines(ns)	0.11	0.17	0.08	0.12
max. m.d.e. spec. test baselines(ns)	0.12	0.19	0.09	0.14
mean m.d.e. spec. test sources (ns)	0.13	0.25	0.08	0.18
max. m.d.e. spec. test sources (ns)	0.21	0.64	0.14	0.53

two to three. The difference between runs 2 and 4 is not so spectacular, because the number of estimated unknown parameters is also doubled for clock function and tropospheric parameters. It should therefore be concluded that making more observations than usual is beneficial (see below).

The most striking results, however, are seen for reliability. In §3.7 attention has already been drawn to the low elevation observations. The results of Table 15 confirm this.
For example, in run 2 an error of 2.74 ns (this is 13.5 times the standard deviation!) is only marginally detectable by statistical testing. This concerns an observation of source 2134+00, a low declination source, which was measured only seven times during the campaign. The same observation has also the largest effect on all estimated unknown

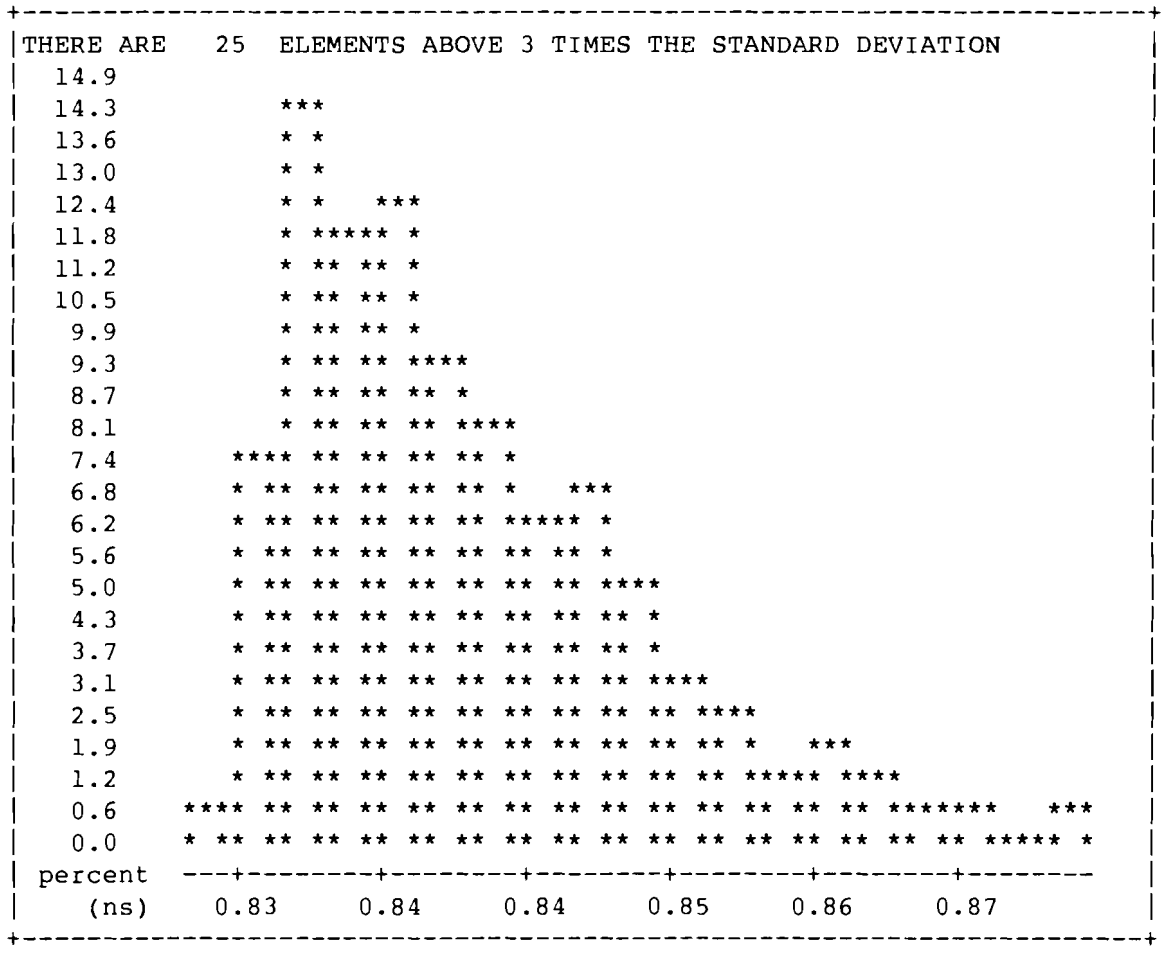

Figure 27: MERIT-SC m.d.e., official schedule

parameters, with $\overline{\lambda}$=13.06. This observation is therefore extremely dangerous in the LSQ fit. The only consolation is that the influence of an error in this observation does not exert the largest influence on the estimated station coordinates ($\overline{\lambda}$=1.85). The largest $\overline{\lambda}$ here is for an observation of 1642+690, in contrast, the source with the highest declination ($\overline{\lambda}$=4.53 with an associated m.d.e. of 1.53 ns).

With this in view it becomes clear from Table 15 that a campaign of one day would in princple give an acceptable level of both precision and reliability. However, because of the probability that a large number of observations will have to be eliminated in the LSQ adjustment for various reasons, a campaign length of two days is to be recommended, although even in this case, special care should be taken with low elevation sources, as errors with a size of 2.5 times the standard deviation (run 4: 0.53 ns) may stay undetected in the source bias test.
Therefore, it is also to be recommended that a careful design of the network be made and the effects of the drop-out of a number of deviations studied beforehand, because one schedule (or design) may be better than another in this respect and much can be gained as regards precision and reliability.

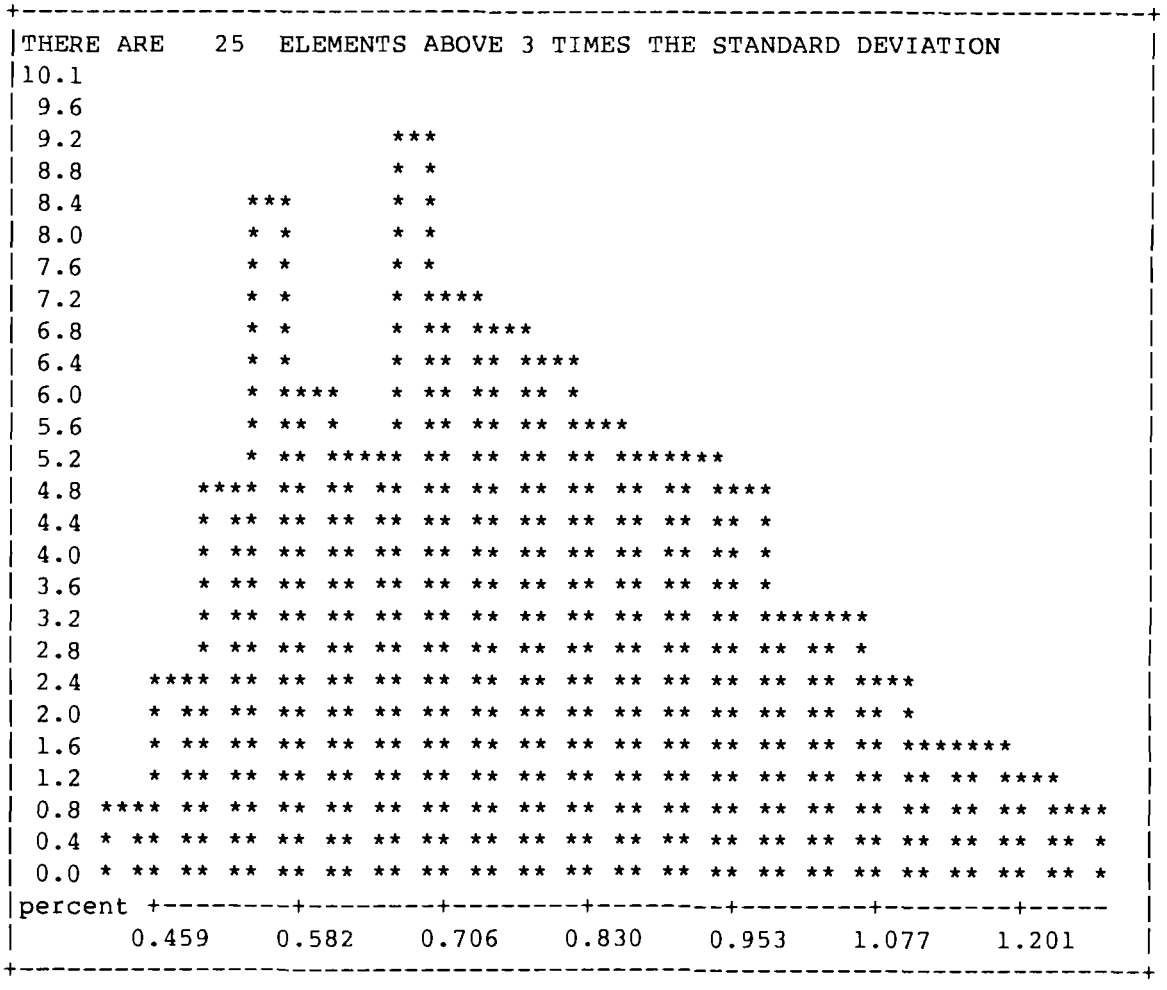

Figure 28: MERIT-SC sqrt($\overline{\lambda}$) all unknowns, official schedule

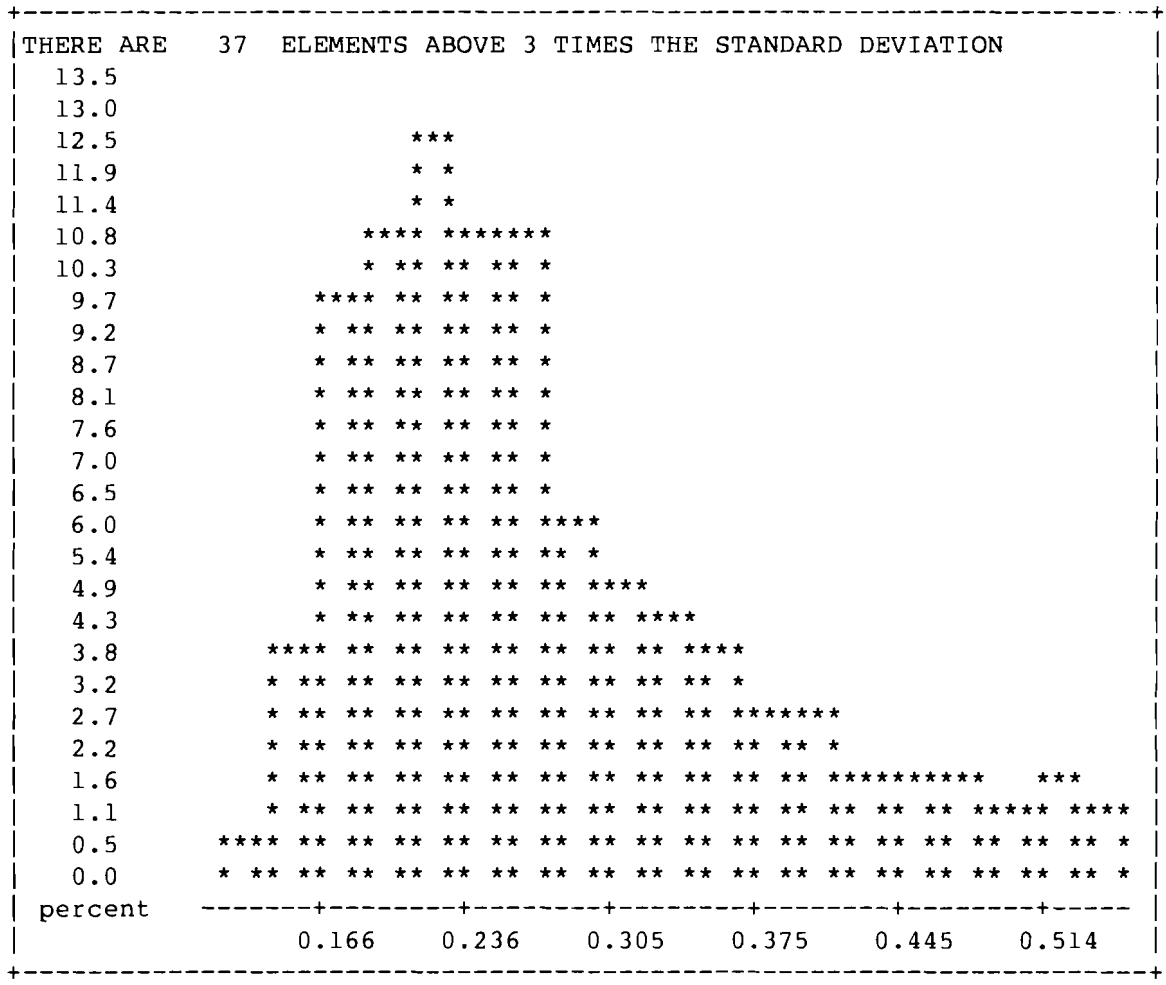

Figure 29: MERIT-SC sqrt($\overline{\lambda}$) coordinates only, official schedule

4.4.3 Network Studies of [Dermanis,1977]

Dermanis in his publication of 1977 studied the precision of estimated Earth orientation parameters and baseline length for a number of assumptions. He selected some observatories, using the criterion that they should be representative of a certain region; therefore, from several neighbouring telescopes only one was chosen and the choice did not reflect the true observational capabilities of the stations. The participating observatories and the experiments studied are listed in Table 16. The geographical locations of the stations and the baselines used in the experiments are shown in Figure 33.
The observing schedule (with a duration of 24 hours and a scan length of 15 minutes) is compiled for all baselines separately by SCHED (§4.3), with a minimum elevation of 8 degrees. The sources used are the same as in Table 9, excluding 0235+164. The a priori standard deviations are determined using (43.1) with estimated fluxes ranging from 3 to 18 Jy, so that values are found ranging from 0.130 to 0.478 ns with an average value of 0.245 ns.

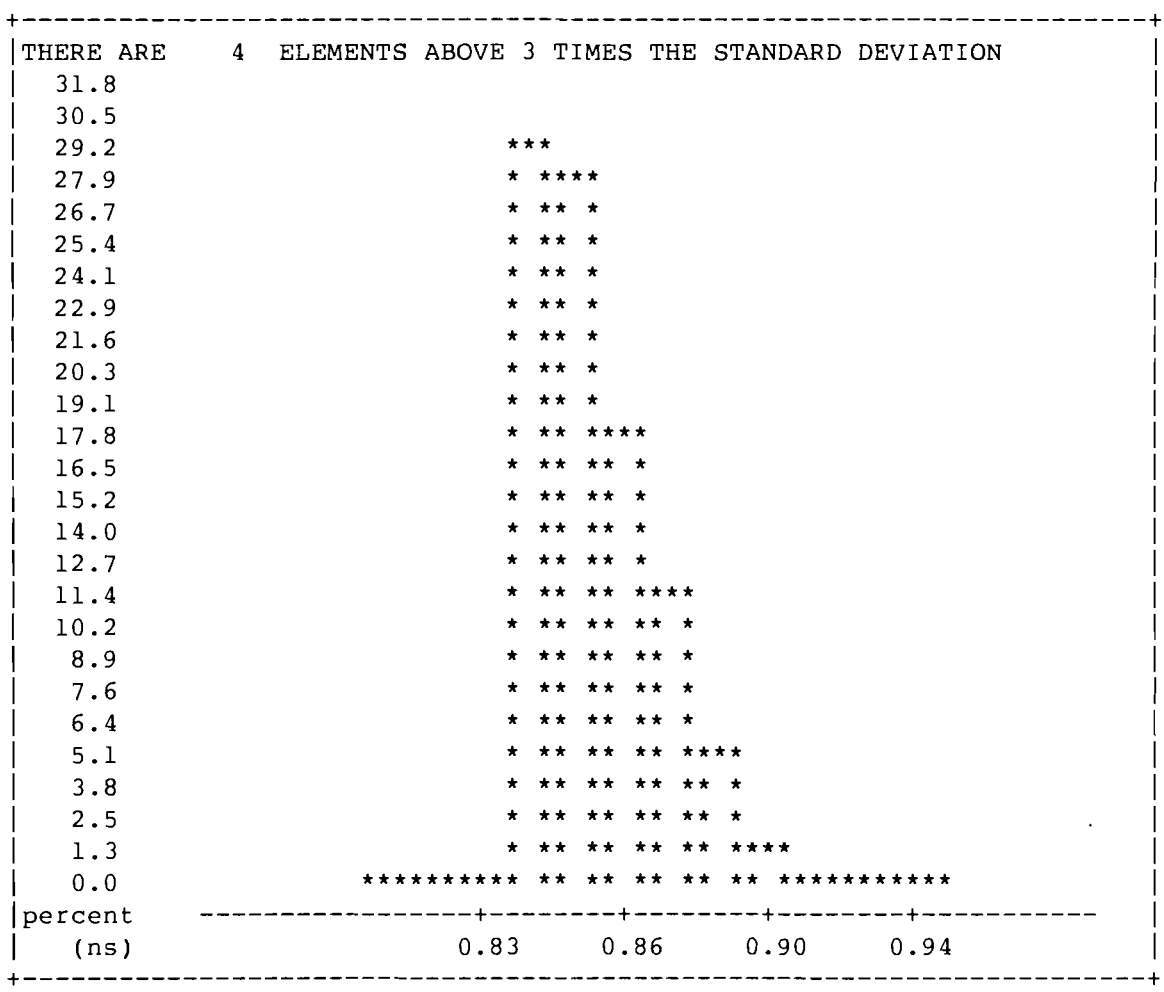

Figure 30: MERIT-SC m.d.e., reference fit

For the set of estimable parameters the station coordinates, second order clock polynomials, one tropospheric zenith delay parameter, all source positions (except the right ascension of 3C273-B) and Earth orientation parameters were chosen.

Apart from a confirmation of the results found by [Dermanis,1977], the main objective of these computations was to investigate the reliability of global VLBI networks. In view of the results of the previous section, here $\overline{\lambda}$ is only computed as the external reliability for all unknown parameters. The main results of these computations are presented in Table 17.

As regards precision, generally speaking, the results of [Dermanis,1977] are confirmed:
As an example one can note that the polar motion recovery in the two and three baseline experiments is about the same. Only the removal of one baseline in experiment 10 results in an increase of the polar motion standard deviation by a factor 1.5 compared to experiment 2. The complex design of experiment 5 does not offer such a dramatic improvement

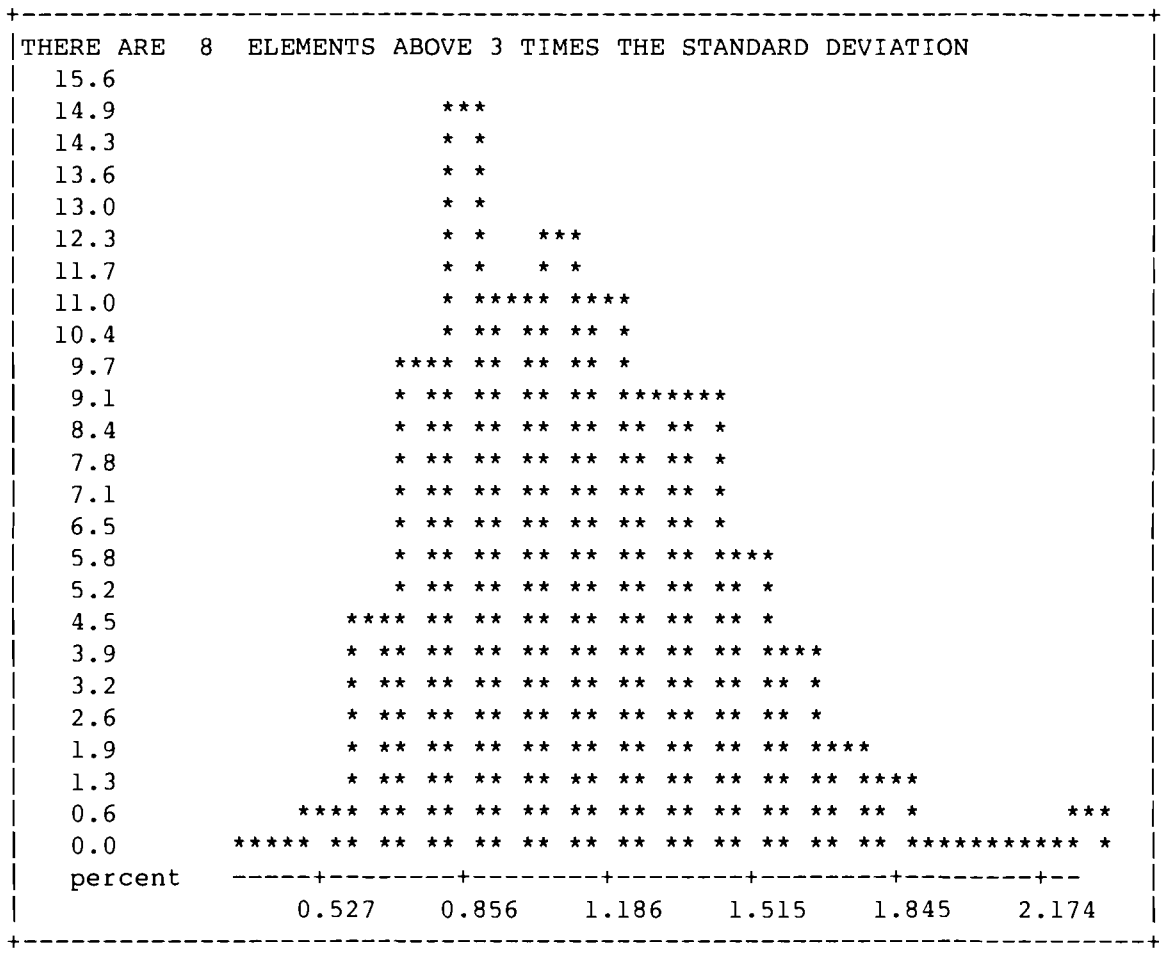

Figure 31: MERIT-SC sqrt($\overline{\lambda}$) all unknowns, reference fit

in precision as one might expect from the increase in the number of observations.
It should also be noted that the standard deviation of UT1 recovery is generally weak for two baseline experiments and somewhat better for three baseline experiments, with the exception of experiment 4.
The estimation of baseline length varies with station configuration. It is especially poorly determined for baselines in directions approximately perpendicular to the equatorial plane to stations on the Southern hemisphere. This can partly be explained by visibility considerations, because of the small number of low declination sources present in the experiment. Furthermore one sees that a larger number of baselines increases the precision of the individual baselines only marginally; compare e.g. the experiments 2 and 10.

The results regarding reliability speak for themselves. A bias per baseline or per station cannot be detected for two baseline experiments but will be absorbed in the clock offset parameter. Moreover, it should be noted that the magnitude of the m.d.e.'s depends mainly on how often a source is observed; compare experiments 2 and 10. Due to the fact that the experiment is not scheduled as a purely simultaneous one, the closure phase relation (triangle condition) is absent and this condition

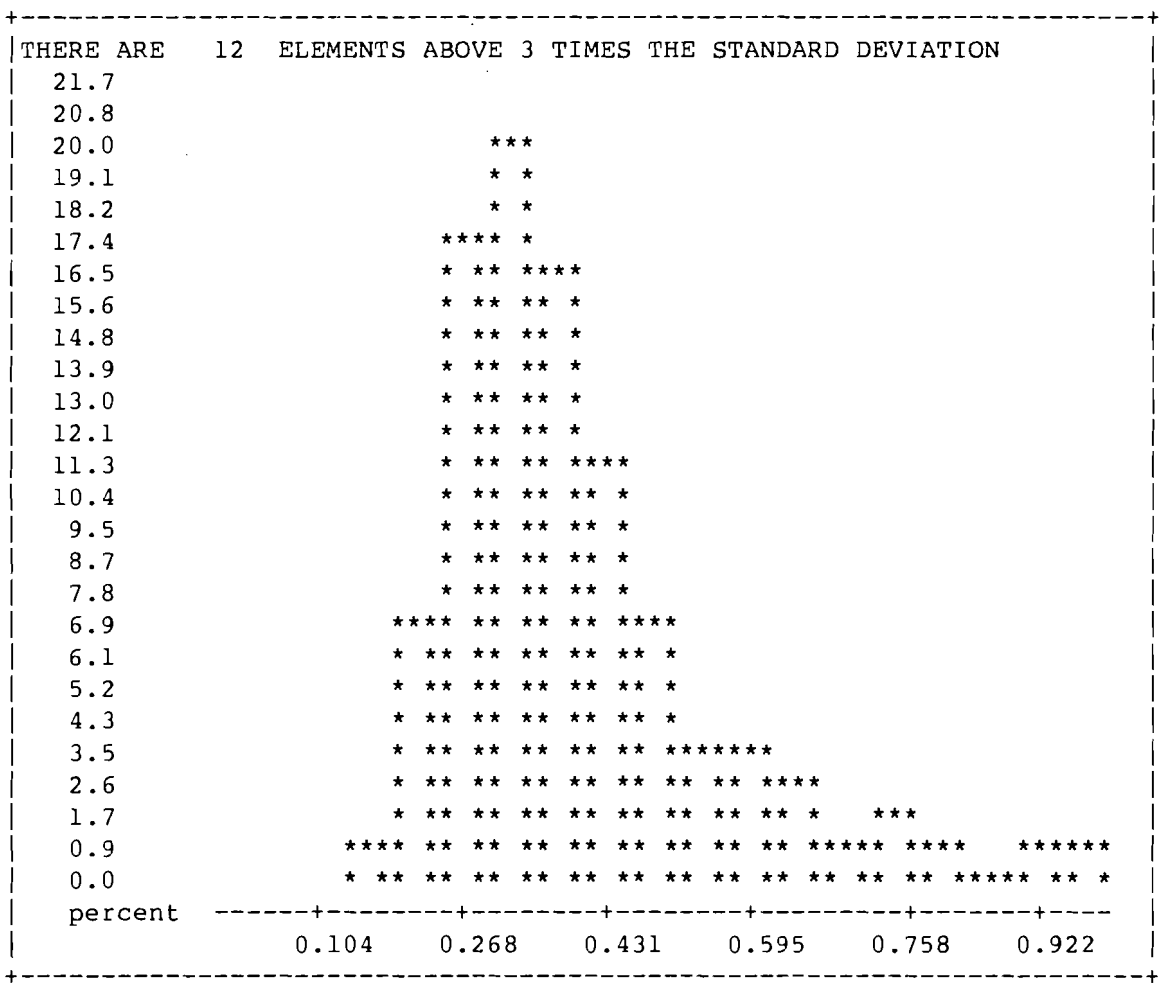

Figure 32: MERIT-SC sqrt($\overline{\lambda}$) coordinates only, reference fit

determines the likelihood of error detection for the most part. It is, however, clear that by introducing more baselines the external reliability in particular, is improved.
Finally, it can be seen that the histograms have a pleasant appearance: the distribution of the m.d.e.'s and $\overline{\lambda}$ is smooth and relatively few large values are found.

Table 16.

Simulated Global VLBI Network

Approximate Station Coordinates		
LOCATION	West longitude	latitude
1. Canberra, Australia	211.0	-35.2
2. Kauai, Hawaii, USA	160.0	22.0
3. Fairbanks, Alaska, USA	148.0	65.1
4. Haystack, Massachusetts, USA	71.5	42.5
5. Sao Paulo, Brazil	47.0	-24.1
6. Madrid, Spain	4.0	40.2
7. Onsala, Sweden	348.1	57.4
8. Johannesburg, South Africa	332.0	-26.2

EXPERIMENTS	
No.	Participating Baselines
1	2-3, 2-4, 3-4
2	3-4, 3-7, 4-7
3	4-5, 4-6, 5-6
4	5-6, 5-8, 6-8
5	1-2, 2-3, 2-4, 3-4, 3-7, 4-5, 4-6, 4-7, 5-6,5-8, 6-7, 6-8
7	2-4, 4-5
8	2-4, 4-6
10	3-4, 4-7

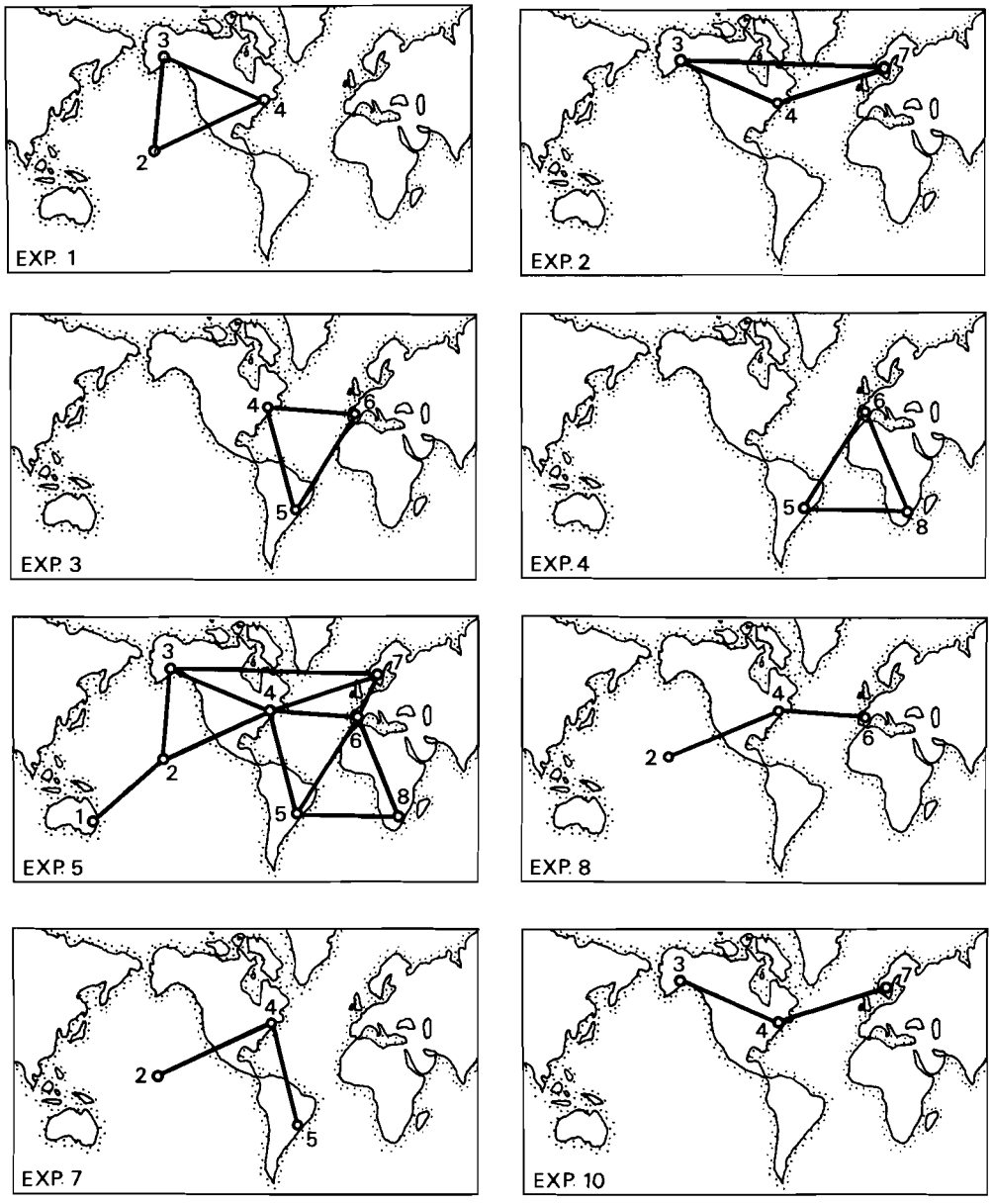

After [Dermanis,1977]

Figure 33: Baselines in Global VLBI Experiments 1-10

Table 17.

Precision and Reliability Global VLBI Experiments

I T E M	EXP1	EXP2	EXP3	EXP4	EXP5	EXP7	EXP8	EXP10
f. sigma base 1-2 (cm)	----	----	----	----	11.5	----	----	----
f. sigma base 2-3 (cm)	9.5	----	----	----	5.2	----	----	----
f. sigma base 2-4 (cm)	8.5	----	----	----	4.7	9.6	8.6	----
f. sigma base 3-4 (cm)	5.9	8.0	----	----	3.3	----	----	8.8
f. sigma base 3-7 (cm)	----	8.6	----	----	3.7	----	----	9.9
f. sigma base 4-5 (cm)	----	----	30.3	----	13.6	37.6	----	----
f. sigma base 4-6 (cm)	----	----	4.7	----	3.1	----	5.4	----
f. sigma base 4-7 (cm)	----	7.9	----	----	3.2	----	----	8.7
f. sigma base 5-6 (cm)	----	----	28.5	37.3	12.4	----	----	----
f. sigma base 5-8 (cm)	----	----	----	4.9	3.8	----	----	----
f. sigma base 6-7 (cm)	----	----	----	----	2.2	----	----	----
f. sigma base 6-8 (cm)	----	----	----	38.0	13.6	----	----	----
f. sigma Xp (mas)	1.26	1.35	1.24	1.23	0.53	1.62	1.54	1.99
f. sigma Yp (mas)	1.68	1.39	0.93	1.11	0.49	1.20	1.81	1.51
f. sigma UT1 (10^{-13})rad/d	1.0	0.5	1.0	2.0	0.1	1.0	0.8	0.6
mean m.d.e. data-sn. (ns)	1.06	1.09	1.08	1.15	1.04	1.15	1.12	1.11
max. m.d.e. data-sn. (ns)	1.88	1.89	2.00	2.17	2.09	2.00	1.99	1.94
sigma m.d.e. data-sn. (ns)	0.27	0.30	0.27	0.30	0.28	0.29	0.30	0.30
mean $\overline{\lambda}$; all unknowns	1.72	1.72	1.72	1.65	1.10	2.22	2.22	2.22
max. $\overline{\lambda}$; all unknowns	3.15	5.39	3.09	3.55	2.64	4.41	3.91	5.45
sigma $\overline{\lambda}$; all unknowns	0.38	0.54	0.37	0.35	0.23	0.54	0.53	0.56
mean m.d.e. test stat.(ns)	0.09	0.09	0.09	0.11	0.08	----	----	----
max. m.d.e. test stat.(ns)	0.09	0.09	0.09	0.11	0.07	----	----	----
mean m.d.e. test base (ns)	0.18	0.18	0.18	0.22	0.18	----	----	----
max. m.d.e. test base (ns)	0.18	0.18	0.18	0.22	0.20	----	----	----
mean m.d.e. test sour.(ns)	0.40	1.26	0.50	0.50	0.17	1.43	1.52	1.47
max. m.d.e. test sour.(ns)	0.74	5.10	0.60	1.43	0.24	2.64	3.91	5.16

4.4.4 European Geodynamics Network

In this section it is tried to make a start designing a European geodynamics network using VLBI in the Mediterranean area. Comparable, but more detailed studies for Satellite Laser Ranging have been reported by [Van Gelder&Aardoom,1982]. In the present publication, the objective is more to illustrate the applications of the quantities describing precision and reliability than to present a detailed design for geodynamics research using VLBI.

The idea is to start with a dual set-up. One network consists of some reference stations in Northern Europe and six stations in the Mediterra-

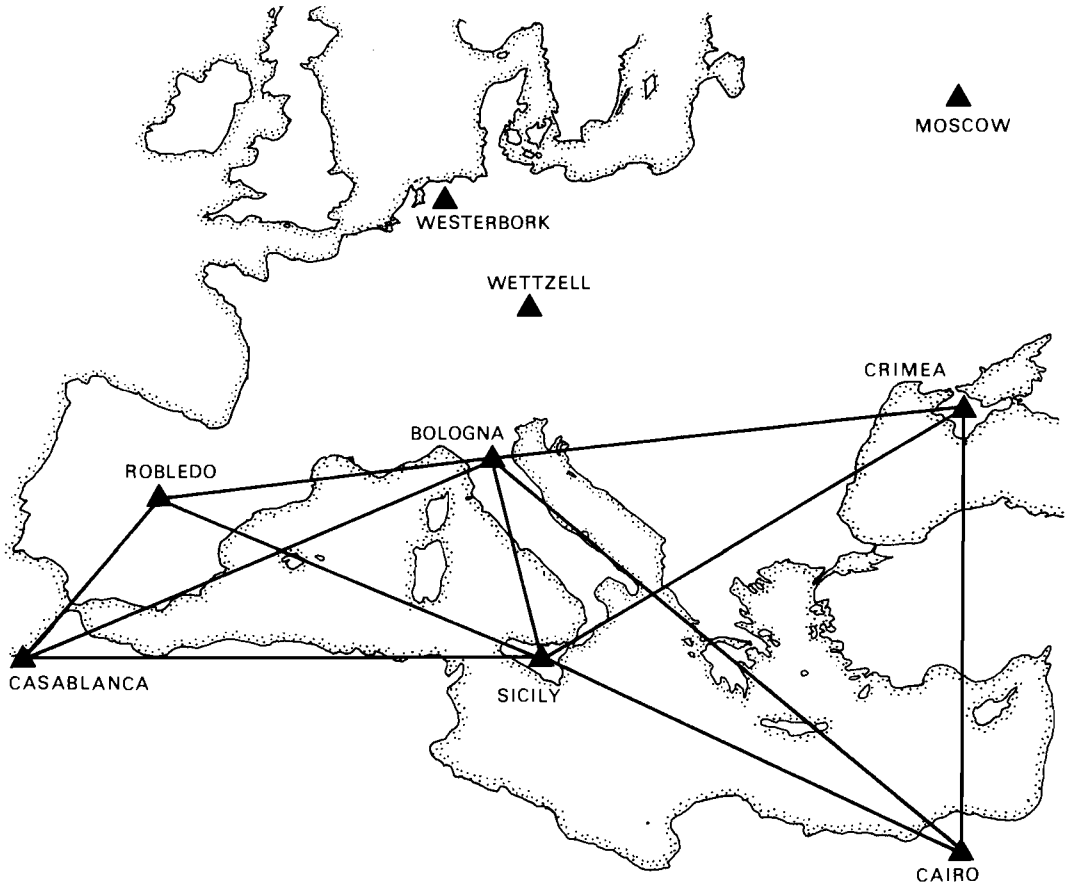

Figure 34: European Geodynamics Network (Diagonal Shape)

nean area and is measured e.g. once every year. The network of the six antennas is observed more regularly.
For the stations the following observatories have been chosen as "reference" stations: Wettzell, Westerbork and Moscow; furthermore, in the tectonically active area: Robledo, Bologna, Sicily and the Crimea. In addition, it is assumed that two transportable VLBI antennas will be available, in this case located in Casablanca and Cairo (Figure 34). By choosing other locations for the two transportable antennas the network can be extended and modified according to available geophysical hypotheses.

In all subsequent LSQ fits to the simulated experiments the same choices are made as before: 72 generated simultaneous observations per baseline for the sources of §4.4.3 according to (43.1) for 24 hours with a lower value of 0.1 ns; station coordinates, second order clock polynomials, tropospheric zenith delay parameters and one set of Earth orientation parameters and source positions (where appropriate) as estimable parameters.

The following designs have been compared: the application of the standard computing model with three possibilities: all source positions held fixed, half the source positions (i.e. the sources 4C67.05, OJ287, 4C39.25, 3C273-B, 2134+00 and 3C454.3) held fixed and all positions estimated. For each of these three possibilities the following four options have been computed: (1) use of only the minimal number of base-

lines with Bologna as the reference station, (2) forming triangles by including ROB-CAS, SIC-CAS, SIC-CAI and CAI-CRI, (3) including the two other diagonals via ROB-SIC and SIC-CRI and (4) all possible baselines. These twelve LSQ fits are summarized in Table 18.

Table 18.

Simulation Results of European Geodynamics Network

	Baselines:	Minimum	Triangle	Diagonal	All
All Sources	μ-max	1.	0.23	0.17	0.17
	σ ROB-CAS (cm)	2.6	1.4	1.3	1.1
	σ BOL-SIC (cm)	2.2	1.4	1.2	1.2
	σ CRI-CAI (cm)	2.9	1.8	1.6	1.3
	mean ∇ (ns)	0.89	0.88	0.87	0.88
	mean $\overline{\lambda}$	1.35	0.98	0.88	0.75
Half the Sources Fixed	μ-max	2.10	1.39	1.18	0.17
	σ ROB-CAS (cm)	2.6	1.4	1.4	1.1
	σ BOL-SIC (cm)	2.2	1.5	1.3	1.2
	σ CRI-CAI (cm)	3.0	1.9	1.7	1.4
	mean ∇ (ns)	0.91	0.88	0.88	0.88
	mean $\overline{\lambda}$	1.64	1.17	1.05	0.89
All Sources Estimable	μ-max	19.30	11.16	9.43	5.10
	σ ROB-CAS (cm)	4.0	2.7	2.4	1.8
	σ BOL-SIC (cm)	3.6	2.6	2.3	1.8
	σ CRI-CAI (cm)	7.4	5.4	4.9	3.5
	mean ∇ (ns)	0.92	0.89	0.88	0.99
	mean $\overline{\lambda}$	1.85	1.31	1.18	0.99

Only the formal standard deviation of the three baselines ROB-CAS, BOL-SIC and CRI-CAI are presented as they are the most important baselines in determining a possible North-South tectonic motion.

The maximum eigenvalues μ_{max} have been computed with respect to the fit with all sources held fixed and a minimum number of baselines.
From Table 18 it becomes obvious that μ_{max} is a very handy tool for describing the mutual precision of two network designs. Hence it is found that introduction of the diagonals does not add much to the precision of the network. Similarly, it is immediately clear that estimation of some source positions is permissible (a μ_{max} of 2.10). On the other hand, however, it is not sensible to estimate all source positions with this station configuration (μ_{max}: 19.30).

Similarly, one can inspect the reliability. It is found that the internal reliability on the basis of the conventional hypothesis is practi-

cally independent of the number of observing baselines. Naturally this is due to the purely simultaneous design. For the external reliability, on the other hand, the difference between $\overline{\lambda}$ in the case of a minimum number of baselines and closed triangles is considerable. A further increase of the number of baselines does not add much. Here again, the positive effect of the closed triangles is clearly demonstrated.

In addition, the same quantities are also computed for the extended network, where all baselines from the three "reference" stations to the six Southern stations have been measured. The two designs for the six stations are studied only with the minimal number of baselines and the triangle shape. One finds the results in Table 19.

Table 19.

Simulation of Extended European Geodynamics Network

	Baselines:	Minimum	Triangle
All Sources Fixed	μ-max	0.25	0.15
	σ ROB-CAS (cm)	1.3	1.0
	σ BOL-SIC (cm)	1.2	1.0
	σ CRI-CAI (cm)	1.5	1.0
	mean $\overline{\nabla}$ (ns)	0.86	0.86
	mean $\overline{\lambda}$	0.73	0.53

One sees that the formal precision of this design is some 50 percent better than the one of the sub-network alone. Furthermore, it should be checked whether the network is stable in a more "absolute" sense. Hence, precisely the latter design is appropriate for regular checking of the small Southern network.

Chapter 5

A L T E R N A T I V E C O M P U T I N G M O D E L S

Summary: In this chapter it is stated that every algorithm included in the formulation of the kinematic model of chapter 3 will not correspond completely to the "real world". Therefore it is advantageous to apply a computing model which is as simple as possible. This is done here for one type of algorithm in the computing model, i.e. those describing rotations of the coordinate frames, such as precession, nutation, Earth rotation and polar motion. First, the question is discussed of what one is really observing with VLBI measurements of the directions of fixed astronomical objects. From this discussion it becomes clear that the computing model with the smallest possible number of hypotheses about the description of the physical phenomena mentioned above, is the geometric model. This model only applies the simultaneity of measurements of several co-observing baselines. The idiosyncrasies of this model as regards precision and reliability are discussed. On practical grounds, an intermediate computing model, called the short-arc model, is also presented. This models the above mentioned phenomena only over a short interval of time.
Computing results using the three types of models (geometric, short-arc, kinematic) are compared for the MERIT Short Campaign, both with a simulation and with the real data of §3.7, and for the simulated European geodynamics network.

5.1 WHY ALTERNATIVE MODELS ARE REQUIRED

5.1.1 Introduction

In chapter 2 all the physical phenomena required to model the "real world" of VLBI measurements were discussed. It should be clear from §2.1 and the discussions in sections 2.3 to 2.7 which describe the phenomena, that every model of such a phenomenon, however carefully designed it might be, is only an approximation. It is therefore advantageous to apply a computing model which requires a minimal number of assumptions for the description of the relevant phenomena. To illustrate the danger of wrong assumptions, chapter 2 concluded with a section on some computational examples indicating that minor changes in the assumptions can cause significant changes in both the orientation and the scale of the network and a change in shape (geometry of the polyhedron). This is also clear from §3.7.3 where real observations were used to show the same thing.

As VLBI can in principle be regarded as a technique for measuring the directions of distant objects in space, it is obvious that many physical

phenomena relevant to VLBI are concerned with rotations. Mentioned are: precession and nutation, the rate of rotation of the Greenwich meridian (UT1) and polar motion. However, also parts of other phenomena can cause a rotation; an example is the E-term of aberration (§2.8).

Now two things are of major interest:
First, the general concept of the "Delft" approach for point positioning (§1.4, items a. and b.) should be recalled, where it is indicated how to formulate a computing model that merely describes the shape of a network and how to define a coordinate system. In §2.2 the difficulties with the introduction of a coordinate system for the kinematic model were indicated.
Second, it is noted that in §2.8 four phenomena were listed which dominate the bottom-line error budget of geodetic VLBI. These are in sequence of decreasing magnitude: dry troposphere at low elevations, wet troposphere, nutation and telescope structure.
Both considerations, the first from the point of view of a general theory which regards rotations of a coordinate frame as non-estimable and therefore of minor interest, the second because it concerns one of the major error sources, justify the conclusion that a way must be found of bypassing the dangers described above and of applying a computing model independent of coordinate frame rotations.

5.1.2 Description of Experiment

To eliminate the rotations, first of all an analysis should be made of the true observational process.
Consider an observer on an Earth which can be assumed to be rigid. At some distance from the Earth (approximately eight thousand million lightyears away) some objects exist that have (or rather show) no proper motion. Since the definition of an inertial coordinate frame says that the system does not undergo any acceleration, it can be stated that these objects do form - to a good approximation - an inertial frame for the observer.
One then decides to study the diurnal motions of these objects by an instrumentally-perfect theodolite which is not necessarily positioned exactly perpendicular to the local equipotential surface of the Earth's gravity field. The theodolite (= the point of intersection of the two cross-hairs in the field of view) is pointed at a certain distant object and the readings on the "vertical" and "horizontal" circles (the quotation marks are added in view of the random position of the theodolite) together with the reading of a perfectly running clock are written down. As the object is moving away from the point of intersection of the two cross-hairs and finally disappears from the field of view, and the object is almost at infinity, the conclusion must be that the Earth is rotating.
After some time, the object appears again in the field of view from the opposite side. When it crosses the "vertical" cross-hair, one reads the clock, rotates the point of intersection of the cross-hairs around the "horizontal" axis to the object and also reads the two circles. The reading of the "horizontal" circle is - by the definition of the experiment - the same as before. The reading on the "vertical" circle is somewhat different. The observer decides to call the difference between

the two time readings: the time required for one "Earth's Rotation", one ERO.
The experiment is repeated several times and the conclusion is that it is a very complex "rotation" since neither the difference between the clock readings, nor the measured angle in the "vertical" plane is constant, or even a linear function of time. Therefore, the ERO cannot be described by a strict mathematical rotation about one axis.

Now one can ask the question: what is the reason for the preference of the "vertical" cross-hair as a reference; why not use the horizontal one? A number of these rotations are measured but completely different time intervals are found which by themselves are again not linearly changing: call these ERO2.

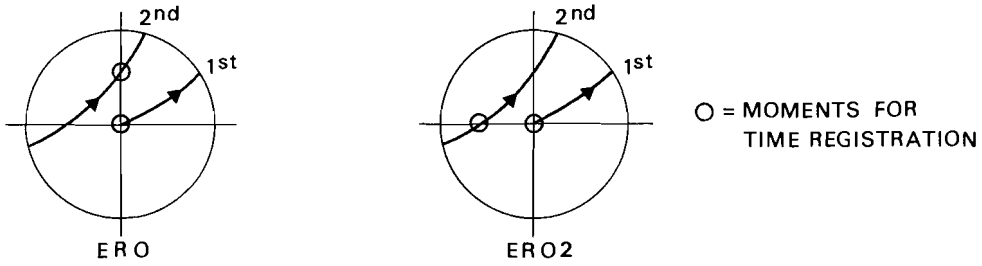

Figure 35: Observed Rotations in a Theodolite-fixed Frame

The observer realizes that a choice must be made and decides to position the theodolite in such a way that the object will not start moving randomly through the field of view, but parallel to the "horizontal" cross-hair. Now a non-ambiguous definition of the Earth's rotation (ERO3) has been found, but the complex changes do not disappear.

However, as one cannot monitor a three dimensional rotation with only one direction, a final experiment is invented. A theodolite is constructed such as the one used in Hipparcos (HIgh Precision PARallax COllecting Satellite), capable of observing three objects simultaneously although they have quite different positions in the sky. The theodolite is, as in the preceding experiment, positioned such that all three sources are at the point of intersection of the cross-hairs and start their motion parallel to the (common) horizontal cross-hair. As the Earth completes its diurnal motion, the theodolite is continuously adjusted, both by changing the horizontal orientation and the direction of the prime axis of the theodolite, to keep the sources at the point of intersection. After exactly 360 degrees rotation on the horizontal circle, the clock time is registered to determine the duration of this ERO4 motion.

5.1.3 Discussion

In the first experiment, a coordinate system, a triad, was defined by setting up the theodolite and leaving it alone. With respect to this "theodolite-fixed" frame of reference the ERO-motion is defined and monitored. The changes in the successive readings for the "vertical" circle and the clock intervals describe the changes of the length of one ERO and the changes in the ERO-pole. The same holds for the second method.
Now at first sight, one is left with two, equally probable definitions of a rotation: ERO3 and ERO4. These are shown in Figure 36, where the irregular helical motion of the Earth's pole is drawn. This illustrates the difference between the two experiments.

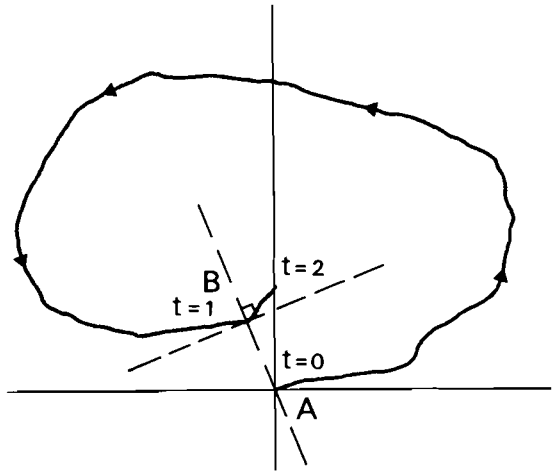

Figure 36: Helical Motion of the Earth's Equator

The reference frame of the theodolite for the third experiment is defined in position A at the start of the experiment and is in position B when the source crosses the vertical cross-hair. The time difference between t0 and t1 is defined as one ERO3.
Continuously adjusting the theodolite during the last experiment is actually trying to maintain the reference frame with a "vertical", or Z-axis, defined to be colinear with the instantaneous rotation axis at the beginning of the experiment. The adjustments required for the orientation of the "vertical" axis of the theodolite, describe the position of the ERO-pole with respect to that at the beginning of the experiment. It is obvious from Figure 36 that the time required to cross the vertical hair again, as measured in this frame, is t2-t0, which differs from t1-t0.

The above description was meant to illustrate the fact that what one measures depends on one's viewpoint. More precisely, it can be stated that it is important to decide what coordinate frame will be adopted to describe the directions. Futhermore, it should be concluded that only one rotation (ERO4) can be observed, regardless how many phenomena constitute this rotation.

Now, some concepts from chapter 2 are recalled:

- precession... the attracting forces of Sun, Moon and planets yield motions of the mean poles of equator and ecliptic; ...it is defined as the rotation from the equator and equinox at epoch to the mean equator of date and mean equinox of date.
- nutation... is the somewhat irregular rotation - due to the attracting forces of Sun and Moon - of the true pole about the mean pole.
- polar motion... consists of the long period components of the effect that the Earth's spinning pole is rotating with respect to a number of observatories fixed to the Earth's crust.
- Earth rotation... the Greenwich mean sidereal time, which is the Greenwich hour angle of the first point of Aries, is given by Newcomb's formula. However, 24 hours of sidereal time do not yield exactly one rotation of the Earth due to precession and nutation. In addition, the angular velocity is subject to periodic and sudden changes due to e.g. Earth tides and movements in the interior of the Earth.

Some quotations are added:

> "Newcomb gives constants, based partly on theoretical considerations but mainly on observation, from which the numerical expressions for ζ_o, z and θ (24.1) can be deduced." [Astron.Eph.Supp.,1974]

> "While nutation and some polar motions arise from related causes, the points of view are quite different. Polar motion takes place in a rotating terrestrial reference frame. Nutation is seen in an inertial celestial reference frame" [Ma,1978].

To summarize:
The long-period, smooth motion of the pole of the equator due to the attracting forces of Sun and Moon on the rigid, non-spherical Earth, together with the motion of the pole of the ecliptic due to the gravitational forces of the planets are taken together in the (observationally derived) formulas of precession. Superimposed on this, the rotations due to the same objects (Sun and Moon) with a periodic character from 19 years to 5 days are taken together as nutation, computed in the J2000 system for a deformable Earth. In this way, the equator and pole at epoch (by agreement the coordinate system defining values) are rotated to a certain equator and pole at the moment of observation from which the ("theoretically forecasted") motions of up to 5 days are filtered out.
Next, one starts from the other side: observers on Earth, fixed to the Earth's crust, follow the diurnal orbit of a number of objects with respect to the instantaneous spinning pole. Any changes in the angle: "pole - point of observation - object" minus the changes already accounted for in the above reasoning for precession and nutation and minus the effects of aberration are interpreted as polar motion and Earth rotation. It should be added here that local distortions due to Earth tides or regional crustal movements also add to the observed angle, but

by averaging over a number of stations and a somewhat longer period these phenomena are (hopefully) filtered out.

5.1.4 Conclusion

In conclusion, it can be stated that with polar motion all motions of the instantaneous rotation axis are described that are not accounted for by precession and nutation (and aberration). A small change in the nutation formulae will thus yield a small change in the polar motion and UT1 results. If it were not impossible for various reasons from the field of mechanics, the Chandler wobble could be a 1.2 year term "forgotten" in the nutation theories. This is in agreement with the fact that nutation, in practice, is a pure theory, based on present-day knowledge about the motions of Sun and Moon and the rheology of the Earth. Better knowledge about especially the latter will improve nutation theories.
Perhaps another definition of nutation is required here, such as: "the theoretically predicted motions of the equatorial pole, based on the ephemeris of Sun and Moon, acting on a non-spherical, deformable and rotating Earth".

Therefore, by measurements of directions only (and this is what VLBI does, in principle), it is impossible to separate e.g. polar motion and nutation, because the only observable one has available is the angle between the instantaneous rotation axis, (parallelly transported to the observing stations) and the fixed source, in two orthogonal directions. Here, time is here just a way of measuring the "horizontal" angle. This is exactly the case demonstrated by the third experiment of §5.1.2.

Naturally one has physical reasons for assuming that the Earth's crust is moving with respect to the pole of rotation and that the pole of rotation is moving with respect to the fixed stars, but what is stated here is that only the sum of the two effects can be measured by direction observations from crust-fixed stations (such as those of VLBI), and that the same applies to the rotation rate of the Greenwich meridian with respect to the fixed stars. Experiments other than those which only measure directions will have to be conducted in order to discriminate between motions of the pole with respect to the crust and of the pole with respect to the fixed stars.
One possibility is placing a number of gravimeters around the North pole and using the differences in readings, via the centrifugal force (at one point it should be zero!) to compute the pole position with respect to the Earth's crust. As one requires in this case exact knowledge of the gravity field of the Earth, the problems with this experiment which are connected with gravity fluctuations due to the Earth's interior and the precision required, need no further explanation!
A better possibility offers the application of gyro's: [Hanse et al.,1984] studied the application of ring laser gyro's, for which it looks now marginally feasible to measure crustal rotations around the vertical to an accuracy of 0.2 arcseconds RMS.
For Earth rotation one imagine measuring the touch-down position in the horizontal plane of a number of free-falling objects from a certain height (Figure 37). They do not fall exactly normal to the equipoten-

tial surface but they move somewhat Eastwards. This is because the horizontal velocity of an object at the top of a tower is larger than the velocity of an object at ground level, due to the Earth's rotation.

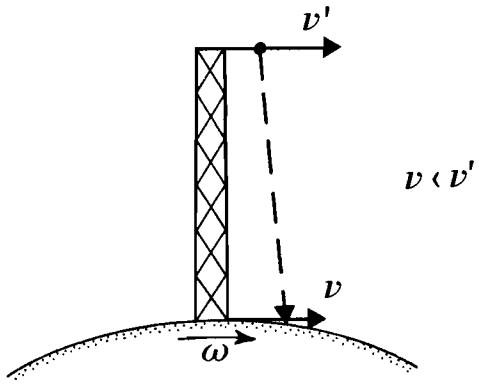

Figure 37: Free-Falling Object on a Rotating Earth

In the above reasoning it was stressed that it would not be possible by measurements of the directions of distant objects alone, to discriminate between the many rotations from very many different origins, but mostly related to the motions of the Earth, Sun and Moon. The most rapidly changing coefficient in nutation is the semi-annual one which changes by 0.006 arcsec per day. Polar motion changes with a rate of approximately 0.002 arcsec per day. In view of these values and of the limited accuracy of the models of these phenomena, the feasability of other computing models will now be investigated. Via the latter models the relative position of a number of stations can be determined without any danger of being affected by the inaccuracies of the former models. It should be noted that all other algorithms such as those of Earth tides and refraction have to be applied in their entirety.

Starting with this goal, two options are now open for defining alternatives to the kinematic computing model:

a)... to define a purely GEOMETRIC computing model in which the rotational motions of the Earth are not used. At any instant of observation, the radio source is observed by a number of baselines and this source position is defined by two separate unknown coordinates in the LSQ adjustment, which are not related (via measured time and knowledge of rotations such as precession) to positions of the same source at other instants of time.

b)... to define -what is called- a "SHORT-ARC" computing model in which the rotational motion models for precession etc. are applied, but where the algorithms are declared only valid for a short period of time, so that after this time new unknowns for the source position coordinates will be introduced.

Especially the first computing model is completely defined in accordance with the preceding sections where it was shown that VLBI can in no way separate the observed rotation angle between spinning pole and the Earth's crust for its causes, so that there is no need to model the phenomena separately. These two computing models may be of use for campaigns with more stations at the highest precision level. They will be discussed and applied in the following sections where delay observations only are used.

5.2 GEOMETRIC COMPUTING MODEL

5.2.1 Concept

This computing model was first discussed by [Aardoom,1972]. The basic idea of the geometric computing model is that two additional unknowns (two source position parameters) are introduced in the LSQ fit for every simultaneous observation by several telescopes. Consequently, at least three co-observing baselines (four stations) should be available: two independent delay observations to solve for the source position and another one to "play the winning game" against the initial number of unknowns: station coordinates, clock parameters, etc.
Only two basic assumptions are required for this model: (a) the stations are at rest with respect to one another for the duration of the campaign and (b) the source position is the same for all co-observing baselines during the correlation interval.

It follows from (a) that rotations such as precession, nutation, polar motion and UT1 can be neglected as they do not affect the relative position of observatories within their polyhedron, but change only their common orientation. On the other hand, Earth tides and antenna structure cannot be neglected because these are the effects that change the station geometry most. The instrumental effect of clock behaviour should also be included.
Assumption (b) is violated in the first place by the retarded baseline effect, which was demonstrated in §3.7.2. Furthermore, refraction effects of dry and wet troposphere and of ionosphere change the observed direction of the astronomical object as a function of baseline as well. On the other hand, the effects of gravitational deflection and annual aberration are common to all baselines and can thus be neglected.

With this in mind, the observation equation for the geometric model can be defined as, cf. (22.7):

$$\begin{aligned} \tau &= -((B) \cdot (U)) / c \\ &\quad + \tau_{RTB} \\ &\quad + \tau_{TRO} \\ &\quad + \tau_{CLO} \\ &\quad + \tau_{ANT} \\ &\quad + \tau_{TID} \\ &\quad + \tau_{ION} \\ &\quad + \tau_{AMB} \end{aligned} \qquad (52.1)$$

It is clear from (52.1) that for the geometric computing model only a simple inner product of the baseline vector and the source vector is required. The source vector (U) is here the observed instantaneous position vector. At this point, however, the question arises how to define the coordinate system. Origin and scale can be defined as the "standard" choice in §3.3: constrain the X-, Y- and Z-coordinates of one station and the velocity of light. The definition of the orientation of the coordinate frame requires a different approach. As there is no Earth rotation axis present in the model formulation to serve as a reference, a logical choice is to constrain three source coordinates, e.g. one right ascension and two declinations. In this way, station coordinates can be estimated with respect to the epoch equator and equinox.

An alternative choice, however, is to constrain 7 stations coordinates (two stations with X,Y,Z and e.g. the Z-coordinate of a third station, depending on the orientation of the network with respect to the coordinate axes). If the arbitrary values are now chosen to be as close as possible to their CIO-system values, this frame is thus defined, in the same way as the adoption of the latitudes (and the longitudes) for the five IPMS-stations define the CIO. By doing this, all source coordinates will be expressed with respect to the CIO-equator and the Greenwich conventional meridian. This, however, is not of any importance because the choice of the coordinate system is arbitrary and the goal of prime interest is to determine the relative position of a number of VLBI observatories.
Please note that, although the geometric model requires in principle no precession and nutation computations, these can nevertheless be useful in the geometric model, but only for determining good approximate values for the linearisation of (52.1) according to the Least Squares requirements.

The implementation of the geometric computing model in DEGRIAS is completely analogous to the kinematic model. It has already been indicated that by a sensible choice of the approximate values of the unknown parameters in the LSQ fit, the computed observations can be the same. As regards the estimable parameters, in equation (31.2) only the three Earth orientation parameters should be excluded: dXp, dYp and dUT1.
During the processing of the observation file DEGRIAS checks whether the source is observed by other baselines at the same time. If this is the case, the same unknown parameters (= same two column numbers in the design matrix) are taken for the source position. If the source has not been observed at the same time before, two additional parameters will be included in the adjustment. If at least two observations are not present for each correlation interval, an error message is printed.

The major disadvantage of the geometric computing model is the large number of unknown parameters. For an observing session of 24 hours and an average scan length of 10 minutes, application of the geometric model means an increase from 26 (13 sources) to 288 source position unknowns. This has two effects. In the first place, the solution of the system of normal equations requires more computing effort because of its larger size. This poses no real problems, however, in view of the application of sparse matrix techniques (§3.2). On the other hand, the formal precision of the estimated unknowns gets worse due to the decreasing number

of redundant observations. Therefore, more observations over a longer campaign are needed to arrive at the same level of (formal) precision. When the observations have already been made, the following considerations need to be balanced: the computation of an LSQ fit using the kinematic model with a better formal precision, but with a higher risk that systematic errors are present due to invalid assumptions concerning model algorithms, or the computation of a solution with the geometric computing model with a worse formal precision, but with a lower risk of systematic errors.
Naturally, the way out of this dilemma is to compute both solutions: if the differences between the estimated results (parameters) of the two computing models after statistical testing are less than can be explained by their respective formal errors, then one may assume that no systematic effects are present and the formal error in the kinematic model results is indeed a realistic one. To compare station coordinates from both solutions, the approach of chapter 6 could be applied.

5.2.2 Estimability Considerations

[Aardoom,1972] analysed the geometric approach from the point of view of estimability. Minimum numbers were derived for participating observatories and observed sources. The basic configuration consists of four stations (which means three independent co-observing baselines for the geometry) with at least 6 different source positions. The relevant numbers which show that the configuration is barely defined in this case are:

observations	estimated parameters
6*3 delays	4*3 station coordinates
7 for coordinate system definition	6*2 source coordinates
	1 scale unit
25	25

Further reference (for other numbers of participating stations) is made also to [Brouwer&Visser,1978] and [Dermanis&Grafarend,1979]. The latter also includes deformations of the station geometry.

The geometric approach is also suitable for demonstrating one of the main characteristics of the "Delft" approach (§1.4), i.e. the formulation of condition equations, because the above calculation of the number of unknowns and observations is not a complete proof of the validity of the minimum requirements. A condition equation containing all observations, on the other hand, provides this proof. In Appendix F a formula is derived for the (hypothetical) two-dimensional case of VLBI observations.

5.3 SHORT-ARC COMPUTING MODEL

In the preceding section it was mentioned that the major disadvantage of the geometric model is its need for many observations. To balance this disadvantage with the advantage of a more hypothesis-free approach, the so-called short-arc computing model was introduced. In this approach, use is made of the algorithms for precession, nutation, polar motion and Earth rotation, just as in the kinematic model, but now just for relating positions of the same source within a limited period of time, e.g. 6 hours. After that period, it is presumed that the path of the source in the sky can no longer be modelled by the routines and new source position parameters are estimated. Hence, one divides the source path into small sections which are treated separately.
DEGRIAS allows several choices for this time interval, ranging from 1 hour to 12 hours. When the VLBI network is not too extended, an optimal choice is probably to take all the positions of the source between its rising and setting as one interval.
That the short-arc computing model is indeed an intermediate between the geometric and the kinematic model is readily seen by increasing the time interval to the duration of the entire campaign, as one then arrives at the kinematic model, or by decreasing the interval to one minute or so, for which the geometric approach is found. By using this computing model, the possible discrepancy of - mainly - the nutation model theories from reality (§2.4.3) will show up in the estimated source parameters; significant deviations could thus yield improved nutation theories.

5.4 COMPARISON OF COMPUTING MODELS

5.4.1 European Geodynamics Network

For comparison with §4.4.4, both the Southern sub-network and the extended network in their triangle shape have been computed with the aid of the geometric model. All relevant options were the same as in §4.4.4.
The results are briefly summarized in Table 20.

The eigenvalues have been computed for the Southern sub-network with respect to the same fit as used in Table 18. The eigenvalues for the extended network have been computed with respect to the corresponding kinematic fit. All numbers indicate that the geometric computing model is hardly applicable to this station configuration, not even with the large number of (relatively short) baselines in the large network, bacause even doubling the number of observations would bring the standard deviations only barely below the decimetre level.

5.4.2 Application to MERIT-SC

5.4.2.1 Simulation

In the same way as was done for the kinematic model (§4.4.2) here a number of simulations is computed with the use of the short-arc and the

Table 20.

Geometric Model Applied to European Geodynamics Network

	Southern Network		Extended Network	
μ-max	32359.	13942.	6712.	5438.
σ ROB-CAS (cm)	49.5	31.6	12.9	11.0
σ BOL-SIC (cm)	41.7	27.1	10.7	9.2
σ CRI-CAI (cm)	98.1	63.5	22.5	21.8
mean ∇ (ns)	1.30	1.01	1.22	1.17
mean $\overline{\lambda}$	4.70	2.54	1.37	1.27

geometric model. In the simulated case only the official schedule is examined; for the results using the observations left in the reference fit of §3.7.2 one is referred to §5.4.2.2.
The set of estimable parameters is chosen as before (station and source coordinates, second order clock polynomial, tropospheric zenith delay and Earth orientation parameters) for 24 hours of observations, with a fixed standard deviation of 0.2 ns. The results should therefore be compared with run 1 of Table 15.
The results are shown in Table 21. Run 1 is a short-arc computation with an interval of 6 hours and run 2 uses an interval of 2 hours. Run 3 is the geometric approach for one day. In addition, for the geometric model a two day campaign is computed in run 4.
It is obvious from the computed results that both with respect to precision and reliabilitity the application of the short-arc computing model is justified. The numbers are not very different from the data of the kinematic approach. The geometric computing model, however, is too weak for use with a set of one day's observations. From run 4 it is clear that at least three days of observations will be required to arrive at a level of formal precision for this station configuration such as that of the kinematic model. The S-basis for the geometric solutions was chosen to be the stations Effelsberg and Haystack, with in addition the Z-coordinate of HRAS.

5.4.2.2 Real observations

As a final test of the computing models developed, the results of a number of adjustment computations of the MERIT-SC data are compared. Here, only simultaneous observations of at least 3 baselines are used and no Earth orientation parameters are estimated. The runs are:

A. using the kinematic model according to the standard fit of §3.7.2, but now all source positions are estimated.

Table 21.

MERIT-SC, Short-arc and Geometric Computing Model

I T E M	RUN 1	RUN 2	RUN 3	RUN 4
number of observations	970	970	970	1875
formal sigma EF-ON baseline (cm)	1.5	1.8	8.8	6.3
formal sigma EF-OV baseline (cm)	7.4	11.0	44.4	30.7
formal sigma HR-ON baseline (cm)	8.2	12.7	33.2	23.0
formal sigma HR-OV baseline (cm)	2.1	3.1	14.6	10.4
formal sigma EF-HR baseline (cm)	8.1	12.9	35.1	24.0
formal sigma OV-ON baseline (cm)	7.1	10.5	41.7	29.1
formal sigma HA-ON baseline (cm)	4.2	6.8	8.3	5.8
formal sigma HA-HR baseline (cm)	3.8	5.7	30.8	21.6
formal sigma HA-OV baseline (cm)	3.4	5.5	41.5	29.4
formal sigma HA-EF baseline (cm)	4.1	6.8	0.0	0.0
mean m.d.e. data-snooping (ns)	0.88	0.92	1.03	1.03
maximum m.d.e. data-snooping (ns)	1.43	1.43	1.43	1.43
sigma m.d.e. data-snooping (ns)	0.07	0.12	0.17	0.17
mean $\overline{\lambda}$ (all unknowns)	1.36	1.83	2.90	2.86
max. $\overline{\lambda}$ (all unknowns)	5.84	5.84	5.84	5.84
sigma $\overline{\lambda}$ (all unknowns)	0.72	1.05	1.34	1.35

B. using the short-arc model, applying a duration of 8.5 hours for each source position interval. All other options are the same as in A.
C. as B, but with 4.5 hours for the interval.
D. as B, but with 2.5 hours for the interval.
E. as B, but with 1 hour for the interval.
F. using the geometric model, again with the same options as before; the S-basis for this solution was chosen as above.

For all runs, the same observations were used and no attempt was made to edit the data according to the results of the statistical testing of each run, so that the differences between the results are directly interpretable as differences following from the computing models. It is immediately clear from Table 22 that relaxation of the computing model via geometric or short-arc approach solves some problems with a biased solution (because of the decrease of the test variate F, at the 5 percent level) at the cost of an increase in the formal errors.
In view, however, of the fact that the differences between the results of the applied short-arc models are all within 2 to 3 times their standard deviation, it can be stated that the models are all applicable. This indicates exactly the choice that one should make (cf. §5.2): the balance between formal error and real biases, which is illustrated in Figure 38. Here one sees that the quoted formal errors for the kinematic model of DEGRIAS applied to the MERIT-SC data are slightly opti-

mistic. A more realistic value is found for run C, where, according to the multi-dimensional F-test, the formal errors present a realistic picture of the true accuracy.

The geometric model, however, shows completely different results. The computed baseline lengths seem to have no relation to the other computed estimates, although the differences can be formally explained by the magnitude of the standard deviations. As regards the MERIT-SC data, therefore only one conclusion is possible: the geometric computing model is not applicable to these data and station configuration. Apart from the fact that the formal precision is bad, it must be that systematic effects other than the ones were tried to be eliminated, are more significant.

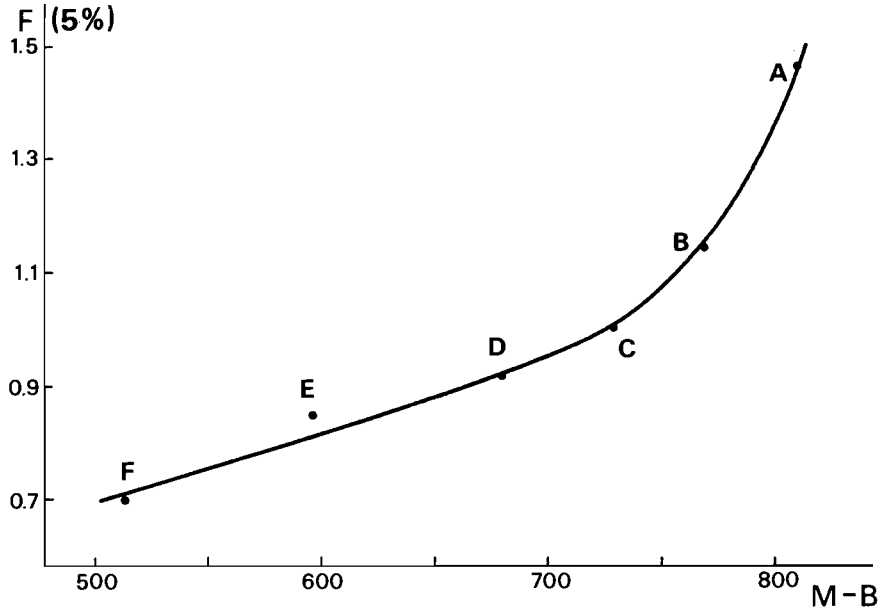

Figure 38: Test Variate and Number of Redundant Observations

5.4.3 Conclusion

The conclusion from the above computations is twofold.
Firstly, it is concluded that the short-arc model presents a good picture of reality since, on the one hand, it eliminates some systematic biases in a solution computed with the kinematic computing model and, on the other hand, it yields somewhat more realistic values for the formal errors.

Secondly, it is concluded that the geometric model, although very attractive from a theoretical point of view, is hardly applicable to realistic VLBI situations. It was found for the MERIT-SC data that the estimates of baseline length deviated too much from the results of the kinematic model.
The conclusion was therefore either that the number of observing baselines should be relatively large (over 20), with in addition a favoura-

Table 22.

Comparison of Computing Models for MERIT-SC

	A	B	C	D	E	F
no. of observations	874	874	874	874	874	874
no. of estim.source coord.	25	67	107	155	241	326
no. of unknowns	62	104	144	192	278	360
length + sigma EF-ON (cm)	2 2	6 2	4 3	8 3	9 4	24 13
length + sigma EF-OV (cm)	18 12	44 13	34 16	44 18	20 27	-193 93
length + sigma HR-ON (cm)	12 14	38 15	32 18	33 20	7 28	-146 65
length + sigma HR-OV (cm)	5 3	15 3	9 4	8 5	7 8	49 18
length + sigma EF-HR (cm)	14 13	38 15	30 7	29 20	4 29	-181 71
length + sigma OV-ON (cm)	16 12	41 13	35 16	46 18	21 26	-171 86
length + sigma HA-ON (cm)	10 9	31 10	27 12	35 14	22 25	36 11
length + sigma HA-HR (cm)	8 7	20 8	21 10	30 11	23 20	-123 75
length + sigma HA-OV (cm)	12 7	31 8	27 10	40 12	35 23	-63 78
length + sigma HA-EF (cm)	12 8	32 10	27 12	34 13	22 24	0 0
Test variate F	1.46	1.14	1.00	0.92	0.84	0.70

ble station configuration, or that, for networks with less stations, observations over longer periods of time (3-4 days) are needed, which is probably not realistic as systematic effects other than the rotations (which one wants to eliminate) become increasingly dominant.

PART II

COMPARISON OF TECHNIQUES

Absolute space, as "the seat of inertia"...
It conflicts with one's scientific understanding to conceive of a thing which acts, but cannot be acted upon.

[Albert Einstein]

Chapter 6

N E T W O R K C O M P A R I S O N

Summary: In the first section of this chapter it is stated that coordinates have only a relative meaning and depend on a number of assumptions. These assumptions should define three translations, three orientations and one scale factor in a 3-D Euclidean space. The relation between different sets of assumptions, called S-bases, is the similarity transformation.
Starting from the similarity transformation, there are two ways of comparing and combining two sets of 3-D Euclidean coordinates for a number of stations. These can be the result of a network measured at the same time by two different techniques (comparison of techniques) or of a network measured twice by the same technique (deformation analysis).
First, it is possible to apply a similarity transformation and an S-transformation, which is a covariance transformation, and to compare the two sets of coordinates directly via an adjustment of the type X1=X2, thus analysing only differences in the shape of the network. A second possible approach is to estimate transformation parameters in the LSQ adjustment as well. Both types of approach are discussed and applied to the case of the Doppler and VLBI coordinates of the ERIDOC network. Furthermore, the technique is used to derive an estimate for the detectable shift of the African plate with respect to the European plate via the network presented in chapter 4.

6.1 COORDINATE SYSTEMS AND FORM ELEMENTS

In every mathematical handbook one finds that coordinates are defined as distances (in certain directions) to a line or a (hyper)plane or surface, this depending on the dimension of the problem (cf. §3.3). This definition leaves open the question whether the space one is examining is Euclidean, Riemannian or other. Distances are simply defined as the shortest path between the point whose coordinates are required and the reference planes, taking into account the metric tensor which describes the geometry of the space. Consequently, the reference planes are agreed upon. Every researcher investigating the space may choose his own set of planes. This set should obviously be complete, i.e. as many planes should be chosen as there are dimensions of the space. In addition, it should be a non-singular choice, which means that the planes should not be parallel (i.e. linearly dependent). This implies that in an N-dimensional space any choice of N linearly independent (hyper)planes or surfaces is equally valid. Consequently, the results computed in one coordinate system are equivalent to the results in another system. But what does one mean by "results"?

By definition, coordinates are not results as they are not the same for every researcher using his own coordinate system. However, the relative position of points (and this is what the geodesist is mostly interested in) is independent of the coordinate system definition, and therefore a "result". The basic tool for describing the relative position of a number of points is called: form element. In the planar case, this is a triangle. It can easily be shown that the Π -quantity [Baarda,1967] which is defined in Figure 39 as a complex number containing a length ratio and an angle, describes the relative position of three points independent of the coordinate system.

Now the discussion is confined to the case of the three dimensional Euclidean space. Three orthogonal planes and the distance between equally spaced marks on the lines of intersection of these planes (the length scale!) have been defined. The point of intersection of the three planes is the origin of the coordinate system. Let there also be a second choice for the planes and length scale. Three points a, b, and c have coordinates (X,Y,Z) with respect to one system and (U,V,W) with respect to the other. As it is known or (in view of the theory of general relativity, for a "small" region) hypothesized that the space is a three dimensional Euclidean one, the coordinates in the one system can be computed from those in the other via a similarity transformation with seven parameters: three translations, three rotations and one scale factor:

$$\begin{pmatrix} U \\ V \\ W \end{pmatrix} = \mu \cdot (R_Z) \cdot (R_y) \cdot (R_x) \cdot \begin{pmatrix} X \\ Y \\ Z \end{pmatrix} + \begin{pmatrix} Tu \\ Tv \\ Tw \end{pmatrix} \qquad (61.1)$$

Here μ is the scale factor, Tu, Tv, Tw are translations along the U, V and W-axis respectively and (R_x), (R_y) and (R_Z) orthogonal rotation matrices, defining successive rotations about the X-axis, the (resultant) Y-axis and the (resultant) Z-axis, which are defined as (coordinate systems right-handed, rotations counter-clockwise as viewed from the end of the positive axis):

$$(R_x) = \begin{bmatrix} 1 & 0 & 0 \\ 0 & \cos\alpha & \sin\alpha \\ 0 & -\sin\alpha & \cos\alpha \end{bmatrix} \qquad (61.2)$$

$$(R_y) = \begin{bmatrix} \cos\beta & 0 & -\sin\beta \\ 0 & 1 & 0 \\ \sin\beta & 0 & \cos\beta \end{bmatrix} \qquad (61.3)$$

$$(R_Z) = \begin{bmatrix} \cos\gamma & \sin\gamma & 0 \\ -\sin\gamma & \cos\gamma & 0 \\ 0 & 0 & 1 \end{bmatrix} \qquad (61.4)$$

Disregarding singular cases, one can now compute the seven transformation parameters: Tu, Tv, Tw, μ, α , β and γ from the relations that seven coordinates (of the possible nine of the three stations) in one

system should be identical to those in the other system. One can therefore compute 36 sets of parameters. Here the transformation is defined as a shift of, and a rotation about the origin. In the geodetic literature this is commonly known as the Bursa model. [Leick&Van Gelder,1975] present some alternative definitions of the translations and rotations as well.
It is now obvious that form elements can be defined as quantities which are invariant under a similarity transformation, because both the length ratio L_{bc}/L_{ba} and the angle "abc" and the ratio of the complex numbers z_{bc} and z_{ba} do not change.

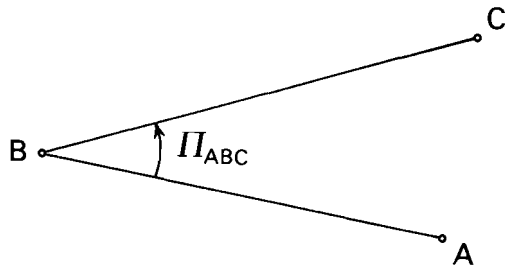

$$\Pi_{ABC} = \frac{L_{BC}}{L_{BA}} + i\alpha_{ABC} = \frac{z_{BC}}{z_{BA}}$$

Figure 39: Definition of Π - Quantity

As the description of the relative positions of a number of stations by means of angles and length ratios is not very practical compared to using coordinates, coordinates are also introduced in the "Delft" approach (§1.4). Here, however, they are called: S-coordinates, where the "S" denotes that, in principle, these coordinates do not mean anything other than a description of the relative positions of a number of points by quantities invariant under a similarity transformation. To the "S", subscripts should be added what the seven quantities which define the coordinate system are.
It was stated above that the reference planes can be chosen at will. This means that it is a matter of taste and convenience how one defines a coordinate system. For a world geodetic system it is obvious that choosing the origin as close as possible to the Earth's centre of mass, with the Z-axis along the rotation axis is the most sensible thing to do, if only in view of the many corrections which depend on latitude.

Now one arrives at the question of how this choice is really made. How, for instance, is the centre of mass of the Earth defined? Nobody has access to this point; its position with respect to the Earth's surface can only be determined via formulae, not via direct geometric measurements. And what about VLBI? VLBI-measurements are in no way (except for some negligibly small relativistic effects) related to the centre of mass of the Earth! How then can VLBI yield geocentric coordinates?
The answer lies in the fact that the reference planes themselves are mostly not chosen but a number of coordinates of points to define the planes. The definition then becomes e.g. $Sa,b;c_Z$ for a choice for the X,Y and Z coordinates of the stations a and b and the Z-coordinate of station c.

For the International Polar Motion Service, for instance, the longitudes and latitudes of the five observatories at the 39.8° parallel have been adopted to define the CIO-pole (§2.2) and not the other way round! Similarly, for VLBI measurements one has to adopt geocentric (X,Y,Z) coordinates of one station in order to define the centre of the Earth.
The same applies to Amersfoort, the origin of the Dutch triangulation network, where the ellipsoidal longitude and latitude of the origin have been chosen as follows: the astronomical longitude of the Leiden astronomical observatory was taken, plus a longitude difference derived from the adjusted observations of the first order triangulation between Leiden and Amersfoort. The latitude was computed as the mean of 13 values determined from astronomical observations from stations all over the country, again corrected via the adjusted triangulation observations. In the same way the network was orientated via the average of 13 Laplace azimuths. It is worth noting that the largest difference in latitude was 5.2 arcseconds, which equals 160 metres! [Claessen&Bruins,1979]. In addition, the maximum difference in azimuth was 7 arcseconds, which is about one metre for a side length of 30 km. These are very large values compared to the "relative" precision of the Netherlands first order triangulation of only a few centimetres.

From many other similar examples (cf. UT1 accuracy from VLBI: about 1 metre, and baseline precision: a few cm) it becomes clear that "absolute" position, orientation and scale of the entire network are determined to one or two orders of magnitude of accuracy less than "relative" position (shape) of the stations within the network (cf. §2.8).

6.2 COMPARISON OF 3-D EUCLIDEAN COORDINATES

6.2.1 Introduction

The comparison of two sets of 3-D coordinates of terrestrial stations is required in two cases. In the first place, the two sets may have been derived by using different measurement systems; this is commonly known as intercomparison of techniques. Secondly, the two sets can originate from two measurement sessions separated in time. In this case the goal is to determine a possible deformation of the network.
Now, in principle two situations are feasible (cf. §6.1):

- both networks are described in the same coordinate system but the shape of the polyhedron of stations is not the same (cf. deformation).

- the shape of the polyhedron of stations is the same for both networks but described in different coordinate systems (cf. intercomparison).

The most common situation is that both the reference frames (e.g. Doppler in a geocentric frame and VLBI in a quasi-geocentric one (§2.2)) and the shapes of the networks (systematic and random biases between Doppler and VLBI, e.g. by the refraction model) are different; hence there is a combination of the two situations mentioned above.
Wherever the expression "the same" is used above, it should be noted that the coordinates are derived from measurements with a random character and they therefore have an error distribution. "The same" means thus: within the limits defined by their stochastic behaviour.

6.2.2 Shape-only Approach

A well-known situation where one wants to check whether the shapes of two geodetic networks are the same, is the two-dimensional closed polygon network which is to be connected to higher order triangulation points. In this case the coordinates of the closed polygon network are computed starting from the published coordinates of two triangulation stations a and b (use of the Sa,b-system; §6.1). Now, for the other trig-points no discrepancies between the published coordinates and the coordinates in the Sa,b-system should be present which are larger than can be explained by the stochastic behaviour of both the Sa,b-system coordinates (error propagation law for the measured directions and distances) and the published triangulation coordinates. This is checked via an LSQ adjustment with both sets of coordinates as observations. If this adjustment shows no significant discrepancies (via statistical testing!), the closed polygon network can be connected to the trig-points by computing the coordinates of all other polygon points in the triangulation system via the error propagation law for correlated observations.
Since the approach described above is concerned with comparing shapes of networks, it follows from §6.1 that the Π-quantity is an appropriate tool. An application is presented in [Wessel&Koudijs,1984].

For the sake of analogy with the next section and because of computer-technical preferences, the approach with form elements (for 3-D its algebraic tool is the quaternion [Quee,1983]) is not chosen here. Instead, use is made of S-coordinates (§6.1) and the adjustment problem is formulated as one using observation equations.

The stochasticity of two sets of coordinates (X) and (Y) is described by the following two variance/covariance matrices:

set X	coordinates		var/covar matrix	
S-basis coordinates	X1 . Xi		QX11 QX12 QX13 =0 =0 =0	
other coordinates in common	Xj . Xm	(QX) =	QX21 QX22 QX23 =0	(62.1)
other correlated coordinates	Xn . Xr		QX31 QX32 QX33 =0	

set Y	coordinates	var/covar matrix	
S-basis coordinates	Y1 . Yi	QY11 * QY12 * QY13 =0 * =0 * =0	
other coordinates in common	Yj . Ym	QY21 * QY22 * QY23 =0 * *	
other correlated coordinates	Yn' . Yr'	QY31 * QY32 * QY33 =0 * *	

(QY) = (62.2)

The number of S-basis coordinates is equal to the number of parameters of the similarity transformation, i.e. seven for 3-D. The values of these S-basis coordinates are the same in both sets (e.g. the trig-point coordinates above), so that:

$$\begin{array}{ccc} X1 & = & Y1 \\ . & . & . \\ . & . & . \\ Xi & = & Yi \end{array} \qquad (62.3)$$

The coordinates j...m refer to stations common to both networks, whereas n...r and n'...r' respectively are coordinates of stations correlated with j...m but not present in both networks.
Assuming that the two sets of coordinates are not correlating, the following adjustment problem is defined, where the (Z)'s are the "weighted mean" coordinates for the two sets as a final value:

$$\begin{bmatrix} Xj \\ . \\ . \\ Xm \\ Yj \\ . \\ . \\ Ym \end{bmatrix} = \begin{bmatrix} 1 & 0 & . & 0 \\ 0 & 1 & & 0 \\ . & & . & . \\ 0 & . & 0 & 1 \\ 1 & 0 & . & 0 \\ 0 & 1 & & 0 \\ . & & . & . \\ 0 & . & 0 & 1 \end{bmatrix} * \begin{bmatrix} Zj \\ . \\ Zm \end{bmatrix} \qquad (62.4)$$

with as the a priori variance/covariance matrix of the "observations":

$$(Q) = \begin{pmatrix} QX22 & 0 \\ & \\ 0 & QY22 \end{pmatrix} \qquad (62.5)$$

The standard Least Squares fit then yields an estimate for (Z). This LSQ fit also offers the possibility of performing statistical testing, e.g. using the w-test (32.3), to search for possible errors or misidentifications in the coordinates.
The correlated coordinates n...r and n'...r' are also adjusted via the formula for correlated observations which are not present in the condition equations of the adjustment problem [Baarda,1967] (v is the correction via the LSQ fit):

$$\begin{pmatrix} vXn \\ . \\ vXr \end{pmatrix} = (QX32) \cdot (QX22)^{-1} \cdot \begin{pmatrix} vXj \\ . \\ vXm \end{pmatrix} \qquad (62.6a)$$

$$\begin{pmatrix} vYn' \\ . \\ vYr' \end{pmatrix} = (QY32) \cdot (QY22)^{-1} \cdot \begin{pmatrix} vYj \\ . \\ vYm \end{pmatrix} \qquad (62.6b)$$

Summarizing this approach, it is stated that using form elements - or the connected S-coordinates - is the "natural" way according to the "Delft" approach for point positioning to compare two sets of coordinates, because it is so closely connected to the shape-only qualities of a set of station coordinates. [Buiten&Richardus] present an application of this approach in the 2-D case, where for the variance/covariance matrix the substitute (criterion) matrix is chosen (§4.2.1).

It is recalled, however, that a requirement of the above approach is that the sets of coordinates are in the same S-system. If, therefore, the coordinates of the stations 1...i in the two sets are not identical before the adjustment, a similarity transformation should be computed on the basis of these seven differences. This yields a unique and unadjusted estimate for the transformation parameters. With these parameters the other coordinates Yj...Ym and Yn'...Yr' can be transformed. The transformed values should then enter the LSQ fit of (62.4). If the computed rotation and scale parameters are not negligibly small (within the linearization area), the var/covar matrix QY should also be transformed.
The other requirement with respect to the same S-system for both sets is that the sub-matrices QX11, QX12, QX13, QX21, QX31, QY11, QY12, QY13, QY21, and QY31 be equal to zero, so that it is clear that those coordinates form the S-basis. Should this not be the case, an S-transformation ([Baarda,1973] or Appendix E) should be performed to redefine both QX and QY as required.

6.2.3 Using Similarity Transformation Parameters

This approach is based on the idea that the polyhedra of stations have exactly the same shape, but are described in different coordinate systems which are related via a coordinate transformation: a shift in origin, three rotations and a scale difference. To check whether this assumption holds, an adjustment problem is formulated. The non-linearized observation equations for this LSQ adjustment are defined as (using the same notation as in the preceding section):

$$(X) = 1 * (Z) \qquad (62.7)$$
$$(Y) = (T) + \mu.(R_Z).(R_Y).(R_X) * (Z)$$

When the rotations and the scale difference are small, it is permissible to linearize this as:

$$\begin{vmatrix} dX1 \\ . \\ dXi \\ dXj \\ . \\ dXm \\ dY1 \\ dY2 \\ dY3 \\ . \\ dYi \\ dYj \\ . \\ dYm \end{vmatrix} = \begin{vmatrix} 0 & . & . & . & . & . & 0 & 1 & 0 & . & . & . & 0 \\ . & & & & & & . & 0 & . & & & & 0 \\ . & & & & & & . & . & & 1 & & & 0 \\ . & & & & & & . & . & & & 1 & & 0 \\ . & & & & & & . & . & & & & . & . \\ 0 & . & . & . & . & . & 0 & 0 & . & . & . & 0 & 1 \\ 1 & 0 & 0 & 0 & -Z & Y & X & 1 & 0 & 0 & . & . & . \\ 0 & 1 & 0 & Z & 0 & -X & Y & 0 & 1 & 0 & . & . & . \\ 0 & 0 & 1 & -Y & X & 0 & Z & 0 & 0 & 1 & . & . & . \\ . & & . & & . & & . & & & & 1 & & 0 \\ . & & . & & . & & . & & & & & . & . \\ . & & . & & . & & . & & & & & 1 & 0 \\ . & & . & & . & & . & & & & & . & . \\ . & & . & & . & & 0 & . & . & . & 0 & 1 \end{vmatrix} * \begin{vmatrix} dT1 \\ dT2 \\ dT3 \\ d\alpha \\ d\beta \\ d\gamma \\ d\mu \\ dZ1 \\ . \\ dZi \\ dZj \\ . \\ dZm \end{vmatrix} \qquad (62.8)$$

For the observations almost nothing changes by comparison with §6.2.2: one has one set of coordinates (X1...Xr) with a priori variance/covariance matrix (QX) and a second set of coordinates (Y1...Yr') with variance/covariance matrix (QY). There is only one crucial difference: it is now possible that there are no coordinates in the range 1...i, and, hence, no S-basis coordinates! In this case the zero matrices (QX11), (QY11), (QX21), (QY21), (QX12), (QY12), (QX13), (QY13), (QX31) and (QY31) disappear from the adjustment problem. However, (QX11) can also have e.g. size 3*3 when only the origin of the coordinate system is defined within the set of the station coordinates of the network, as is the case for geodetic VLBI. At the same time, (QY11) may be of size seven, so that all S-basis coordinates are explicitly defined. After elimination of the transformation parameters which are present in neither of the two networks via a similarity transformation (e.g. in the previous case: compute the translation parameters a priori), the standard Least Squares adjustment will yield a solution for the transformation parameters and the "adjusted" unknown station coordinates (Z), as in §6.2.2. The correlated coordinates (Xn...Xr) and (Yn...Yr') are also computed as before.
This system of observation equations will automatically lead to the approach of the preceding section if the (X)- and (Y)-coordinates are on the same S-basis (coordinates identical, with zero variance) and the transformation parameters are constrained to the a priori values of 0 for translations and rotations and of 1 for the scale factor.

It can be proven theoretically [Teunissen,1985] that in the formulation which uses parameters, the original coordinate definition as present in (QX) and (QY) is of no importance in the adjustment results such as shifting variate and statistical testing via the w-test (42.7). This is already suggested by the fact that the S-transformation is, in fact, a

linearized version of the similarity transformation for covariance transformations, so that the similarity transformation includes the S-transformation for this adjustment problem, so that one then arrives at the approach of §6.2.2.
Here, the main ideas will be illustrated by a number of examples before the conclusions are summarized in §6.6.

6.3 THE "FUSION" SOFTWARE

The FUSION-software is designed to combine and compare two sets of X,Y,Z-coordinates of stations in 3-D Euclidean space according to the theory presented in the preceding two sections. A 1-D and 2-D extension of the software is foreseen but has not been implemented yet.
A step-wise description of the programme flow is as follows:

(1) Input of steering parameters and option list followed by the input of the two sets of coordinates and their covariance matrices.
If required, the coordinates will be referred to their barycentre by means of a translation. In this way, the three translation parameters will be computed as the difference between the position of two barycentres of the respective sets, rather than as a shift in the position of the origins of the coordinate systems of the two sets. This "barycentric approach", when in addition unit matrices are used as a priori variance/covariance matrices, is commonly known as: Helmert's transformation.
This approach has the advantage that four (out of the seven) unknown transformation parameters are not correlated, and they therefore can easily be computed (analytically) [Teunissen,1985]. From a computational point of view, the widespread application of computers, made this argument loose most of its weight. Moreover, a relative position of the barycentres of two networks is even more insignificant than the relative position of the two origins of the two reference frames. On the other hand, it may be that the unit matrix is the best available approximation to the true var/covar matrix that one has. As always, the main problem of the absence of a realistic variance/covariance matrix lies in the interpretation of statistical testing results.

(2) If the approach of §6.2.2 is chosen, an exact similarity transformation with seven parameters is computed from a chosen number of seven coordinates in the two sets. This transformation is then applied to all coordinates of the second set, so that for the seven coordinates the values are exactly the same, and they deviate - hopefully - for all other coordinates by small amounts.
However, partial similarity transformations can also be computed, e.g. where only the translation parameters are used (cf. §6.2.3).

(3) Next, an S-transformation can be computed to re-define the two variance/covariance matrices. If the approach of §6.2.2 is chosen, the new S-basis should be the same as that taken under (2). However, the S-basis can also be chosen otherwise, as mentioned in §6.2.3. For the available S-transformations one is referred to Appendix F.

(4) Statistical testing by means of "data-snooping" of the observations (43.4) is standard procedure in the SCAN-II software package. In this way, all alternative hypotheses are tested that one coordinate at a time is wrong. However, stations do not tend to move exactly along the coordinate axes. With this in mind, a number of non-conventional alternative hypotheses are formulated, as listed below. For a mathematical formulation of the C-vectors (§3.2) one is referred to Appendix G.

a) alternative hypotheses that coordinates included in the S-basis are erroneous.
Coordinates that form part of the S-basis have zero-variance and therefore do not get an LSQ adjustment correction; this, however, does not imply that they are errorless. Consequently, these coordinates should be tested. This is possible in a relative sense, just as an observation can always be tested with respect to other observations.

b) alternative hypotheses that the differences between the two sets of coordinates can be described by a similarity transformation after all, although the parameters for some reason were held fixed to a priori values in the approach of §6.2.3.
Suppose that it is believed that the two sets are identical apart from a translation. Then an adjustment can be executed according to §6.2.3 with only the three translation parameters as unknowns. Statistical testing of the shifting variate (32.1) will tell whether this assumption is valid. If the test is rejected, an alternative hypothesis can be specified to investigate whether the assumption should not have been e.g.: three translations plus a scale difference. If the w-test for this alternative hypothesis is accepted, a new adjustment should be executed where one solves for such an additional transformation parameter.

c) alternative hypotheses that a station is shifted in local horizontal North/South or East/West direction or in height.
It has been stated already that it is very unlikely that an error occurs in exactly the X-, Y- or Z-direction. However, errors in the (local) horizontal plane or perpendicular to the Earth's surface can readily be expected. An example is a possible levelling error in the height difference of the ground survey tie connecting the permanent marks of two space geodetic techniques in an intercomparison experiment.

(5) Next, the weight matrix is computed by taking the inverse of the matrix (Q) (62.5), taking into account possible zero sub-matrices. Here it should be remarked, however, that the incorporation of other correlated coordinates as mentioned in §6.2.2 is not yet implemented.
The coefficients of the observation equations are computed via (62.8). If either one of the transformation parameters is not to be included in the adjustment, its coefficients are set to zero.
The computed minus observed (C-O) values follow directly from the non-linearized observation equations (62.4) and (62.7), using the approximate values of the unknowns and the observations (= input coordinates).

(6) Execution of the adjustment and statistical testing by means of the central module of SCAN-II (§3.2) and output of all relevant data about observations and unknowns.

6.4 APPLICATION TO PROJECT ERIDOC

6.4.1 Introduction

In §3.6.1 the main intentions of Project ERIDOC were described and VLBI results for the station coordinates were shown in Table 6. In [Brouwer et al.,1983] Doppler coordinates of the antenna phase centres have been published, computed via the GEODOP-III software using precise ephemeris in a multi-station fit. Including the ground survey tie between the VLBI antenna reference point and the Doppler antenna phase centre, these coordinates are shown in Table 23. For the variance/covariance matrix the a posteriori one of the GEODOP-III LSQ fit is chosen.

Table 23.

ERIDOC Doppler Coordinates

Station	X-coord. (m)	Y-coord. (m)	Z-coord. (m)
1 Effelsberg	4033952.46	-486973.42	4900429.77
2 Chilbolton	4008312.90	100668.33	4943794.20
3 Westerbork	3828605.90	-443860.42	5064920.47
4 Jodrell Bank	3822848.47	153818.79	5086283.61
5 Onsala	3370970.94	-711451.65	5349662.71

Now the two sets of coordinates (Tables 6 and 23) are applied to show the comparison of techniques by adjustment of coordinates.

In the first place, the effect of the dependence of the S-basis is shown. As all coordinates are stochastic quantities, the values of the computed similarity transformation parameters depend on the choice of the seven coordinate differences from which they are computed. For a number of choices these parameters are listed in Table 24. This table shows a bizarre effect because of the large differences between the computed parameters. This highlights how irrelevant these parameters are and consequently the same applies to those data such as position, orientation and scale.

Table 24.

ERIDOC Transformation Parameters Depending on S-basis

2 points +1 coord	DXGEO (m)	DYGEO (m)	DZGEO (m)	R(x) arcsec	R(y) arcsec	R(z) arcsec	μ (ppm)
1+5+Z4	-42.88	-34.25	6.24	-0.45	-0.34	1.43	-0.85
2+5+Z1	-39.24	-52.23	0.69	0.07	-0.15	1.14	-0.74
2+4+Z5	-79.43	7.26	21.76	-1.18	-1.59	2.67	0.52
2+5+Z4	-78.68	-5.77	31.73	-1.20	-1.78	-1.97	-0.74
1+4+Z5	-42.91	-30.92	1.03	-0.44	-0.25	1.59	-0.18
5+3+Z2	-25.60	-68.44	-13.36	0.51	0.47	0.85	0.30

6.4.2 Direct Results of VLBI-Doppler Comparison

It is well-known that VLBI and Doppler are not referred to the same coordinate frame. VLBI uses a quasi-geocentric frame where the coordinates of one station are arbitrarily held fixed and Doppler is connected via a model for the gravitational field of the Earth to the centre of gravity. Therefore, in this case the approach of estimating transformation parameters is considered to be the most direct method. The results of the LSQ adjustment executed in this way are shown in Table 25. The values of the transformation parameters have of course only the "relative" meaning mentioned above. However, the scale factor of -.84 ppm has about the same order of magnitude as the values obtained from global data [Hothem et al.,1982]. The rotation parameters present a measure for the orientation differences between the VLBI and the Doppler coordinate systems. The VLBI results are referred to the smoothed BIH-data of Circular D, which are inherently different from the orientation integrated into the Doppler ephemeris. For a possible further interpretation of the results, it should be noted that the extent of the ERIDOC network is small compared to the Earth's radius.

Please note that the post-fit residuals of the X-, Y- and Z- coordinates as a result of this adjustment are different for VLBI and Doppler, due to the different variance/covariance matrices. Compare e.g. the residuals of Onsala, with the superior VLBI position. The VLBI coordinates of Effelsberg do not get a correction because of their arbitrary character: they are part of the S-basis and have a zero-variance.

The multi-dimensional F-test (32.1) for this adjustment yields a value of 4.43, with a critical value of 1.81. The test is therefore rejected: the two polyhedra of stations do not have the same shape. Since the null-hypothesis is not accepted, a number of alternative hypotheses are formulated according to §6.3 and tested with the one-dimensional w-test to search for errors. The following alternative hypotheses are used

Table 25.

Comparison of ERIDOC VLBI and Doppler Results I

DXGEO (m)	-43.27 +/- 1.67						
DYGEO (m)	-38.92 +/- 2.71						
DZGEO (m)	+6.15 +/- 1.74						
SCALE	0.99999916 +/- 0.00000023						
R(x) (arcsec)	-0.32 +/- 0.08						
R(y) (arcsec)	-0.36 +/- 0.06						
R(z) (arcsec)	1.34 +/- 0.06						
STATION	VLBI RESIDUALS			DOPPLER RESIDUALS			
	X(m)	Y(m)	Z(m)	X(m)	Y(m)	Z(m)	
EFF	0.0	0.0	0.0	+0.02	-0.03	+0.06	
ONS	0.01	0.00	0.01	-0.23	-0.05	-0.16	
JOD	-0.07	-0.02	-0.16	+0.22	+0.49	+0.34	
CHI	+0.28	+0.02	+1.03	-0.22	-0.13	-0.11	
WBK	-0.13	-0.02	-0.24	-0.23	-0.05	-0.16	
	w-TEST (geocentric)			w-TEST (local)			
	X	Y	Z	ϕ	λ	h	
EFF	0.98	1.05	1.18	1.08	0.82	2.93	
ONS	1.74	1.77	2.22	0.92	0.92	5.12	
JOD	1.49	1.31	1.56	0.48	1.23	2.51	
CHI	2.89	0.70	2.88	1.18	0.61	4.42	
WBK	3.78	0.51	2.31	1.76	1.07	4.25	

here: (1) one of the X-, Y- or Z-coordinates of the stations is erroneous, and (2) one of the stations is erroneously shifted in either the local horizontal ϕ - or λ -direction or in height.

As regards the first type of alternative hypothesis, it should be remarked that, using the S-transformation of Appendix G, the VLBI coordinates of Effelsberg can be tested as well, although they have a zero-variance. The test values are also listed in Table 25.
Indeed, the w-tests indicate a discrepancy in the vertical direction. The size of the marginally detectable error (m.d.e.), connected with this w-test, shows that the discrepancy has a magnitude of about 1 metre. The conclusion thus might be that a height error in the ground survey tie in either of these stations is responsible for the observed discrepancy. The geometry of the network, however, is too weak to be able to arrive at a definite conclusion. Reasons for this are: the remote position of Onsala with very accurate VLBI coordinates, the inaccurate VLBI coordinates of Chilbolton (cf. Table 6) and the inaccurate Doppler coordinates of Jodrell Bank due to few observed satellite passes [Brouwer et al.,1983]. A further investigation into this matter has not led to a definite conclusion either.

From the residuals presented in this section, it can concluded be that the level of agreement between the two sets of coordinates is around 0.5 metre; not that large, considering the hidden height error.

6.4.3 Dependence on Variance/Covariance Matrix

This dependence is illustrated in three ways. Firstly, it is investigated what happens when the shape-only approach (§6.2.2) is chosen; secondly, the results are compared for different choices of the station with arbitrary coordinates; and thirdly the results are shown for a completely different variance matrix, notably the unit matrix.

The post-fit residuals of the first adjustment are listed in Table 26. It is clear that all S-basis coordinates get a zero correction. The parameters computed in the a priori similarity transformation can be found in Table 24. In addition, it is noted that the w-test values are exactly the same as in the adjustment of §6.4.2. The same applies to the multi-dimensional F-test. They are therefore independent of the chosen S-basis.
Similarly, the adjustment can be performed with respect to a number of other S-bases, but the same test results will always be found.

Table 26.

Comparison of ERIDOC VLBI and Doppler Results II

STATION	VLBI RESIDUALS			DOPPLER RESIDUALS		
	X(m)	Y(m)	Z(m)	X(m)	Y(m)	Z(m)
EFF	0.0	0.0	0.0	0.0	0.0	0.0
ONS	0.0	0.0	0.0	0.0	0.0	0.0
JOD	0.04	-0.04	0.0	0.31	+0.57	0.0
CHI	+0.38	+0.01	+1.17	-0.26	-0.06	-0.33
WBK	-0.11	-0.03	-0.21	0.50	0.08	0.18

Now the results are compared of the computed translation parameters for different choices for the arbitrary coordinates of the reference station. If the values of Table 6 for the five ERIDOC stations are chosen successively for this purpose, the corresponding a posteriori variance/covariance matrices can be computed via a simple S-transformation applied to the var/covar matrix of the DEGRIAS fit. Then four var/covar matrices are found with in each case a different station having a zero variance. With these matrices four additional comparisons can be made as in the previous section (again with the same test results), so that five sets of translation parameters can be compared in Table 27.

Table 27.

Translation Parameters as a Function of S-basis

Fixed Station:	EFF	ONS	CHI	JOD	WES
DXGEO (m)	-43.27	-43.28	-43.56	-43.20	-43.14
DYGEO (m)	-38.92	-38.92	-38.94	-38.90	-38.90
DZGEO (m)	+6.15	+6.14	+5.11	+6.31	+6.39

It is now clear that from the same set of coordinates several sets of adjusted translation parameters can be computed, differing by up to 1.20 m, which are therefore dependent on the choice of the S-basis. If all statistical tests are accepted, the values should of course lie within the range set by their standard deviations (Table 25). Since the S-transformation applied here was only concerned with a shift in position, the estimated rotation and scale parameters are the same for all solutions. However, more extended S-transformations, ultimately leading to the approach of §6.2.2, will yield the same effect for the latter parameters as well.

Now a completely different a priori var/covar matrix is chosen: diagonal matrices are taken with a standard deviation of 0.5 metres for all Doppler coordinates and 0.2 metres for all VLBI coordinates except Effelsberg. The results of the corresponding LSQ fit are shown in Table 28. It is obvious that not only the transformation parameters and the post-fit residuals but also the test values are different. Consequently, this adjustment can lead to different conclusions. In this case, the height error seems to be present at another station.

6.5 APPLICATION TO EUROPEAN GEODYNAMICS NETWORK

The approach of comparing two sets of 3-D coordinates which includes alternative hypotheses for error detection can also be applied for determining tectonic motions (§6.1). As an example this is done for establishing marginally detectable shifts in North/South direction in the stations Cairo, Casablanca and Sicily of the European geodynamics network (§4.4.4). The size of the tectonic motion that can be detected by the adopted measurement design is naturally the size of the marginally detectable error for an alternative hypothesis.
Here two cases can be considered: first, the size of the shift that can be determined for the design with only the six Southern stations, where only the minimal number of baselines have been measured, and second, the design of the complete network, thus including Wettzell, Westerbork and Moscow, with a triangle-shape in the Southern part.

Table 28.

Comparison of ERIDOC VLBI and Doppler Results III

DXGEO (m)	-45.38 +/- 5.21						
DYGEO (m)	-40.41 +/- 5.07						
DZGEO (m)	+5.35 +/- 4.63						
SCALE	0.99999944 +/- 0.00000053						
R(x) (arcsec)	-0.25 +/- 0.15						
R(y) (arcsec)	-0.40 +/- 0.19						
R(z) (arcsec)	1.34 +/- 0.12						
STATION	VLBI RESIDUALS			DOPPLER RESIDUALS			
	X(m)	Y(m)	Z(m)	X(m)	Y(m)	Z(m)	
EFF	0.0	0.0	0.0	-0.14	0.00	+0.12	
ONS	0.02	0.01	0.05	-0.15	-0.07	-0.33	
JOD	-0.06	-0.05	-0.09	+0.35	+0.29	+0.59	
CHI	+0.08	+0.04	+0.12	-0.48	-0.23	-0.72	
WBK	-0.07	0.00	-0.07	0.43	0.02	0.40	
	W-TEST (geocentric)			w-TEST (local)			
	X	Y	Z	ϕ	λ	h	
EFF	0.41	0.00	0.42	0.30	0.44	1.78	
ONS	0.63	0.29	1.73	0.27	0.39	2.53	
JOD	1.02	0.79	1.72	0.10	0.75	2.28	
CHI	1.35	0.64	2.07	0.22	0.61	2.54	
WBK	1.06	0.06	0.99	0.24	0.17	1.44	

The marginally detectable errors at the 0.1 percent level are then respectively:

mm	South network	Full network
m.d.e. Cairo	7.0	5.0
m.d.e. Casablanca	9.0	6.0
m.d.e. Sicily	8.0	6.9

From this data, it can be concluded, in view of the adopted average standard deviation of the single observation (0.1 ns), that a shift with a magnitude of about half the level of the a priori standard deviation of the VLBI measurements can be detected by this network configuration, under the severe restriction that no systematic or other biases are present other than Gaussian noise of the observations, an assumption, which is to be doubted with the preceding chapters in mind.

6.6 CONCLUSIONS

Two approaches have been discerned for the comparison of two sets of Euclidean coordinates for a 3-D network. The first is based on the interpretation of differences in shape only; the second also yields estimates for differences in position, orientation and scale between the two sets, via the seven (or less) parameters of a similarity transformation. It is shown that the results of statistical testing are completely equivalent in both approaches as these are quantities independent of the S-system. The transformation parameters, however, have only a relative meaning and their magnitude depends completely on the chosen S-system, although their error bounds can be indicated. Thus, the choice between the two approaches can be made on the basis of computational considerations only (programming preferences).
To this conclusion it can be added immediately that it is of paramount importance to have a good a priori variance/covariance matrix for the two sets of coordinates to serve as input to the intercomparison fit. Only then can valid statements about the comparison results be made because a reliable interpretation of statistical testing is possible only in this case.

Furthermore, it is obvious that an error still is present in the ERIDOC comparison which cannot be detected because of the poor reliability of the comparison due to the station configuration. It is clear that a height error is present in one of the stations but no final decision can be taken. The agreement between VLBI and Doppler coordinates is nevertheless at the half metre level.

With this in mind, it should be concluded that great care should be taken in connecting (by conventional surveying means) the reference points of two techniques in intercomparison experiments, especially when the network is small in either size (as compared to the radius of the Earth) or in number of stations. This is primarily because the reliabilty of such an intercomparison experiment is poor and errors in the ground survey tie may easily affect the conclusions about the intercomparison experiment. In this respect, the increase by 50 percent in the magnitude of the shift of the stations on the African plate that can be detected with respect to the European stations for three as against six European reference observatories, is a typical example of what a difference a careful design can make.

Finally, it is noted that an extension of the FUSION software is required to allow an approach where not only 3-D Euclidean coordinates but also ellipsoidal ϕ, λ and h can serve as input. In this way, the comparison of triangulation and space techniques results becomes possible (cf. RETrig).

PART III

CONCLUDING REMARKS

Chapter 7

C O N C L U S I O N S & R E C O M M E N D A T I O N S

7.1 SYNOPSIS

Objectives

In retrospect, this publication which concerns the principles, assumptions and methods of geodetic VLBI has become a subsidence of knowledge, some old, some new, from the fields of astronomy, geophysics and geodesy, which is rather voluminous, since it is intended to be read by people from all these disciplines.
It is a result of a research project whose main objectives were originally formulated as follows:

- To study possible computing models for the geodetic analysis phase of VLBI and to implement the results in a software package to be able to investigate the precision and reliability of VLBI observations;

- To develop a general approach for evaluating intercomparison experiments because the ultimate accuracy of world-wide geodetic positioning can only be achieved by a combination of several techniques;

- to cooperate in the organization and measurement of one or more VLBI experiments in order to verify the results of the above two studies also using "real" observations, since the proof of the pudding is in the eating.

Summary of results

In addition to the fact that geodetic VLBI in the Netherlands has become operational as a result of the research project mentioned above, the following scientific merits of this publication can be summarized.

In chapter 2 all the physical phenomena relevant to VLBI observations were reviewed. Models of these phenomena were described for implementation, together with a general Least Squares module, in the DEGRIAS software package (= DElft Geodetic Radio Interferometry Adjustment System) for the geodetic analysis phase of VLBI. The conclusion (§2.8) was that the accuracy of the standard DEGRIAS computing model, called the kinematic model, is at the one decimetre level for intercontinental baselines and is a few centimetres for shorter distances.
Secondly, it was concluded that the following phenomena dominate the VLBI error budget in general when the improvement in accuracy on intercontinental baselines from one decimetre to one centimetre is required: refraction due to "dry" troposphere at low elevations, refraction due to "wet" troposphere, nutation and telescope structure.
For two of these factors a remedy was investigated.

First, the effect of the eliminating observations made below 10 degrees elevation in VLBI experiments was studied (see below).
Second, the so-called geometric computing model was studied in chapter 5 as an alternative which does not rely on the modelling of the rotational motions of the Earth, and which, therefore, eliminates possible inaccuracies in (mainly) nutation theories and UT1. The model makes use only of the simultaneity of the observations of several co-observing baselines. Another type of computing model, called the short-arc model, which applies the models for precession etc. over only a limited period of time and estimates separate source position parameters for time intervals of 2-12 hours, is added as an intermediate third possibility.

Both on the basis of simulation computations and on the basis of adjustment of actually observed data from a portion of the MERIT Short Campaign (=to Monitor Earth Rotation and to Intercompare the Techniques of observation and analysis) the following conclusions were drawn regarding the design and analysis of a geodetic VLBI experiment:

- Low elevation observations (below 10 degrees) should be excluded from the observation schedule as the magnitude of the correction for tropospheric refraction becomes less certain and these observations are of poor reliability. This means that comparatively large errors may remain undetected (by statistical testing) in the LSQ fit and in addition, that an undetected error has a large impact on the estimated unknown parameters such as station coordinates.

- Moreover, it can be stated that the reliability of a geodetic VLBI experiment is generally poor because of the large difference between the number of scheduled observations and the number of weighted observations in the final Least Squares fit. Reasons for this are: bad spots on tape, weather conditions, clock system failures etc.. It was found that in some cases errors up to 12 times the standard deviation of the observations were not detectable by statistical testing. Therefore, a single observation may have a large influence on the estimated station coordinates. One example was given where the introduction of one single observation made a difference of 19 cm in the estimated baseline length with an effect on statistical testing, which was hardly noticeable. This is especially true of single baseline experiments, as their reliability is even poorer.

- Also for multi-station experiments, however, it should be noted that deficiences in the modelling of the physical phenomena may affect the orientation and the scale of the network geometry considerably. Especially scale effects due to refraction should be mentioned. Once again in geodetic measuring practice it is therefore obvious also for VLBI that the "relative" positions of the observatories are estimable by at least one order of accuracy better than their "absolute" ones.

- Bearing the above in mind, it is concluded that the formal errors of the LSQ results using the kinematic computing model are generally somewhat optimistic. On the other hand, it was shown that the geometric computing model requires at least 3 times as many observations to arrive at the same level of formal precision for the estimated parameters. Although very attractive from a theoretical point of view, it

is thus not very practical, not to say hardly applicable in practice, unless many (>20) baselines are co-observing in an intercontinental network. The short-arc approach is a promising alternative where the formal errors and the "true" errors are balanced.

- As a possible remedy, the operation of a network configuration with more than two baselines (so that closed triangles can be formed) has the advantage of improved likelihood of error detection and is therefore to be recommended.

- Furthermore, it is concluded that much can be gained with a careful design of the experiment with respect to precision and reliability.

- Finally, it is concluded that the accuracy really improves when more observations are made. Therefore, it is recommended that 48 hours instead of 24 hours of observations are taken for VLBI measurements for geodynamic applications.

The methods of analysing precision and reliability are finally applied to the design of a European geodynamics network. It is shown that a set-up with a large campaign observing e.g. once a year and a small campaign observing more regularly, is capable of determining positions at the accuracy level required for the detection of crustal motions in the Mediterranean area.

For the intercomparison of techniques, the method was studied by which one compares two sets of 3-D Euclidean coordinates. Here, as above, the importance of applying statistical testing procedures to detect e.g. errors in the ground survey tie between the reference points of the two techniques or identification errors was stressed. Furthermore, it was shown that the approach which makes a comparison using transformation parameters and that which uses S-transformations yield similar results. This has led to the development of the FUSION software package.

The DEGRIAS package was applied to the VLBI measurements of ERIDOC (=European Radio Interferometry and DOppler Campaign) which was organized during the research project, together with the Geodetic Institute of Bonn University. For this experiment it was found that the Mark-II two channel 40 MHz Bandwidth Synthesis approach yielded a precision of less than 10 cm for the baseline where hydrogen masers were present at both observatories. By comparison of the VLBI coordinates and the Doppler coordinates of the ERIDOC stations with the use of FUSION, it was found that they are comparable to the 0.5 metre level, although an error in the height of one of the stations is still present; the location of this error could not be established as the reliability of the network configuration was too poor.
In addition, the intercomparison approach is also applicable to the detection of deformations of a network by crustal motions. For the design of the European network described above it was found that a shift of about half of the magnitude of the standard deviation of the VLBI observations of the African stations to the North could be reliably detected.

7.2 RECOMMENDATIONS FOR FURTHER RESEARCH

Any publication marks only one phase in a continuous line of development. Therefore, this study is concluded with a number of possible activities, which can be regarded as improvements or enhancements of the research here presented.

(1) First of all, an upgrade of DEGRIAS from prototype software to production software is required. This includes both the improvement of the computing model via introduction of the J2000 ephemerides, the increase in the number of estimable parameters (e.g. precessional constant and gravitational deflection parameter), the extension of the applied statistical tests for error detection and the introduction of real telescope idiosyncrasies in the design module.

(2) The upgraded DEGRIAS package should then be incorporated into the hardware and software facilities of the Netherlands Foundation for Radio Astronomy at Dwingeloo/Westerbork to enable an active participation of this observatory in geodetic VLBI, both with respect to the scheduling, the observations and the final data analysis. In view of the correlator for Connected Element Radio Interferometry which already exists at Westerbork, attention should now also focus on the correlation and fringe analysis phase.

(3) A final test of the applicability of the short-arc and (possibly) the geometric computing model by comparison with the kinematic model should be made via a specially designed and organized multi-station intercontinental VLBI experiment.

(4) Even more than in the present study, from now on, emphasis should be placed on the intercomparison aspects of VLBI and other geodetic space techniques. On the one hand, the need is felt for an ERIDOC-II experiment with a careful design of the intercomparison aspects with both Doppler satellite positioning, Satellite Laser Ranging and the terrestrial control network (RETrig).
On the other hand, however, the extension of DEGRIAS is also required to be able to handle VLBI data obtained in connection with QUASAT (QUAsar SATellite) because this could improve the baseline geometry over long distances, and additional information about the Earth's gravity field could be acquired for other types of intercomparison.

(5) Finally, it is felt that for many practical applications the use of natural sources and intercontinental baselines is not required. It is, therefore, recommended that the ideas and software developed here be applied to the case of radio-interferometry with artificial satellites as emitting objects, notably the Macrometer® concept. In this case, it is even more important to place emphasis on the correlation and fringe analysis phase; cf. (2).

Appendix A

THE POSITION OF THE SUN

In DEGRIAS, the approximate position of the Sun is required for working out the gravitational deflection (§2.5.2). Define (with T in Julian centuries since 1900.0 [Astron.Eph.Supp.,1974]):

L = geometric mean ecliptic longitude with respect to the mean equinox of date (in degrees)

$$= 279.696678 + 36000.768925 * T \qquad (A.1)$$

μ = mean anomaly (in degrees)
= geometric mean longitude minus mean longitude of perigee

$$= 358.475833 + 35999.049750 * T \qquad (A.2)$$

e = eccentricity of the Earth's orbit

$$= 0.01675104 - 0.00004180 * T \qquad (A.3)$$

ε = mean obliquity of the ecliptic (in degrees)

$$= 23.452294 - 0.0130125 * T \qquad (A.4)$$

R_e = Sun's distance from the Earth

$$= 1 - 0.0167 * \cos\mu \qquad (A.5)$$

The longitude (L_S) of the true Sun can be computed as:

$$L_S = L + 1/4 * e*(8 - e^2) * \sin\mu + 5/4 * e^2 * \sin(2*\mu) + 13/12 * e^3 * \sin(3*\mu) \qquad (A.6)$$

Under the assumption that the Sun's latitude is zero, its ecliptic longitude L_S and its right ascension α_S and declination δ_S are related by:

$$(P_S) = \begin{pmatrix} U_S \\ V_S \\ W_S \end{pmatrix} = R_S * \begin{bmatrix} \cos(\alpha_S) * \cos(\delta_S) \\ \sin(\alpha_S) * \cos(\delta_S) \\ \sin(\delta_S) \end{bmatrix} = R_S * \begin{bmatrix} \cos(L_S) \\ \sin(L_S) * \cos\varepsilon \\ \sin(L_S) * \sin\varepsilon \end{bmatrix} \qquad (A.7)$$

so that the apparent position vector of the Sun in the true equatorial frame of date is known. Due to several approximations in the above formulae, the accuracy of this computed position of the Sun is about 0.01 degrees.

Appendix B

THE COSECANT LAW FOR TROPOSPHERIC PATH DELAY

Several methods exist for scaling the tropospheric path delay in zenith direction as derived from (26.7) and (26.11) to other elevations. The coefficients of five models are shown here; μ is the elevation angle.

1. the strict cosecant model (26.2):

$$1/\sin\mu \tag{B.1}$$

2. the Marini model [Schuh,1984], where the constants are computed for an average value of location and weather:

$$1/(\sin\mu + 0.00123/(\sin\mu + 0.010)) \tag{B.2}$$

3. the Chao-model (26.3):

$$1/(\sin\mu + 0.00143/(\tan\mu + 0.0445)) \tag{B.3}$$

4. the model of the GEODOP-III software package for evaluating NNSS satellite Doppler observations [Lawlinakis,1976]:

$$1/\sin(\mathrm{sqrt}(\mu^2+6.25)) \tag{B.4}$$

5. the [Saastamoinen,1972] model including values for pressure,temperature and humidity such that the zenith path delay is two metres:

$$(1 - 1.32*10^{-3}*\mathrm{cotan}^2\mu) \;/\; \sin\mu \tag{B.5}$$

Assuming a value of 2 metres for the zenith path delay, the corrections as a result of these models at different elevation angles are shown in Table 29.
Disregarding models 1 and 5, it appears that all models yield equal results (to within the range of cm) for elevations above 10 degrees. Taking into account the main applications of the models it can be concluded that there exists a general agreement about the behaviour of the troposphere above this elevation. However, differences with a magnitude of decimetres are found at 5 degrees elevation.

It is therefore recommended that observations below 10 degrees elevation should not be included in VLBI experiments, on the one hand because the models deviate by so much in this elevation range that one cannot be certain as to which of them is valid and on the other hand because an error in the zenith path delay is multiplied by a factor 10 at low elevations.

Table 29.

Dry Tropospheric Effect (in metres)

elevation μ	45°	30°	10°	5°	1°
model 1	2.828	4.000	11.518	22.948	114.598
model 2	2.822	3.980	11.090	20.036	32.124
model 3	2.822	3.982	11.104	20.410	49.340
model 4	2.825	3.987	11.177	20.531	42.574
model 5	2.825	3.984	11.028	18.988	-

Another reason for the above recommendation is that it was shown in §3.7.3 that low elevation observations have a large impact on the geometry of the LSQ adjustment (large $\overline{\lambda}$ -parameter (42.11)) and errors may therefore easily affect the estimated unknowns such as station coordinates.

Appendix C

IONOSONDE VERSUS DUAL-FREQUENCY IONOSPHERIC CORRECTION

In this appendix an indication of the accuracy of the ionospheric refraction model based on the ionosonde method presented in §2.6.3 is given as compared to the correction derived by dual frequency observations. In Table 30 the ionospheric refraction corrections are shown for 111 observations on the Effelsberg-HRAS baseline during the MERIT Short Campaign (§3.7).
The coordinates of Effelsberg are: 50° 20' North, 6° 53' East and of HRAS: 30° 28' North, 103° 57' West. This means a baseline length of 8100 kilometres, a latitude difference of 20 degrees and a time (geographical longitude) difference of 7.5 hours. In particular these last two figures are important with regard to the method applied here: spatial and temporal extrapolation of the activity of the ionosphere, starting from values observed at only one station.
The f_oF2 values are observed by the ionosonde equipment of the Royal Netherlands Meteorological Institute (KNMI) in De Bilt, The Netherlands, which is situated at: 52° 6' North, 5° 12' East.

According to (26.15), (26.16) and (26.17), the observed data (hourly readings) for f_oF2 are extrapolated (in time and position) and the computed value for the ionospheric path delay is shown in the fourth column of Table 30 for those observations during the first two days of the MERIT-SC where the ionospheric path delays could also be computed from the simultaneous observations at S- and X-band (column 3). The time of observation and the times of sunrise (SR) and sunset (SS) at the two stations are listed in column 1. In the fifth column the difference between the model and the S/X-result is listed, marked by asterisks in the last column to show more clearly systematic effects.
It is obvious from Table 30 that there are some systematic trends in the differences between the S/X and ionosonde method corrections, especially during the first day. However, the mean value, of the difference is almost zero (no real bias) and the maximum difference is only 0.56 ns, which can be seen from Figure 40. More important, however, is the fact that the RMS spread is only 0.23 ns, which is somewhat below the average level of the a priori standard deviations of the MERIT-SC on the longer baselines.
In conclusion, it can be stated that the model, although far from perfect, is accurate to an acceptable level, especially in view of the fact that the results for shorter baselines will be better due to a stronger correlation between the real ionospheric behaviour at one position and the observed values at the weather station. Improvements as indicated in the discussion of §2.6.3 will eliminate most of the systematic effects shown, except perhaps for observations taken during sunrise or sunset at one of the stations. An accuracy level of 0.1 ns would then be feasible.

Table 30.

Difference between S/X and Ionosonde Model

TIME h m		OBSERV.DELAY (in μs)	IONOSPH. PATH DELAY (ns) S/X	MODEL	DIFF	PLOT
2239		-12495.797709	0.660	0.418	0.242	**
2258		7393.196559	2.221	2.119	0.102	*
2309		-13974.792890	0.606	0.462	0.144	*
2319		-3205.756151	0.884	0.912	-0.028	
2327		8939.024950	1.332	1.503	-0.171	**
0003	SS-H	5918.848427	1.045	1.277	-0.232	**
0043		2502.755800	0.770	1.055	-0.285	***
0127		-1207.747520	0.471	0.853	-0.382	****
0133		44.064714	0.499	1.059	-0.560	******
0140		-10870.743999	0.156	0.644	-0.488	*****
0234		-3626.578087	0.349	0.764	-0.415	****
0246		-7325.152416	0.159	0.480	-0.321	***
0253		-8546.537889	0.105	0.453	-0.348	***
0317		-10930.068234	0.000	0.292	-0.292	***
0324		-9841.617002	0.082	0.304	-0.222	**
0336		-2380.978832	0.193	0.594	-0.401	****
0351		7866.922554	0.269	0.687	-0.418	****
0412		-1396.193657	0.214	0.519	-0.305	***
0424		-13029.406975	0.049	0.118	-0.069	*
0433		-6611.984193	-0.025	0.265	-0.290	***
0449		5313.097010	0.184	0.452	-0.268	***
0555	SR-E	-4070.640790	-0.056	-0.046	-0.010	
0612		-15777.285199	-0.205	-0.457	0.252	***
0920		-1741.742525	-0.557	-0.828	0.271	***
0942		-4597.924382	-0.685	-1.006	0.321	***
0952		-4420.342865	-0.665	-0.936	0.271	***
1039		-8057.528409	-0.843	-1.087	0.244	**
1126		5706.810704	-0.464	-0.537	0.073	*
1140		-12028.339878	-1.090	-1.257	0.167	**
1158		-12231.715826	-1.176	-1.356	0.180	**
1212		-3819.715014	-0.849	-0.887	0.038	
1218	SR-H	1059.764809	-0.517	-0.588	0.071	*
1308		-3292.747658	-0.439	-0.462	0.023	
1316		-15960.748331	-1.296	-1.285	-0.011	
1326		-11698.551897	-1.128	-1.114	-0.014	
1332		-16296.546207	-1.319	-1.278	-0.041	
1346		-6394.689589	-0.424	-0.446	0.022	
1353		-13573.145589	-1.009	-0.972	-0.037	
1550		6705.786031	0.696	0.849	-0.153	**
1559		-14614.561955	-0.686	-0.758	0.072	*
1624		3278.929726	0.552	0.633	-0.081	*
1632		-10923.402340	-0.659	-0.596	-0.063	*
1641		-16051.096764	-0.729	-0.909	0.180	**
1815	SS-E	8037.021538	1.311	1.002	0.309	***
1822		-8240.179006	0.263	-0.034	0.297	***
1911		-12343.606567	0.143	-0.211	0.354	****
1925		4392.492924	1.127	0.758	0.369	****

2001		-15821.987009	0.067	-0.287	0.354	****
2010		-2043.646801	0.945	0.537	0.408	****
2018		2247.002659	1.135	0.755	0.380	****
2047		-5108.051036	0.853	0.473	0.380	****
2055		835.846618	1.124	0.749	0.375	****
2140		-9084.012604	0.750	0.456	0.294	***
2149		-1010.121839	1.078	0.820	0.258	***
2235		-12492.106673	0.641	0.479	0.162	**
2359		5924.667243	1.181	1.293	-0.112	*
0039		2508.603908	0.852	1.001	-0.149	*
0123	SS-H	-1202.072696	0.495	0.685	-0.190	**
0129		51.653714	0.520	0.828	-0.308	***
0136		-10863.556369	0.106	0.378	-0.272	***
0230		-3627.575318	0.312	0.504	-0.192	**
0242		-7320.301969	0.115	0.273	-0.158	**
0256		-8286.977678	0.066	0.253	-0.187	**
0313		-10923.440312	-0.109	0.120	-0.229	**
0320		-9837.375023	0.023	0.201	-0.178	**
0332		-2382.631814	0.216	0.481	-0.265	***
0347		7869.913879	0.292	0.627	-0.335	***
0408		-1398.173510	0.184	0.438	-0.254	***
0420		-13026.354015	-0.038	0.021	-0.059	
0429		-6604.317240	-0.115	0.159	-0.274	***
0436		4184.712500	0.219	0.472	-0.253	***
0445		5316.209644	0.227	0.411	-0.184	**
0518		-456.610904	0.112	0.243	-0.131	*
0551		-4063.206179	-0.025	0.016	-0.041	
0608	SR-E	-15776.829479	-0.284	-0.388	0.104	*
0701		-11235.555087	-0.472	-0.532	0.060	*
0710		9296.552945	-0.080	0.116	-0.196	**
0717		-1017.494601	-0.269	-0.243	-0.026	
0758		-16222.707051	-0.891	-0.980	0.089	*
0853		256.682986	-0.523	-0.351	-0.172	**
0916		-1735.815480	-0.622	-0.494	-0.128	*
0948		-4414.696546	-0.751	-0.872	0.121	*
0955		-9139.290803	-0.957	-1.190	0.233	**
1035		-8052.491897	-0.936	-1.221	0.285	***
1043		-10886.337295	-1.011	-1.457	0.446	****
1052		4366.300871	-0.730	-0.738	0.008	
1101		7570.761642	-0.511	-0.534	0.023	
1122		5712.953277	-0.579	-0.625	0.046	
1128		470.379419	-0.909	-0.935	0.026	
1136		-12024.404030	-1.162	-1.500	0.338	***
1148	SR-H	-4731.252937	-1.001	-1.254	0.253	***
1154		-12231.126371	-1.278	-1.714	0.436	****
1214		1065.895116	-0.678	-0.804	0.126	*
1257		-8807.692333	-1.157	-1.216	0.059	*
1304		-3286.925988	-0.610	-0.704	0.094	*
1312		-15959.067755	-1.434	-1.709	0.275	***
1322		-11699.876797	-1.382	-1.469	0.087	*
1328		-16295.281476	-1.429	-1.674	0.245	**
1349		-13567.315850	-1.214	-1.281	0.067	*
1432		-16910.134234	-1.500	-1.372	-0.128	*
1440		-10571.827600	-0.664	-0.647	-0.017	
1546		6712.613298	0.482	0.637	-0.155	**

```
|  1555      -14611.689714 -0.979 -0.880 -0.099  *          |
|  1620 SS-E   3285.859462  0.430  0.509 -0.079  *          |
|  1637      -16049.269246 -1.094 -0.988 -0.106  *          |
|  1804        7556.230773  1.151  1.081  0.070  *          |
|  1818       -8234.061966  0.167 -0.040  0.207  **         |
|  1907      -12338.321496 -0.054 -0.097  0.043             |
|  1914        2497.515165  1.040  0.944  0.096  *          |
|  1921        4395.290500  1.156  1.071  0.085  *          |
|  1957      -15817.799606 -0.157 -0.214  0.057  *          |
+-----------------------------------------------------------+
```

It should be added here that application of the model would be facilitated if VLBI-campaigns were scheduled only in those periods of the year when the ionosphere is less active, e.g. June and July (Figure 10), although this should be balanced against a somewhat larger irregularity and perhaps other more prominent systematic effects during this period. One could even add weight this remark by also stating that with the use of dual frequency observations the best results can be achieved for VLBI campaigns during summer time, because second-order effects are always present.

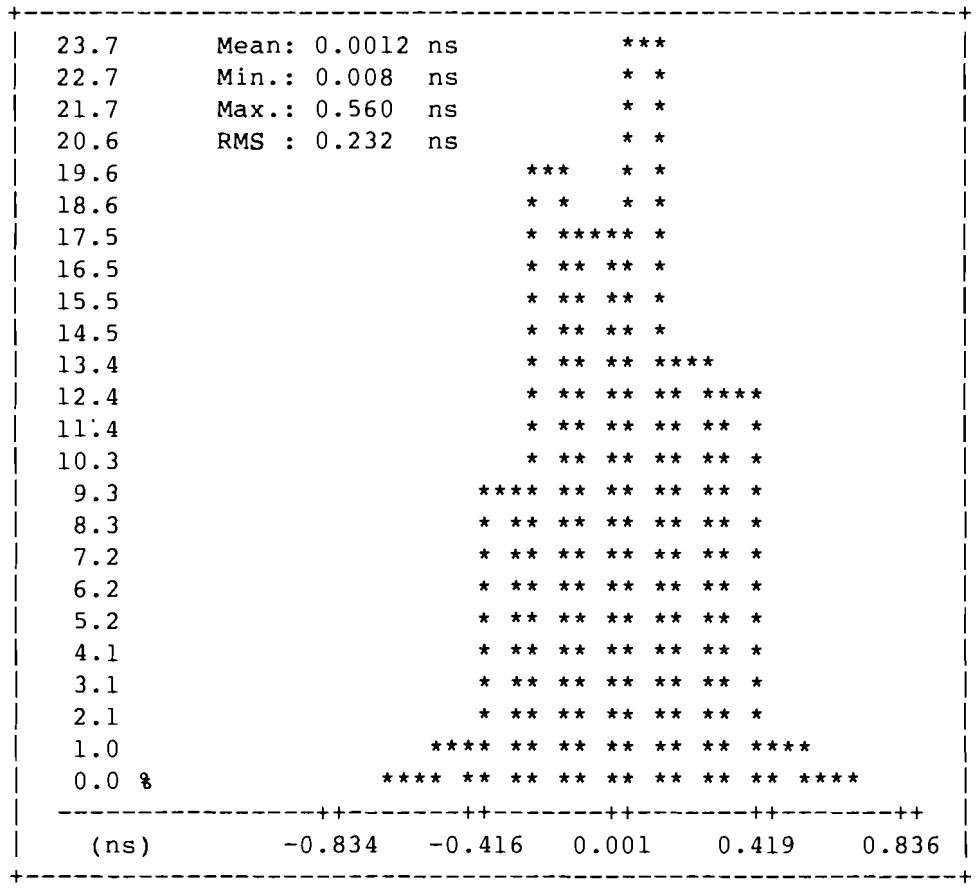

Figure 40: Overview of Differences in the Ionospheric Correction

Appendix D

DOWN-WEIGHTING OF OBSERVATIONS

Down-weighting of individual observations according to a certain (prescribed) recipe, is often applied to a Least Squares adjustment in order to achieve an acceptable solution. In the so-called "Danish Method", the location of possible measurement errors (or outliers) by an iterative computation of LSQ fits is regarded as a philosophy [Krarup & Kubik,1983]. During this iteration, the weights of the individual observations in a given LSQ fit are multiplied by an exponential function with a quantity containing the post-fit residual of the previous LSQ fit as an argument. For different applications (such as: photogrammetric block adjustment, levelling networks, resection), different exponential functions are developed, with a numerical value depending on the sequence number of the iteration as well.

The danger of such an approach is that it is possible to down-weight, due to a mixture of several errors, a non-erroneous observation at the start of the iteration sequence. Convergence to a wrong solution is then possible. This is particularly true of ill-conditioned problems. Nevertheless, some iterative down-weight procedure is included in the DEGRIAS software package for eliminating the influence of outliers on the final LSQ fit. It will be shown below that this influence lies mainly in the weighted RMS-spread of the residuals and not in the computed solution for the estimable unknowns.
This result follows from the two formulae for the computation of the adjusted observations and the post-fit residuals of the LSQ fit:

$$X = A.(A^T.P.A)^{-1}.A^T.P.\ x \qquad (D.1)$$

$$v = (I-A.(A^T.P.A)^{-1}.A^T.P).x \qquad (D.2)$$

where

x = "observed" observation vector
X = "adjusted" observation vector
v = post-fit residual vector; see (32.2)
A = design matrix
P = weight matrix of the observations, here assumed to be diagonal, so that:

$$Pii = \sigma_o^2 / \sigma_i^2 \qquad (D.3)$$

From the formulae (D.1) and (D.2) it can be seen that the matrix $A.(A^T.P.A)^{-1}.A^T.P$ determines which part of the observed values x will be regarded as "signal", i.e. adjusted X (and thus, via X=A.Y, estimated parameters) and which part as "noise", i.e. post-fit

residuals. As the above matrix projects the observed vector x, according to (D.1), onto the space where it fulfills all condition equations of the adjustment problem, it is a projector [Teunissen,1984b], here denoted by M, so that (D.1) and (D.2) become:

$$X = M.x \qquad (D.4)$$

$$v = (I-M).x \qquad (D.5)$$

Now the question remains of how possible errors in x are devided between X and v. Naturally, this depends on the number of redundant observations. Two limiting cases are considered:
First, assume a situation where no redundant observations are present at all. In this case the numbers of observations and estimable parameters are equal and A becomes square and invertable. It then follows from (D.1) that M is a unit-matrix so that (D.4) becomes X=x and (D.5) v=0. In this situation, therefore, all measurement errors are completely transferred to the adjustment result X and no error is shown in the post-fit residuals (on which all statistical testing is based).
Second, it is assumed that an infinite number of redundant observations is present. Although this situation is not feasible in practice, it is clear that $(A^T.P.A)^{-1}$, which is the variance/covariance matrix of the unknown parameters, goes to zero for an increasing number of observations, so that M approaches a zero-matrix. According to (D.5) v then equals x, so that any error in the observations immediately becomes visible in the corresponding post-fit residual.

It will now be shown that the computing model for geodetic VLBI approximates fairly well the latter situation. Therefore, the behaviour of the marginally detectable error (m.d.e.; §4.2.3) is studied for a change in the standard deviation. This m.d.e. is defined as the size of an error in a certain observation which is detectable with at least a probability β by the w-test (32.3) using a significance level α. It is computed as (42.6), (42.8):

$$\nabla i = \sigma_o \cdot \mathrm{sqrt}(\lambda_o/(Ci^T.P.(I-M).Ci)) \qquad (D.6)$$

or

$$\nabla i = \sigma_o / \mathrm{sqrt}(Pi/Ni) * \sigma i \qquad (D.7)$$

The column vector Ci in (D.6) is used to denote the sequence number of the observation for which the m.d.e. is computed (42.4). λ_o is the non-centrality parameter of the statistical test and is computed from the assumed α and β.

Now a relation is to be found between the m.d.e. and the a priori standard deviation. To compute their dependence, (D.7) is differentiated (linearized) with respect to σ_i.

---Start of intermezzo---

For this differentiation the derivative of the inverse of a matrix is needed. This can be found from:

put $B = A^{-1}$, so that $A.B = I$ (D.8)

$\rightarrow$ $A.dB + dA.B = 0$ (D.9)

$\rightarrow$ $A^{-1}.A.dB + A^{-1}.dA.B = 0$ (D.10)

$\rightarrow$ $dB = -A^{-1}.dA.B$ (D.11)

Hence, the derivative of the inverse of a matrix is:

$$d(A^{-1}) = -A^{-1}.dA.A^{-1} \quad \text{(D.12)}$$

---End of intermezzo---

Using (D.12) for the linearization of Ni with respect to Pi one finds:

$$\begin{aligned} dNi = {} & dPi - dPi.Ai.(A^T.P.A)^{-1}.Ai^T.Pi \\ & +Pi.Ai.(A^T.P.A)^{-1}.Ai^T.dPi.Ai.(A^T.P.A)^{-1}.Ai^T.Pi \\ & -Pi.Ai.(A^T.P.A)^{-1}.Ai^T.dPi \end{aligned} \quad \text{(D.13)}$$

$$\begin{aligned} \rightarrow dNi &= dPi*(1-2*Ai.(A^T.P.A)^{-1}.Ai^T.Pi+(Ai.(A^T.P.A)^{-1}.Ai^T.Pi^2) \\ &= dPi * (1 - 2*(Pi-Ni)/Pi + ((Pi-Ni)/Pi)^2) \end{aligned}$$

$$\rightarrow dNi = Ni^2 / Pi^2 * dPi \quad \text{(D.14)}$$

Linearize also equation (D.3) according to:

$$dPi = -2 / \sigma_o * Pi^{1\frac{1}{2}} * d\sigma i \quad \text{(D.15)}$$

and (D.7) according to:

$$d\nabla i = \sigma_o * sqrt(\lambda_o) * -\tfrac{1}{2}*Ni^{-1\frac{1}{2}} . dNi \quad \text{(D.16)}$$

Substitution of (D.14) and (D.15) in (D.16) then yields:

$$d\nabla i = sqrt(\lambda_o) * sqrt(Ni/Pi) * d\sigma i \quad \text{(D.17)}$$

Use is now made of the fact that the trace of a projector equals the dimension of its range [Teunissen,1984b]. The trace of M, therefore, equals the number of unknowns. The trace of I is of course the number of observations. From this it follows that the sum of all values Ni/Pi, which are the main diagonal elements of the matrix I-M, is equal to the number of conditions in the LSQ adjustment.
Furthermore, one sees that all diagonal elements have a value between 0 and 1, because:

$$Ni/Pi = Ci^T.(I-M).Ci \quad \text{(D.18)}$$

$$= Ci^T.I.Ci - Ci^T.M.Ci \quad \text{(D.19)}$$

and since M is a projector, which has the property: M.M=M,

$$Ni/Pi = 1 - Ci^T.M.M.Ci$$
$$= 1 - ||M.Ci||^2 \qquad (D.20)$$

Application of the cosine rule - where μ is the angle between the unit vector Ci and its projection - then yields:

$$Ni/Pi = 1 - ||Ci|| \; . \; ||M_{Ci}|| \; . \; \cos\mu$$
$$= 1 - \cos^2\mu \quad = \quad \sin^2\mu \qquad (D.21)$$

which is between 0 and 1. For a VLBI network, the ratio between the number of delay observations and the number of unknown parameters is typically 15:1. For 1500 observations this means an average value for Ni/Pi of 14/15 = 0.933, so that an average value is found for sqrt(Ni/Pi) of 0.966 and for sqrt(Pi/Ni) of 1.035.
Since there is only one type of observable and all observations contribute in an equivalent way to the system of condition equations, no large deviations from this average value is to be expected, so that the following relation is valid:

$$sqrt(Ni/Pi) \cong sqrt(Pi/Ni) \cong 1 \qquad (D.22)$$

and by combining (D.7) and (D.17) one finds:

$$\nabla i+d \; \nabla i \cong sqrt(\lambda_o * Ni/Pi) * (\sigma i+d \; \sigma i) \qquad (D.23)$$

This relation expresses the fact that a change in the standard deviation of one of the (non-correlated) VLBI delay observations yields an equivalent change in the m.d.e. of this observation whilst all other m.d.e.'s remain constant. Inverse dependence is found for the closely related w-value which is the result of the one-dimensional test.
This can also be derived from the fact that (32.3) reduces to

$$wi = -xi \; / \; \sigma \; i \qquad (D.24)$$

for many redundant observations and a relatively large xi, which means a large error for this i-th observation and no errors in all other observations.

This proves the correctness of some down-weighting for the VLBI case.
As a concluding remark, it can be added that the limiting case of the continued down-weighting of the LSQ adjustment is the L1-norm solution, where a number of observations equal to the number of estimable unknowns have weight one and all other observations have weight zero.

Appendix E

A GENERAL 3-D S-TRANSFORMATION

Introduction

The geodetic analysis phase of VLBI involves the estimation of a number of unknown parameters Y which have a linear (linearized) relation with experimental data X (observations) according to: X=A.Y. The question of how to define vector Y so that it is estimable from X involves the so-called datum-problem and the question of configuration defects which are the result of an insufficient measurement set-up. The latter is not considered here; one is referred to §4.4.1.
The datum-problem deals with coordinate system definition: coordinates are not estimable from observations alone. If, for instance, in a levelling network only height differences are measured, it requires an arbitrary choice for the height of one of the stations to be able to compute the heights of all other stations from the measured height differences. If a different choice is made, other heights are found.
The relation between these two sets of results is obviously described by a similarity transformation. Datum (or coordinate system) definition therefore requires a number of assumptions equal to the number of parameters in the similarity transformation. For VLBI (3-D) this number is seven. A system B.Y=0 of seven equations should therefore be added to X=A.Y to find one solution (out of the countless possible ones). The S-transformation [Baarda,1973] describes the relation between the (differential) quantities Y for different choices of B.Y=0. As the variance/covariance matrix of Y is dependent on the choice of B.Y=0 as well, the S-transformation is primarily applied to transform the precision description to other datums.

A General Formula

The formula for the S-transformation can be derived directly from the linearized similarity transformation under the assumption that the approximate values describe the identity transformation. Using P as the transformation parameter matrix, the similarity transformation is:

$$Y2 = P.Y1 \qquad (E.1)$$

As P=1, the unit matrix (because of the above assumptions for the approximate values), it follows as the linearized equation, using T as the coefficient matrix:

$$dY2 = dY1 + T.dP \qquad (E.2)$$

Using the theory of generalized inverses one finds for the description of a group of S-transformations depending on the choice for matrix B (see [Teunissen,1984b] for an extensive discussion):

$$\begin{aligned} dY2 &= S.dY1 \\ &= (I - T.(B.T)^{-1}.B).dY1 \end{aligned} \qquad (E.3)$$

3-D S-transformation, Euclidean Coordinates Only

The 3-D similarity transformation (E.1) is defined as:

$$\begin{pmatrix} X \\ Y \\ Z \end{pmatrix} = \mu \cdot R_z(C) \cdot R_y(B) \cdot R_x(A) \cdot \begin{pmatrix} Xi \\ Yi \\ Zi \end{pmatrix} + \begin{pmatrix} U \\ V \\ W \end{pmatrix} \qquad (E.4)$$

Linearization with approximate values A=B=C=0, μ=1 yields:

$$\begin{pmatrix} dX \\ dY \\ dZ \end{pmatrix} = \begin{pmatrix} dXi \\ dYi \\ dZi \end{pmatrix} + \begin{pmatrix} d\mu & dC & -dB \\ -dC & d\mu & dA \\ dB & -dA & d\mu \end{pmatrix} \cdot \begin{pmatrix} Xi \\ Yi \\ Zi \end{pmatrix} + \begin{pmatrix} dU \\ dV \\ dW \end{pmatrix} \qquad (E.5)$$

so that (E.2) becomes:

$$\begin{pmatrix} dX \\ dY \\ dZ \end{pmatrix} = \begin{pmatrix} dXi \\ dYi \\ dZi \end{pmatrix} + \begin{pmatrix} Xi & 0 & -Zi & Yi & 1 & 0 & 0 \\ Yi & Zi & 0 & -Xi & 0 & 1 & 0 \\ Zi & -Yi & Xi & 0 & 0 & 0 & 1 \end{pmatrix} \cdot \begin{pmatrix} d\mu \\ dA \\ dB \\ dC \\ dU \\ dV \\ dW \end{pmatrix} \qquad (E.6)$$

For n points the matrix T therefore has the following shape:

$$T = \begin{bmatrix} Xa & 0 & -Za & Ya & 1 & 0 & 0 \\ Ya & Za & 0 & -Xa & 0 & 1 & 0 \\ Za & -Ya & Xa & 0 & 0 & 0 & 1 \\ Xb & 0 & -Zb & Yb & 1 & 0 & 0 \\ Yb & Zb & 0 & -Xb & 0 & 1 & 0 \\ Zb & -Yb & Xb & 0 & 0 & 0 & 1 \\ : & : & : & : & : & : & : \end{bmatrix} \begin{matrix} --- \\ . \\ . \\ 3xn \\ . \\ . \\ --- \end{matrix} \qquad (E.7)$$

Matrix B has size 7x3n. Three special cases of B are mentioned here:

1) If B is taken as the transpose of T, the so-called minimum norm solution is found, which has a minimal value for the trace of the variance/covariance matrix. For this matrix the notation Bm is used.

2) If B is taken as (I7 | 0), the "standard" solution with seven fixed station coordinates is found: e.g. two points are completely fixed plus the Z-coordinate of a third point. This matrix is denoted as Bs.

3) In case 2 a singular situation may occur. A planar network, for instance, parallel to the equatorial plane cannot be fixed by a choice of two points with X,Y,Z and an additional X of a third point. Therefore, a B-matrix is derived in the following section where neither of the coordinates of the third point is chosen to be fixed, but instead the direction at this point perpendicular to the plane through the three points is chosen. This B-matrix is denoted as Bp.

Derivation Bp-matrix

The vector representation of a plane through three points a,b and c is:

$$\begin{pmatrix} X \\ Y \\ Z \end{pmatrix} = \begin{pmatrix} Xa \\ Ya \\ Za \end{pmatrix} + \lambda * \begin{pmatrix} Xb-Xa \\ Yb-Ya \\ Zb-Za \end{pmatrix} + \mu * \begin{pmatrix} Xc-Xa \\ Yc-Ya \\ Zc-Za \end{pmatrix} \qquad (E.8)$$

The vector (N), perpendicular to this plane, is:

$$\begin{pmatrix} Nx \\ Ny \\ Nz \end{pmatrix} = \begin{bmatrix} (Yb-Ya) * (Zc-Za) - (Zb-Za) * (Yc-Ya) \\ (Zb-Za) * (Xc-Xa) - (Xb-Xa) * (Zc-Za) \\ (Xb-Xa) * (Yc-Ya) - (Yb-Ya) * (Xc-Xa) \end{bmatrix} \qquad (E.9)$$

Consequently, the formula for the plane through a,b and c is:

$$Nx * X + Ny * Y + Nz * Z = \text{constant} \qquad (E.10a)$$

If point c is now confined to this plane, so that the rotation of the plane about the line a-b is fixed, the following relation should hold:

$$Nx * dXc + Ny * dYc + Nz * dZc = 0 \qquad (E.10b)$$

Matrix Bp therefore has the following shape:

$$Bp = \begin{array}{c} \begin{array}{ccccc} \text{a} & & \text{b} & \text{c} & \text{d,e,..} \\ \hline \end{array} \\ \begin{bmatrix} 1\ 0\ 0 & 0\ 0\ 0 & 0\ 0\ 0 & 0.. \\ 0\ 1\ 0 & 0\ 0\ 0 & 0\ 0\ 0 & 0.. \\ 0\ 0\ 1 & 0\ 0\ 0 & 0\ 0\ 0 & 0.. \\ 0\ 0\ 0 & 1\ 0\ 0 & 0\ 0\ 0 & 0.. \\ 0\ 0\ 0 & 0\ 1\ 0 & 0\ 0\ 0 & 0.. \\ 0\ 0\ 0 & 0\ 0\ 1 & 0\ 0\ 0 & 0.. \\ 0\ 0\ 0 & 0\ 0\ 0 & Nx\ Ny\ Nz & 0.. \end{bmatrix} \end{array} \qquad (E.11)$$

3-D S-transformation including other VLBI unknown parameters

As not only station coordinates are of interest in VLBI, now source coordinates, scale and orientations are also introduced to T as unknown parameters.

1. Source coordinates

Let α and δ be right ascension and declination, then the following similarity transformation exists, using rotations only:

$$\begin{bmatrix} \cos\alpha \,.\, \cos\delta \\ \sin\alpha \,.\, \cos\delta \\ \sin\delta \end{bmatrix} = R_Z(C).R_Y(B).R_X(A).\begin{bmatrix} \cos\alpha i.\cos\delta i \\ \sin\alpha i.\cos\delta i \\ \sin\delta i \end{bmatrix} \qquad \text{(E.12)}$$

so that linearization yields (omitting the suffix "i"):

$$\begin{bmatrix} d(\cos\alpha \,.\, \cos\delta) \\ d(\sin\alpha \,.\, \cos\delta) \\ d(\sin\delta) \end{bmatrix} = \begin{bmatrix} 0 & dC & -dB \\ -dC & 0 & dA \\ dB & -dA & 0 \end{bmatrix} . \begin{bmatrix} \cos\alpha \,.\, \cos\delta \\ \sin\alpha \,.\, \cos\delta \\ \sin\delta \end{bmatrix} \qquad \begin{matrix} a \\ \text{(E.13b)} \\ c \end{matrix}$$

From (E.13c) it follows:

$$\cos\delta \,.\, d\delta = \cos\alpha \,.\, \cos\delta \,.\, dB - \sin\alpha \,.\, \cos\delta \,.\, dA$$

$$\rightarrow \quad d\delta = -\sin\alpha i \,.\, dA + \cos\alpha i \,.\, dB + 0 \,.\, dC \qquad \text{(E.14)}$$

In the same way one finds from (E.13b):

$$\cos\alpha \,.\, \cos\delta \,.\, d\alpha - \sin\alpha \,.\, \sin\delta \,.\, d\delta = -\cos\alpha \,.\, \cos\delta \,.\, dC + \sin\delta \,.\, dA \qquad \text{(E.15)}$$

Substituting (E.14) in (E.15), one finds:

$$\cos\alpha \,.\, \cos\delta \,.\, d\alpha = (\sin\delta - \sin^2\alpha \,.\, \sin\delta) \,/\, dA + \sin\alpha \,.\, \cos\alpha \,.\, \sin\delta \,.\, dB - \cos\alpha \,.\, \cos\delta \,.\, dC$$

$$\rightarrow \quad d\alpha = \cos\alpha.\tan\delta \,.\, dA + \sin\alpha.\tan\delta \,.\, dB - 1 \,.\, dC \qquad \text{(E.16)}$$

Some useful checks on the formulae (E.14) and (E.16) are:
- use $\delta=0$, an equatorial source: $d\alpha = -dC$, which is correct since a right ascension change is then a rotation about the Z-axis,
- use $\alpha=0$, a source in Aries: $d\delta = dB$, which is correct since a declination change is then a rotation about the Y-axis.

[Teunissen,1984b] derived these formulae by a different method as well.

2. Scale and orientations

For the scale parameter S and the orientations O1 and O2 connected to polar motion and the 1950.0 precession axis, plus the orientation O3 for UT1, the following identities hold:

$$dS = 1 \,.\, d\mu \qquad \text{(E.17)}$$

$$\begin{aligned} dO1 &= 1 \,.\, dA \\ dO2 &= 1 \,.\, dB \\ dO3 &= 1 \,.\, dC \end{aligned} \qquad \text{(E.18)}$$

The complete T matrix now reads for n stations, m sources, p sets of orientation parameters and one scale factor:

$$
\begin{bmatrix}
Xa & 0 & -Za & Ya & 1 & 0 & 0 \\
Ya & Za & 0 & -Xa & 0 & 1 & 0 \\
Za & -Ya & Xa & 0 & 0 & 0 & 1 \\
\vdots & \vdots & \vdots & \vdots & \vdots & \vdots & \vdots \\
0 & -\sin\alpha & \cos\alpha & 0 & 0 & 0 & 0 \\
0 & \cos\alpha.\tan\delta & \sin\alpha.\tan\delta & -1 & 0 & 0 & 0 \\
\vdots & \vdots & \vdots & \vdots & \vdots & \vdots & \vdots \\
0 & 1 & 0 & 0 & 0 & 0 & 0 \\
0 & 0 & 1 & 0 & 0 & 0 & 0 \\
0 & 0 & 0 & 1 & 0 & 0 & 0 \\
\vdots & \vdots & \vdots & \vdots & \vdots & \vdots & \vdots \\
1 & 0 & 0 & 0 & 0 & 0 & 0
\end{bmatrix}
\begin{matrix}
--- \\ . \\ 3xn \\ --- \\ --- \\ 2xm \\ --- \\ --- \\ 3xp \\ . \\ --- \\ 1
\end{matrix}
\qquad \text{(E.19)}
$$

Together with an appropriate choice of the Bs matrix this forms the general 3-D S-transformation for VLBI.

Appendix F

CONDITION EQUATION FOR THE 2-D VLBI CASE

Introduction

More observations than unknown parameters will result in an adjustment problem. In addition to the LSQ adjustment with observation equations (§3.1), an adjustment with condition equations is also possible. In the "Delft" approach for point positioning (§1.4) this second method is, in principle, preferred, because one has a direct check on whether the network construction is determined or not via the condition equations. Furthermore, it is possible to do statistical testing per condition equation, thus enabling a better detection of errors. Lastly, it supports the line-of-thought that only the shape of the network is determined by the observations and not its position, orientation or its scale. By adjustment via condition equations, one therefore bypasses the zero-order design problem (datum definition).
In this appendix, the condition equation for the two-dimensional (2-D) case of VLBI is derived, via an algorithm found by G.Strang van Hees. At the same time the disadvantage of the adjustment problem with condition equations is shown, the complexity of the formulae, as compared to the simple version (22.3). Such an approach results therefore in more complicated software; this is why for LSQ adjustment mostly the first approach is chosen.

Derivation

Section 5.2.2 shows the balance between observations and unknowns in the 3-D case. In the planar case (Figure 41) 3 stations, i.e. two independent baselines, with measurements of three different sources are required for a barely determined configuration of the network. A fourth observed source will thus yield one condition equation, as follows:

observations	unknown parameters
8 = 2 baselines * 4 sources	6 station coordinates
	4 source positions
4 for coordinate definition	1 scale unit
12	11

In Figure 41 the distances CA0, CA1, CA2, CA3, CB0, CB1, CB2 and CB3 are measured; call these a0, a1, a2, a3, b0, b1, b2 and b3. Unknowns are AA0=A and BB0=B and the angles $\mu 1$, $\mu 2$ and $\mu 3$. One then finds (and equivalently for 2 and 3):

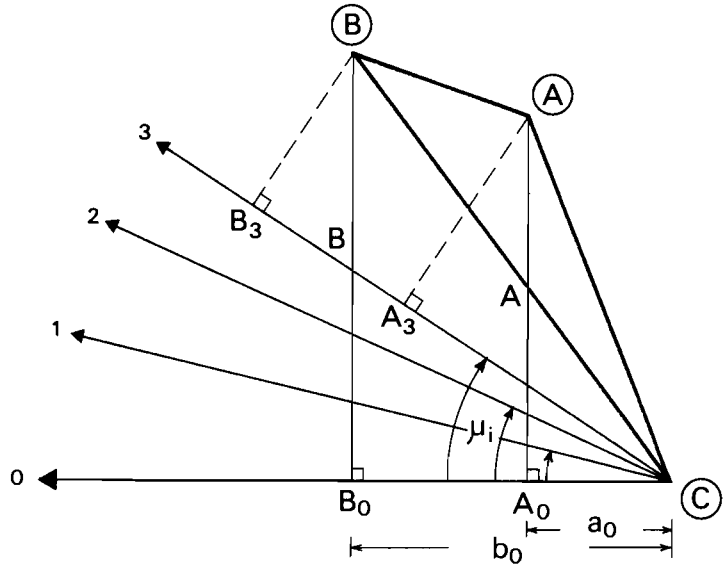

Figure 41: Two-dimensional VLBI

$$a1 = a0.\cos(\mu 1) + A.\sin(\mu 1) \qquad (F.1)$$
$$b1 = b0.\cos(\mu 1) + B.\sin(\mu 1)$$

Solving this system for $\cos(\mu 1)$ and $\sin(\mu 1)$ and eliminating $\mu 1$ via $\sin^2(\mu 1)+\cos^2(\mu 1)=1$ one finds, with some rearrangement of factors:

$$\frac{A^2}{B^2} * \frac{(b0^2-b1^2)}{(a1b0-a0b1)^2} - 2* \frac{A}{B} * \frac{(a0b0-a1b1)^2}{(a1b0-a0b1)^2} * \frac{(a0^2+a1^2)}{(a1b0-a0b1)^2} = \frac{1}{B^2} \qquad (F.2)$$

or, introducing the abbreviations P1, Q1 and R1:

$$P1 * (A/B)^2 - 2*Q1 * (A/B) + R1 = 1/B^2 \qquad (F.3)$$

Now taking the difference of equations (F.3) for 1 and 2 and for 1 and 3 one finds the following two equations with only one unknown, viz. A/B:

$$(P1-P2) * (A/B)^2 - 2 * (Q1-Q2) * (A/B) + (R1-R2) = 0$$
$$(P1-P3) * (A/B)^2 - 2 * (Q1-Q3) * (A/B) + (R1-R3) = 0 \qquad (F.4)$$

The fact that the two roots of each equation are equal yields the required condition equation. The first root is a0/b0, which can easily be found, but this root is introduced by taking the square in $\sin^2(\mu 1)+\cos^2(\mu 1)=1$.

The product of two roots Z1 and Z2 of a quadratic equation $u.Z^2+v.Z+w=0$ is $Z1*Z2=w/u$. Now $Z1=a0/b0$ and one finds by putting the other two roots of the two equations equal:

$$(R1-R2) \;.\; (P1-P3) = (R1-R3) \;.\; (P1-P2) \qquad (F.5)$$

Elaborating this equation and rearranging the terms, one arrives at the following equation which contains all observations. It is the (non-linear) condition equation.

$$0 = (a0b0 \; a1b1 \; a2b2 \; a3b3) \; * \qquad (F.6)$$

$$* \begin{bmatrix} 0 & b3^2 & b1^2 & b2^2 \\ b2^2 & 0 & b3^2 & b0^2 \\ b3^2 & b0^2 & 0 & b1^2 \\ b1^2 & b2^2 & b0^2 & 0 \end{bmatrix} - \begin{bmatrix} 0 & b2^2 & b3^2 & b1^2 \\ b3^2 & 0 & b0^2 & b2^2 \\ b1^2 & b3^2 & 0 & b0^2 \\ b2^2 & b0^2 & b1^2 & 0 \end{bmatrix} * \begin{matrix} (a0^2) \\ (a1^2) \\ (a2^2) \\ (a3^2) \end{matrix}$$

Appendix G

SPECIAL ALTERNATIVE HYPOTHESES FOR "FUSION"

In §6.3 the FUSION software for the comparison of two sets of 3-D Euclidean coordinates was described. Some special alternative hypotheses for the w-test (42.7) were indicated there, which facilitate the detection of possible errors in the station coordinates. The mathematical formulation of the C-vectors connected with these hypotheses (42.4) is now presented.

a) an error in S-basis coordinates.
To give the general idea, it may be worthwhile studying a small levelling network which should be connected to known points. Let it consist of four points, with H1, H2, H3 and H4 as published heights and h1, h2, h3 and h4 as newly determined heights, where 1 is the S-basis-point with zero-variance. Now, the four alternative hypotheses that at one of these stations the height difference h-H is erroneous can be specified by the following (transposed) C-vectors (42.4): (1,0,0,0), (0,1,0,0), (0,0,1,0) and (0,0,0,1). This will lead to w-values that can be tested statistically. However, as 1 has zero-variance and therefore gets no correction, w=0 for h1-H1. Therefore, the alternative hypothesis "1 is erroneous, 2, 3 and 4 are OK" is reworked as: "1 is OK; 2, 3 and 4 are equally erroneous", formulated by C-vector (0,-1,-1,-1).
This can be interpreted as follows: if 2, 3 and 4 all get a correction of, say, +15 cm, this should be read as: 1 has sunk 15 cm!
It is naturally a matter of interpretation whether the first or the second hypothesis is true. In an ordinary levelling network it would be highly coincidential if all points were lifted by 15 cm. However, when measuring in a tectonically-active area, the matter is not so trivial and it could easily be the case that point 1 is the only stable point.

It can be shown that this C-vector is a column of the S-transformation matrix to the S-basis of station 1 (see Appendix E). This is true because the S-matrix is essentially derived from the (linearized) relation (= similarity transformation) between the unknowns in one S-system and those in another (§4.2.2).
In the same way, the C-vector in the three dimensional case is found as the appropriate column for the X-, Y- and Z-coordinates of the S-basis-point from the S-matrix (E.3), with (E.7) as the choice for T and Bs (the "standard" choice of Appendix E) for B.

b) an error in the choice of similarity transformation parameters.
If, for some reason, one or more transformation parameters are not estimated in the adjustment, one should test whether this is justified.

The columns of the (linearized) system of observation equations (62.8) do represent exactly the relation between the coordinates and the similarity transformation parameters. Consequently, these columns can be taken as C-vector.
In this way, the following C-vectors can be composed for the alternative hypotheses that a given transformation parameter is erroneous (if n= the number of stations in both sets):

scale	:	(C) = (X1,Y1,Z1,X2,Y2,Z2, ... ,Xn,Yn,Zn)
DX	:	(C) = (1,0,0,1,0,0, ... ,1,0,0)
DY	:	(C) = (0,1,0,0,1,0, ... ,0,1,0)
DZ	:	(C) = (0,0,1,0,0,1, ... ,0,0,1)
R_X	:	(C) = (0,Z1,-Y1,0,Z2,-Y2, ... ,0,Zn,-Yn)
R_Y	:	(C) = (-Z1,0,X1,-Z2,0,X2, ... ,-Zn,0,Xn)
R_Z	:	(C) = (Y1,-X1,0,Y2,-X2,0, ... ,Yn,-Xn,0)

It should be noted that if one of the parameters is estimated in the adjustment, the corresponding w-test value will of course be (practically) zero.

c) an error in local horizontal East/West or North/South direction or in height.
The C-vectors related to this type of alternative hypothesis are specified as vectors in the these directions. Consequently their formulation is:

North/South (ϕ):		(C) = (X , Y, -sqrt(X^2+Y^2)/Z)
East/West (λ)	:	(C) = (Y , -X , 0)
height (h)	:	(C) = (X , Y , Z)

Appendix H

REFERENCES

Aardoom, L., 1972: "ON A GEODETIC APPLICATION OF MULTIPLE-STATION VLBI", Publ. Netherlands Geodetic Commission, Vol.5, No.2, Delft.

Aardoom, L., 1983: "FEATURES OF THE EARTH'S ROTATION", Zenit, p.156-163 (in Dutch).

Aardoom, L., 1984: "SHORT REPORT VISIT CDP INVESTIGATOR'S MEETING", Fall 84, not published (in Dutch).

Alberda, J.E., 1974: "PLANNING AND OPTIMIZATION OF NETWORKS: SOME GENERAL CONSIDERATIONS", Boll. Geod. Sc.A., 33.

Astron.Eph.Supp., 1974, Astronomical Ephemeris, Explanatory Supplement, Her Majesty's Stationary Office, London.

Baarda, W., 1966: "POLYGON THEORY IN THE COMPLEX PLANE, PART 1-IV", Dept. of Geodesy, Delft (in Dutch).

Baarda, W., 1967: "ADJUSTMENT THEORY, PART I + II", Dept. of Geodesy, Delft (in Dutch).

Baarda, W., 1968: "A TESTING PROCEDURE FOR USE IN GEODETIC NETWORKS", Publ. Netherlands Geodetic Commission, Vol. 2, No. 5, Delft.

Baarda, W., 1972: "A PERSONAL REPORT ON ACTIVITIES IN S.S.G. NO. 1.14: SPECIFICATIONS FOR FUNDAMENTAL NETWORKS IN GEOMETRIC GEODESY", XVth General Assembly of IUGG, Moscow; AIG Proc., Tome 24, Paris.

Baarda, W., 1973: "S-TRANSFORMATIONS AND CRITERION MATRICES"; Publ. Netherlands Geodetic Commission, Vol. 5, No. 1, Delft.

Baars, J.W.M., J.F. van der Brugge, J.L. Casse, J.P. Hamaker, L.H. Sondaar, J.J. Visser, K.J. Wellington, 1973, "THE SYNTHESIS RADIO TELESCOOP AT WESTERBORK", Proc. IEEE, Vol. 61.

Bare, C.C., B.G. Clark, U.I. Kellerman, M.H. Cohen, D.L. Jauncey, 1967: "INTERFEROMETER EXPERIMENT WITH INDEPENDENT LOCAL OSCILLATORS", Science, Vol. 157.

BIH, 1978, Annual Report, Bureau International de l'Heure, Paris.

Beyer W., J. Campbell, F.J. Lohmar, H. Seeger, A. Sudau, F.J.J. Brouwer, G.J. Husti, G. Lundqvist, B. Rönnäng, R.T. Schilizzi, R.S. Booth, P. Richards, S. Tallquist, 1982: "PROJECT 'ERIDOC' (EUROPEAN RADIO-INTERFEROMETRY AND DOPPLER CAMPAIGN)", in: Proc. Symp. No. 5, IAG-meeting Tokyo, NOAA Techn. Report NOS95/NGS24, Rockville.

Bock, Y., 1980: "A VLBI VARIANCE-COVARIANCE ANALYSIS INTERACTIVE COMPUTER PROGRAM", Report No. 298, Dept. of Geod. Science, Ohio State University, Columbus.

Bock, Y., 1983: "ON THE TIME DELAY WEIGHT MATRIX IN VLBI GEODETIC PARAMETER ESTIMATION", Report No. 348, Dept. of Geod. Science, Ohio State University, Columbus.

Bos, A., E. Raimond, H.W. van Someren Greve, 1981, Astron. Astrophysics, 98, 251.

Broten, N.W., T.H. Leyg, J.L. Locke, C.W. McLeish, R.S. Richards, J.L. Ten, H.P. Gush, R.M. Chrisholm, J.A. Galt, 1967: "LONG BASELINE INTERFEROMETRY: A NEW TECHNIQUE", Science, Vol. 156, 1592.

Brouw, W.N., 1973: "SOME THOUGHTS ON APERTURE SYNTHESIS CELESTIAL POSITIONS", Note 143, Neth. Found. for Radio-Astronomy, Dwingeloo.

Brouwer, F.J.J. & P. Visser, 1978: "RADIOINTERFEROMETRY; ASTRONOMY AND GEODESY", graduate thesis, Dept. of Geodesy, Delft (in Dutch).

Brouwer, F.J.J., D.T. van Daalen, J.T. Gravesteijn, H.M. de Heus, J.J. Kok, P.J.G. Teunissen, 1982: "THE DELFT APPROACH FOR THE DESIGN AND COMPUTATION OF GEODETIC NETWORKS", in: "Forty Years of Thought...", Anniversary edition on the occasion of the 65th birthday of Professor W.Baarda, Geodetic Computing Centre, Delft.

Brouwer, F.J.J. 1982a: "MEASURES FOR PRECISION AND RELIABILITY IN PLANNING, ADJUSTING AND TESTING A EUROPEAN VLBI-CAMPAIGN; A SURVEY OF CURRENT AND FUTURE MEASUREMENTS", in: Proc. Intern. Symposium on Geod. Networks and Computations, Bayerische Akademie der Wissenschaften, editor R.Sigl, München.

Brouwer, F.J.J. 1982b: "SELECTED TOPICS IN GEODETIC VLBI", Proc. "Meeting on Geodetic Applications of VLBI"; Report 82.3, Netherlands Geodetic Commission, Delft.

Brouwer, F.J.J., G.J. Husti, W. Beyer, J. Campbell, B. Hasch, F.J. Lohmar, H. Seeger, G. Lundqvist, B. Rönnäng, A. van Ardenne, R.T. Schilizzi, B. Anderson, R.S. Booth, P.N. Wilkinson, P. Richards, S. Tallquist, 1983: "DATA ANALYSIS OF PROJECT 'ERIDOC' (EUROPEAN RADIO-INTERFEROMETRY AND DOPPLER CAMPAIGN)", paper presented at the IUGG/IAG General Assembly, Section 2 "Space Techniques", Hamburg.

Brouwer, F.J.J. (ed.), 1984: "EUROPEAN VLBI FOR GEODESY AND ASTROMETRY", account of a working meeting, 3-4 nov. 1983, Netherlands Geodetic Commission, Delft.

Buiten, H.J. & P. Richardus, 1982: "JUNCTION OF CONTROL SURVEYS BY ADJUSTMENT COMPARED WITH COORDINATE TRANSFORMATION", in: "Forty Years of Thought...", Anniversary edition on the occasion of the 65th birthday of Professor W.Baarda, Geodetic Computing Centre, Delft.

Campbell, J., 1979a: "PHASE VERSUS DELAY IN GEODETIC VLBI", Proc. Conf. "Radio Interferometry Techniques for Geodesy", MIT, NASA CP 2115, Washington.

Campbell, J., 1979b: "DIE RADIOINTERFEROMETRIE AUF LANGEN BASEN ALS GEODAETISCHES MESSPRINZIP HOHER GENAUIGKEIT", Reihe C, Heft 254, Deutsche Geod. Komm., München.

Campbell, J. & F.J. Lohmar, 1982: "ON THE COMPUTATION OF IONOSPHERIC PATH DELAYS FOR VLBI FROM SATELLITE DOPPLER OBSERVATIONS", in Proc. Symp. no. 5, IAG, Tokyo, NOAA-TR: NOS95-NGS24, Rockville.

Campbell, J., 1982: "VLBI FOR GEODESY AND GEOPHYSICS; STATUS AND PROSPECTS", Proc. "VLBI-techniques", CNES, Toulouse,

Carter, W.E., 1981: "NGS FORMAT FOR VLBI DATA", NGS-document 810121 ;FOR2:55.

Carter, W.E., 1983: "THE APPLICATIONS OF RADIO INTERFEROMETRIC SURVEYING IN GEODESY", NGS/NOAA, Rockville.

Chao, C.C., 1970: "A PRELIMINARY ESTIMATION OF TROPOSPHERIC INFLUENCE ON THE RANGE AND RANGE RATE DATA DURING THE CLOSEST APPROACH OF THE MM71 MARS MISSION", JPL, TM 391-129, Pasadena, California.

Clark, T.A., C.C. Counselman, P.G. Ford, L.B. Hanson, H.F. Hinteregger, W.J. Klepczynski, C.A. Knight, D.S. Robertson, A.E.E. Rogers, J.W. Ryan, I.I. Shapiro, A.R. Whitney, 1979: "SYNCHRONIZATION OF CLOCKS BY VLBI", IEEE, Vol. IM-28, no. 3.

Claessen, W.A. & G. Bruins, 1978: "THE NETHERLANDS TRIANGULATION SERVICE", Cadastral Service, Apeldoorn (in Dutch).

De Munck, J.C., 1982: "IONOSPHERIC CORRECTION FOR (PSEUDO) RANGE MEASUREMENTS TO SATELLITES", Proc. General Meeting of the IAG, Tokyo.

Dermanis, A., 1977: "DESIGN OF EXPERIMENT FOR EARTH ROTATION AND BASELINE PARAMETER DETERMINATION FROM VLBI", Report No. 245, Dept. of Geodetic Science, O.S.U., Columbus.

Dermanis, A. & E. Grafarend, 1981: "ESTIMABILITY ANALYSIS OF GEODETIC, ASTROMETRIC AND GEODYNAMICAL QUANTITIES IN VLBI", Geophys. J. R. Astron. Soc., 65.

Dicke, R.H., 1969: "AVERAGE ACCELERATION OF THE EARTH'S ROTATION AND THE VISCOSITY OF THE DEEP MANTLE", J.Geophys.Res., Vol.74, No. 25.

Enslin, H., 1978: "DETERMINATION OF THE ROTATION OF THE EARTH", in "Tidal Friction and the Earth's Rotation", ed. P.Brosche, Springer Verlag, Berlin.

Fansalow, J., O.J. Sovers, J.B. Thomas, F.R. Bletzacker, T.J. Kearns, E.J. Cohen, G.H. Purcell, D.H. Rogsted, L.J. Skjerve, L.E. Yomig, 1981: "DEVELOPMENT OF A RADIO-ASTROMETRIC CATALOG BY MEANS OF VLBI

OBSERVATIONS", proc. Ref. Coord. Syst. for Earth Dynamics, D.Reidel publ.comp., Dordrecht.

Flock, W.L., S.D. Slabin, E.U. Smith, 1982: "PROPAGATION EFFECTS ON RADIO RANGE AND NOISE IN EARTH-SPACE TELECOMMUNICATIONS", Radio Science, Vol. 17, No. 6.

Fujimoto, M.K., S. Aoki, K. Nakajima, T. Fukishima, S. Matsuzaka, 1982: "GENERAL RELATIVISTIC FRAMEWORK FOR THE STUDY OF ASTRONOMICAL/GEODETIC REFERENCE COORDINATES", in Proc. Symp. no. 5, IAG, Tokyo, NOAA-TR: NOS95-NGS24, Rockville.

Greve, A., 1981: "METROLOGY OF THE EFFELSBERG 100 M RADIO REFLECTOR", Zeitschrift für Vermessungswesen, no. 6.

Gubanow, V.S., 1973: "SERIES EXPANSION OF THE ANNUAL ABERRATION WITH RESPECT TO FUNDAMENTAL ARGUMENTS", Soviet Astron.-AJ, Vol.16, No.5.

Hagfors, T., 1976: "THE IONOSPHERE", in Astrophysics, part B "Radio Telescopes", ed. M.L. Meeks, Academic Press, New York.

Hanse, J., W.H. Egli, M. Ignagni, 1984: "POLAR MOTIONS MEASUREMENT STUDY", Report AFGL-TR-84-0261, United States Air Force, Hanscom AFB, Massachusetts.

Herring, T.A., B.E. Corey, C.C. Counselman, I.I. Shapiro, B.O. Rönnäng, O.E.H. Rydbeck, T.A. Clark, R.J. Coates, C. Ma, J.W. Ryan, N.R. Vandenberg, H.F. Hinteregger, C.A. Knight, A.E.E. Rogers, A.R. Whitney, D.S. Robertson, B.R. Schupler, 1981: "GEODESY BY RADIO INTERFEROMETRY: INTERCONTINENTAL DISTANCE DETERMINATIONS WITH SUB-DECIMETER PRECISION", J. Geophys. Res., Vol. 86, No. B3.

Hopfield, H.S., 1977: "TROPOSPHERIC CORRECTION OF ELECTROMAGNETIC RANGING SIGNALS TO A SATELLITE: STUDY OF PARAMETERS", Proc. IAG-symp. on Refraction, Neth. Geod. Comm., Delft.

Hothem, L.D., T. Vincenty, R.E. Moose, 1983: "RELATIONSHIP BETWEEN DOPPLER COORDINATES AND OTHER ADVANCED GEODETIC MEASUREMENT SYSTEMS USING GLOBAL DATA", Proc. of the 3rd International Geodetic Symposium on Satellite Doppler Positioning, Las Cruces.

Kaplan, G.H., 1981: "THE IAU RESOLUTIONS ON ASTRONOMICAL CONSTANTS, TIME SCALES AND THE FUNDAMENTAL REFERENCE FRAME", US Naval Observatory, Circular no. 163, Washington.

Klobuchar, J.A., 1978: "IONOSPHERIC EFFECTS ON SATELLITE NAVIGATION AND AIR TRAFFIC CONTROL SYSTEMS", AGARD lecture series, no. 93.

Kok, J.J., 1981: "AN ALGORITHM FOR THE REDUCTION OF SPARSE SYMMETRIC MATRICES, FOR USE IN LEAST-SQUARES ADJUSTMENT PROGRAMMES", IAG. Symp. on Optimization of Design and Computation of Control Networks, Sopron, Hungary.

Kok, J.J., 1984: "ON DATA SNOOPING AND MULTIPLE OUTLIER TESTING", NOAA technical report NOS/NGS/30, Rockville, Md.

Krarup, T. & K. Kubik, 1983: "THE DANISH METHOD, EXPERIENCE AND PHILOSOPHY", Reihe B, Heft 98, Deutsche Geod. Komm., München.

Larden, D.R., 1980: "SOME GEOPHYSICAL EFFECTS ON GEODETIC LEVELLING NETWORKS", Proc. 2nd Symp. on Redef. NAD, Ottawa.

Lawlinakis, A., 1976: "PROGRAM PREDOP", Dept. of Energy, Mines and Resources, Survey and Mapping Branch, Report SMB-1214E, Ottawa.

Leick, A. & B.H.W. van Gelder, 1975: "ON SIMILARITY TRANSFORMATIONS AND GEODETIC NETWORK DISTORTIONS BASED ON DOPPLER SATELLITE OBSERVATIONS", Report No. 235, Dept. of Geod. Science, O.S.U., Columbus.

Leick, A., 1978: "THE OBSERVABILITY OF THE CELESTIAL POLE AND ITS NUTATIONS", Report No. 262, Dept. of Geod. Science, O.S.U., Columbus.

Lundqvist, G., 1984: "RADIO INTERFEROMETRY AS A PROBE OF TECTONIC PLATE MOTION", Ph.D. Thesis, TR No. 150, Onsala Space Observatory.

Lynn, P.A., 1973: "AN INTRODUCTION TO THE ANALYSIS AND PROCESSING OF SIGNALS", Macmillan Press Ltd, London.

Ma, C., 1978: "VLBI APPLIED TO POLAR MOTION, RELATIVITY AND GEODESY", Ph.D. Thesis, NASA/GFSC TM 79582.

Mc Lintock, D.N., 1980: "VLBI AND GEODETIC APPLICATIONS", Ph.D. Thesis, Dept. of Surveying, University of Nottingham.

Melbourne, W., R. Anderle, M. Feissel, R. King, D. McCarthy, D. Smith, B. Taply, R. Vincente, 1983: "MERIT STANDARDS", MERIT Commission on Standards.

Melchior, P., 1966: "THE EARTH TIDES", Pergamon Press, Oxford.

Melchior, P., 1978: "THE TIDES OF THE PLANET EARTH", Pergamon Press, Oxford.

Michelson, A.A., 1890: "ON THE APPLICATIONS OF INTERFERENCE METHODS TO ASTRONOMICAL MEASUREMENTS", Phil. Mag., 30, 1-21.

Misner, C.W., K.S. Thorne J.A., Wheeler, 1970: "GRAVITATION", Freeman and Company, San Francisco.

Moran, J.M., P.P. Crowther, B.F. Burke, A.H. Barret, A.E.E. Rogers, J.A. Ball, J.C. Carter, C.C. Bare, 1967: "SPECTRAL LINE INTERFEROMETRY WITH INDEPENDENT TIME STANDARDS AT STATIONS SEPARATED BY 845 KM", Science, Vol. 157.

Moran, J.M. & B.R. Rosen, 1979: "THE ESTIMATION OF PROPAGATION DELAY THROUGH THE TROPOSPHERE FROME MICROWAVE RADIOMETER DATA", Proc. Confer. on Radio Interferometry Techniques for Geodesy, NASA-CP 2115, Washington, D.C.

Mueller, I.I., 1980: "REFERENCE COORDINATE SYSTEMS FOR EARTH DYNAMICS; A PREVIEW", Proc. IAU Colloquium 56, Warsaw, Poland, Reidel Publ. Comp., Dordrecht.

Munk, W.H., & G.F. Macdonald, 1975: "THE ROTATION OF THE EARTH", Cambridge University Press, Cambridge.

Newcomb, S., 1895a: "THE ELEMENTS OF THE FOUR PLANETS AND THE FUNDAMENTAL CONSTANTS OF ASTRONOMY", Washington.

Newcomb, S., 1895b: "TABLES OF THE SUN", APAE, 6, part I.

Newcomb, S., 1897: "A NEW DETERMINATION OF THE PRECESSIONAL CONSTANT WITH THE RESULTING PRECESSIONAL MOTIONS", APAE, 8, part I.

Nibbelke, P., 1984: "ADJUSTMENT OF GEODETIC NETWORKS ON THE ELLIPSOID", graduate thesis, Dept. of Geodesy, Delft (in Dutch).

Nottarp K. & R. Kilger, 1982: "DESIGN OF WETTZELL TELESCOPE", Proc. Symp. "VLBI-techniques", CNES, Toulouse.

Preuss, E., 1984: "RADIOINTERFEROMETRIE MIT GROSSEN BASISLAENGEN (VLBI)", Physik in unsere Zeit, Bonn.

Quee, H. 1983: "QUATERNION ALGEBRA APPLIED TO POLYGON THEORY IN THREE DIMENSIONAL SPACE", Ph.D. Thesis, Publ. Netherlands Geodetic Commission, Vol. 7, No. 2, Delft.

Robertson, D.S., 1975: "GEODETIC AND ASTROMETRIC MEASUREMENTS WITH VERY-LONG-BASELINE INTERFEROMETRY", Ph.D. Thesis, Massachusetts Institute of Technology.

Robertson, D.S. & W.E. Carter, 1981: EARTH ROTATION INFORMATION DERIVED FROM MERIT AND POLARIS VLBI OBSERVATIONS", Proc. IAU-colloquium No. 63, Grasse, France.

Rogers, A.E.E., 1970: "VLBI WITH LARGE EFFECTIVE BANDWIDTH FOR PHASE-DELAY MEASUREMENTS", Radio Science, Vol. 5, no. 10.

Rogers, A.E.E., R.J. Cappallo, H.F., Hinteregger, J.I. Levine, E.F. Nesman, J.C. Webber, A.R. Whitney, T.A. Clark, C. Ma, J. Ryan, B.E. Corey, C.C. Counselman, T.A. Herring, I.I. Shapiro, C.A. Knight, D.B. Shaffer, N.R. Vandenberg, R. Lacasse, R. Mauzy, B. Rayhrer, 1983: "VLBI: THE MK-III SYSTEM FOR GEODESY, ASTROMETRY AND APERTURE SYNTHESIS", Science, Vol. 219.

Russell, B., 1977: "THE ABC OF RELATIVITY", Unwin Paperbacks, London.

Saastamoinen, J., 1972: "ATMOSPHERIC CORRECTION FOR THE TROPOSPHERE AND STRATOSPHERE IN RADIO RANGING OF SATELLITES", in Geoph. Monogr. S., Vol. 15, "The Use of Artificial Satellites for Geodesy", ed. S.W. Henriksen et al:, A.G.U., Washington, D.C.

Schaffer, D.B., 1984: "VLBI GEODESY: TECHNIQUES AND RECENT RESULTS", proc. IAU Symp. No. 110, ed. R. Fanti et al., D. Reidel Publ. Comp., Dordrecht.

Schilizzi, R.T., 1982: "ASTRONOMICAL VLBI, THE PAST, PRESENT AND FUTURE", Proc. Meeting on Geodetic Applications of VLBI", ed. F.J.J.Brouwer, Report 82.3, Neth. Geod. Comm., Delft.

Schilizzi, R.T., B.F. Burke, R.S. Booth, R.A. Preston, P.N. Wilkinson, J.F. Jordan, E. Preuss, D. Roberts, 1984: "THE QUASAT PROJECT", Proc. IAU Symp. No. 110 "VLBI and Compact Radio Sources", ed. R. Fanti et al., D. Reidel Publ. Comp., Dordrecht.

Schuh, H., 1984: "BONNER VLBI-AUSWERTE PROGRAM", internal document Geodetic Institute Bonn (not published).

Schut, T.G., 1983: "WESTERBORK SYNTHESIS RADIO TELESCOPE MEASUREMENTS: A GEODETIC ANALYSIS", graduate thesis, Dept. of Geodesy, Delft (in Dutch).

Schwiderski, E.M., 1978: "GLOBAL OCEAN TIDES, PART I, A DETAILED HYDRODYNAMICAL INTERPOLATION MODEL", US Naval Surface Weapons Center, TR-3866, Dahlgren, Va.

Shapiro, I.I. & C.A.Knight, 1969: "GEOPHYSICAL APPLICATIONS OF LONG BASELINE RADIO INTERFEROMETRY", Conf. public. "Earthquake Displacement Fields and the Rotation of the Earth", D.Reidel Publ. Comp., Dordrecht.

Shapiro, I.I., C.C. Couselman, T.A. Herring, 1979: "ANALYSIS OF LASER RANGING AND VLBI OBSERVATIONS FOR GEODETIC PURPOSES", Report AFGL-TR-, Dept. of Earth and Planetary Sciences, MIT, Cambridge, Mass..

Smith, E.K. & S. Weintraub, 1953: "THE CONSTANTS IN THE EQUATION FOR ATMOSPHERIC REFRACTIVE INDEX AT RADIO FREQUENCIES", Proc. IRE, 41, 1035-1037.

Spoelstra, T.A.Th., 1983a: "THE INFLUENCE OF IONOSPHERE REFRACTION ON RADIO ASTRONOMY INTERFEROMETRY", Astron. and Astroph. 120,313.

Spoelstra, T.A.Th., 1983b: "CORRECTING VLBI OBSERVATIONS FOR IONOSPHERIC REFRACTION", Proc. Symp. on "Beacon Satellite Studies of the Earth's Environment", ed. T. Tyagi, New Delhi.

Spoelstra, T.A.Th. & H. Kelder, 1984: "EFFECTS PRODUCED BY THE IONOSPHERE ON RADIO INTERFEROMETRY", Radio Science, Vol. 19, No. 3.

Teunissen, P.J.G., 1984a: "QUALITY CONTROL IN GEODETIC NETWORKS", Math./Phys.Geod. Section, Report 84.2, Dept. of Geodesy, Delft.

Teunissen, P.J.G., 1984b: "GENERALIZED INVERSES, ADJUSTMENT, THE DATUM PROBLEM AND S-TRANSFORMATIONS", Math./Phys.Geod. Section, Report 84.1, Dept. of Geodesy, Delft.

Teunissen, P.J.G., 1985: "THE GEOMETRY OF GEODESIC INVERSE LINEAR MAPPING AND NON-LINEAR ADJUSTMENT", Ph.D. Thesis, Publ. Netherlands Geodetic Commission, Vol. 8, No. 1, Delft (in press).

Thomas, J.B., 1972: "AN ANALYSIS OF LONG BASELINE RADIO INTERFEROMETRY", Part I,II,III, JPL Techn. Report 32-1526, Pasadena, California.

Thomas, J.B., 1981: "AN ANALYSIS OF RADIO INTERFEROMETRY WITH THE BLOCK-O SYSTEM", NASA/JPL Publication 81-49, Pasadena, California.

Thomas, J.B., O.J. Sovers, J.L. Fanselow, E.J. Cohen, G.H. Purcell Jr., D.H. Rogstad, L.J. Skjerve, D.J. Spitzmesser, 1983: "RADIO INTERFEROMETRIC DETERMINATION OF SOURCE POSITIONS, INTERCONTINENTAL BASELINES, AND EARTH ORIENTATION WITH DSN ANTENNAS", TDA Progress Report 42-73, NASA/JPL, Pasadena.

Trask, D., A. Niell, A. Rogers, T. Herring, J. Davidson, D. Schaffer, J. Ryan, T. Clark, 1982: "ERROR SOURCES IN THE DETERMINATION OF BASELINES BY VLBI", NASA/GSFC, presentation CDP investigator's meeting 28th Oct. (not published).

Tsimis, E., 1973: "CRITICAL CONFIGURATIONS (DETERMINANTAL LOCI) FOR RANGE AND RANGE-DIFFERENCE SATELLITE NETWORKS", Report No.191, Department of Geodetic Science, Ohio State University, Columbus.

Van Antwerpen, A., F.J.J. Brouwer, R. Nicolai, P. Visser, 1978: "A TENSOR ANALYTICAL APPROACH TO THE DIRECT METHOD OF GEODESY IN CURVED SPACE", paper 10th semester course "Geodetic Computations and Projections", Dept. of Geodesy, Delft (in Dutch).

Vandenberg N.R., T.A. Clark, L.N. Foster, A.R. Whitney, G. Lampe, 1980: "AUTOMATION OF THE MK-III FIELD SYSTEM", Proc. Conf. "Radio Interferometry Techniques for Geodesy", MIT, NASA CP2115.

Van Gelder, B.H.W. & L.Aardoom, 1982: "SLR NETWORK DESIGN IN VIEW OF RELIABLE DETECTION OF PLATE KINEMATICS IN THE EAST MEDITERRANEAN", Math./Phys. Geod. Section, Report 82.3, Dept. of Geodesy, Delft.

Van Vleck, J.H. & D.Middleton, 1966: Proc. IEEE, 54,2.

Wahr, J., 1979: "THE TIDAL MOTIONS OF A ROTATING, ELLIPTICAL, ELASTIC, AND OCEANLESS EARTH", Ph.D. Thesis, University of Colorado.

Wahr, J., 1981: "THE FORCED NUTATIONS OF AN ELLIPTICAL, ROTATING, ELASTIC AND OCEANLESS EARTH", Geophys. J. Royal Astr. Soc., Vol. 64, No.3.

Wessel, P.F.H. & H. Koudijs, 1984: "THE POINT POSITIONING METHOD OF THE NETHERLANDS RAILWAYS", NGT-Geodesia, Vol. 26, No. 10 (in Dutch).

Wilkins, G.A. (ed.), 1980: "PROJECT MERIT", Royal Greenwich Observatory, England.

Woolard, E.W., 1953: "ASTRONOMICAL PAPERS PREPARED FOR THE USE OF THE AMERICAN EPHEMERIS AND NAUTICAL ALMANAC", XV, US Govt. Printing Off., Washington.

Woolard, E.W. & G.M. Clemence, 1966: "SPHERICAL ASTRONOMY", Academic Press, New York.